# NUCLEAR MAGNETIC RESONANCE STUDIES IN CHEMISTRY

BODLEIAN LIBRARY OXFORD
DEPOSITED
THESIS
9.4.70

# NUCLEAR MAGNETIC RESONANCE STUDIES IN CHEMISTRY

A thesis submitted to the Board of
the Faculty of Physical Sciences in
the University of Oxford
in partial fulfilment of the
requirements of the degree of
Doctor of Philosophy

by

Christopher Hall, B.A.

November 1969

Trinity College,
Oxford.

Physical Chemistry Laboratory
South Parks Road,
Oxford.

Acknowledgements

I thank my supervisor, Professor R.E. Richards, F.R.S., for his keen interest and guidance, and for the opportunity to work in his laboratory during the years 1966-69.

I am grateful to Dr. R.R. Sharp, from whom over the course of two years I have learned a great amount, for innumerable discussions on many aspects of the research described in this thesis; and also to Dr. D.W. Kydon for long, useful discussions and collaboration on the chlorine exchange problem.

I am indebted to Dr. J.D. Halliday for his instruction in the use of the high field superconducting solenoid spectrometer and for the gift of some carefully prepared caesium n.m.r. reference samples.

I thank Dr. A.J. Downs and Mr. C. Adams for recording a Raman spectrum for me.

This thesis was typed by Mrs. G. Haydon and the diagrams were drawn by Mr. W. Hanna, whom I am very happy to thank for their care and skill. I thank Mr. V. Hall for his help in the production of the diagrams.

I acknowledge the financial support of a Research Studentship of the Northern Ireland Ministry of Education.

I am indebted to my wife for her assistance in many ways and for her encouragement throughout the writing of this thesis.

| Chapter | | Page |
|---|---|---|
| I | Magnetic relaxation of $^{23}Na$ and $^{81}Br$ in aqueous solutions of the alkali halides . . . . . | 1 |
| | 1. Introduction: some aspects of magnetic relaxation studies of pure liquids and ionic solutions . . . . . | 2 |
| | 2. Experimental aspects . . . . . | 13 |
| | 3. Experimental results . . . . . | 21 |
| | 4. Discussion . . . . . | 22 |
| II | Studies of the $^{133}Cs$ ion resonance shift in solution . . . . . | 34 |
| | 1. Introduction . . . . . | 35 |
| | 2. Experimental account . . . . . | 54 |
| | 3. Further studies of the HRS theory and the $^{133}Cs$ ion resonance shift in solution . . . . . | 55 |
| | 4. Conclusion . . . . . | 85 |
| III | An n.m.r. study of chlorine exchange in aqueous solutions of chloride in the presence of chlorine . . . | 94 |
| | 1. Introduction . . . . . | 95 |
| | 2. Theory of chemical exchange effects on the n.m.r. spectra of quadrupolar nuclei . . . . . | 96 |
| | 3. Experimental aspects . . . . . | 107 |
| | 4. Determination of subsidiary parameters . . . . . | 120 |
| | 5. Discussion of the effect of chemical exchange on linewidths of quadrupolar nuclei in the light of theory . . . . . | 140 |
| | 6. Experimental results . . . . . | 151 |
| | 7. General conclusions . . . . . | 168 |
| APPENDIX I: | Lorentzian line-fitting program . . . . . | 170 |
| APPENDIX II: | Numerical data relating to Chapter III . . . . . | 173 |
| APPENDIX III: | Solutions of the Bloch equations modified to allow for the effects of chemical exchange . . . . . | 178 |
| REFERENCES: | . . . . . | 193 |
| SUMMARY: | . . . . . | 197 |

# CHAPTER I

## Magnetic Relaxation of $^{23}Na$ and $^{81}Br$ in aqueous solutions of the alkali halides

## 1. Introduction: some aspects of magnetic relaxation studies of pure liquids and ionic solutions

### i. Preliminary

The ways in which non-equilibrium nuclear magnetisations relax towards equilibrium states are many and various, and involve many kinds of forces acting on the spins. However it is a general result of relaxation theory that the rates at which these relaxations occur are determined both by the intensity of the interaction responsible for relaxation and by the characteristics of the motions in the neighbourhood of the spin modulating the interaction. In principle, observed n.m.r. relaxation parameters can be interpreted in such a way that information on the microscopic motion of the system is obtained (Pople 1967; Dwek and Richards 1967).

However it is perhaps fair to state that n.m.r. has at present made few unique contributions to an understanding of the liquid state. The generally low information content of n.m.r. signals from mobile liquids has to be set against the natural complexity of the liquid lattice. The recent monograph on water by Eisenberg and Kauzmann (1969) for example refers to only three pieces of information derived from magnetic resonance experiments:

a) the spin-echo determination of the $H_2O$ self-diffusion coefficient (which may alternatively be measured by a variety of other methods);

b) proton chemical shift data which are relevant to liquid water structure theories;

c) measurements of $^{1}H$, $^{2}D$ and $^{17}O$ relaxation times from which a number of motional correlation times may be estimated.

This introduction does not constitute a thoroughgoing survey of nuclear magnetic relaxation studies on liquids or even on electrolyte solutions. It is intended to be illustrative of the problems and achievements in this field and to lead naturally into the presentation and discussion of the new data on ion resonances which form the remainder of the Chapter.

ii. Nuclear magnetic relaxation in pure liquids

The numerous investigations in this field (largely by proton magnetic resonance) have been fully reviewed by Hertz (1967), and it is sufficient here to discuss briefly the interpretation of the relaxation data of water as an example relevant to the rest of this Chapter in which some important concepts are introduced (Bloembergen, Purcell and Pound 1946).

Relaxation theory (Abragam 1961) shows that the spin-lattice relaxation time ($T_1$) for relaxation by dipolar coupling of two identical spins is given by

$$T_1^{-1} = \frac{3}{2}\gamma^4\hbar^2 I(I+1)[J^{(1)}(\omega) + J^{(2)}(2\omega)] \qquad (1.1)$$

where $\gamma$ is the magnetogyric ratio of the nucleus of spin I, J are spectral densities of certain functions of lattice parameters (Fourier transforms of the autocorrelation function describing the random motion of the dipolar coupling) and $\omega$ is the Larmor frequency of the spin.

Now the spectral densities are considered for the case of water. Immediately it is clear that two distinct sets of protons must be taken into account: those situated in the same molecule and those in different molecules. In the first case, modulation of the coupling depends only on changes in the angles relating the interspin vector to the laboratory frame; the vector itself is of fixed length. Thus, the motion of importance is molecular rotation. In contrast, the intermolecular dipolar coupling of spins is more complicated, involving relative translational and orientational motion. It is customary to neglect the rotational motion in this case and treat the intermolecular contribution to the relaxation rate as an effect of pure translational Brownian motion.

Several approaches to the problem of describing molecular rotation have been suggested. Bloembergen, Purcell and Pound (1946) supposed that the

motion is approximately classical and obeys a diffusion equation in which the diffusion coefficient is given by Stokes' Law. The rotational correlation time is then given by

$$\tau_{rn} = \frac{4\pi a^3 \eta}{3kT} \qquad (1.2)$$

where a is the molecular hard-sphere radius and $\eta$ is the solvent viscosity. Hertz (1967) has expanded this model somewhat to include rotational diffusion by jumps of different lengths. It should be noted that the n.m.r. rotational correlation time $\tau_{rn}$ is expected to be equal to one-third of the molecular reorientation time $\tau_r$ which may, for example, be determined from dielectric relaxation measurements.

On the other hand Steele (1963a, b) has suggested that for molecules which interact rather weakly (mobile, nonpolar liquids) the rotational friction coefficient (upon which the Stokes' Law dependence turns) may be very small, and that the rotational correlation time in such circumstances is governed by the molecular moment of inertia. Atkins (1969) has considered the quantum mechanical analogue of this, in which gas-like rotation of molecules in the liquid is allowed at defect sites in which the molecules are sufficiently unhindered.

There are no clear criteria to assist in deciding the range of validity of the two approaches. Moniz, Steele and Dixon (1967) have shown that some nonpolar organic liquids have relaxation times in agreement with the inertial formulation. There is also much evidence that the bulk viscosity provides a good correlating parameter for some other liquids (Bloembergen, Purcell and Pound 1946). Recently however Atkins, Loewenstein and Margalit (1969) have presented some evidence in support of gas-like rotation in the polar liquids $NH_3$ and $ND_3$.

The translational contribution to the relaxation time may also be evaluated (Abragam 1961) by solving a diffusion equation and employing the

Debye-Stokes diffusion coefficient, such that the translational correlation time $\tau_t$ is given by

$$\tau_t = \frac{12a^3\eta}{kT} = 9\tau_{rn} \qquad (1.3)$$

Again other more extended descriptions have been given (Hertz 1967) involving translational jump distances and other microscopic parameters.

Thus the following relations are derived for a mobile liquid (using a Stokes' Law diffusion description of both rotational and translational motion, and assuming that the extreme narrowing inequalities $\omega\tau_{rn} \ll 1$ and $\omega\tau_t \ll 1$ are satisfied):

intermolecular: $$J^{(1)}(\omega) + J^{(2)}(2\omega) = \frac{4}{3b^6}\tau_{rn} = \frac{16\pi\eta a^3}{9b^6 kT} \qquad (1.4)$$

where b is the distance between spins;

intramolecular: $$J^{(1)}(\omega) + J^{(2)}(2\omega) = \frac{4\pi N}{45a^3}\tau_t = \frac{16\pi^2 N\eta}{15kT} \qquad (1.5)$$

where N is the number of spins in unit volume of solution.

Therefore from equations (1.1), (1.4), (1.5)

$$T_1^{-1} = 8\pi\gamma^4\hbar^2 I(I+1)\left(\frac{a^3}{3b^6} + \frac{\pi N}{5}\right)\frac{\eta}{kT} \qquad (1.6)$$

This formula predicts the observed relaxation time of protons in water with reasonable accuracy (Abragam 1961), although there is evidence that the Debye-Stokes rotational correlation time generally proves to be rather longer than the true correlation time (see for example O'Reilly and Schacher 1963). Improved formulae for the correlation time have been given (for example Hill 1954) and tested against experimental data (Herbison-Evans and Richards 1964; Assink and Jonas 1969).

An experimental separation of the inter- and intra-molecular parts of the relaxation can often be made by dilution of the liquid under study with some magnetically inert liquid (frequently $D_2O$). This method does not work satisfactorily in the case of $H_2O$, but results on other liquids indicate that both the terms of equation (1.6) are essentially correct.

The $^2D$ spin-lattice relaxation of $D_2O$ is dominated by the interaction of the nuclear quadrupole moment with the electric field gradients within the molecule. Since the spins are oriented with respect to laboratory axes ($H_o$) and the field gradients are fixed in the molecular frame, the thermal molecular reorientation modulates this interaction. The analysis for $I = 1$ or for any value of $I > \frac{1}{2}$ in the limit of extreme narrowing is similar to that for intramolecular relaxation by dipolar coupling. The relaxation time is given by:

$$T_1^{-1} = \frac{3}{40} \frac{2I + 3}{I^2(2I-1)} \left(1 + \frac{\bar{\eta}^2}{3}\right)\left(\frac{e^2Qq}{\hbar}\right) \tau_{rn} \qquad (1.7)$$

where $\bar{\eta}$ is the asymmetry parameter of the field gradient tensor, $(e^2Qq/\hbar)$ is the nuclear electric quadrupole coupling constant; the Debye-Stokes formula for $\tau_{rn}$ given in equation (1.2) may be used.

Thus $^2D$ relaxation time data from pure $D_2O$ give directly the rotational correlation time $\tau_{rn}$, provided that the quadrupole coupling constant is known. This simple analysis has been applied also to $H_2{}^{17}O$ ($^{17}O$ relaxation) and the results from both are in substantial agreement with those obtained from $^1H$ relaxation data (Eisenberg and Kauzmann 1969).

It is clear from the elementary theory given above that the spin part of equation (1.1) is much more easily handled than the lattice part J. This results from the great complexity of any model description of the liquid state. As long as the model involves only a few microscopic parameters, it is probably seriously oversimplified. As soon as more

than a few parameters are allowed, the validity of the model is likely to be experimentally underdetermined.

One example of a way in which the foregoing theory is oversimplified is that no allowance is made for correlation in the motions of several adjacent particles. All the correlation functions used in the derivation of equation (1.6) and (1.7) are essentially two particle autocorrelation functions. In fact, taking the $H_2O$ molecule as an example, it is clear that the translational motions of two spins in the same molecule are completely correlated. This is not a feature customarily included in the analysis of the intermolecular part of the relaxation equation. In a rather weaker fashion, some degree of correlation must be anticipated in the motions of adjacent water molecules which are linked by hydrogen bonds.

iii. The effect of electrolytes on the relaxation of solvent nuclei

The addition of ionic solutes to $H_2O$ and other liquids generally alters the observed relaxation time of the solvent nuclei (for example $^1H$ and $^2D$). The dissolved ions are in a sense "impurities" in the pure liquid lattice and in their vicinity the relaxation behaviour of the solvent is modified. In some cases, the hydration spheres of the ions exchange only slowly with the bulk liquid and separate n.m.r. relaxation times can in principle be measured from these distinct zones. For singly-charged diamagnetic ions with which this Chapter is concerned, no longlasting hydration sphere is formed and the observed relaxation time is a value averaged over all solvent environments.

Proton spin-lattice relaxation times of aqueous solutions of diamagnetic salts have been extensively studied. On the whole salts which are considered to be structure-breaking by other criteria (such as the evidence of viscosity B-coefficients) reduce the water correlation time and structure-forming salts increase it (Hertz 1967; Engel and Hertz 1968). Indeed Samoilov (1965) has based his theory of hydration to a large extent upon such data. The proton data appear to lead unambiguously to these conclusions, but the further

matters of separating the correlation times of $H_2O$ molecules in the anion and the cation hydration or of determining hydration numbers is, as always with individual ionic quantities, more difficult. A simple three-site model has been used by Hertz in which the bulk solvent and the hydration spheres of the cation and the anion are characterised by three correlation times and three populations.

The effect of diamagnetic salts on the $^2D$ relaxation has been studied by Hertz and Zeidler (1964); these data may also be interpreted on a three site model, and the correlation times are in good agreement with those from $H_2O$ measurements. It is important here to anticipate that the ions may effect not only the reorientational correlation time of the solvent molecules but also the field gradient at the $^2D$ nucleus. Thus there is an ambiguity in the case of the quadrupolar relaxation mechanism in attributing changes in the relaxation time to changes in correlation time. This is true to only a slight extent in the case of the dipolar relaxation of protons in $H_2O$.

iv. Solute resonances

The data now available (Deverell 1969) on the relaxation times of simple ionic solute nuclei are in some ways complementary to the solvent data which have been discussed. There are certain clear and important differences between the microdynamic information which is bound up in the relaxation times of monatomic ion nuclei (mostly of alkali halides) and that obtainable from solvent data.

1. Ion resonances are influenced only by the solvation regions of the solution and therefore provide a direct probe into solvation phenomena.

2. Ion nuclear magnetic resonance is one of the few techniques available in the study of solutions which yields information specific to one ion species in solution.

3. With the exception of $F^-$, all the ion resonances studied are of nuclei possessing nuclear electric quadrupole moments, which relax by quadrupolar interaction (some dipolar contribution is detectable in Li relaxation). However for alkali metal and halide ions there is no molecular frame in which the components of the electric field gradient tensor are fixed. Such a frame does exist for a stable hydration complex. In general, both solvent molecules and other ions contribute to this fluctuating field gradient.

An important experimental limitation on ion resonance work should be mentioned:

4. Whereas the solvent concentration is large and approximately constant even in the presence of large quantities of solute, the studies of solute resonances are handicapped both by relatively low concentrations and by the need to observe less sensitive nuclei. There is need at present for low concentration relaxation time data friom ionic solutes.

It is immediately clear from these characteristic features of the monatomic ion resonances that the analysis of relaxation time data will be more intractable than for the solvent. In a concentrated solution both solvent molecules and other ions can be expected to contribute to the ion relaxation. The ion-ion contribution to the relaxation may be removed in principle by use of the infinite dilution (zero concentration) reference state, obtained from data at finite concentrations by extrapolation. This procedure is satisfactory only if low concentration data are available or if the functional dependence of the relaxation time on concentration is known. At present the data and the theory do not fully meet either requirement.

Furthermore, the origins of the field gradients acting on the ion nuclei to produce relaxation have not clearly been identified. Diffusing ions and diffusing dipolar solvent molecules generate field gradients, but it has been suggested (Deverell 1966) that the repulsive overlap of

closed shell ions may be very effective in producing field gradients at the nucleus also. A similar interaction with solvent molecules may also be important, and being short-range in nature may be very dependent on the finer details of the mutual orientation of the solvent molecule and the ion.

The calculation of an expression for the relaxation time of ion nuclei in solution, analogous to equation (1.7) for solvent nuclei, and based upon a model of diffusing ions and rotating dipoles has been performed independently by Hertz (1961) and by Valiev (1960). The details need not be discussed here, but several comments can be made. As before the factor containing nuclear parameters is easily determined. The calculation proper concerns the evaluation of the intensity of the power spectrum of the fluctuating action of the field gradient on the nucleus. The theory restricts itself to determining the effects of solvent rotations in the first hydration sphere. The motions of the individual solvent molecules within the hydration spheres are assumed to be uncorrelated. The expressions obtained involve a number of drastic approximations and are very unwieldy, but do predict the relaxation rates at infinite dilution in water well (Deverell 1969). However evidence from a number of sources (Deverell 1969; Speight and Armstrong 1967) has strongly suggested the inadequacy of this model to account for the interionic contribution to relaxation. Furthermore Hertz, Stalidis and Versmold (1969) have recently shown by analysis of the concentration dependence of the new data on aqueous solutions that for a number of alkali halides the solvent term is probably only fortuitously correct and that the repulsive overlap interaction between ion and solvent molecule is probably a more important cause of field gradients than solvent electric dipoles.

As was mentioned in connection with solvent studies, the changes in the bulk viscosity have frequently been used to explain changes in relaxation times. Deverell, Frost and Richards (1965) showed that many electrolyte solutions obey a simple empirical relation which may be written

$$T_2^{-1} = (A + Bc)\eta/T = T_1^{-1} \qquad (1.8)$$

to which form the full expressions of Hertz and Valiev may be reduced if it be assumed that the correlation times are governed by Debye-Stokes relations and depend linearly on $\eta/T$.

The Debye relation has been very commonly used to correlate proton relaxation times in non-hydrogen-bonded liquids. Rather surprisingly, proton spin-lattice relaxation rates in water and electrolyte solutions are also approximately proportional to $\eta/T$ (Jones and Powles 1964).

The observation that proton relaxation rates often vary as $\eta/T$ has been explained by the fact that protons sample every possible environment in a liquid or solution in a time short compared to $T_2$ and are therefore well represented by a bulk property like viscosity. Since ionic nuclei in electrolyte solutions experience an environment atypical of the bulk solution, doubt has been expressed (Jones and Powles 1964, Arnold and Packer 1968) that bulk viscosity can provide a measure of their correlation times. Nevertheless a substantial body of data shows the converse to be true. Itoh and Yamagata (1959) found that $^{127}I$ linewidths in aqueous iodide solutions vary with temperature approximately as $\eta/T$. Richards and Yorke (1963) and Deverell, Frost and Richards (1965) have tested equation (1.8) by varying solvent composition and solute concentration in solutions of bromides and iodides at constant temperature. In solutions less concentrated than 4 molal the data could be correlated to $\eta/T$ by allowing for concentration dependent ion-ion interactions, although these same data were inconsistent with the model underlying equation (1.8) Eisenstadt and Friedman (1967) have found a most unusual deviation from equation (1.8), however, for $^{23}Na$ relaxation rates. Results from NaCl solutions at one-quarter and one-half molar showed that $(T_1)^{-1}$ is accurately proportional to $\eta^0/T$ ($\eta^0$ is the viscosity of pure water) with an appreciable positive intercept in the limit $\eta^0 \to 0$. The viscosity of NaCl at these concentrations (less than 0.5

molar) differs little from that of pure water so that replacing $\eta$ by $\eta^0$ would not materially after the correlation. Two other salts, $NaPF_6$ and $NaClO_4$, also at half molar, showed $^{23}Na$ relaxation rates proportional to $\eta/T$, but these data extrapolated approximately to zero. Very recent studies (Hall, Haller and Richards 1969) of $^{81}Br$ and $^{35}Cl$ relaxation as a function of temperature in mixed solvents of methanol-water suggest an intercept as $\eta/T \rightarrow 0$ in equation (1.8). In these solutions $(T_2)^{-1}$ remains quantitatively linear with $\eta/T$ when viscosity varies by more than an order of magnitude. Identical effects upon relaxation rate were obtained when viscosity was changed with both temperature and concentration.

The present investigation (Hall, Richards, Schulz and Sharp 1969) was prompted by an interest to explore further the unexpected dependence noted by Eisenstadt and Friedman and by Hall, Haller and Richards (1969) of ionic relaxation rates on temperature. Measurements of $(T_2)^{-1}$ are presented for $^{23}Na$ and $^{81}Br$ in aqueous solutions of several salts as a function of temperature and concentration. Changing both these variables simultaneously for a given salt provides an exacting test for the dependence of linewidth on $\eta/T$ and permits the separation of ion-ion from ion-solvent interactions by extrapolation of data to zero concentration.

An empirical relation that correlates adequately all previously published data from related systems is:

$$(T_2)^{-1} = [A_{c_{H_2O}} + B(c)]\eta/T + D \qquad (1.9)$$

This equation is similar in form to the theoretical result (1.8) discussed above and will be used here as a test correlation for the relaxation data. A and B terms may tentatively be assigned as measures of ion-solvent and ion-ion interactions respectively by analogy with equation (1.8). More precise interpretation of these quantities based on the formulae of Hertz and Valiev of diffusing charges and solvent dipoles is open to some questions as mentioned previously. The D term does not suggest, a priori, any simple interpretation and required for its elucidation measurements over

a much wider range of conditions than have so far been reported. However establishing a correlation such as (1.9), valid for several nuclei and partner ions over a broad range of temperature and concentration, should be useful for pointing out mechanisms of relaxation. The correlation may also serve as an empirical basis for interpreting data from ions in solutions of more complex chemical composition.

## 2. Experimental Aspects

$^{81}$Br linewidths were measured using a Varian V-4200 spectrometer. Signals were recorded as first derivatives of the absorption mode and are quoted as linewidths at maximum slope $\Delta\nu_s$. Control runs were taken to ensure that the r.f. power level applied did not produce saturation broadening. A correction was made for field inhomogeneity, which was about 8Hz, by observing the width of the $^{23}$Na resonance in samples for which the true width was known from spin-echo measurements. Modulation broadening was corrected from a calibration curve of selected $^{81}$Br resonances measured by the side-band method at 2kHz modulation frequency. Temperature was controlled within $\pm 0.1^{\circ}$C for both spin-echo and wideline methods and was checked by a thermocouple immersed in a dummy sample.

Solutions were prepared with AnalaR grade chemicals that had been dried overnight at 120°C. Samples were sealed in pyrex tubes immediately after preparation. A trace of sodium thiosulphate was added to a control tube as a test for oxidation of $Br^-$ but no effect on the linewidth was detected. Viscosities were determined using Ostwald viscometers in a constant temperature bath regulated to $\pm$ 0.1°C. Measured values agree with those taken from the literature within about 2 per cent.

Longitudinal relaxation times, $T_1$ for $^{23}$Na were determined by the spin-echo method at 20 MHz using a $\pi$-$\tau$-$\pi/2$-$\tau'$-$\pi$ pulse sequence. Signals were averaged over about fifty trials at varying values of $\tau$ by a boxcar integrator

| Concentration /mol $kg^{-1}$ | Temperature /K | $(T_1)^{-1}/S^{-1}$ | $\eta$/cp | $10^3\ \eta/T$ /cp $K^{-1}$ |
|---|---|---|---|---|
| 1.00 | 358 | 9.2 | 0.38 | 1.06 |
| | 328 | 11.4 | 0.55 | 1.68 |
| | 317 | 12.4 | 0.66 | 2.08 |
| | 297 | 18.5 | 0.97 | 3.27 |
| | 288 | 20.7 | 1.19 | 4.13 |
| 1.40 | 358 | 8.6 | 0.39 | 1.09 |
| | 328 | 11.7 | 0.57 | 1.74 |
| | 317 | 12.7 | 0.68 | 2.14 |
| | 297 | 18.7 | 0.98 | 3.30 |
| | 288 | 22.0 | 1.21 | 4.21 |
| 2.00 | 358 | 10.0 | 0.41 | 1.14 |
| | 328 | 11.8 | 0.60 | 1.83 |
| | 317 | 14.2 | 0.71 | 2.24 |
| | 297 | 19.9 | 1.01 | 3.40 |
| | 288 | 24.0 | 1.26 | 4.37 |
| 3.00 | 358 | 11.0 | 0.47 | 1.31 |
| | 328 | 13.3 | 0.67 | 2.03 |
| | 317 | 15.5 | 0.78 | 2.46 |
| | 297 | 21.5 | 1.10 | 3.70 |
| | 288 | 27.7 | 1.38 | 4.80 |
| 4.00 | 358 | 11.5 | 0.52 | 1.45 |
| | 328 | 15.1 | 0.73 | 2.24 |
| | 317 | 17.3 | 0.88 | 2.78 |
| | 297 | 23.5 | 1.24 | 4.17 |
| | 288 | 30.8 | 1,54 | 5.35 |
| 6.00 | 358 | 13.6 | 0.65 | 1.82 |
| | 328 | 19.8 | 0.92 | 2.80 |
| | 317 | 21.9 | 1.11 | 3.50 |
| | 297 | 31.6 | 1.59 | 5.34 |
| | 288 | 41.3 | 1.99 | 6.91 |

TABLE 1.1

$^{23}$Na n.m.r. relaxation times and viscosities of aqueous NaBr (Data obtained by Dr. R.R. Sharp).

| Concentration /mol kg$^{-1}$ | Temperature /K | $\Delta\nu_{\frac{1}{2}}$/Hz | $\eta$/cp | $10^3\eta/T$ /cp K$^{-1}$ |
|---|---|---|---|---|
| 1.00 | 353 | 127 | 0.38 | 1.08 |
| | 333 | 143 | 0.51 | 1.53 |
| | 313 | 190 | 0.70 | 2.24 |
| | 298 | 229 | 0.95 | 3.19 |
| | 283 | 308 | 1.36 | 4.80 |
| 1.40 | 353 | 123 | 0.39 | 1.10 |
| | 333 | 152 | 0.53 | 1.59 |
| | 313 | 192 | 0.73 | 2.33 |
| | 298 | 227 | 0.97 | 3.25 |
| | 283 | 318 | 1.41 | 4.97 |
| 2.00 | 353 | 132 | 0.42 | 1.19 |
| | 333 | 156 | 0.56 | 1.68 |
| | 313 | 188 | 0.77 | 2.46 |
| | 298 | 235 | 1.01 | 3.39 |
| | 283 | 338 | 1.45 | 5.12 |
| 3.00 | 353 | 135 | 0.46 | 1.30 |
| | 333 | 169 | 0.62 | 1.86 |
| | 313 | 212 | 0.84 | 2.68 |
| | 298 | 270 | 1.10 | 3.69 |
| | 283 | 372 | 1.56 | 5.51 |
| 4.00 | 353 | 143 | 0.52 | 1.48 |
| | 333 | 186 | 0.69 | 2.07 |
| | 313 | 237 | 0.93 | 2.97 |
| | 298 | 308 | 1.24 | 4.16 |
| | 283 | 478 | 1.75 | 6.18 |

TABLE 1.2

$^{81}$Br linewidths and viscosities of aqueous NaBr

| Concentration /mol $kg^{-1}$ | Temperature /K | $\Delta\nu_{\frac{1}{2}}$/Hz | $\eta$/cp | $10^3\eta/T$ /cp $K^{-1}$ |
|---|---|---|---|---|
| 0.50 | 353 | 125 | 0.36 | 1.02 |
| | 333 | 148 | 0.47 | 1.40 |
| | 313 | 165 | 0.64 | 2.04 |
| | 298 | 278 | 0.85 | 2.86 |
| | 283 | 338 | 1.22 | 4.30 |
| 1.0 | 353 | 132 | 0.36 | 1.03 |
| | 333 | 164 | 0.47 | 1.40 |
| | 318 | 224 | 0.63 | 2.02 |
| | 298 | 310 | 0.83 | 2.79 |
| | 283 | 364 | 1.16 | 4.11 |
| 1.5 | 353 | 140 | 0.37 | 1.04 |
| | 333 | 174 | 0.47 | 1.41 |
| | 313 | 237 | 0.63 | 2.00 |
| | 298 | 312 | 0.81 | 2.72 |
| | 283 | 413 | 1.12 | 3.95 |
| 3.0 | 353 | 164 | 0.39 | 1.11 |
| | 333 | 212 | 0.49 | 1.46 |
| | 313 | 306 | 0.63 | 2.00 |
| | 298 | 389 | 0.80 | 2.67 |
| | 283 | 480 | 1.05 | 3.70 |
| 4.0 | 353 | 201 | 0.41 | 1.17 |
| | 333 | 241 | 0.51 | 1.53 |
| | 313 | 338 | 0.65 | 2.06 |
| | 298 | 401 | 0.80 | 2.67 |
| | 283 | 534 | 1.03 | 3.65 |

TABLE 1.3

$^{81}$Br linewidths and viscosities of aqueous CsBr

(Many data here obtained by Dr. G.W. Schulz).

| Concentration /mol kg$^{-1}$ | Temperature /K | $\Delta\nu_{\frac{1}{2}}$/Hz | $\eta$/cp | $10^3\eta/T$ /cp K$^{-1}$ |
|---|---|---|---|---|
| 0.498 | 353 | 111 | 0.38 | 1.08 |
| | 333 | 143 | 0.50 | 1.50 |
| | 313 | 173 | 0.69 | 2.22 |
| | 298 | 233 | 0.94 | 3.16 |
| 0.950 | 353 | 122 | 0.41 | 1.15 |
| | 333 | 148 | 0.53 | 1.58 |
| | 313 | 181 | 0.73 | 2.32 |
| | 298 | 240 | 0.99 | 3.31 |
| 1.84 | 353 | 133 | 0.45 | 1.27 |
| | 333 | 168 | 0.58 | 1.75 |
| | 313 | 213 | 0.81 | 2.57 |
| | 298 | 272 | 1.09 | 3.65 |
| | 283 | 358 | 1.57 | 5.53 |
| 2.99 | 353 | 152 | 0.51 | 1.46 |
| | 333 | 184 | 0.67 | 2.00 |
| | 313 | 238 | 0.91 | 2.90 |
| | 298 | 304 | 1.21 | 4.07 |
| | 283 | 416 | 1.73 | 6.11 |
| 4.00 | 353 | 175 | 0.57 | 1.62 |
| | 333 | 211 | 0.74 | 2.22 |
| | 313 | 266 | 1.00 | 3.20 |
| | 298 | 349 | 1.34 | 4.51 |
| | 283 | 492 | 1.91 | 6.75 |
| 4.98 | 353 | 187 | 0.64 | 1.82 |
| | 333 | 229 | 0.83 | 2.51 |
| | 313 | 317 | 1.13 | 3.61 |
| | 298 | 393 | 1.50 | 5.04 |

TABLE 1.4

$^{81}$Br linewidths and viscosities of aqueous LiBr

Figure 1.1

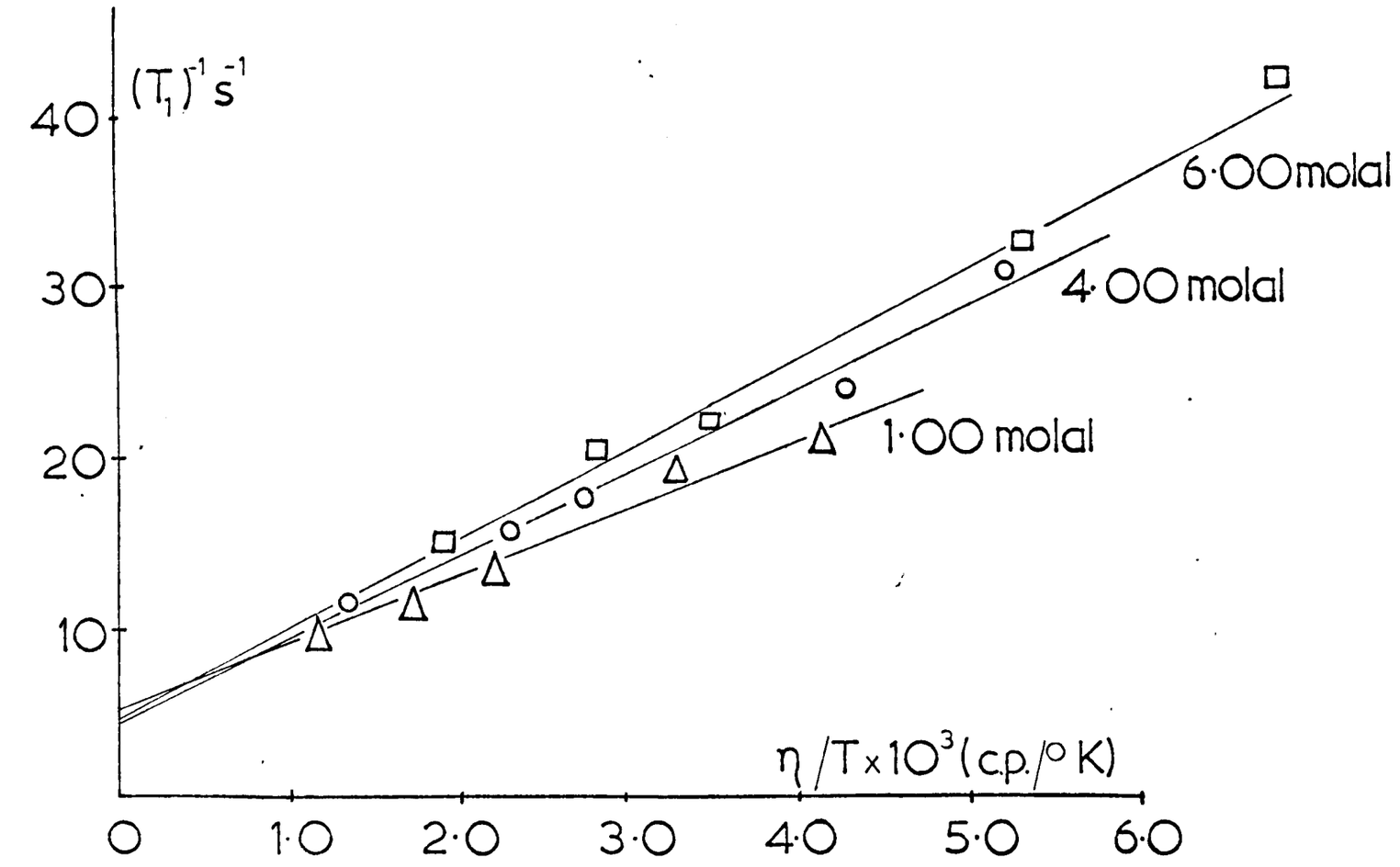
$T_1^{-1}(^{23}Na)$ *versus* solution $\eta/T$

for aqueous NaBr solutions

Figure 1.2

n.m.r. linewidths of $^{81}Br$ *versus* $\eta/T$

for aqueous NaBr solutions


$(T_1)^{-1}\,s^{-1}$
40
30
20
10
6·00 molal
4·00 molal
1·00 molal
$\eta/T \times 10^3$ (c.p./°K)
0
1·0
2·0
3·0
4·0
5·0
6·0

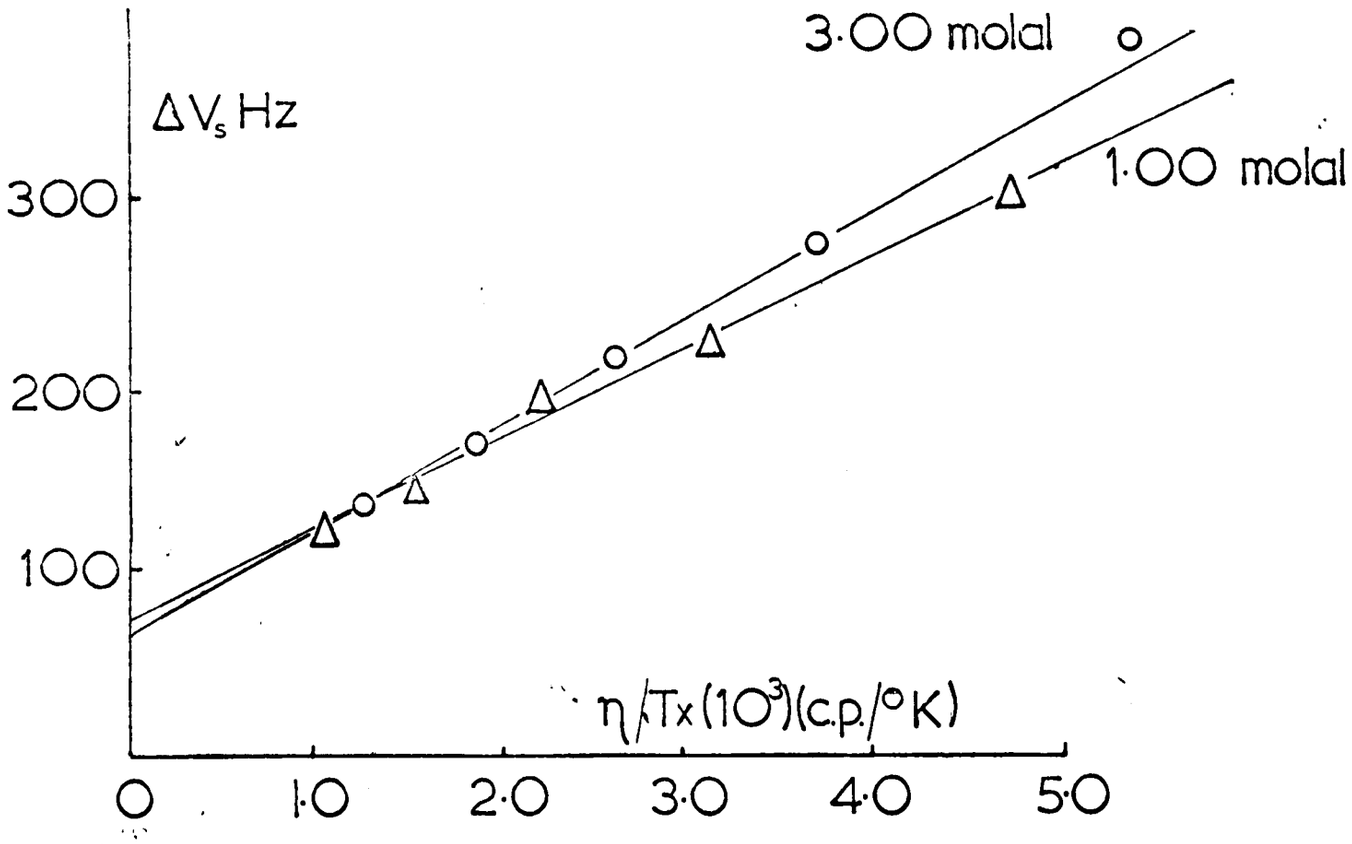
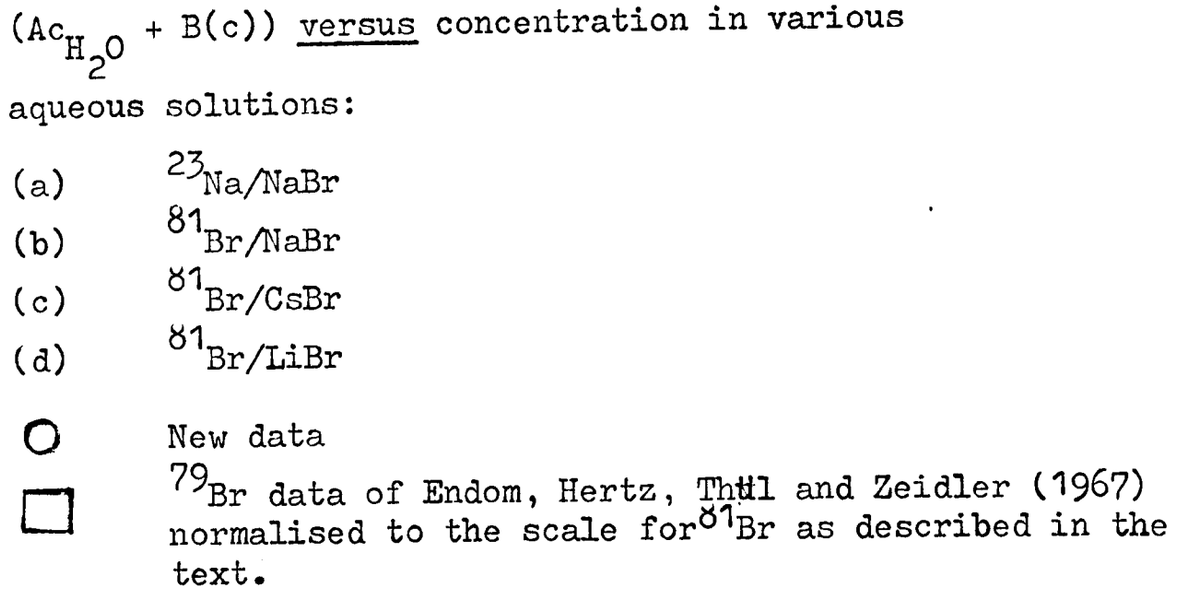
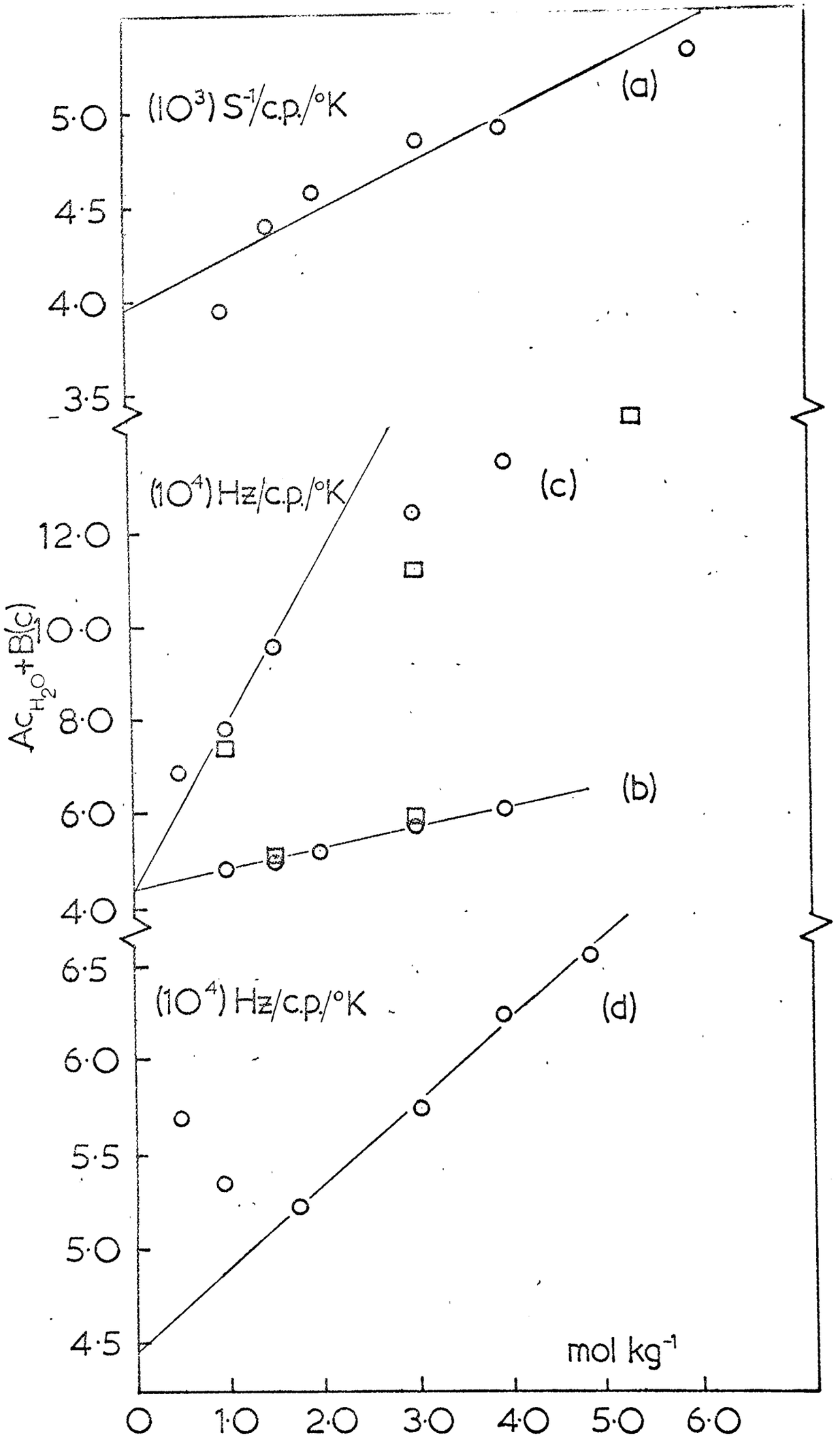

$\Delta V_s$ Hz
300
200
100
3·00 molal
1·00 molal
$\eta/T \times (10^3)$ (c.p./°K)
0
1·0
2·0
3·0
4·0
5·0

Figure 1.3


($Ac_{H_2O}$ + B(c)) versus concentration in various aqueous solutions:
(a) $^{23}$Na/NaBr
(b) $^{81}$Br/NaBr
(c) $^{81}$Br/CsBr
(d) $^{81}$Br/LiBr
New data
$^{79}$Br data of Endom, Hertz, Thül and Zeidler (1967) normalised to the scale for $^{81}$Br as described in the text.


(10³) S⁻¹/c.p./°K
(a)
5·0
4·5
4·0
3·5
(10⁴) Hz/c.p./°K
(c)
12·0
10·0
8·0
6·0
4·0
$AC_{H_2O}+B(c)$
(b)
6·5
(10⁴) Hz/c.p./°K
(d)
6·0
5·5
5·0
4·5
mol kg⁻¹
0
1·0
2·0
3·0
4·0
5·0
6·0

| Salt see note 1 | c/mol $kg^{-1}$ | D see note 2 | B(c → 0) see note 2 |
|---|---|---|---|
| NaBr $^{81}Br$ | 1.00 | 72 | 0.40 x ($10^4$) |
| | 1.40 | 70 | |
| | 2.00 | 66 | |
| | 3.00 | 62 | |
| | 4.00 | 56 | |
| LiBr $^{81}Br$ | 0.498 | 52 | 0.42 x ($10^4$) |
| | 0.950 | 60 | |
| | 1.84 | 74 | |
| | 2.99 | 71 | |
| | 4.00 | 72 | |
| | 4.98 | 69 | |
| CsBr $^{81}Br$ | 0.50 | 51 | 3.1 x ($10^4$) |
| | 1.00 | 61 | |
| | 1.50 | 44 | |
| | 3.00 | 39 | |
| | 4.00 | 44 | |
| NaBr* $^{79}Br$ | 1.40 | 140 | |
| | 3.00 | 146 | |
| | 7.00 | 138 | 0.58 x ($10^4$) |
| CsBr* $^{79}Br$ | 1.00 | 145 | 4.3 x ($10^4$) |
| | 3.00 | 145 | |
| | 5.40 | 145 | |
| NaI* $^{127}I$ | 1.01 | 270 | |
| | 4.00 | 330 | |
| | 7.00 | 395 | |
| KI* $^{127}I$ | 3.00 | 190 | |
| | 5.00 | 190 | |
| CsI* $^{127}I$ | 2.00 | 260 | |
| NaBr $^{23}Na$ | 1.00 | 4.8($s^{-1}$) | 0.25 x ($10^3$) |
| | 1.40 | 3.8($s^{-1}$) | |
| | 2.00 | 4.2($s^{-1}$) | $/s^{-1}K^{-1}$ x |
| | 3.00 | 3.9($s^{-1}$) | $cp^{-1}mol^{-1}kg$ |
| | 4.00 | 4.0($s^{-1}$) | |
| | 6.00 | 3.9($s^{-1}$) | |

TABLE 1.5 Notes

1. * Linewidths data of Endom, Hertz, Thül and Zeidler (1967).
2. Parameters B and D of equation (1.9). Units Hz $K^{-1}$ $cp^{-1}$ $mol^{-1}$ kg and Hz unless marked otherwise.

and recorded on a chart recorder. Reproducibility of results using this method ranged between 4 and 10 per cent depending on concentration. (These $^{23}Na$ relaxation data were obtained by Dr. R.R. Sharp.)

## 3. Experimental results

### i. New measurements

For reasons outlined in the Introduction and assessed more fully in Section 4 the available data on the relaxation rates of aqueous $^{23}Na$, $^{79}Br$, $^{81}Br$ and $^{127}I$ ion resonances are analysed in terms of equation (1.9). Tables 1.1, 1.2, 1.3 and 1.4 contain the n.m.r. linewidth and viscosity data. Figures 1.1 and 1.2 show plots of equation (1.9) for several concentrations of $^{23}NaBr$ and $Na^{81}Br$. The observed intercepts on the y axis define D, and the slopes define $(Ac_{H_2O} + B(c))$. In figure 1.3 (a)-(d) the slopes of the $\eta/T$ correlations are plotted as a function of concentration. Intercepts of these curves define A (the limiting slope at infinite dilution of equation (1.2)) and the form of the c dependence of B is shown. For the $^{81}Br$ resonance, B shows no concentration dependence when $Li^+$ and $Na^+$ are counterion but is dependent upon concentration when $Cs^+$ is the counterion. Approximate values of $B(c \rightarrow 0)$ were chosen by extrapolating plots of $(Ac_{H_2O} + B(c))$ for different salts to a common infinite dilution value. A rather puzzling minimum appears near c = 1 molal in Figure 1.3 (d). No similar feature is seen in corresponding plots of other salts, which may indicate that data from the lowest concentration of $Li^{81}Br$ contains systematic error. Table 1.5 gives $B(c \rightarrow 0)$ and D for various ion resonances in alkali halide solutions.

### ii. Comparison with other measurements

The measurements described in Section 3.i are correlated well by equation (1.9) and this correlation may now be tested with data from other laboratories.

Linewidths of $^{79}Br$ and $^{81}Br$ should experimentally be in the same ratio as the squares of the quadrupole moments, namely 1.45. The results for $Na^{79}Br$ and $Cs^{79}Br$ of Endom, Hertz, Thül and Zeidler (1967) may therefore be compared with the present data. It is again found that equation (1.9) is obeyed, and the values of B and D obtained, adjusted for the change of isotope, are shown in Table 1.5 and Figure 1.3 (b, c). The observed ratio of linewidths generally exceeds 1.45 by about 10 to 30 per cent, which is larger than experimental uncertainty. A few measurements of $^{79}Br$ and $^{81}Br$ in the same system have been made and it is verified that the ratio of linewidths is $1.46 \pm 0.01$. Hertz (1961) has also verified this ratio although his linewidths are systematically slightly broader than those reported here.

Linewidths for $^{127}I$ as a function of temperature in solutions of KI, NaI, and CsI have been reported by the same authors. The data correlate quite well with equation (1.9), and the appropriate parameters are listed in Table 1.5.

The temperature variation of $^{23}Na$ relaxation times in aqueous NaCl has been reported by Eisenstadt and Freidman (1967). The $^{23}Na$ data for 1 molal NaBr given here agree with their data for 0.555 M NaCl to better than 10 per cent, which is satisfactory.

## 4. Discussion

### i. Significance of the viscosity correlation of n.m.r. linewidths

The data presented in the previous section of this Chapter have shown that n.m.r. linewidths of several ions in aqueous alkali halide solutions depend functionally upon concentration and temperature in a manner given by equation (1.9). The accurate linearity that is often evident between linewidth and $\eta/T$ is in fact surprising since molecular correlation times near an ion are not expected to bear any obvious relation to bulk viscosity. It is desirable therefore to compare the proposed correlation (1.9) with

others, such as the Arrhenius plot, that possess more immediate physical significance.

A linear Arrhenius plot provides a very simple interpretation of temperature dependence in terms of molecular dynamics in the system. The slope of the plot is proportional to the height of a potential barrier encountered at some point in the course of a dynamical process that causes fluctuating field gradients at the ionic nucleus. By a simple extension, a curved Arrhenius plot can formally be considered as arising from a spectrum of activation energies pertaining to a variety of dynamical paths that can be followed during the molecular motion. Many of the n.m.r. linewidths do in fact show marked curvature in their Arrhenius plots (see Endom, Hertz, Thül and Zeidler 1967). These same data are linear in /T within experimental error, however, as can be shown by statistical methods. Thus it may be said that equation (1.9), in which A, B and D are chosen empirically, but are independent of concentration and temperature, can be used to predict to a first approximation the degree of curvature in Arrhenius plots of the same data. In this respect viscosity over temperature appears to provide the more satisfactory correlation.

A quantitative test of the linearity obtained from both types of correlation can be made by fitting linewidth data from various systems to an equation of the form:

$$y = a_o + a_1 x + a_2 x^2 \qquad (1.10)$$

For the Arrhenius correlation, $y = \ln\Delta\nu$ and $x = 1/T$ while for the correlation 1.9 $y = \Delta\nu$ and $x = \eta/T$. In order to obtain coefficients $a_o$, $a_1$, $a_2$ whose relative values may be compared, the variable ($\Delta\nu$, $\ln\Delta\nu$, $\eta/T$ and $1/T$) are expressed on scales that range from zero at the minimum measured values to one at maximum measured values. Thus a suitably scaled linewidth is $(\Delta\nu)_r = (\Delta\nu - \Delta\nu_{min})/(\Delta\nu_{max} - \Delta\nu_{min})$. Using these units, $a_o \sim 0$ and $a_1 + a_2 \sim 1.00$ for both correlations, and the ration $a_2/a_1$ is a measure of deviation from linearity. Systematic curvature is probably present inthe linewidth data for a given salt when the mean of

| $a_{2,m}$ | $\sigma$ | $\lvert a_{2,m}\rvert/\sigma$ | P | Salt | Correlation |
|---|---|---|---|---|---|
| 0.119 | 0.056 | 2.15 | 0.036 | $^{23}$NaBr | $(\Delta\nu)_r$ versus $(\eta/T)_r$ |
| -0.046 | 0.062 | 0.744 | 0.45 | Li$^{81}$Br | $(\Delta\nu)_r$ versus $(\eta/T)_r$ |
| 0.0076 | 0.057 | 0.133 | > 0.50 | Na$^{81}$Br | $(\Delta\nu)_r$ versus $(\eta/T)_r$ |
| -0.307 | 0.101 | 3.04 | 0.002 | Cs$^{81}$Br | $(\Delta\nu)_r$ versus $(\eta/T)_r$ |
| 0.502 | 0.064 | 8.01 | $\sim 10^{-13}$ | $^{23}$NaBr | $(\ln\Delta\nu)$ versus $(1/T)_r$ |
| 0.239 | 0.053 | 4.49 | $5\times10^{-4}$ | Li$^{81}$Br | $(\ln\Delta\nu)$ versus $(1/T)_r$ |
| 0.354 | 0.054 | 6.55 | $\sim 10^{-9}$ | Na$^{81}$Br | $(\ln\Delta\nu)$ versus $(1/T)_r$ |
| 0.092 | 0.131 | 0.69 | 0.50 | Cs$^{81}$Br | $(\ln\Delta\nu)$ versus $(1/T)_r$ |

TABLE 1.6(a) Test of linearity of n.m.r. linewidth data in correlation with equation (1.9) and Arrhenius plots.

| Correlation | Concentration | $a_o$ | $a_1$ | $a_2$ |
|---|---|---|---|---|
| $\tau_r$ versus $\eta/T$ | 0.50 M | -0.011 | 1.088 | -0.080 |
| $\tau_r$ versus $\eta/T$ | 1.00 M | -0.002 | 0.994 | 0.010 |
| $\ln\tau_r$ versus $1/T$ | 0.50 M | 0.057 | 0.156 | 0.666 |
| $\ln\tau_r$ versus $1/T$ | 1.00 M | 0.002 | 0.692 | 0.306 |

TABLE 1.6(b) Coefficients from equation (1.10) for dielectric relaxation times in aqueous NaBr (Hasted and El Sabeh 1953)

this ratio averaged over all concentrations differs from zero by more than about twice the standard deviation in the mean. Table 1.6 (a) contains a tabulation of mean second order coefficients $a_{2,m}$ from equation (1.10) appropriate to the various salts investigated. Standard deviations in the mean, $\sigma$, are likewise tabulated along with the probabilities P that the measured deviations from linearity are not statistically significant. Data from $^{23}$NaBr, Na$^{81}$Br, Li$^{81}$Br are undoubtedly linear in $\eta/t$ within experimental error but very clearly do not give linear Arrhenius plots. The opposite situation appears to hold for Cs$^{81}$Br. Standard deviations are also larger for these data, however, and since coefficients for this salt were averaged over only five concentrations, we are not entirely confident that the curvature is real.

Another remarkable feature of the $\eta/T$ correlation is that n.m.r. linewidths extrapolate to an almost constant value with vanishing $\eta/T$, regardless of solute concentration or species of counterion. Thus the intercept D is uniquely defined in a given solvent by the nuclear species being observed. Two exceptions to the rule of a constant intercept for a given resonance have been noted by Eisenstadt and Freidman (1967) for $^{23}NaPF_6$ and $^{23}NaClO_4$ at half molar concentration. In all cases involving alkali halide solutions, however, D is nearly constant for a given nucleus independent of concentration.

Thus we find that viscosity provides the most generally successful correlation of alkali halide linewidths at high concentration. The accuracy of the correlation is somewhat disconcerting since no accurate theoretical relation exists between bulk viscosity and molecular dynamics in the neighbourhood of an ion. We shall not discuss this question further here but rather consider various mechanisms of relaxation that are consistent with equation (1.9).

ii. Relaxation at infinite dilution

Extrapolation of a correlation time from the infinite dilution ionic linewidths is a difficult problem, especially since the quadrupole coupling constant, as well as $\tau_c$, may be temperature dependent. Beginning, however, with the assumption that all temperature dependence of the n.m.r. linewidths is contained in $\tau_c$, we have examined measures of the solute and solvent translational correlation times and the solvent reorientational correlation time in solution to see whether any of these quantities alone could explain the observed temperature dependence of the n.m.r. linewidths.

Ionic and solvent translational correlation times are proportional to the respective inverse self-diffusion coefficient, $(D^s)_{ion}^{-1}$ and $(D^s)_{H_2O}^{-1}$. Self-diffusion of aqueous alkali metal and halide ions is associated with an activation energy about equal to that for viscous flow. Activation energies for $(D^s)_{Na^+}^{-1}$ and $(D^s)_{Br^-}^{-1}$ which can be obtained at infinite dilution from the limiting ionic conductivities (Robinson and Stokes 1965) are respectively 4.2 - 4.5 and 3.8 - 4.2 kcal/mole between 15 and 55°C. These values are significantly higher than the activation energies, 2.6 - 3.2 and 2.3 - 2.8 kcal/mole, for $^{23}Na$ and $^{81}Br$ nuclear magnetic relaxation at low concentration in the same temperature range.

Arnold and Packer (1968) have recently discussed the validity of correlating solute relaxation rates in ionic solutions with $(D^s)_{ion}^{-1}$, a procedure that they consider preferable to the viscosity correlation in view of the unambiguous theoretical relation between self-diffusion coefficients and translational correlation times. They justify this procedure on the fact that although viscosity of KI solutions decreases with increasing concentration below about 4 molal, the $^{127}I$ linewidth increases monotonically over the same concentration region. From equation (1.9) we interpret this behaviour as indicative of interionic interactions (a non-zero B coefficient in equation (1.9)). Furthermore they have shown that $(D^s)_{ion}^{-1}$ varies linearly and monotomically with the $^{127}I$ linewidth. The infinite dilution activation energy for $(D^s)^{-1}$ is 3.8 - 4.2 kcal/mole between 15 and 55°C, a

value substantially larger than the activation energy (2.4 - 2.9 kcal/mole) (Endom, Hertz, Thül and Zeidler 1967) for the $^{127}I$, linewidths in aqueous KI. Therefore the temperature dependence for aqueous $^{127}I$ as well as for $^{23}Na$ and $^{81}Br$, does not appear to support the hypothesis of a physical connection between $(D^s)_{ion}^{-1}$ and $\tau_c$.

It is difficult to obtain a detailed picture of translational and reorientational correlation times of the solvent in hydration spheres. Crude estimates of these quantities may be obtained from the concentration dependence of $(D^s)_{H_2O}^{-1}$ and of the dielectric relaxation time, $\tau_r$, respectively. A change in the activation energy of $(D^s)_{H_2O}^{-1}$ on $\tau_r$ with concentration should give a qualitative idea of the activation energy for solvent translation or reorientation near an ion. In pure water both $(D^s)_{H_2O}^{-1}$ and $\tau_r$ are directly proportional to $\eta^o/T$ (Wang 1965; Simpson and Carr 1958; Hasted, Ritson and Collie 1948) and therefore possess the same activation energy ($E_A$ = 4.5 kcal/mole at 298K). Krynicki (1966) has demonstrated from his accurate proton relaxation data on water that the product $(T_1\tau_r^{-1})$ is constant to $\pm$ 3% from 273.3 to 368.4K. Rather surprisingly, activation energies for $(D^s)_{H_2O}^{-1}$ and $\tau_r$ show the opposite behaviour in aqueous NaBr; $E_A$ for $(D^s)_{H_2O}^{-1}$ increases very slightly with concentration, relative to $E_A$ for $\eta/T$ while $E_A$ for $\tau_r$ decreases substantially (Figures 1.4 and 1.5). This behaviour can be rationalized on the basis of the solvation model of Frank and Wen (1957). These authors suggest that near small ions, solvent molecules are directionally bound by electrostrictive forces. Since the electrostrictively bound solvent does not possess the required geometric configuration for hydrogen bonding to the normal water structure, and since the solvated ion efficiently transmits thermal shocks which destabilize hydrogen bonded solvent structure, it is postulated that a region of relatively mobile non-structured solvent exists just beyond the strongly electrostricted layer. This model suffices to explain 'structure forming' and 'structure breaking' effects in a variety of kinetic, thermodynamic and spectroscopic properties of solutions.

From his survey of criteria for structure breaking and forming, Kay (1968)

Figure 1.4

Inverse self-diffusion coefficients of water in aqueous NaBr *versus* solution $\eta/T$

Data at 273.2 K from Endom, Hertz, Thül and Zeidler (1967)

Data at 298.2 K from McCall and Douglass (1965)

| | |
|---|---|
| x | pure water |
| o | 1 mol $kg^{-1}$ |
| □ | 2 mol $kg^{-1}$ |

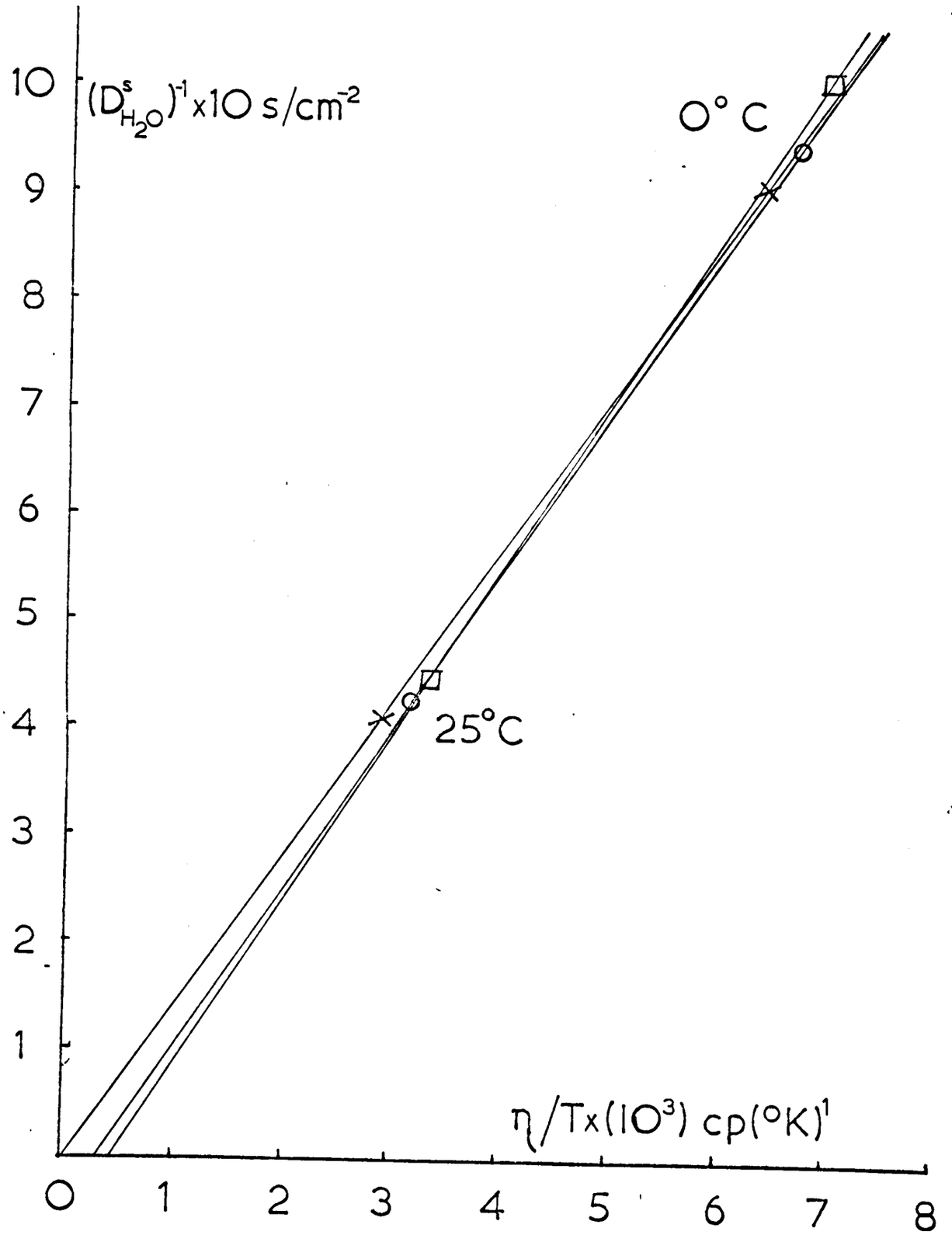

10
9
8
7
6
5
4
3
2
1
$(D^s_{H_2O})^{-1} \times 10$ s/cm$^{-2}$
0° C
25°C
$\eta/T \times (10^3)$ cp(°K)$^1$
0
1
2
3
4
5
6
7
8

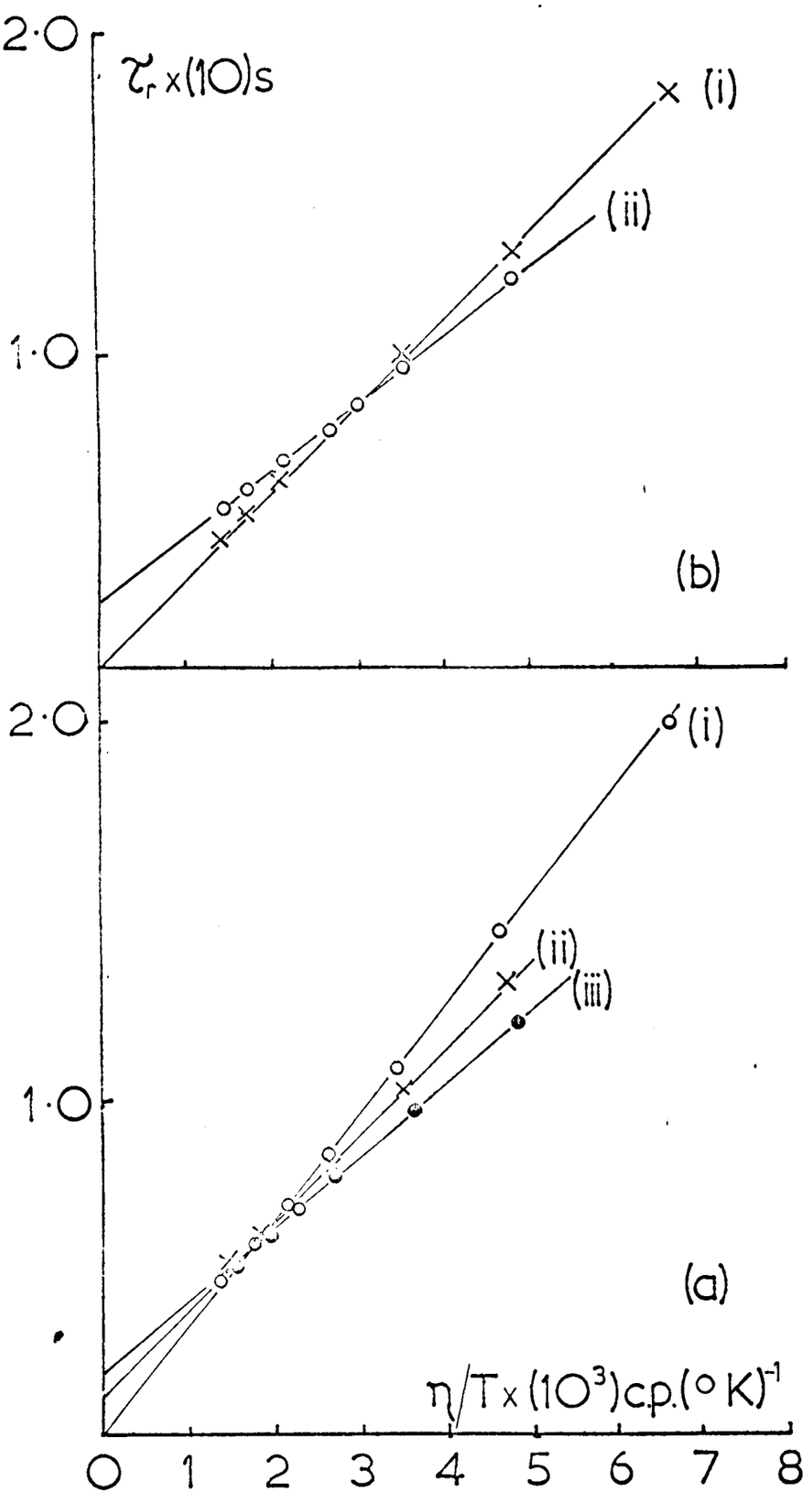
Figure 1.5

(a) Dielectric relaxation times $\tau_r$ of water *versus* $1/T$ for

i. pure water
ii. 0.5 mol NaBr $kg^{-1}$
iii. 1.0 mol NaBr $kg^{-1}$

(b) Dielectric relaxation times $\tau_r$ of water *versus* $1/T$ for

i. pure water
ii. 0.5 mol NaCl $kg^{-1}$


2·0
$\tau_r \times (10)s$
(i)
(ii)
1·0
(b)
2·0
(i)
(ii)
(iii)
1·0
(a)
$\eta/T \times (10^3)$ c.p. $(^\circ K)^{-1}$
0 1 2 3 4 5 6 7 8

concludes that among the alkali metal and halide ions, $K^+$, $Rb^+$, $Cs^+$, $Cl^-$, $Br^-$, and $I^-$ are strong structure breakers while $Li^+$ and $F^-$ are electrostrictive structure makers. $Na^+$ is not clearly in either category, presumably because decreased solvent mobility in the electrostricted region approximately equals increased solvent mobility in the structure broken region.

This picture of solvation predicts that both self-diffusion and solvent reorientation should be facilitated in structure broken regions and hindered in electrostrictively bound region. Therefore large qualitative differences in the activation energies for these motions in solvation spheres would not be expected. The observed dissimilarity in behaviour between $\tau_r$ and $(D^s)_{H_2O}^{-1}$ may indicate that strongly electrostricted solvent does not contribute to high frequency dielectric dispersion whereas the electrostricted layers will surely affect solvent self-diffusion. However the molar lowering of $\tau_r$ for $Na^+$ and $Br^-$ (Hasted and El Sabeh 1953) unambiguously indicates that in the outer hydration region of these ions molecular reorientation occurs with an activation energy of approximately the correct magnitude to account for the n.m.r. relaxation. Quite possibly $(D^s)_{H_2O}^{-1}$ possesses a similarly small activation energy in this region. The hypothesis that an electrostrictively bound solvent layer on $Na^+$ contributes little to quadrupolar relaxation is not unreasonable since such a layer probably contains elements of octahedral or tetrahedral symmetry associated with small equilibrium electric field gradients. A suggestive quantitative similarity between dielectric relaxation in 0.50 and 1.00 M NaBr and the $^{23}Na$ and $^{81}Br$ linewidths is evident from an analysis of data in Figure 1.5 (a). Dielectric relaxation times in aqueous NaBr remain accurately linear in $\eta/T$ at least up to 1.00 M (see Table 1.6 (b)) in spite of the fact that the mean activation energies of $\tau_r$ and $\eta/T$ differ considerably. This behaviour indicates that solvent reorientation (and possibly also translation) in the outer solvation region could explain the good linearity of the n.m.r. linewidths with $\eta/T$.

The following simple calculation indicates that activation energies of

the n.m.r. data for $^{23}Na$ and $^{81}Br$ are of proper magnitude to explain the temperature dependence of $\tau_r$ in accord with Frank and Wen's model. We begin with a hypothesis that both the dielectric relaxation time in the total hydration sphere (as defined above) and the ionic n.m.r. relaxation rate are proportional to the average solvent reorientation time in the structure broken region. Water molecules strongly electrostricted to the ionic surface of $Na^+$ are assumed to contribute negligibly to dielectric dispersion in the centimetre wavelength region as well as to the n.m.r. relaxation.

Writing the bulk dielectric relaxation time, $\tau_r$, as a sum of relaxation times in the solvation sphere, $\tau_r^+$ and $\tau_r^-$, and in non-solvating water $\tau_r^o$, we have

$$\tau_r = (1 - x^+ + x^-)\tau_r^o + x^+\tau_r^+ + x^-\tau_r^-.$$

$x^+$ and $x^-$ refer to mole fractions of solvent in cation and anion hydration spheres respectively. $\tau_r^+$ and $\tau_r^-$ are by assumption taken as proportional to the infinite dilution n.m.r. relaxation rates of cation and anion, that is, $\tau_r^{\pm} = Q^{\pm}(T_2^r)^{\pm}$. Using linewidth data of $^{23}Na$ and $^{81}Br$, extrapolated to infinite dilution, for $\tau_r^{\pm}$ and dielectric relaxation data from 1 M aqueous NaBr (Figure 1.5 (b)) for $\tau_r$, $Q^+$ and $Q^-$ can be chosen to reproduce the temperature dependence of $\tau_r$. Allowing $x^+/x^- = r$ to assume any value in the range $0.5 < r < 1.5$, the total fraction of solvent in hydration spheres is calculated to be $x^+ + x^- = 0.80 \pm 0.02$. The mean reorientation time of the structure broken region at 25°C is calculated to be $(\tau_r^+ + \tau_r^-)/2 = 7.3(10^{-12})$s. This value is necessarily shorter than the dielectric relaxation time in pure water ($8.2 \times 10^{12}$s at 25°C) since $\tau_r$ decreases in NaBr solution. The fraction of solvent in structure broken regions of both ions is large with 15 to 25 water molecules comprising each hydration sphere. Including a possible electrostrictively bound layer around $Na^+$, the picture obtained is one in which virtually all solvent in 1 molal salt solution is affected in its hydrogen bond forming capability by the presence of ions. Such a picture is consistent with the solvation model of Frank and Wen.

The above discussion is concerned with the molecular motions in which the hydration sphere can explain the relatively small temperature dependence of aqueous $^{23}Na$ and $^{81}Br$ nuclear magnetic relaxation. These arguments have proceeded of necessity from an assumption that the nuclear quadrupole coupling constant does not possess a large negative temperature coefficient. Such a temperature dependence could occur for example if the hydration number decreases rapidly with increasing temperature as has been suggested by Eisenstadt and Friedman (1967). Vibrational degrees of freedom within the electrostricted layer could also contribute to magnetic relaxation in $Na^+$. These motions have been analysed quantitatively by Valiev and Zripov (1966), who found this contribution to be small for $Al(H_2O)_6$. Further work on aquo complexes is desirable to test more thoroughly Valiev's results.

iii. Interpretation of concentration dependence of relaxation

N.m.r. linewidths of a given ion in various salts should extrapolate to a common limiting value at zero concentration, at which point interactions with counterions vanish. Similarly, by plotting equation (1.9) for a series of concentrations and extrapolating to c = 0, the limiting slopes $A_i$ should approach a single value independent of the counterion. This value is characteristic of the ion-solvent interaction. It is evident from Figure 1.3, however, that a single value of A in equation (1.9) is not obtained if the B term is linear in solute concentration. Thus we conclude that B contains higher powers in concentration which become important at least above 1 molal. This result is similar to that of Jones and Powles (1964) who have found that the proton relaxation rate in aqueous solutions is also non-linear in concentration, even at concentrations well below 1 molal.

It was mentioned in the Introduction to this Chapter that the mechanism responsible for an interionic term in the relaxation is in some doubt. The uncertainty concerns the details of the interaction rather than the correlation time. Both the model of Hertz (and the closely similar one of Valiev) and the overlap mechanism suggested by Deverell predict a correlation time $\tau_{ii}$ for the ion-ion interaction that is the same as that for translational self-diffusion, namely:

$$\tau_{ii} = \text{const.} \quad \frac{1}{D_{cat}^{s} + D_{anion}^{s}}$$

where $D_{cat}^{s}$ and $D_{anion}^{s}$ are self-diffusion coefficients for cation and anion.

In order to obtain quantitative B coefficients, it is necessary to extrapolate the slopes of equation (1.9) somewhat arbitrarily to a common limiting value, at zero concentration. For the $^{81}Br$ resonance we have chosen a limiting slope $A = 44.5\ (10^{3})/Hz\ K^{-1}\ cp^{-1}$. This value was used above to calculate the n.m.r. correlation time. Magnitudes of the B coefficients from our temperature data are obviously in qualitative agreement with the trend of cation effects observed by Deverell, Frost and Richards (1965), who found that cations produce an interionic contribution to the relaxation of $^{81}Br$ and $^{127}I$ in the order:

$$Li^{+} \leq Na^{+} < K^{+} < Rb^{+} < Cs^{+}$$

Furthermore, information concerning the temperature dependence of $\tau_{ii}$ may be inferred from the fact that our plots of linewidth against $\eta/T$ extrapolate to the same approximate intercept for a given nucleus regardless of solution composition. Thus the intercept is independent of concentration and consequently the contribution of an ion-ion interaction to the n.m.r. linewidth apparently vanishes with $\eta/T$. Whether the ion-ion interaction is accurately proportional to $\eta/T$ is open to some question, however, in view of the possible curvature of the $Cs^{81}Br$ data, in which this interaction is relatively very large.

An approximate activation energy can be assigned the ion-ion interaction, which has a magnitude proportional to the difference between infinite dilution and finite concentration linewidths. This activation energy has the value $3.5 \pm 0.3$ kcal/mole and is therefore in accord with typical measured values for ionic self-diffusion. Thus our temperature data do not conflict with either mechanism of the ion-ion interaction discussed above.

# CHAPTER II

## Studies of the $^{133}Cs$ ion resonance shift in solution

# 1. Introduction

## i. Review

This Chapter describes a series of experiments designed to test a theory of the chemical shifts of ion resonances in electrolyte solutions (Halliday, Richards and Sharp 1969). The evaluation of this theory has been hitherto, and is in the present work, largely based on consideration of $^{133}Cs$ data on solutions of Cs salts in a variety of solvents. It is equally expected to apply to other simple monatomic closed-shell ions.

Carrington, Dravnicks and Symons (1960) first demonstrated that the $^{133}Cs$ resonance frequency in solutions of CsCl to which other electrolytes are added is a linear function of the mole fraction of additive in the range 1 to 6 mol/kg $H_2O$. The constant of proportionality between the shift and the concentration in a particular solvent and at constant temperature depends on the identity of the added ions, particularly the counterion.

A more extensive n.m.r. investigation, comprising measurements on aqueous solutions of many simple salts which yield monatomic ions, was carried out by Deverell (1966). The ion resonances studied included $Na^+$, $K^+$, $Rb^+$, $Cs^+$, $Cl^-$, $Br^-$, $I^-$, $Sr^{2+}$, $Mg^{2+}$, and $La^{3+}$. He found that the linearity of the isothermal ion resonance shifts with salt concentration was a general feature of the results at higher concentrations ($\geq$ 2 mol/kg $H_2O$) At the lower end of the accessible concentration range there was a consistent display of curvature in such correlations ($\leq$ 2 mol/kg $H_2O$). It was found that in this region the plot of the shift against activitywas linear, although nonlinear at salt concentrations above 2 mol/kg $H_2O$. The extrapolated resonance frequency of each ion at infinite dilution (zero concentration) was found to be independent of counterion.

When the free ion is dissolved in an infinite quantity of solvent there is an ion-solvent interaction which causes a shift in the resonance frequency of the free ion nucleus. As the salt concentration is increased

there is a further shift in the resonance frequency which is attributed to a combination of ion-ion interactions and modifications of the ion-solvent interaction brought about by the presence of the salt. Thus

$$\sigma = \sigma_{is}(c) + \sigma_{ii}(c) \tag{2.1}$$

where $\sigma$ is the observed shielding constant, $\sigma_{is}$ is the ion-solvent contribution to the shielding constant, and $\sigma_{ii}$ is the ion-ion contribution to the shielding constant. We require that in the limit of $c \rightarrow 0$, $\sigma_{ii}$ vanishes and $\sigma_{is} \rightarrow \sigma_{is}^{o}$, the infinite dilution shielding constant. Deverell's results then suggested

$$\sigma - \sigma_{is}^{o} = c\,(\sigma_{ii}' + \sigma_{is}') \tag{2.2}$$

or in terms of chemical shifts ($\delta$) measured relative to the infinite dilution resonance frequency to a first approximation is

$$\delta = c(\delta_{ii} + \delta_{is}) \tag{2.3}$$

where c represents an activity below about 2 mol $kg^{-1}$ ($H_2O$) and a concentration above this point; and where $(\delta_{ii} + \delta_{is})$ is a "molal shift" or an "activity shift" characteristic of the temperature, solvent and counterion. In fact we may expect that $\delta_{is}(c)$ will be a rather weak function of concentration compared with $\delta_{ii}(c)$ and thus

$$\delta_{ii} + \delta_{is} \approx \delta_{ii} \tag{2.4}$$

for a first approximation. This has proved a useful assumption in subsequent work, as it has focussed attention on $\delta_{ii}(c)$, a quantity which we might expect to be able to calculate. The basis of these equations and the assumptions they contain will be discussed more fully below.

Deverell also demonstrated from his results on aqueous solutions of alkali and alkaline earth halides that there is a uniformity in the effect of counterions on the nuclear resonance frequencies of different ions. Thus the efficacy of the halide ions in producing low field shifts

of cation resonances is

$$F^- < Cl^- < Br^- < I^-$$

a series which applies to all the cations investigated. Similarly, the powers of the various cations in producing low field shifts in halide ion resonances may be ordered.

$$Na^+ < Li^+ < K^+ < Rb^+ < Cs^+$$

Furthermore, apart from the inversion of $Li^+$ and $Na^+$ in the latter series, the trends are those which would be expected if the shift were caused by repulsive overlap of ions during collisions in solution. Similar rankings of counterions in producing resonance shifts had earlier been found by Bloembergen and Sorokin (1958) in crystals, and attributed to such a mechanism. Deverell produced semiquantative evidence supporting a similar interpretation for solutions.

The inaccessibility of low concentrations has been a serious shortcoming of most spectroscopic methods of studying ions in solution. Thus the n.m.r. studies described above were limited to solutions stronger in salt than 0.2 mol/kg solvent. This fact, together with the absence of a theory of concentrated solutions of the rank of the extended Debye-Hückel theory of more dilute systems, has severely limited the contributions of spectroscopy to knowledge of electrolyte solutions. However the work of Halliday (1969) shows that in favourable cases n.m.r. methods can now reach into the "dilute" solution region. $^{133}Cs$ is such a favourable case since the resonance of the dissolved $Cs^+$ ion is extremely narrow ($T_2 \approx 13$ s, 2 mol CsCl/kg $H_2O$) and shows very large solvent and concentration shifts. Using a high field (5 T) superconductive solenoid of great stability and signal accumulation techniques shifts were measured to very high accuracy down to concentrations as low as 5 mol $dm^{-3}$. Under these circumstances it was possible to carry through a detailed investigation of the agreement between experiment and the quantitative predictions of an extended Debye-Hückel model (Halliday, Richards and Sharp 1969), which will be

discussed in some detail in Section 3.

It is appropriate to conclude this brief general experimental survey of previous work at this point, and make some comments on the theoretical formulation of the problem.

1. The simple ion-resonances of the alkali metals, the alkaline earths and the halogens, together with others such as that of lanthanum, consist in each case of a single Lorentzian line in most common solvents. The position of the resonance in the frequency spectrum is determined by the time average of the instantaneous resonance frequencies of the ion as it passes through a continuous sequence of situations in solution. We may attempt to predict the chemical shift by considering it to be caused by binary interactions between the ion and the other particles in the solution, averaged over their possible configurations.

2. Formally, the observed shielding constant $\sigma$ may be expressed as an average over the canonical ensemble:

$$\sigma = \langle\bar{\sigma}\rangle = \left\{ \int_V \cdots \int d\underline{R}d\underline{R}'d\underline{r}d\underline{\Omega}\bar{\sigma}(\underline{R},\underline{R}';\underline{r},\underline{\Omega})\exp[-\beta U(\underline{R},\underline{R}';\underline{r},\Omega)] \right\}/Z \qquad (2.5)$$

where $\underline{R},\underline{R}'$ are the N,N' position vectors of the N,N' ions and counterions in the system; $\underline{r},\underline{\Omega}$ are the n position and orientation vectors of the n solvent molecules and $\beta = 1/kT$; and

$$Z = \int \cdots \int \exp[-\beta U] d\underline{R}d\underline{R}'d\underline{r}d\underline{\Omega} \qquad (2.6)$$

where U is the potential energy of configuration $(\underline{R},\underline{R}',\underline{r},\underline{\Omega})$. It is assumed that the observed shielding constant $\sigma$ is the mean of the N individual ion shielding constants, which are the sums of pairwise interactions of the ions with the other particles. Thus the interactions with like ions, counterions and solvent molecules may be separated:

$$\bar{\sigma}(\underline{R},\underline{R}',\underline{r},\underline{\Omega}) = \frac{1}{N}\sum_{i}^{N}\left(\sum_{j\neq i}^{N}\sigma_i(\underline{R}_{ij}) + \sum_{j}^{N'}\sigma_i(\underline{R}'_{ij}) + \sum_{j}^{n}\sigma_i(\underline{r}_{ij},\underline{\Omega}_j)\right) \tag{2.7}$$

Substituting equation (2.7) into equation (2.5) gives rise to three contributions to $\sigma$ from like-ion, counterion and solvent interactions; for example, the like ion contribution to the shielding constant is found to be

$$\bar{\sigma}_{ii} = \left\{\frac{1}{N}\sum_{i}^{N}\int\cdots\int_{V}d\underline{R}d\underline{R}'d\underline{r}d\underline{\Omega}\sum_{j\neq i}^{N}\sigma_i(\underline{R}_{ij})\exp(-\beta U)\right\}/Z \tag{2.8}$$

However since all ions i are indistinguishable, all N terms of the summation are equal upon integration. Thus the problem can be simplified by considering the interaction of one ion (labelled 1) with all others

$$\bar{\sigma}_{ii} = \left\{\int\cdots\int d\underline{R}d\underline{R}'d\underline{r}d\underline{\Omega}\sum_{j\neq 1}^{N}\sigma_1(\underline{R}_{ij})\exp(-\beta U)\right\}/Z \tag{2.9}$$

Thus $\bar{\sigma}_{ii}$ is the sum of N-1 terms, all of which are equal, since no ion j is preferred. Hence considering one such term

$$\bar{\sigma}_{ii} = \left\{(N-1)\int\cdots\int d\underline{R}_1 d\underline{R}_2\cdots d\underline{R}_N d\underline{R}'d\underline{r}d\underline{\Omega}\sigma_{12}(\underline{R}_{12})\exp(-\beta U)\right\}/Z \tag{2.10}$$

$$= (N-1)\iint\sigma_{12}(\underline{R}_{12})\left\{\int\cdots\int\frac{d\underline{R}_3\cdots d\underline{R}_N d\underline{R}'d\underline{r}d\underline{\Omega}\exp(-\beta U)}{Z}\right\}dR_1 dR_2 \tag{2.11}$$

$$\text{But}\quad \left(\int\cdots\int d\underline{R}_3\cdots d\underline{R}_N d\underline{R}'d\underline{r}d\underline{\Omega}\exp(-\beta U)\right)/Z = \frac{\rho^{(2)}}{N(N-1)} \tag{2.12}$$

where $\rho^{(2)}$ is a conventionally defined pair-distribution function. Therefore

$$\bar{\sigma}_{ii} = \frac{1}{N}\iint\sigma_{12}(\underline{R}_{12})\rho^{(2)}d\underline{R}_1 d\underline{R}_2 \tag{2.13}$$

$$= \frac{V}{N}\int\sigma_{12}(\underline{R}_{12})\rho^{(2)}d\underline{R}_{12} \tag{2.14}$$

$$= \frac{4\pi}{\rho}\int\sigma_{ii}(R)\rho^{(2)}R^2 dR \tag{2.15}$$

where $\rho = N/V = Lc$, L is Avogadro's number, c is the volume concentration of electrolyte; R is now a polar position coordinate, and $\sigma_{12}$ is now called $\sigma_{ii}$ for continuity of notation. Similar expressions are obtained for the ion-counterion and ion-solvent contributions to $\sigma$.

$$\bar{\sigma}'_{ii} = \frac{4\pi}{\rho'} \int \sigma'_{ii}(R')\rho^{(2)} dR' \qquad (2.16)$$

$$\bar{\sigma}_{is} = \frac{4\pi}{\rho_s} \iint \sigma_{is}(r,\underline{\Omega})\rho^{(2)} dr d\underline{\Omega} \qquad (2.17)$$

At this point it should be emphasised that the only simplification which has been made is that of assuming that the observed shielding constant is a sum of pairwise interactions. The problem of calculating the shielding constant thus resolves itself into finding manageableexpressions for $\sigma_{ii}$, $\sigma'_{ii}$, $\sigma_{is}$ and a radial pair distribution function $\rho^{(2)}$.

3. Thus relative to an arbitrary reference frequency the observed shift at any concentration of solute c is given generally by

$$\delta'_{obs}(c) = (\delta^{o}_{is})' + \delta_{is}(c) + \delta_{ii+}(c) + \delta_{ii-}(c) \qquad (2.18)$$

If the shifts are referred to the infinite dilution frequency, as has been customary, then

$$\delta_{obs}(c) = \delta_{is}(c) + \delta_{ii+}(c) + \delta_{ii-}(c) \qquad (2.19)$$

The ion-ion contribution (ii) has been separated into like-ion and counterion contributions; the remaining notation is obvious. In general $\delta_{is}(c)$ will include the effects of a number of different phenomena; the displacement of solvent molecules from the neighbourhood of the probe ion, and modifications in the orientation and motion of solvent molecules caused by other ions in the solution may be expected to be important. For solutions of mixed electrolytes the last two terms will be sums over the various species in the system.

It should be noted that the infinite dilution resonance frequency, whilst conceptually very simple as a referencing point, is not experimentally convenient as it can only be obtained by a long extrapolation of experimental data. This is particularly liable to error in the case of nonaqueous solvents in many of which relatively large changes of ion resonance frequency occur at very low concentrations.

4. The complexity of the model required is evident from the last paragraphs, but it is important to anticipate this at the outset. The acceptable assumptions and simplifications depend somewhat on the mechanism proposed for the interaction between the particles which causes the shift. Thus if the interaction is very short range an adequate model of the first solvation sphere may be a satisfactory basis for a theory. If the interactions between the ion and the remainder of the solution converge only slowly when integrated over successive shells of particles then a good radial distribution function will be required.

5. The ion-ion contributions to the chemical shift appear more amenable to calculation than those contributions represented by other terms in equation (2.18). The spherical symmetry and simple electronic structure of the closed shell monatomic ions are simplifying features, and the use of an extended Debye-Hückel model would seem to provide a good foundation upon which to build a predictive theory.

6. The ion-solvent interaction immediately appears to present greater difficulties, in that steric factors can be expected to be of great importance in determining the interaction of a solvent molecule with an ion.

A brief resume of the Debye-Hückel theory - in only sufficient detail to provide some basis for the later discussion - is given below and is followed by an account of the theory of ion-resonance shifts applied by Halliday, Richards and Sharp to the $^{133}Cs$ ion.

ii. The Debye-Hückel theory

A central feature of the Debye-Hückel theory of dilute electrolyte solutions is the calculation of the pair distribution function for a solution of ions (Résibois 1968).

Let $\alpha$ and $\beta$ be labels for the ion species; the volume concentrations of the two sorts of ions are $\rho_\alpha$, $\rho_\beta$, and their charges are $eZ_\alpha$ and $eZ_\beta$.

The pair distribution function for two ions in a vacuum is

$$\rho^{(2)} = \rho_\alpha \rho_\beta \gamma_{\beta\alpha}(R) \tag{2.20}$$

where $$\gamma_{\beta\alpha} = \exp\left( - \beta \frac{Z_\alpha Z_\beta e^2}{R} \right)$$

But this is inapplicable to a system containing other ions. Instead we write

$$\gamma_{\beta\alpha} = \exp\left(-\beta e Z_\beta \Phi_\alpha(R)\right) \tag{2.21}$$

where $\Phi_\alpha(R)$ is the total electric potential at $\underline{R}$, due to ion $\alpha$ at the origin and all the other ions taken in an average manner. First it is assumed that Poisson's equation applies:

$$\nabla^2 \Phi_\alpha(R) = \frac{4\pi}{\epsilon} q_\alpha(R) \tag{2.22}$$

where $q_\alpha$ is the charge density at $\underline{R}$. $q_\alpha$ of course is determined by the distribution that is sought. However it may be assumed that

$$q_\alpha(R) = eZ_\alpha \delta(R) + \sum_\gamma eZ_\gamma \rho_\gamma \gamma_{\gamma\alpha}(R) \tag{2.23}$$

where the first term takes account of the presence of ion $\alpha$ at the origin, and the second postulates that all ion distribute themselves about $\alpha$ in the same fashion as does $\beta$.

It follows that

$$\nabla^2\Phi_\alpha(R) = -\frac{4\pi e}{\epsilon} Z_\alpha \delta(R) - \frac{4\pi e}{\epsilon} \sum_\gamma Z_\gamma \rho_\gamma \exp\left[-\beta e Z_\gamma \Phi_\alpha(R)\right] \qquad (2.24)$$

which is the Poisson-Boltzmann equation, from which $\Phi_\alpha$ is calculable in principle. The difficulty of solving it is considerable, but in addition it contains physical inconsistencies (Fowler and Guggenheim 1939), which can be simply expressed as follows:

It can be shown that $\rho^{(2)} = \rho^{(2)'}$ where $\rho^{(2)'}$ is defined by equation (2.20) with $\alpha$ and $\beta$ interchanged.
This requires that

$$Z_\beta \Phi_\alpha = Z_\alpha \Phi_\beta$$

which in turn requires $\Phi_\alpha = Z_\alpha \Phi$ (2.24a)

where $\Phi$ is independent of $Z_\alpha$; however, such a solution is not consistent with the Poisson-Boltzmann equation (2.24). It has been customary to remove this inconsistency by taking the approximate form of (2.24) obtained by expansion of the last term

$$\nabla^2\Phi(R) = -\frac{4\pi}{\epsilon} \delta(R) - \frac{4\pi e}{\epsilon Z_\alpha} \sum_\gamma \rho_\gamma Z_\gamma + \left(\frac{4\pi e^2 \beta}{\epsilon} \sum_\gamma Z_\gamma^2 \rho_\gamma\right) \Phi(R) \qquad (2.25)$$

which from the electroneutrality condition $\sum_\gamma e Z_\gamma \rho_\gamma = 0$ and the definition

$$\kappa^2 = \frac{4\pi e^2 \beta}{\epsilon} \Sigma Z_\gamma \rho_\gamma \qquad (2.26)$$

may be written

$$\nabla^2\Phi(R) = -\frac{4\pi}{\epsilon} \delta(R) + \kappa^2 \Phi(R) \qquad (2.27)$$

which is the linearised Poisson-Boltzmann equation. Solutions of this are readily obtained (boundary condition $\Phi \to 0$ as $R \to \infty$)

$$\Phi(R) = \frac{e}{\epsilon R} \exp(-\kappa R) \qquad (2.28)$$

Thus from equations (2.20), (2.21) and (2.25) the distribution function. is found

$$\rho_{DH}^{(2)} = \rho_\alpha \rho_\beta \exp\left\{-\beta e Z_\beta \left[\frac{eZ_\alpha}{\epsilon R}\exp(-\varkappa R)\right]\right\} \qquad (2.29)$$

Again, the important approximations contained in the derivation of this result must be recognised:

A] The linearisation of the Poisson-Boltzmann equation is valid only insofar as the inequality

$$\beta e Z_\gamma \Phi_\alpha(R) \ll 1 \qquad (2.30)$$

is satisfied. It is possible, though difficult (Fowler and Guggenheim 1939) to solve the complete Poisson-Boltzmann equation (2.24), but this is no advance since it is only the linearised form of it that is physically consistent and acceptable (see above). Therefore there is no rigorous way of extending the Debye-Hückel argument to nondilute systems. The result of the Debye-Hückel theory given in equation (2.29) must therefore be regarded as valid only in the limit of infinite dilution. The range of concentrations in which it may be expected to be a good approximation can be estimated from (2.27); note that since $\Phi_\alpha$ is a function of R it must be satisfied for all important values of R.

B] Several different problems concern the treatment of the solvent as a dielectric continuum (of dielectric constant $\epsilon$).

It is probably an acceptable approximation in most cases to write the Coulomb energy of two ions, $R_{12}$ apart, in a solution as $(Z_\alpha Z_\beta e^2)/R_{12}\epsilon$ when the two ions are separated by many solvent molecules. On the other hand, there can be no question that this formula is quite invalid for two ions in contact. At intermediate separations, the strong electric forces acting on the dipolar solvent molecules cause various degrees of dielectric saturation, reducing $\epsilon$. These considerations restrict the validity of the dielectric approximation in the case of water to solutions whose ionic strengths are less than about 0.01 mol $kg^{-1}$.

Furthermore the presence of dissolved electrolyte is known to alter the bulk dielectric constant of a solvent. Thus in general $\epsilon$ is a function of concentration.

At small interionic separations the molecular nature of the solvent profoundly influences the distribution of ions for other reasons. Since the solvent is composed of particles, packing geometry becomes important, and it is necessary to take into account correlation between the positions of solvent molecules and the positions of ions. In short the Debye-Hückel model does not provide a good $\rho^{(2)}$ for short interionic distances. That is, the Debye-Hückel model does not furnish an adequate way of calculating the complicated integral expression on the left of equation (2.12) under such circumstances. Curve A of figure 2.1 shows the form of the Debye-Hückel distribution function $\rho_{DH}^{(2)}$ as a function of distance for oppositely charged ions. A better distribution function $\rho^{(2)*}$ would show oscillations of the type shown in the second curve B at small values of R.

The limiting form of the Debye-Hückel distribution function may be extended by incorporation of an additional parameter a, the sum of the hard-sphere radii of the ions or the distance of closest approach of the ion centres. The extended Debye-Hückel potential has the form

$$\Phi(R) = \frac{e\exp[-\kappa(R-a)]}{\epsilon R(1+\kappa a)} \qquad (2.31)$$

Although values of a are found usually to be a few tenths of nm, a is customarily treated as an adjustable parameter, varied to obtain concordance between theory and experiment. The extended Debye-Hückel theory is useful in predicting thermodynamic properties of electrolyte solutions up to ionic strengths of 0.1 mol $kg^{-1}$.

iii. The HRS modified Debye-Hückel radial distribution function

The contents of section i and ii can be used to obtain the expressions used by HRS in their analysis of $^{133}Cs$ ion resonance shifts.

Firstly it is postulated that the observed shift in the ion resonance as the concentration varies (at constant temperature) is solely the result of the ion-ion interactions (equation (2.4)). There is evidence in support of this approximation from several sources.

Then by combining equations (2.15), (2.20), (2.21) and (2.31) an expression for this shift as a function of c, $\epsilon$, T, $Z_\alpha$. $Z_\beta$, $\sigma_{ii}(R)$ is obtained for an assumed extended Debye-Hückel distribution function $\rho^{(2)}_{DH}$

$$\sigma \sim \bar{\sigma}_{ii} = 4\pi\rho \int_a^\infty \sigma_{ii}(R)\exp(-\beta e Z_\beta \Phi_\alpha)R^2 dR \qquad (2.32)$$

where

$$\Phi_\alpha = \frac{eZ_\alpha}{\epsilon R}\exp[-\varkappa(R-a)/(1+\varkappa a)] \qquad (2.32a)$$

Now it is necessary to recognise the shortcomings of the Debye-Hückel model at small interionic separations (R ~ a). In the HRS model this is done by the following considerations.

Because of the molecular nature of the solvent there is a strong tendency for two ions of opposite charge in very close proximity either to be separated by one solvent molecule diameter, or two, or else to be in contact (see schematic illustrations in Figure 2.2). The graininess of the notional continuum is imposed on the distribution function for small values of R. If one ion is separated from another by a single solvent molecule, and this molecule is then displaced, the ions may be expected to move together. Referring to Figure 2.1 HRS suggested that ions separated by a distance R such that $a < R \leq \beta$ would experience a resultant force tending to drive them together (R = a); similarly ions instantaneously situated between $\beta$ and $\alpha$ are driven apart to the comparatively stable

Figure 2.1

Variation of $\rho^{(2)}$ (continuum solvent) and of $\rho^{(2)*}$ (particle solvent) with distance from central ion.

(For explanation of other symbols see text.)

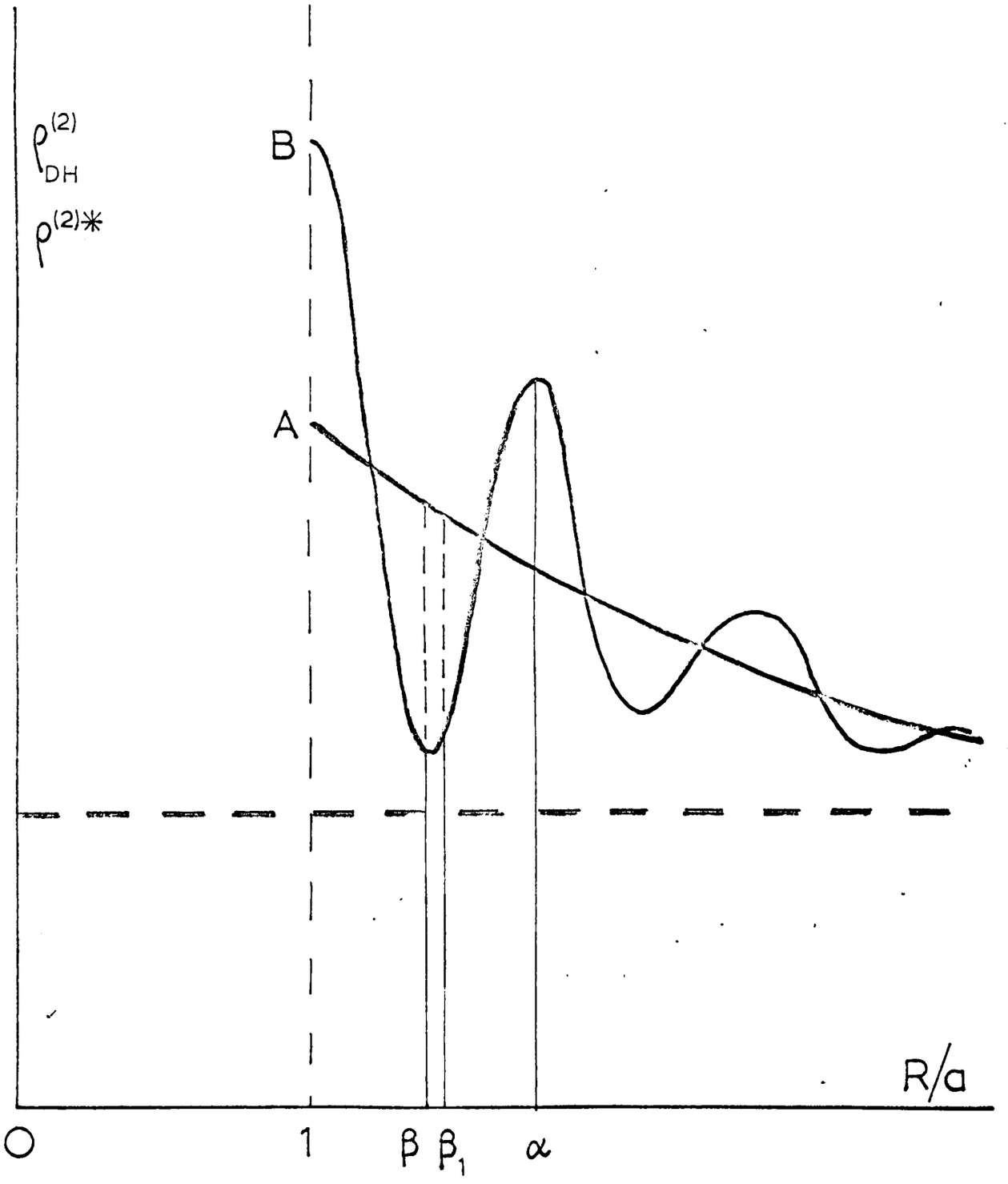

$\rho^{(2)}_{DH}$
$\rho^{(2)*}$
B
A
R/a
O
1
β
$\beta_1$
α

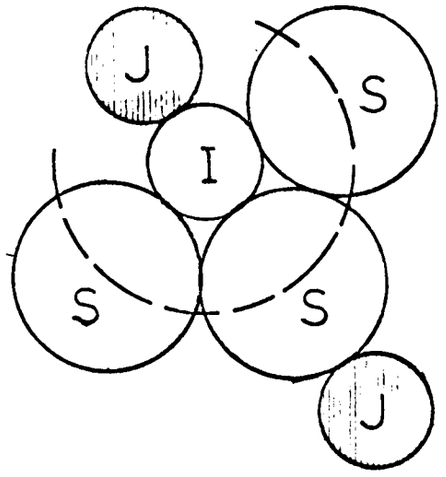
Figure 2.2

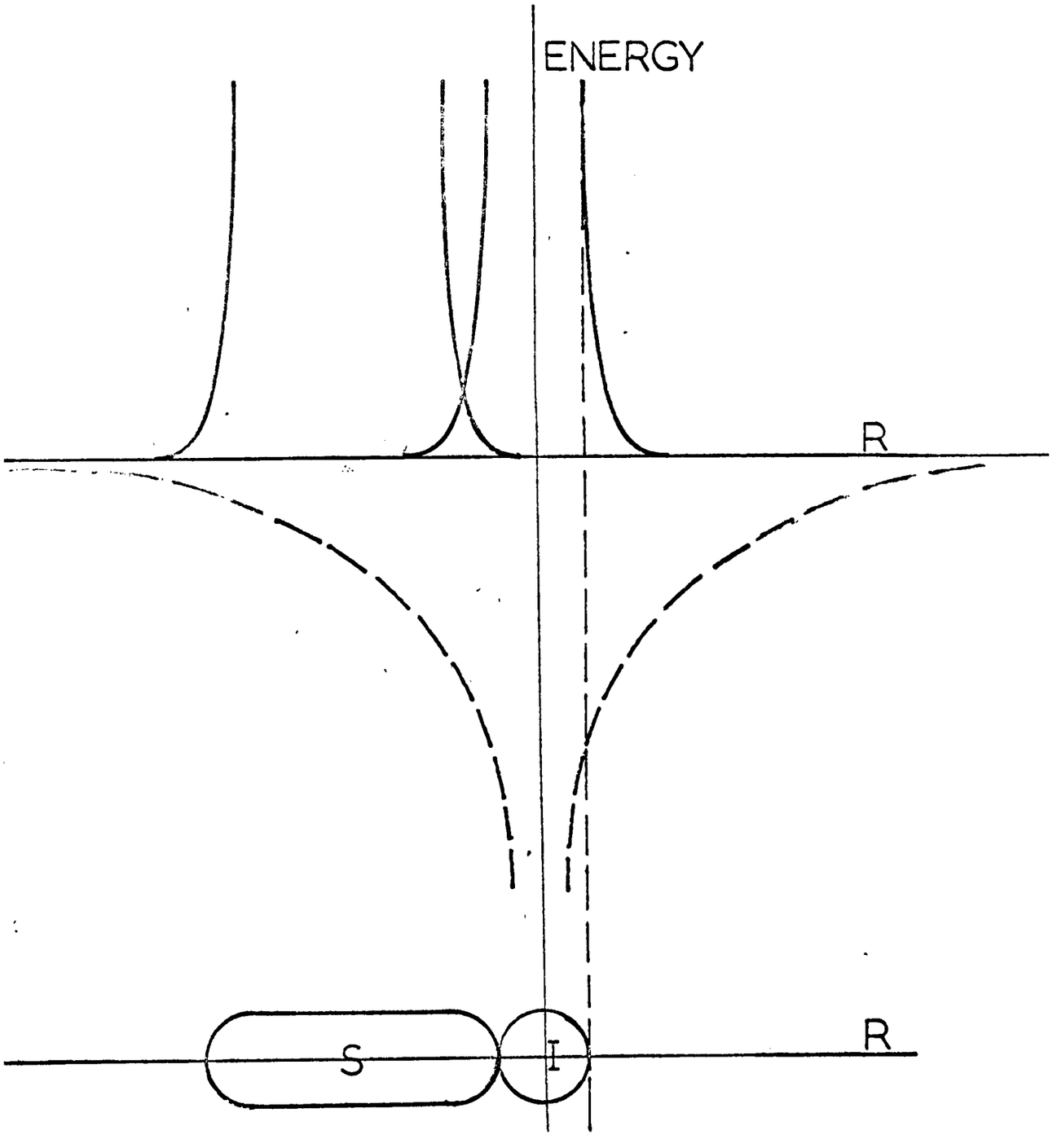
a Typical configuration of three ions I, J and J in a hard-disk solvent S

b Potential energy profile for the approach of an ion towards another ion I of opposite charge and a solvent molecule S.

Full lines: short-range repulsive energy.

Broken lines: interionic Coulomb energy.


J
S
I
S
S
J


ENERGY
R
R
S
I

configuration $R = \alpha$. Of course, Figure 2.1 is schematic and implies spherical symmetry; in fact, the lattice geometry around the ion can be expected to be very complicated. However it is well-known that radial distribution functions of the form of that in Figure 2.1 (B) are obtained experimentally by x-ray methods (for example Lawrence and Kruh 1967).

In the present case, the form of the oscillating $\rho^{(2)*}$ is not known; it would of course be generated by inclusion of an oscillating short-range repulsion energy in the $U(R,R',r,\Omega)$ of equation (2.12). However it is true that the areas under the curves $\rho_{DH}^{(2)}$ $\rho^{(2)*}$ are equal in the limit $(R/a) \rightarrow \infty$. The numbers, N, N*, of ions inside spheres of radius $R_o$ for the two distribution functions are

$$N = 4\pi\rho \int_a^{R_o} \rho_{DH}^{(2)} R^2 dR \qquad (2.33)$$

and

$$N^* = 4\pi\rho \int_a^{R_o} \rho^{(2)*} R^2 dR \qquad (2.34)$$

and $$N \simeq N^*, \; R_o/a \rightarrow \infty .$$

Figure 2.3 shows the behaviour of N and N* as $R_o$ is increased from a to large values. The value of $N^*(R_o)$ oscillates about $N(R_o)$; there are points $\beta_i$ where $N = N^*$, and one such point $\beta_i$ is associated with each extremum in $\rho^{(2)*}$. Although not precisely true, there is probably no great error in the approximation $\beta_1 = \beta$.

From the foregoing

$$\int_a^{\beta_1} \rho^{(2)*} R^2 dR = \int_a^{\beta_1} \rho_{DH}^{(2)} R^2 dR \qquad (2.35)$$

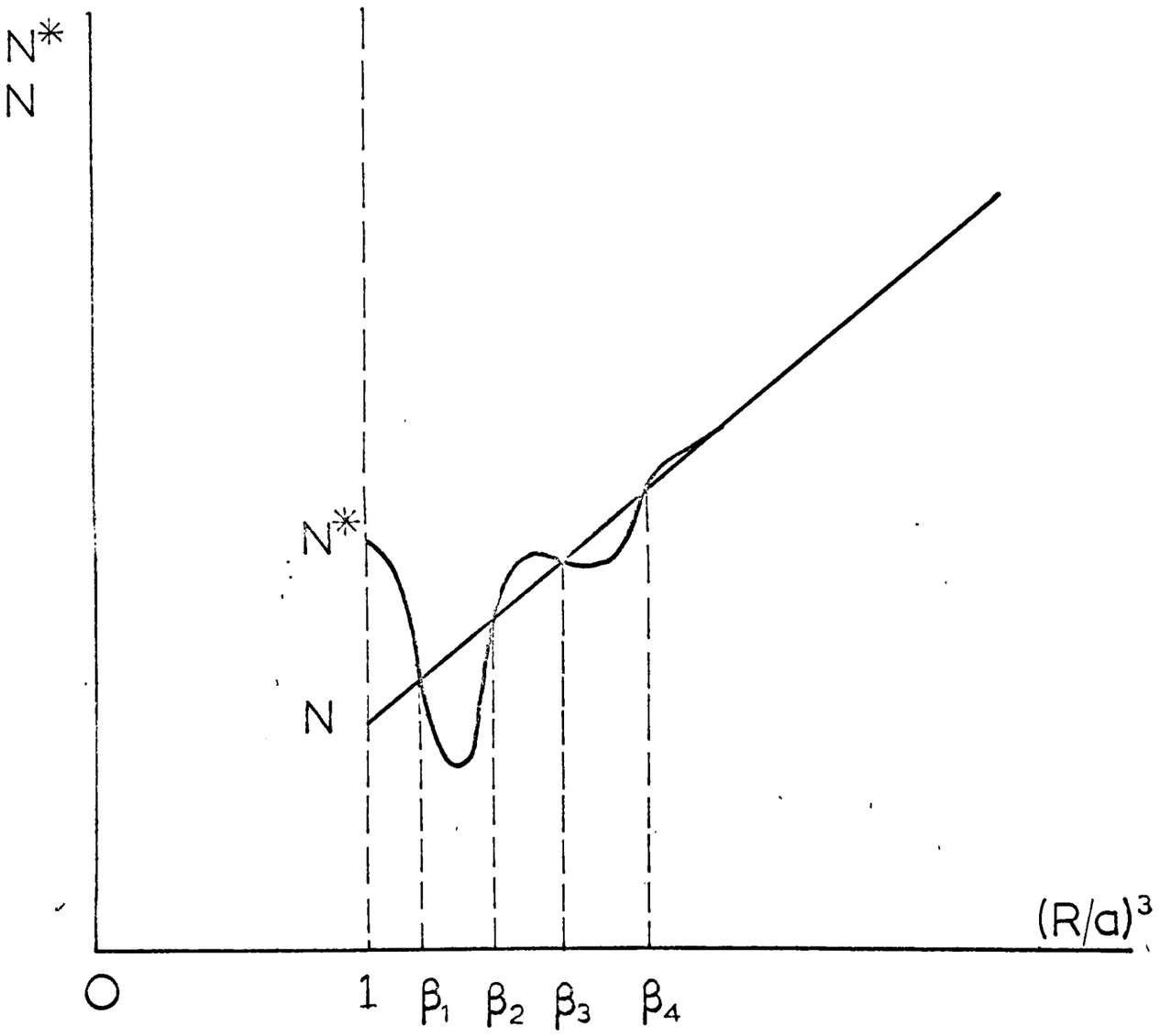
The HRS theory postulates that $\beta \approx \beta_1 \approx a + \frac{1}{2}$ (diameter of solvent molecule) and therefore

$$\int_a^{\beta} \rho^{(2)*} R^2 dR = \int_a^{\beta} \rho_{DH}^{(2)} R^2 dR \qquad (2.36$$

where it is noted that $\rho_{DH}^{(2)}$ is the extended Debye-Hückel pair distribution

Figure 2.3

Variation of N and N* with $(R/a)^3$, showing the number of ions within a sphere of radius R/a about the central ion for continuum and for particle solvents.


N*
N
N*
N
(R/a)³
O
1
β₁
β₂
β₃
β₄

function. Thus the assumption is made that the probability of one ion being in contact with another in the solution is obtained by integrating the Debye-Hückel pair distribution function between limits a and β. Therefore from equations (2.29) and (2.33)

$$\sigma = 4\pi\rho\sigma_{ii}(a)\int_a^{\beta} \exp(-\beta e Z_\beta \Phi_\alpha) R^2 dR + 4\pi\rho\int_\beta^{\infty}\sigma_{ii}(R)\exp(-\beta e Z_\beta \Phi_\alpha)\, R^2 dR \quad (2.37)$$

where $\Phi_\alpha$ is given by equations (2.24a) and (2.28).

iv. Interactions contributing to the interionic term in the chemical shift

HRS considered three types of interaction between ions as possible causes of the observed ion resonance shift:

A the short-range repulsive force between ions resulting from the overlap of their filled orbitals;
B the electrostatic polarisation of the ionic orbitals by other ions;
c the van der Waals' forces between the ions.

The structure of the Ramsay shielding formula (Abragam 1961) shows that the change in the resonance frequency of a free nucleus caused by the presence of electrons bound to it can be considered in two parts: thus

$$\sigma = \sigma_d + \sigma_p \quad (2.38)$$

respectively the diamagnetic and the paramagnetic parts. $\sigma_d$ describes the induced circulation of the electronic charge in the polarising magnetic field (classically as required by Lenz's Law) such that the field at the nucleus is slightly reduced. The other term $\sigma_p$ derives from the interaction of electronic orbital angular momentum (through its associated magnetic moment) with the external field. Because evaluation of the paramagnetic part requires knowledge of excited states $|n\rangle$, the average energy approximation is usually applied to express $\sigma_p$ in terms of the ground state ket $|0\rangle$, and a mean excitation energy $\Delta$:

$$\sigma_p = \frac{4}{3}\left(\frac{e\hbar}{2mc}\right)^2 \Delta^{-1} \sum_{kj} \langle 0 | \underline{l}_j \cdot \frac{\underline{l}_k}{r_k^3} | 0 \rangle \qquad (2.39)$$

For an unperturbed ion in an S state, $\sigma_p$ vanishes, but $\sigma_d$ is large and increases with the nuclear charge of the ion. Any perturbation of the ion, which causes orbital angular momentum to be mixed into the ground state, produces a contribution $\sigma_p$. Ikenberry and Das (1965) have demonstrated that changes in $\sigma_d$ are relatively negligible compared with $\sigma_p$ for closed shell ions.

The calculation of the repulsive overlap term carried out by HRS closely follows the method used by Ikenberry and Das in their studies of the ion shifts of the same ions in the solid state, and involves evaluation of the paramagnetic part of the Ramsay formula. It is not necessary to enter into details of the calculation here but the result is quoted for reference:

$$\text{Repulsive overlap: } \sigma_{ii}(R) = -\frac{4\alpha^2}{3\Delta}\langle r^{-3}\rangle_p \left[ |S^{\sigma s}|^2 + |S^{\sigma\sigma}|^2 + |S^{\pi\pi}|^2 - 2S^{\pi\pi}S^{\sigma\sigma} \right] \qquad (2.40)$$

where $\alpha$ is the fine structure constant

$\Delta$ the mean excitation energy

and S overlap integrals between the outermost s and p orbitals of the adjacent ions. The radial dependence of $\sigma_{ii}(R)$ comes directly from the radial dependence of the overlap integrals, which vary exponentially with R, and have been the subject of several calculations, notably by Hafemeister and Flygare (1965). The change in shielding constant with concentration may now be evaluated after substitution of equation (2.40) into equation (2.37). In the case of the repulsive overlap contribution only the first term of equation (2.37) is used.

The contributions to the shielding constant from the polarisation and van der Waals' interactions will not be discussed here, since results showed that for those ions for which experimental data were available

($Cs^+$, $Rb^+$, $K^+$, $I^-$, $Br^-$, and $Cl^-$) the repulsive overlap term was completely dominant. Thus Deverell's earlier conclusion (1966) was fully supported.

v. Concentration dependence of the chemical shift

The concentration dependence of $\sigma$ (or $\delta$) predicted by equation (2.37) is in agreement with the $^{133}Cs$ resonance data in the electrolyte concentration range 0.02 to 2.0 mol $dm^{-3}$ in the cases of aqueous solutions of CsCl, CsBr, CsI, CsOH and $CsNO_3$. It was found by HRS that the computed and experimental shifts obeyed an empirical equation

$$\log(\delta) = g\log(c) + D \qquad (2.41)$$

over that concentration range (g and D constant); and that the computed results obeyed this law also to slightly higher concentrations. This feature of the shifts will be discussed in Section 3(i).

In the case of non-aqueous solvents and of aqueous mixed solvents, the functional form of equation (2.41) was found (though not tested over such a great concentration range), but the observed values of g were systematically rather larger than those predicted. In terms of equation (2.37) the solvent is characterised chiefly by its dielectric solvent $\epsilon$ which determines g.

vi. Solvent shifts

The variation of the infinite dilution shielding constant from one solvent to another and as a function of solvent composition in mixed solvents is very marked and is a set of data of great interest. Very little progress has been made towards understanding it; some brief remarks will be made in Section 4 on this subject.

## 2. Experimental Account

$^{133}Cs$ resonance frequencies were determined from measurements on a 5.02T broad-line n.m.r. spectrometer incorporating an extremely stable superconductive solenoid magnet. The construction and operation of this spectrometer have been fully described by Halliday (1969) and by Halliday, Hill and Richards (1969). The field variations during early experiments (late 1968) were not greater than 1 part/$10^7$ per day. After an interruption in operation of the spectrometer as the result of the appearance of a helium leak in the solenoid dewar vessel, the performance appeared to deteriorate somewhat and field drifts of 2 to 4 parts/$10^7$ per day were measured.

The spectra were obtained by electronic sweep of the $H_1$ frequency, usually in crystal-locked 1 Hz steps, at various rates, typically 1 Hz $s^{-1}$. Spectra were accumulated in a Northern Scientific computer of average transients. $H_o$ modulation at approximately 2 kHz was employed, and its amplitude optimised to produce maximum centre-band signal strength. The $^{133}Cs$ resonance frequency at the fixed magnetic field of the superconductive solenoid was $\sim$ 28.010MHz.

The magnet inhomogeneity linewidth varied from 12 to 22 Hz (half-height full linewidth) over the course of the experiments. The estimated uncertainty in the measured resonance frequencies is about $\pm$ 1 Hz, but poorer in very dilute solutions.

Samples were contained in handblown spherical bulbs, the shape of which rendered susceptibility corrections unnecessary. Preliminary studies showed that random differences between sample bulbs did not produce detectable shifts in resonance frequency.

Temperature control was achieved by passing a gentle heated air flow through the cylindrical probe and over the sample bulb. A platinum resistance sensor incorporated into the probe body provided control signals for the heater relay. Sample temperature was determined by a calibrated thermocouple

attached to the probe close to the sample bulb. The temperature stability achieved was excellent and the absolute temperature calibration estimated to be $\pm$ 0.3 K.

Materials: double distilled water
CsCl, MeOH, HOAc AnalaR grade
NaBr AnalaR grade
$MgBr_2$, $CaBr_2$, CsBr BDH reagent grade

Methanol was purified by three distillations and acetic acid by drying fresh AnalaR material over $Mg(ClO4)_2$.

Samples were made up by weight for all experiments except those concerned with the effects of ionic strength, which were made up by volume from volumetrically prepared stock solutions. Halide ion concentrations of all samples used in ionic strength experiments and many samples used in other experiments were confirmed by silver titration. Methanol solvent was analysed for water content by refractometry: the water content was estimated as < 0.6%.

## 3. Further studies of the HRS theory and the $^{133}Cs$ ion resonance shifts in solution

### i. Preliminary

The remainder of this Chapter is concerned with the following topics:

ii) additional discussions of some aspects of the HRS theory;

iii) - v) new experimental data on the effects of (a) temperature, (b) solvent dielectric constant and (c) ionic strength on the concentration dependence of the $^{133}Cs$ shift.

These matters are discussed in turn below.

ii. Aspects of the HRS theory

It has been mentioned previously that Halliday (1969) found that $^{133}Cs$ ion resonance shifts obeyed the following empirical concentration-functional law

$$\log(\delta_{obs}) = g_o \log(c) + D \qquad (2.41)$$

where $\delta_{obs}$ is the observed shift relative to infinite dilution and where $g_o$ is a constant characteristic of the solvent and temperature only. (The constant D was incorrectly omitted by HRS in their original formulation.) This relationship was most strenuously tested for aqueous solutions of Cs salts and found to hold in the concentration range $0.02 < c < 2.0$ mol $kg^{-1}H_2O$. However the data available indicated that outside these limits

$$\frac{d\log(\delta)}{d\log(c)} > g_o \qquad (2.41)$$

The relationship was found to hold for $Cs^+$ ion shifts in other solvents, although the concentration ranges spanned by the data were smaller than for water. The values of $g_o$ varied from solvent to solvent. HRS found that the shifts predicted by equation (2.37) also obeyed equation (2.41), and thus made use of the very convenient parameter g to test agreement between the calculated and the observed shifts.

It is appropriate therefore to consider the following:

a) the status of the relationship (2.41) in the light of equation (2.37);

b) errors involved in the use of relationship (2.41) to obtain infinite dilution shifts by extrapolation;

c) alternative methods of comparing calculated and observed shifts.

a) As a preliminary to all the discussion that follows, a useful simplification in the form of equation (2.37) is introduced and justified. The HRS equation for the observed shift may be written out fully

$$\delta_{obs}(c) = \delta(a) 4\pi \left(\frac{c'N}{10^3}\right) \int_a^{a+r_s} R^2 \exp\left(\frac{-Z_\alpha Z_\beta e^2}{\epsilon RkT(1+\kappa a)}\right) \exp\left[-\kappa(R-a)\right] dR \qquad (2.43)$$

from equation (2.37) and (2.40), recalling that only the first term of equation (2.37) is retained. $r_s$ is the radius of the solvent molecule, so that $a + r_s \simeq \beta$. $\varkappa$ is defined by equation (2.26); a practical definition is

$$\varkappa^2 = \frac{8\pi e^2 IN}{\epsilon kT} \tag{2.44}$$

where the ionic strength I is introduced:

$$I = \frac{10^3 \Sigma_\gamma Z_\gamma^2 \rho_\gamma}{2N} \tag{2.45}$$

$$= \frac{1}{2} \Sigma Z_\gamma^2 c_\gamma \tag{2.46}$$

$c_\gamma$ being the concentration of ion $\gamma$.

The integration can of course be carried out numerically; however at any concentration it is possible to find a value of R, $R_e$, such that the double exponential factor may be removed from the integral:

$$\delta_{obs}(c) = \delta(a) 4\pi \left(\frac{cN}{10^3}\right) \exp\left(-\frac{Z_\alpha Z_\beta e^2}{\epsilon k R_e T} \frac{\exp[-\varkappa(R_e - a)]}{(1 + \varkappa a)}\right) \int_a^{a+r_s} R^2 dR \tag{2.47}$$

$$= \delta(a) \frac{4\pi}{3} \left(\frac{cN}{10^3}\right) \exp\left(-\frac{Z_\alpha Z_\beta e^2}{\epsilon k R_e T} \frac{\exp[-\varkappa(R_e - a)]}{(1 + \varkappa a)}\right) \left(R_m^3 - a^3\right) \tag{2,48}$$

where $R_m = a + r_s$

Now it can be shown that $R_e$ is almost constant over a large range of concentration. For example the entries in Table 2.1 show that the ratio of the integral of equation (2.43) to the exponential factor of equation (2.48) is effectively a constant, independent of concentration, at least up to about 1 mol $dm^{-3}$. Furthermore, the actual value of $R_e$ used ($a < R_e < R_m$) has a relatively negligible effect on the concentration dependence of the calculated shift (Table 2.1).

| dielectric constant | ionic strength mol $dm^{-3}$ | $A_1$ see note 1 | $A_2$ see note 1 | $A_3$ see note 2 | $A_1/A_3$ | $A_2/A_3$ |
|---|---|---|---|---|---|---|
| 78.54 ($H_2O$, 298K) | 0.001 | 5.0990 | 4.5492 | 1.2566 | 4.0578 | 3.6202 |
| | 0.010 | 4.4397 | 3.9626 | 1.0970 | 4.0471 | 3.6122 |
| | 0.100 | 3.1891 | 2.8542 | 0.7882 | 4.0463 | 3.6212 |
| | 1.000 | 1.8751 | 1.7015 | 0.4700 | 3.9891 | 3.6202 |
| 40.00 | 0.001 | 23.1844 | 18.5624 | 5.4869 | 4.2254 | 3.3830 |
| | 0.010 | 16.1735 | 12.9643 | 3.8294 | 4.2235 | 3.3855 |
| | 0.100 | 7.3681 | 5.9560 | 1.7546 | 4.1993 | 3.3945 |
| | 1.000 | 2.5255 | 2.1238 | 0.6195 | 4.0771 | 3.4282 |

Notes: 1 $$A_1, A_2 = \exp\left(-\frac{e^2 \exp[-\varkappa(R_e - a)]}{\epsilon R_e kT(1+\varkappa a)}\right)$$

$a = 0.35$ nm

$R_e = 0.42$ nm for $A_1$ and $= 0.45$ nm for $A_2$

2 $$A_3 = 4\pi\left(\frac{N}{10^3}\right)\int_a^{R_m} R^2 \exp\left(-\frac{e^2 \exp[-\varkappa(R-a)]}{\epsilon RkT(1+\varkappa a)}\right) dR$$

$a = 0.35$ nm, $R_m = 0.50$ nm. Numerically integrated.

TABLE 2.1

It follows from equation (2.48) that for a simple solution of an electrolyte

$$\ln \delta_{obs}(c) = \ln A + \ln c - \frac{Z_\alpha Z_\beta e^2}{\epsilon k R_e T} \frac{\exp[-\varkappa(R_e - a)]}{1+\varkappa a} \qquad (2.49)$$

where $A = \delta(a)\frac{4\pi}{3}\left(R_m^3 - a^3\right)\left(\frac{N}{10^3}\right)$

Thus

$$\frac{d\ln \delta_{obs}}{d \ln c} = \frac{d \log \delta_{obs}}{d \log c} = 1 + \frac{Z_\alpha Z_\beta e^2}{\epsilon k R_e T} \frac{\varkappa}{2}\left(R_e - a \frac{a}{1+\varkappa a}\right) \frac{\exp[-\varkappa(R_e - a)]}{1 + \varkappa a} \qquad (2.50)$$

This is easily evaluted and Figure 2.4 shows that, over the concentration range 0.02 to 2.0 mol $dm^{-3}$ in which the relation $\log(\delta_{obs}) = g\log(c) + D$ is believed to hold for aqueous solutions, equation (2.50) predicts a substantially but not by any means precisely constant value of g. The log-log relationship is not in any sense fundamental, but merely an adequate approximation over a limited concentration range. The linear region is in fact centred upon a point of inflexion in equation (2.31), the locus of which is

$$I_{infl} = \frac{\epsilon k T}{8\pi R_e^2 e^2 N} \qquad (2.51)$$

At concentrations sufficiently low that $\varkappa a \ll 1$, $(d\ln(\delta_{obs})/d\ln(c))$ may be expanded as a power series in c:

$$\frac{d\ln\delta_{obs}}{d\ln c} = 1 + \frac{Z_\alpha Z_\beta e^2}{\epsilon k R_e T}\left[R_e \frac{mc^{\frac{1}{2}}}{2} - \frac{m^2}{2}\left(a^2 + R_e^2\right)c + \frac{m^3 c^{3/2}}{2}\left(a^3 + \frac{3}{2}a^2 R_e + \frac{R_e^3}{2}\right)\ldots\right] \qquad (2.52)$$

where $m = (8\pi e^2 N/\epsilon k T)^{\frac{1}{2}}$ for a 1:1 electrolyte.

Evaluating the first four terms for T = 298K and $R_e$ = .42 nm yields

$$\frac{d\ln\delta_{obs}}{d\ln c} = 1 - \frac{810c^{\frac{1}{2}}}{\epsilon^{3/2}} + \frac{16840c}{\epsilon^2} + \frac{257300c^{3/2}}{\epsilon^{5/2}} \qquad (2.53)$$

Figure 2.4

Calculated variation of

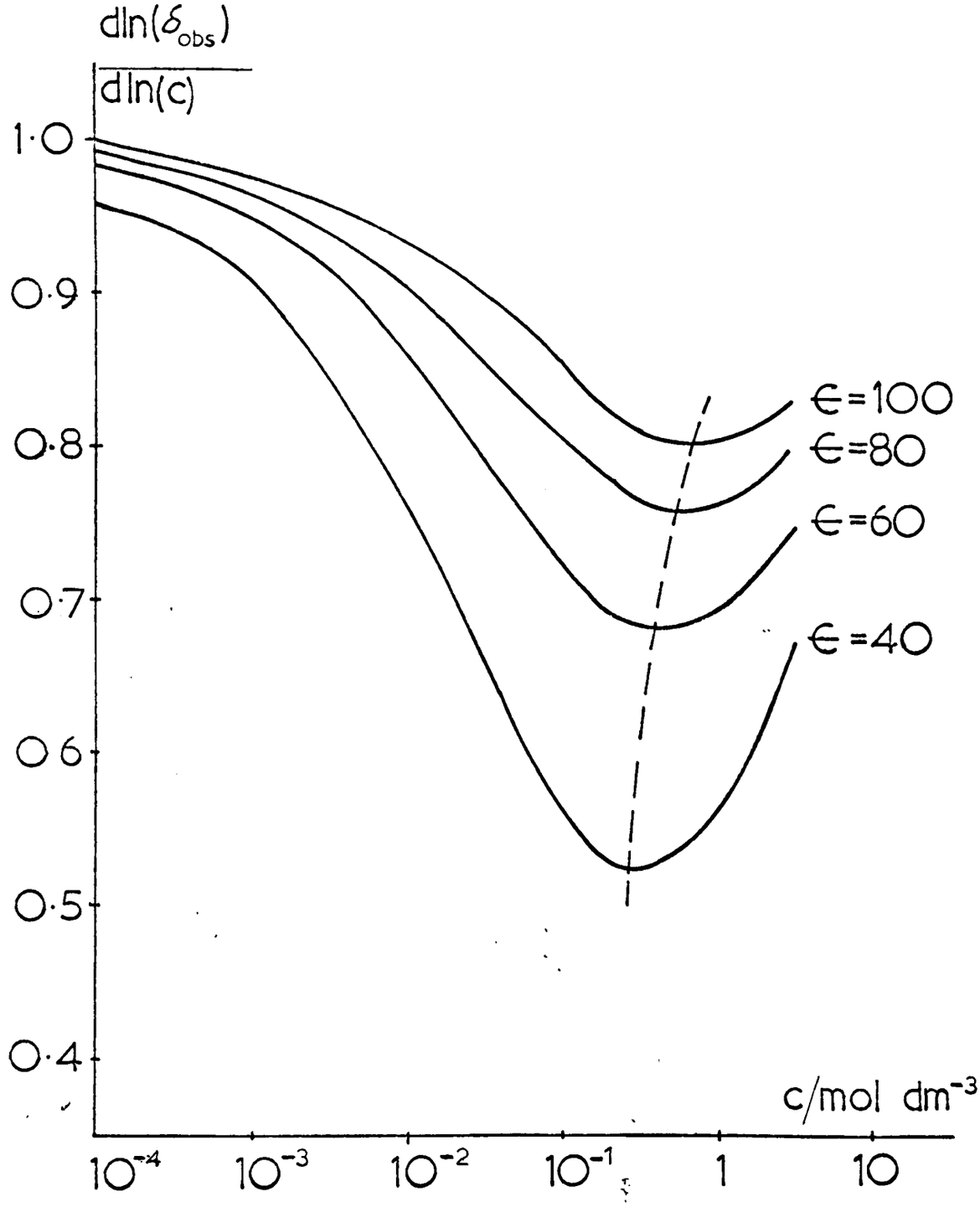
$$g \equiv \frac{d\ln\delta_{obs}}{d\ln c}$$ versus concentration c

for a number of dielectric constants $\epsilon$

$R_e = 0.42$ nm

$a = 0.35$ nm

$T = 298K$


dln(δobs)
dln(c)
1·0
0·9
0·8
0·7
0·6
0·5
0·4
ϵ=100
ϵ=80
ϵ=60
ϵ=40
c/mol dm-3
10-4
10-3
10-2
10-1
1
10

Values of $(d\ln\delta_{obs}/d\ln c)$ evaluated from expression (2.53) are in good agreement with those from the full expression (2.50) up to about 0.02 mol $dm^{-3}$ solvent.

Therefore we can state the following general conclusions.

i) The HRS theory predicts that the law $\log(\delta_{obs}) = g\log(c) + D$ will hold approximately, over a limited range of concentrations, centred upon a concentration determined mainly by the solvent dielectric constant and given in equation (2.51) above. This concentration is in fact that for which

$$\varkappa = R_e^{-1}$$

In other words, the concentration region for which the log-log law holds is that in which the radius of the Debye-Hückel ionic atmosphere is approximately equal to the mean distance over which the interionic approaches are considered effective in contributing to the shift.

ii) As the concentration of the electrolyte approaches zero, the screening effects of the ionic atmosphere become increasingly unimportant, and as

$$I \to 0,\ g \equiv \frac{d\ln\delta_{obs}}{d\ln c} \equiv \frac{c}{\delta_{obs}} \frac{d\delta_{obs}}{dc} \to 1 \qquad (2.54)$$

For very large values of $\varepsilon$, the ionic atmosphere effect is very small, and $g \sim 1$ throughout the concentration range.

b) The $\log(\delta_{obs}) = g\log(c) + D$ relationship cannot be used to obtain the infinite dilution shift from a set of experimental shift measurements graphically. The relationship presupposes that the shift values are already referenced to the infinite dilution shift. As has been mentioned briefly previously the matter of determining the infinite dilution shift corresponding to a set of shift data is one which causes some difficulty; HRS varied the infinite dilution shift by trial and error so that the

linearity of the log-log plot was optimised.

An equivalent procedure involves the non-linear least-squares fitting of data to the expression

$$\delta' = D'c^g + b \qquad (2.55)$$

where the $\delta'$ are arbitrarily referenced shift data, b is the infinite dilution shift and $D' = \exp(D)$. Although this procedure has been applied to some Cs shift data it clearly requires caution, since as has been shown above g is not expected to be independent of concentration. If very low concentration data were available (perhaps < 0.001 mol $dm^{-3}$ solvent) then it might be assumed

$$\delta' = D'c + b \qquad (2.56)$$

but such data are not yet available for any ion nucleus.

An apparently much more satisfactory means of determining the infinite dilution shift is achieved by making a least squares fit of shift data (preferably at low concentrations) to equation (2.48), which may be written in the following form:

$$\delta_{obs} = Ac \exp\left(-\frac{Z_\alpha Z_\beta e^2}{\epsilon kTR_e} \frac{\exp[-\kappa(R_e - a)]}{1 + \kappa a}\right) = \delta' - B \qquad (2.57)$$

where $\delta_{obs}$ is the shift measured relative to the infinite dilution shift as zero, and $\delta'$ is an arbitrarily referenced experimental shift. The infinite dilution shift is given by B. The results of applying this fitting procedure to the data of Halliday (1969) on CsBr in aqueous solution are illustrated in Figure 2.5, which shows also for comparison the linear log-log plot. It has been assumed that $\epsilon$ has the value 78.5, the bulk dielectric constant of water at 298 K. The infinite dilution shift estimated by the linear log-log fit (curve B) is 16.91 parts/$10^6$ and that estimated from the fit represented by curve A is 16.97 parts/$10^6$, both measured to

Figure 2.5

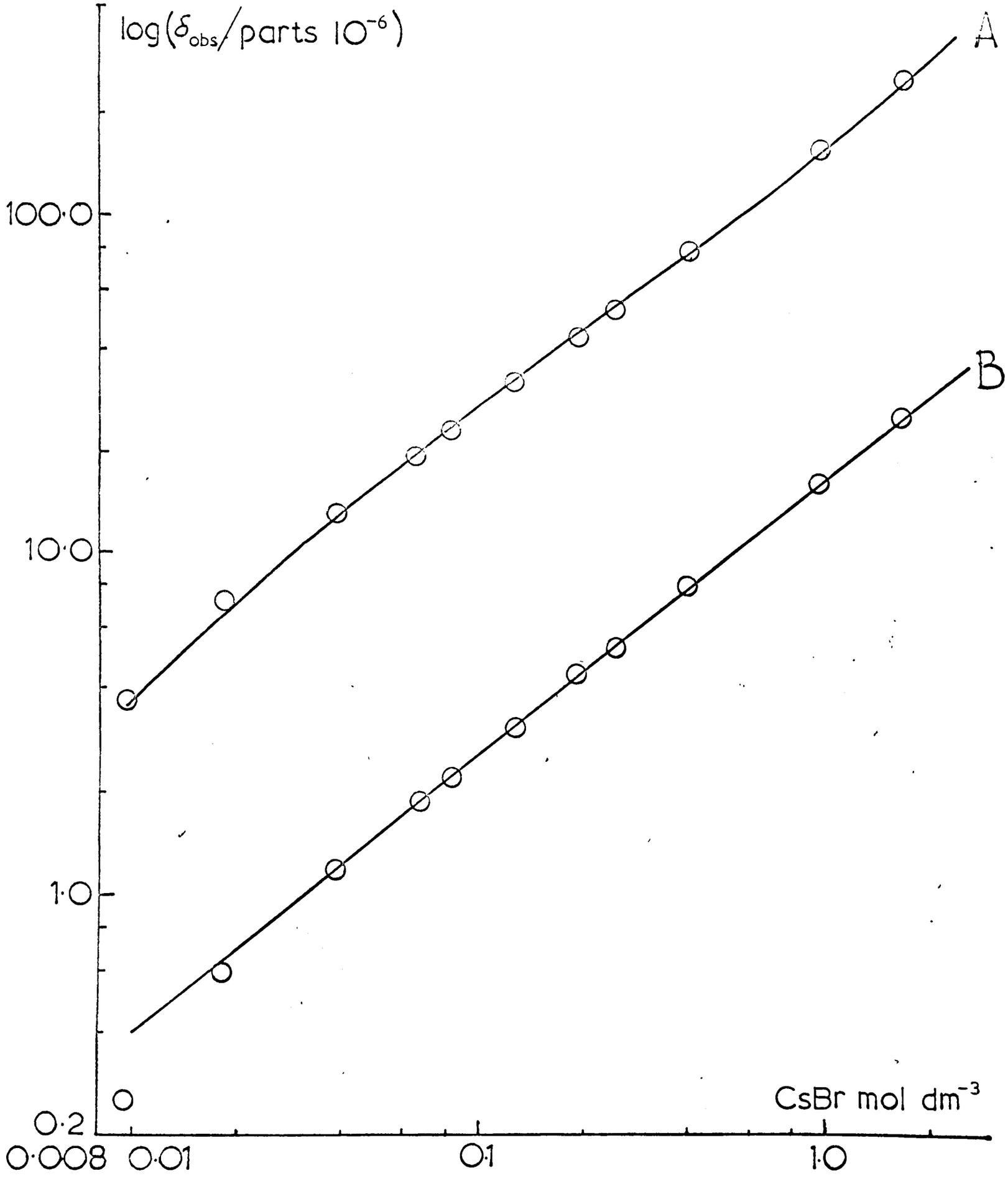
$CsBr/H_2O$: $^{133}Cs$ shift data from
Halliday, Richards and Sharp (1969)

A: curve and infinite dilution resonance frequency determined by least squares fit to equation (2.57).
Infinite dilution shift 16.97 parts/$10^6$ to high field of $^{133}Cs/CsCl/H_2O$ 1.994 mol $kg^{-1}$.

B: curve and infinite dilution resonance frequency determined by least squares fit to equation (2.41).
Infinite dilution shift 16.91 parts/$10^6$ to high field of $^{133}Cs/CsCl/H_2O$ 1.994 mol $kg^{-1}$.

All data refer to 298K.

Note upper curve A displaced by a factor of 10, for clarity of display.


log(δobs/parts 10⁻⁶)
A
B
100·0
10·0
1·0
0·2
0·0008
0·01
0·1
1·0
CsBr mol dm⁻³

high field of the $^{133}Cs$ resonance of 1.994 mol $kg^{-1}$ aqueous CsCl at the same temperature. The difference between the two estimates is 0.06 parts/$10^6$, that is, 1.7 Hzat 28.010 MHz. Thus in the present case the error introduced by using the former method is very small, and this is generally so for aqueous solutions. For solutions in solvents of lower dielectric constant, the error can be much more serious (see Section iii) for the movement of the resonance at very low concentrations is much greater. In addition the success of the linear log-log fit almost certainly depends on the fortunate circumstance that the data related to the appropriate concentration range (see above).

c) The question of how to make an extrapolation of the measured resonance frequencies to the state of infinite dilution is closely related to the matter of how to test the validity of the HRS theory. It is important to avoid any risk of circularity in the argument. The form of equation (2.37) makes it essential to obtain a value for the infinite dilution shift (and this is anyway of great importance as the fundamental ion-solvent interaction parameter), and it seems reasonable to try to do so by the method just described.

If the estimated infinite dilution resonance frequency is now used as a new reference point for the data at finite concentrations, then it is important to recognise that the shift of origin may itself to some extent predispose the data to fit the relationship used in the extrapolation. This relationship is the very HRS equation which we may wish to test. The only way to avoid this problem is to make measurements down to very low concentrations, thus making the extrapolation to infinite dilution as "short" as possible and reducing the scope for error.

It is of particular interest to test whether the bulk dielectric constant of the solvent (or solution) is indeed a good parameter for use in equation (2.57). One direct way of testing for this is to fit the experimental data to equation (2.57), allowing A, B and the dielectric constant itself $\epsilon$ to be determined by least squares or some similar criterion.

This may be done by standard differential correction methods (see, for example, McCalla 1967 ). The results for the $^{133}Cs$ shift in aqueous solutions of CsCl, CsBr, $CsNO_3$ and CsOH are shown in Table 2.2. The data included have been limited to concentrations below 0.45 mol $dm^{-3}$. Although this range is rather arbitrary, it is an attempt to restrict the test to concentrations where equation (2.48) may reasonably be expected to be valid. It must be understood that this test makes extremely stringent demands on the quality of the data. First, the restriction of the data to low concentrations means that the number of points in each data set is rather small, and that the shift variation is also rather small. Second, the best least squares values of A, B and $\epsilon$ are extremely sensitive to the data errors. With this in mind the results do appear to show that for aqueous solutions of Cs, the bulk dielectric constant is a good measure of the degree of attenuation of the Coulomb force between the ions. In considering the "best" values of $\epsilon$ listed in Table 2.2, it should be borne in mind that as the dielectric constant increases the exponential Debye-Hückel factor in the concentration dependence of the shift approaches unity asymptotically. Therefore the sensitivity of the shift to changes in the dielectric constant is much less for high values of the dielectric constant than for low values. (This may be seen for example in Figure 2.6). Thus the deviations of the $\epsilon$ values of Table 2.2 from the true water value of 78.5 are easily accounted for by small experimental errors. There is, at least, no evidence from these results to suggest that the use of the bulk water dielectric constant is inappropriate.

Two further examples of the same procedure are described in Sections (iii) and (iv).

A very sensitive display of the effect of the solvent dielectric constant on the concentration dependence of the shift can be made as follows.

| electrolyte | maximum concentration included in data set/ mol $dm^{-3}$ | best value of $\epsilon$ see note 1 | best value of infinite dilution shift B/Hz see notes 1 and 2 |
|---|---|---|---|
| CsBr | 0.127 | 62.1 | 477.0 |
| CsBr | 0.405 | 90.2 | 473.5 |
| CsCl | 0.450 | 99.0 | 470.0 |
| $CsNO_3$ | 0.112 | 87.5 | 474.5 |
| CsOH | 0.231 | 101.1 | 471.5 |

Notes: 1 best values of $\epsilon$ and B determined from equation (2.57) by the principle of least squares.

2 infinite dilution shifts B are measured to high field of $^{133}Cs/CsCl$ 1.994 mol $kg^{-1}$ aqueous solution at 298K.

Data from Halliday 1969

TABLE 2.2

Define a function F(c, $\epsilon$) by

$$F = - \frac{Z_\alpha Z_\beta e^2}{\epsilon k R_e T} \frac{\exp[-\varkappa(R_e - a)]}{(1+\varkappa a)} \tag{2.58}$$

so that by equation (2.48)

$$\delta_{obs} = A c \exp(F) \tag{2.59}$$

Consider an experimental ion resonance shift in a solvent S

$$\delta^s_{obs} = A^s c \exp(F^s) \tag{2.60}$$

At one particular concentration $c_1$, within the concentration range over which equation (2.48) may be expected to apply, the shift is

$$\delta^{s1}_{obs} = A^s c_1 \exp(F^{s1}) \tag{2.61}$$

$A^s$ is not calculable precisely on the basis of present knowledge and may be removed:

$$\left( \frac{\delta^s_{obs}\ c_1}{\delta^{s1}_{obs}\ c} \right) = \exp(F^s - F^{s1}) \tag{2.62}$$

Now it is possible to compare the effect on the shift of the changing concentration in solvent S (dielectric constant $\epsilon^s$) with the predicted effect of concentration in a reference solvent H (dielectric constant $\epsilon^h$) since the relation

$$\frac{\log \left( \frac{\delta^s_{obs} c_1 \exp F^{h1}}{\delta^{s1}_{obs}\ c} \right)}{F^h} = \frac{F^s - F^{s1} + F^{h1}}{F^h} \tag{2.63}$$

should be found.

For S ≡ H, the right-hand side of equation (2.63) is identically equal to one at all concentrations, and the left-hand side function of the experimental data should be independent of concentration and equal to one also. Figure 2.6 shows that this is approximately true of the data of Halliday for Cs salts in $H_2O$ up to about 1 mol $dm^{-3}$, above which the validity of (2.48) may be assumed to fail. Other curves in Figure 2.6 show the value of the function $(F^s - F^{s1} + F^{h1})/F^h$ for other values of $\epsilon^s$. $c_1$ equals 0.1 mol $dm^{-3}$ in this case. It should be noted that this plot appears to be much more sensitive in revealing deviation and scatter about the predicted curves than the simple plots of shift versus concentration used earlier.

Such plots (called for brevity Q-plots hereafter) may appear unnecessarily complicated in form. In fact, they reveal in a rather direct way the effect of different dielectric constants on the ionic atmosphere factor in the observed chemical shift data. Both the linear concentration dependence and the concentration-independent factor in the shift data are removed to reveal the Debye-Hückel factor. Then the Debye-Hückel factor itself is normalised to 1 for some reference solvent (usually water).

Two further examples of these plots are given in Sections 3 iii, iv, for MeOH solutions of CsCl and for HOAc-$H_2O$ solutions of CsBr.

Figure 2.6

$Q_1$ (points) and $Q_2$ (curves) <u>versus</u> Cs salt concentration

□ $CsCl/D_2O$

△ $CsCl/H_2O$

○ $CsBr/H_2O$

◇ $CsCl/H_2{}^{18}O$

Data from Halliday (1969)

$$Q_1 = \frac{\log\left(\frac{\delta^s_{obs} c_1 \exp F^{h1}}{\delta^{s1}_{obs} c}\right)}{F^h}$$

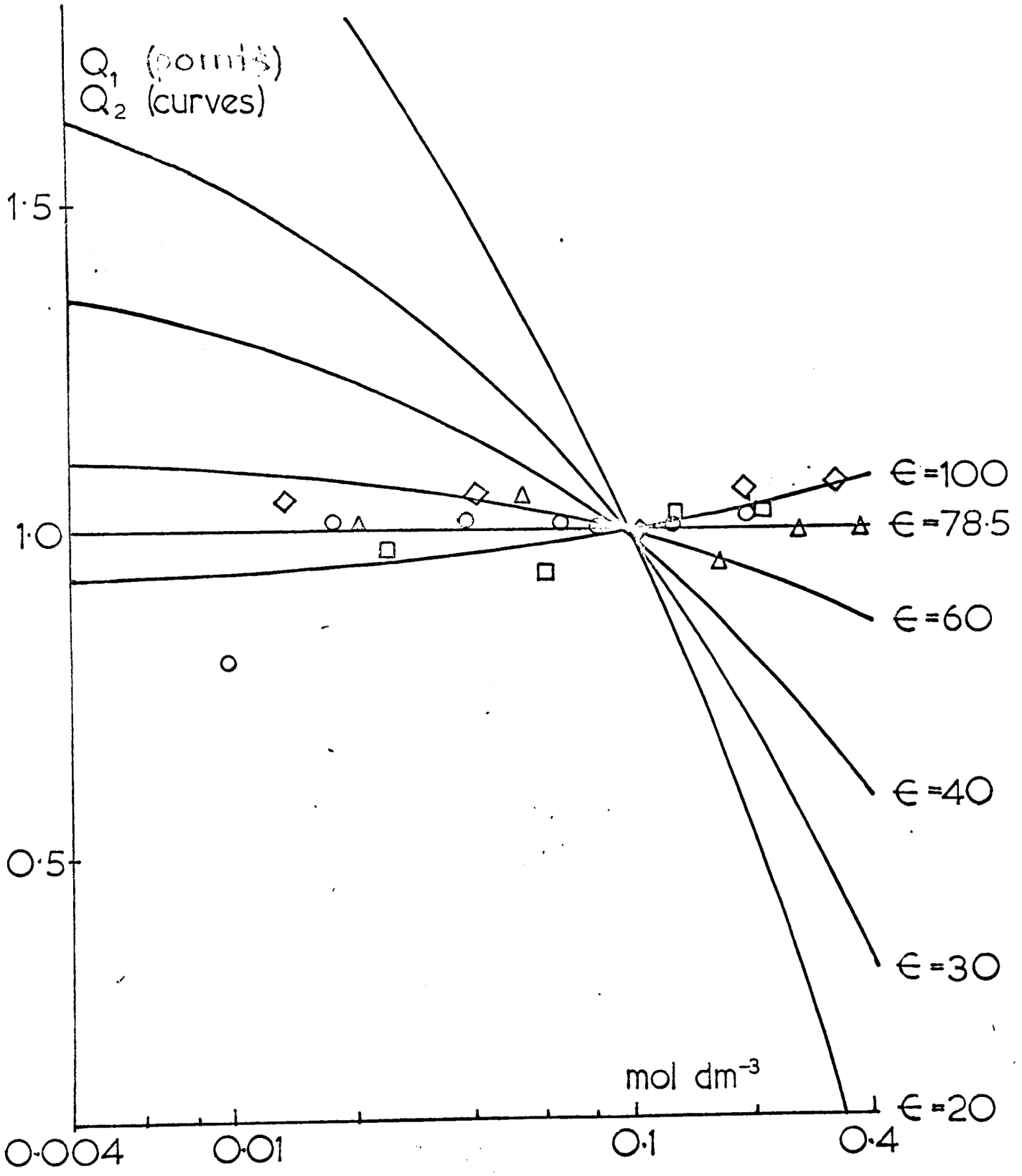
$$Q_2 = \frac{F^s - F^{s1} + F^{h1}}{F^h}$$

(see equation (2.63)).

$h = s = H_2O$ for $Q_1$

$c_1 = 0.1$ mol $dm^{-3}$

$h = H_2O$ for $Q_2$; s: various $\epsilon$


Q1 (points)
Q2 (curves)
1·5
1·0
0·5
ϵ=100
ϵ=78·5
ϵ=60
ϵ=40
ϵ=30
ϵ=20
mol dm⁻³
0·004
0·01
0·1
0·4

iii. CsCl/MeOH: the effect of temperature on the concentration dependence of the $^{133}Cs$ shift

New data for the effect of temperature on the concentration dependence of the $^{133}Cs$ shift have been obtained for the CsCl/MeOH system. The HRS equations indicate that the dielectric constant enters the equations only in combination with the absolute temperature T. However for most solvents the product $\varepsilon T$ is almost constant, and thus the effect of temperature on the shift is expected to be very small. This was in fact found by HRS for the system $CsBr/H_2O$ at three temperatures in the range 25-90°C. In the case of MeOH the variation in $\varepsilon T$ is just sufficiently great to offer some hope that the effect might be detectable.

Figure 2.7 (a) shows the $^{133}Cs$ shift relative to an infinite dilution resonance frequency obtained by extrapolation of the equation (2.57), as a function of concentration at three temperatures. The solid lines show the best least squares fit to this equation at each temperature, using the appropriate bulk dielectric constant. It is seen that equation (2.57) can provide a very good fit to the observed data; nonetheless it is important not to be misled into concluding from this that the fitted equation is necessarily the only, or even the best, equation for this purpose. Table 2.3 (column 5) shows that the A values of equation (2.57) determined from the data by the least squares principle differ slightly from one temperature to another. Although there is no explicit temperature dependence of A in equation (2.49) this is not entirely unexpected, since the quantity $\delta(a)$ describes the shift caused by replacing a solvent molecule in the solvation sphere by an ion. It is very probable that the effect of temperature on the motion of the solvent molecules and on the energy of interionic collisions renders this quantity temperature dependent.

It is desirable to have evidence that the bulk dielectric constant is an appropriate parameter to use in equation (2.57); and that the apparent temperature dependence of A is not an artefact of the fitting procedure used. The fuller procedure, in which the dielectric constant is

Figure 2.7

$^{133}Cs$ shift data (CsCl/MeOH) relative to infinite dilution shifts listed in Table 2.3, column 6 at three temperatures

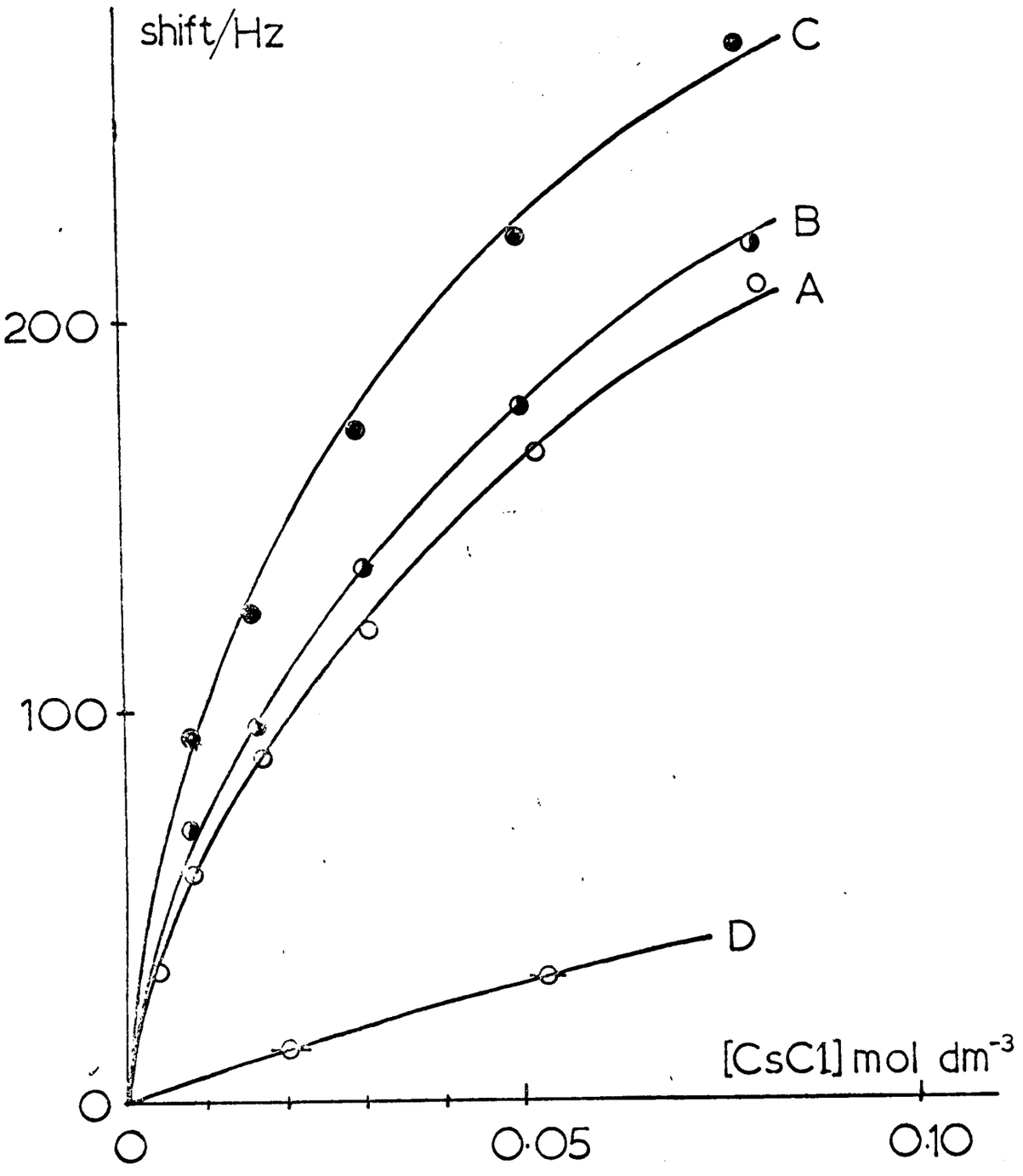
A 298K

B 308.3K

C 326K

Dielectric constant data from International Critical Tables and Maryott and Smith 1951

D $CsCl/H_2O$ (Halliday 1969) for comparison


shift/Hz
C
B
A
200
100
D
[CsCl] mol dm$^{-3}$
0
0
0·05
0·10

| 1 | 2 | 3 | 4 | 5 | 6 | 7 | 8 | 9 | 10 |
|---|---|---|---|---|---|---|---|---|---|
| T/K | concentration mol/kg | concentration mol/dm$^3$ (calcd.) | observed chemical shift/Hz see note 1 | best values of constants see note 2 | | best values of constants see note 3 | | | ε of solvent see note 4 |
| | | | | A | B | A | B | ε | |
| 298 | 0.1033 | 0.0813 | 1537 | | | | | | |
| | 0.0671 | 0.0528 | 1579 | | | | | | |
| | 0.0395 | 0.0311 | 1624 | | | | | | |
| | 0.0218 | 0.0171 | 1656 | | | | | | |
| | 0.0110 | 0.0087 | 1687 | | | | | | |
| | 0.0052 | 0.0041 | 1711 | 218 | 1745 | 260 | 1737 | 32.6 | 36.5 |
| 308.3 | 0.1033 | 0.0803 | 1781 | | | | | | |
| | 0.0671 | 0.0521 | 1823 | | | | | | |
| | 0.0395 | 0.0307 | 1864 | | | | | | |
| | 0.0218 | 0.0169 | 1905 | | | | | | |
| | 0.0110 | 0.0085 | 1935 | 202 | 2001 | 248 | 1988 | 30.7 | 33.5 |
| 326 | 0.1033 | 0.0785 | 1781 | | | | | | |
| | 0.0671 | 0.0510 | 1829 | | | | | | |
| | 0.0395 | 0.0300 | 1878 | | | | | | |
| | 0.0218 | 0.0166 | 1926 | 190 | 2050 | 261 | 2041 | 27.5 | 28.7 |
| | 0.0110 | 0.0084 | 1956 (see note 5) | | | | | | |

$^{133}$Cs shift data from CsCl/MeOH system at 298, 308.3, 326 K.

Notes: 1 Observed shifts referenced to:

298 K $^{133}Cs/CsCl/H_2O$ 1.994 mol (kg $H_2O$)$^{-1}$
(data from Halliday 1969)

308.3 and 326 K $^{133}Cs/CsCl/H_2O$ 3.349 mol (kg $H_2O$)$^{-1}$.

(All observed shifts are to high field of reference).

Measuring frequency 28.010 MHz.

2 A and B obtained by least squares fit of data at each temperature to equation (2.57) using the known solvent bulk dielectric constant.

3 A, B and ε obtained by least squares fit of data at each temperature to equation (2.57).

4 Solvent bulk dielectric constants from Maryott and Smith 1951.

5 For purposes of fitting data point rejected as apparently erroneous (see Figure 2.8); deviation > 3 standard deviations of other data.

TABLE 2.3

treated as a parameter to be determined from the data by the principle of least squares, has been applied to these measurements. The results are set out in Table 2.3 column 10, and strikingly support the use of the bulk dielectric constant. The estimated values of $\epsilon$ are in close agreement with the bulk dielectric constants of the solvents. A similar result was found earlier from the analysis of $^{133}Cs$ shift data in $H_2O$ (see Section ii), although the scatter in the estimated dielectric constant was rather larger. Further evidence for the same conclusion is given in the next section.

The small variation of A noted in column 5 (Table 2.3) is not supported by the A values obtained by the complete fitting procedure (column 7); the important feature however is that the A values are approximately constant, as expected from the definition of A given in equation (2.49). Thus the regression of the three sets of data to an equation in which only the functional form of the concentration dependence is specified yields an essentially constant value of A and a solvent parameter which is very close to the bulk dielectric constant in each case. This must be considered very sound confirmation of the validity of the HRS theory.

It is clear from Figure 2.7 (A, B, C) that the intersection of the shift-concentration plot with the infinite dilution line c = 0 is extremely acute for the CsCl/MeOH system at all three temperatures. Thus rather small changes in the best fitted curves result in comparatively large movements of the origin frequency (the infinite dilution shift). By comparison the intersection of line D ( ,CsCl/$H_2O$) appears to be experimentally much more clearly defined. This difference is directly attributable to the dielectric constant difference between MeOH and $H_2O$. It is fortunate that the early work (Halliday 1969) was largely concerned with aqueous solutions where graphical extrapolation to infinite dilution is comparatively straightforward. It is especially important in solvents of low dielectric constant to carry measurements down to as low concentrations as possible if errors in extrapolation are to be kept small. The experience of the CsCl/MeOH system suggests that data in the range 0.01 to 0.10 mol $dm^{-3}$ are satisfactorily

described by the HRS theory. Measurements at concentrations much below this range are precluded at present by poor signal-to-noise ratios. The insolubility of CsCl in pure MeOH prevented extension of these measurements to higher salt concentrations.

Figure (2.8) shows the predictions of equation (2.63) compared with the experimental data in the form of a Q-plot. The agreement is very satisfactory. The bulk dielectric constants of the solvents have been assumed for the predicted curves.

The possibility that the large shift of the resonance frequency at very low concentrations of salt in these solutions is the effect of preferential solvation by water impurity appears to be ruled out both by the temperature dependence and the direction of the shift.

iv. CsBr/HOAc-$H_2O$: a mixed solvent study

It has been shown in the previous section that the HRS theory appears to account very satisfactorily for the concentration dependence of the $^{133}Cs$ resonance frequency in CsCl/MeOH solutions. This section describes the results of $^{133}Cs$ shift measurements on solutions of CsBr in acetic acid - water mixtures of three compositions. Acetic acid itself has an exceptionally low dielectric constant (6.2) and although itself a poor solvent for salts of Cs, may be mixed with water to improve its solvent powers.

$^{133}Cs$ shift data (298K) obtained are tabulated in Table 2.4. It was found that the low concentration data in each solvent could be fitted very well to equation (2.57), using the bulk dielectric constants. This is shown in Figure 2.9. On the other hand the "best" curve through all the data from each solvent was a very poor fit: the differences between the calculated and observed resonance frequencies were nearly all considerably

Figure 2.8

$Q_1$ (points) and $Q_2$ (curves) versus concentration for $^{133}Cs$ shifts in CsCl/MeOH systems.

For explanation of $Q_1$, $Q_2$ see Figure 2.6

A $\epsilon = 32.6$

B $\epsilon = 30.7$

C $\epsilon = 28.7$

D reference solvent $\epsilon = 78.54$ ($H_2O$)

△ 298 K

○ 308.3K

□ 326K

Data normalised at 0.0218 mol $kg^{-1}$ ($c_1$).

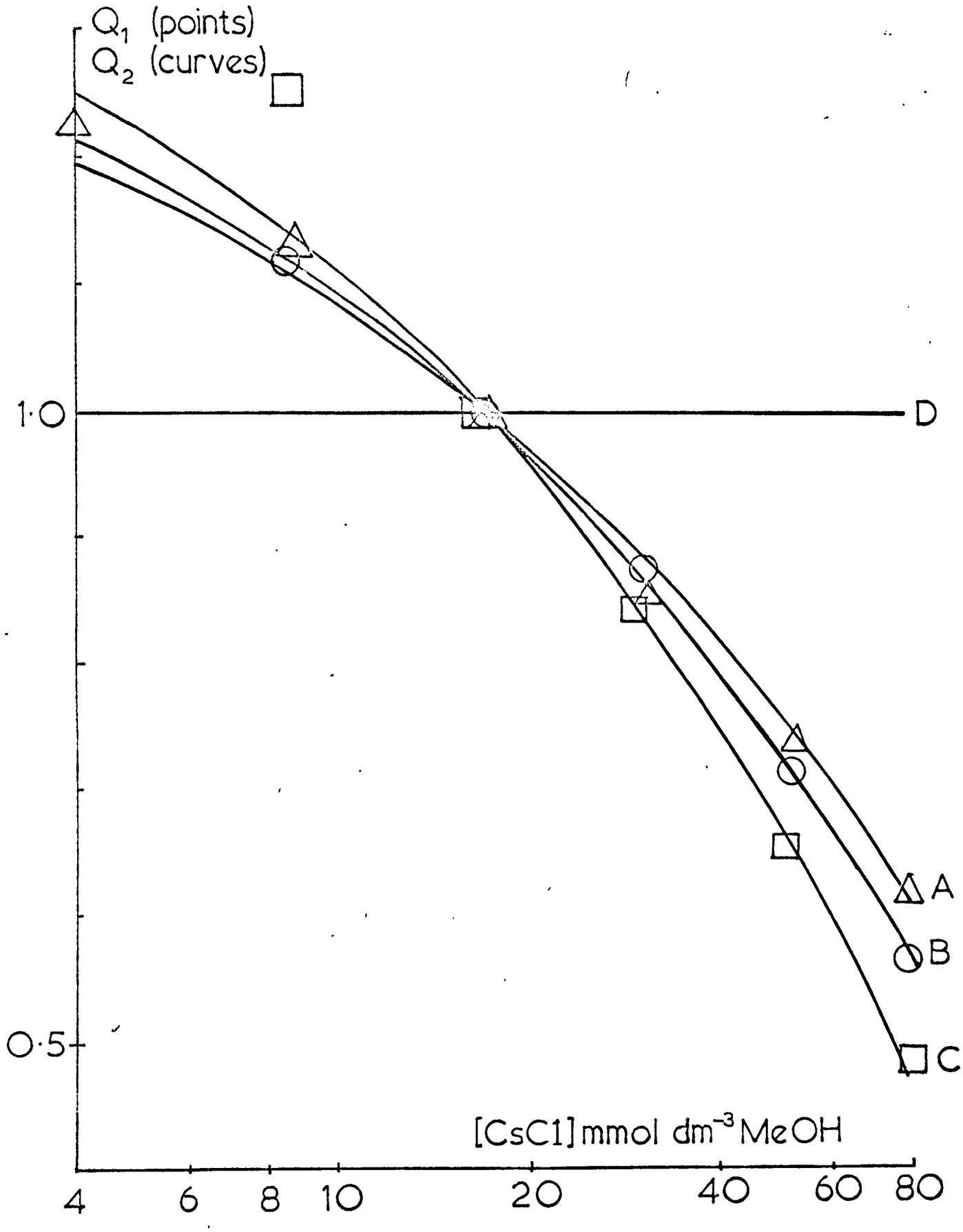

Q1 (points)
Q2 (curves)
1·0
0·5
D
A
B
C
[CsCl] mmol dm⁻³ MeOH
4
6
8
10
20
40
60
80

Figure 2.9

$^{133}Cs$ shifts versus concentration for CsBr/HOAc-$H_2O$ systems (shifts referenced to infinite dilution shifts B, Table 2.4 column 7).



0.2 mole fraction HOAc
0.8 mole fraction $H_2O$



0.4 mole fraction HOAc
0.6 mole fraction $H_2O$



0.7 mole fraction HOAc
0.3 mole fraction $H_2O$

Curves show best least squares fit of data to equation (2.57) using solvent bulk dielectric constants:

A $\epsilon = 57.2$

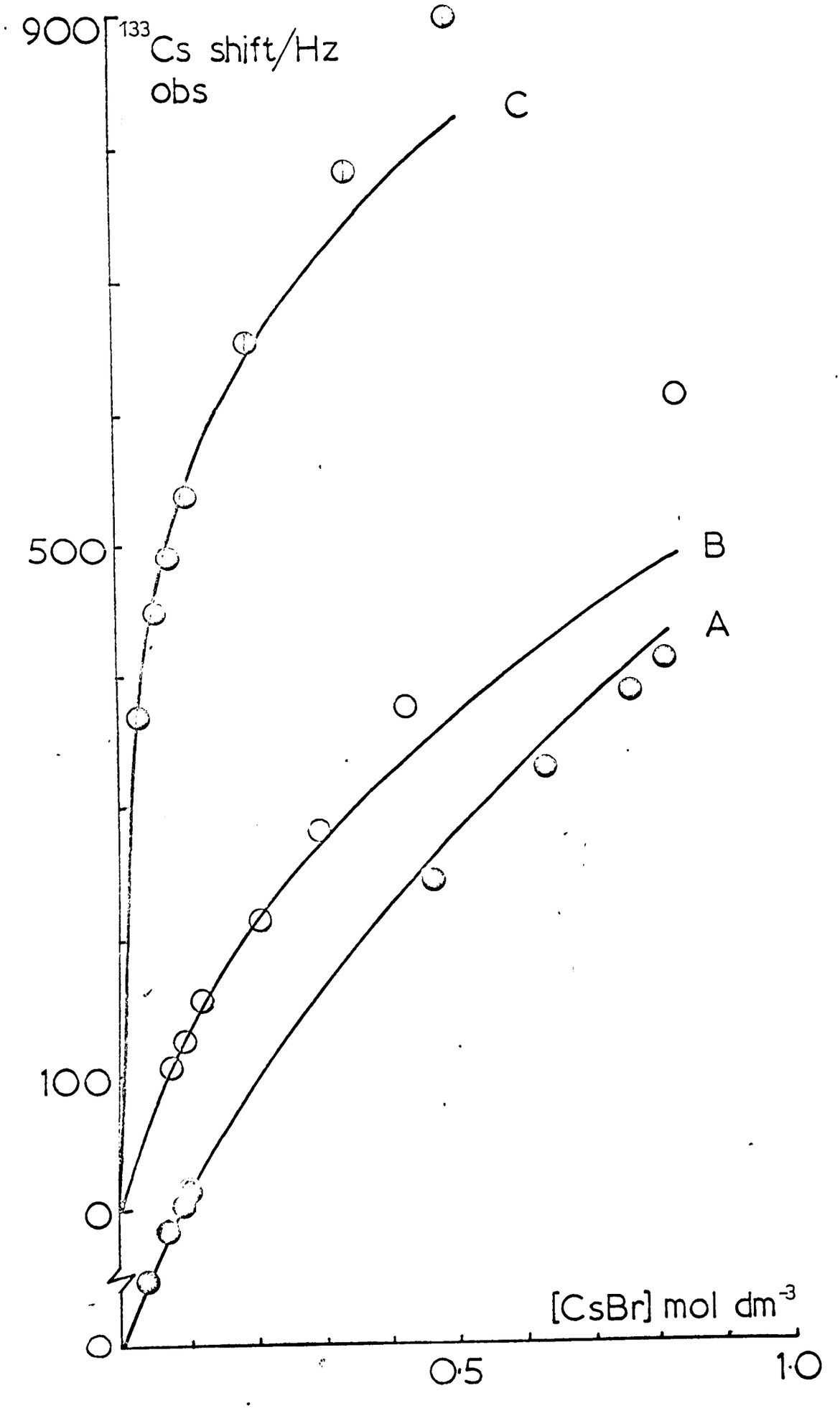
B $\epsilon = 42.5$

C $\epsilon = 23.8$

$R_e = 0.435$ nm

a = 0.365 nm

T = 298K


900
500
100
0
0
$^{133}$Cs shift/Hz
obs
C
B
A
[CsBr] mol dm$^{-3}$
0·5
1·0

| 1 | 2 | 3 | 4 | 5 | 6 | 7 | 8 | 9 | 10 |
|---|---|---|---|---|---|---|---|---|---|
| solvent composition mole fraction | | CsBr concentration | | observed chemical shift/Hz see note 4 | best values of constants see note 1 and note 2 | | | | ε of solvent see note 3 |
| $H_2O$ | HOAc | mol $kg^{-1}$ | mol $dm^{-3}$ (calcd) | | A | B | ε | ε | |
| 0.80 | 0.20 | 0.032 | 0.034 | 829 | | | | | |
| | | 0.054 | 0.057 | 794 | | | | | |
| | | 0.081 | 0.085 | 776 | | | | | |
| | | 0.092 | 0.097 | 762 | | | | | |
| | | 0.093 | 0.098 | 757 | | | | | |
| | | 0.435 | 0.457 | 530 | 294 | 881 | 56 | | |
| | | 0.600 | 0.630 | 442 | data not | | | | |
| | | 0.723 | 0.759 | 387 | included (see | | | | |
| | | 0.772 | 0.811 | 362 | text) | | | 111 | 57.2 |
| 0.60 | 0.40 | 0.060 | 0.064 | 795 | | | | | |
| | | 0.077 | 0.082 | 777 | | | | | |
| | | 0.108 | 0.115 | 748 | | | | | |
| | | 0.193 | 0.202 | 687 | 235 | 904 | 41 | | |
| | | 0.280 | 0.297 | 623 | data no | | | | |
| | | 0.402 | 0.427 | 524 | included (see | | | | |
| | | 0.785 | 0.834 | 290 | text) | | | 108 | 42.5 |
| 0.30 | 0.70 | 0.022 | 0.024 | 797 | | | | | |
| | | 0.051 | 0.054 | 711 | | | | | |
| | | 0.068 | 0.072 | 671 | | | | | |
| | | 0.094 | 0.100 | 625 | | | | | |
| | | 0.185 | 0.196 | 508 | 330 | 1164 | 33 | | |
| | | 0.318 | 0.337 | 383 | data no | | | | |
| | | 0.470 | 0.499 | 264 | included (see | | | | |
| | | | | | text) | | | 35 | 23.8 |

TABLE 2.4

(Continued on following page)

Notes:

1 Values of constant determined by best fit of data to equation (2.57)

columns 6 and 7: Λ and B found from low concentration data only, using bulk dielectric constant of solvent, shown in column 10.

2 column 7: ε determined from low concentration data only by principle of least squares

column 8: ε determined from all data at each solvent composition by principle of least squares.

3 dielectric constants interpolated from data of Borovikov and Fialkov 1965

4 observed chemical shifts referenced to $^{133}Cs/CsCl/H_2O$ 3.349 mol (kg $H_2O$)$^{-1}$.
Measuring frequency 28.010 MHz.

$^{133}Cs$ shift data from CsBr/HOAc-$H_2O$ systems at 298K.

TABLE 2.4 continued.

greater than the estimated experimental uncertainty. This strongly suggests that the HRS theory does not adequately describe the concentration dependence of the shift at the higher concentrations.

Figure 2.9 shows the experimental shift data, together with the best curves fitted through the 4 or 5 lowest concentration points of each set. The manner in which the experimental data at higher concentrations deviate from these curves is clear. No deviation is discernible in the case of the water-rich solvent mixture (curve A) right up to the highest concentration for which there is a shift datum. In contrast, as the dielectric constant of the solvent falls (curves B and C) the deviation is evident at concentrations above approximately 0.2 mol $dm^{-3}$.

The validity of using the bulk dielectric constant in this analysis may be supported in the same way as it was in the previous sections, by determining an empirical $\epsilon$ by least squares fitting of the data to equation (2.57). Again it is found that if all data from each solvent are included the fit is rather poor, and in two cases the estimated $\epsilon$ values appear to be very unreasonable (Table 2.4); whereas, if the fitting is restricted to the low concentration points, then $\epsilon$ values are obtained which are in remarkably good agreement with the true bulk dielectric constants of the solvents. It must be emphasised that this result is independent of any choice of the infinite dilution shift, which is also simultaneously determined.

Figure 2.10 shows the Q-plot of these data sets. In this figure the infinite dilution shifts of Table 2.4 (column 7) have been used. It can be seen that at least for the 0.40 and 0.70 mole fraction acetic acid solutions the data show good agreement with theory. The displacement between the observed points for the water-rich system and the corresponding curve (A) is probably attributable to experimental error in the datum point which was used in normalising the data. It should be recalled that this kind of plot shows up experimental error very clearly.

Figure 2.10

$Q_1$ (points) and $Q_2$ (curves) <u>versus</u> concentration for CsBr/HOAc-$H_2O$ systems (298K).

A $\epsilon = 57.2$

B $\epsilon = 42.5$

C $\epsilon = 23.8$

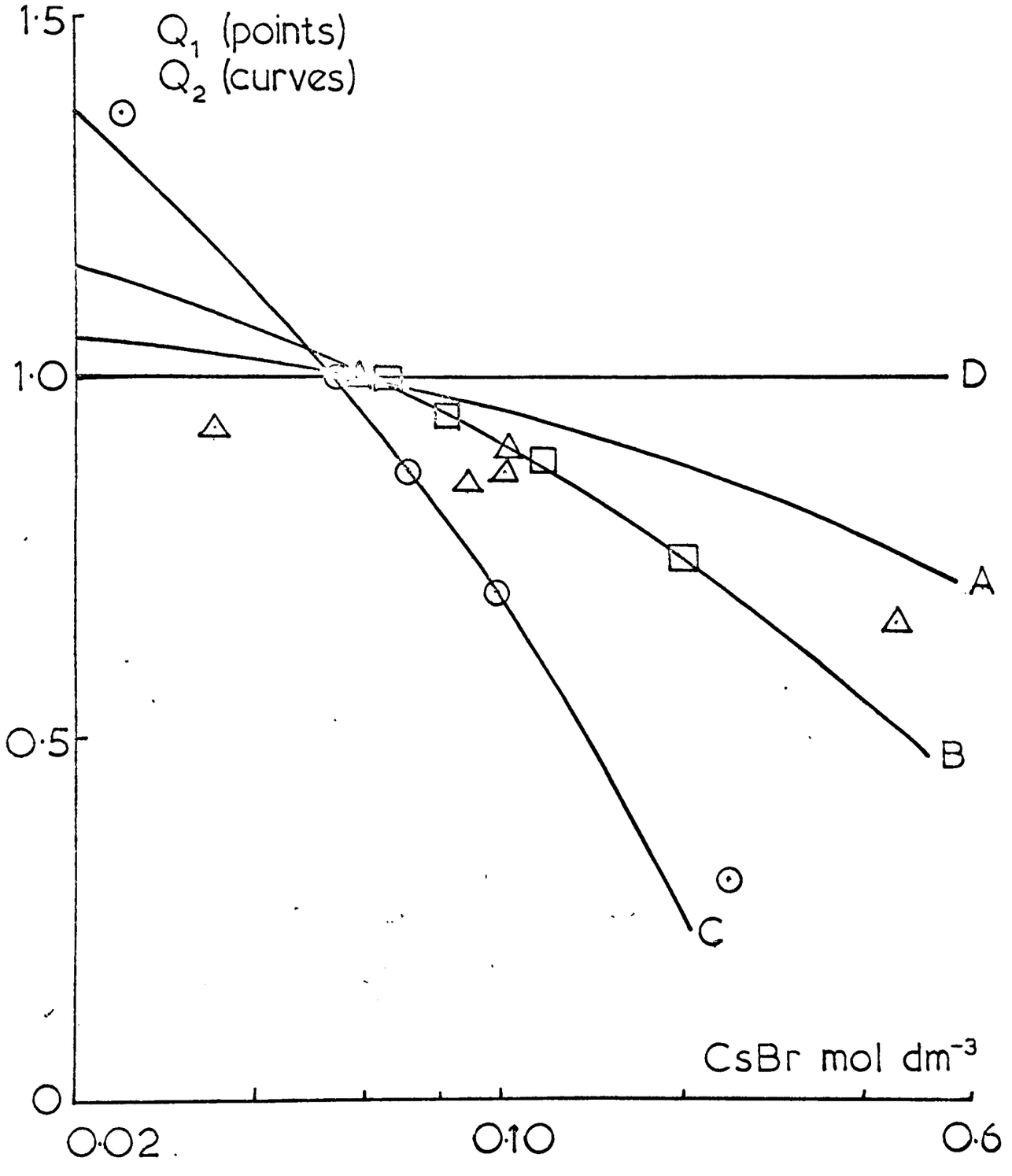
D $\epsilon = 78.54$ reference solvent ($H_2O$)

△ 0.2 mole fraction HOAc, data normalised at datum point 0.057 mol $dm^{-3}$

□ 0.4 mole fraction HOAc, data normalised at datum point 0.064 mol $dm^{-3}$

○ 0.7 mole fraction HOAc, data normalised at datum point 0.054 mol $dm^{-3}$

For definitions of $Q_1$ and $Q_2$ see Figure 2.6


1·5
1·0
0·5
0
$Q_1$ (points)
$Q_2$ (curves)
D
A
B
C
CsBr mol dm$^{-3}$
0·02
0·10
0·6

v. The influence of ionic strength on the $^{133}Cs$ resonance frequency

By introducing divalent cations into a CsBr solution, it is possible to change the ionic strength of the solution without necessarily altering the concentration of the anion which is dominant in causing the observed shift of the $^{133}Cs$ resonance. This possibility allows an interesting test of the HRS theory, which is described in the present section.

We shall consider three series of solutions which are of constant $Br^-$ concentration, but between which the ionic strength is changed by varying the $Na^+/M^{2+}$ concentration ratio. Each solution of a series contains in addition the same small concentration of $Cs^+$ ion. Thus the $^{133}Cs$ n.m.r. is used as a probe with which the effects of changing the ionic strength may be studied.

In general, as has been discussed at length earlier in this chapter, the observed shift of an ion resonance in a particular system is a sum of solvent, like-ion and counterion shifts: in the present case

$$\delta_{obs} = \delta(Cs^+-H_2O) + \delta(Cs^+-Cs^+) + \delta(Cs^+-Br^-) + \delta(Cs^+-Mg^{2+}) + \delta(Cs^+-Na^+) \qquad (2.64)$$

The solution compositions are listed in Table 2.5, which summarises also the experimental chemical shift data.

It is assumed

i) that $\delta(Cs^+-Cs^+)$ may be neglected because of the small $Cs^+$ concentration:

ii) that $\delta(Cs^+-M^{2+})$ and $\delta(Cs^+-Na^+)$ are sufficiently small to be neglected because of the small size of the $Mg^{2+}$, $Ca^{2+}$ and $Na^+$ ions. It is known from Deverell (1969) that these ions produce very small molal shifts in ions and their effects on a cation may be confidently assumed to be very small.

| concentration mol $dm^{-3}$ | | | | concn. mol $dm^{-3}$ | ionic strength mol $dm^{-3}$ | reference solution for shift data of column 8 | observed chemical shift/Hz | shift/Hz relative to infinite dilution (see notes 1 and 2) | ε (see note 4) |
|---|---|---|---|---|---|---|---|---|---|
| $[Cs]$ | $[Br^-]$ | $[Na^+]$ | M | $[M^{2+}]$ | I | | $\pm 1$Hz | | |
| 0.03 | 0.30 | 0.27 | Mg | 0.00 | 0.30 | 3.830 | -1049 | 188 | 74.70 |
| | | 0.21 | | 0.03 | 0.33 | mol $kg^{-1}$ | -1053 | 184 | 74.46 |
| | | 0.15 | | 0.06 | 0.36 | $CsBr/H_2O$ | -1054 | 183 | 74.22 |
| | | 0.09 | | 0.09 | 0.39 | (note 1) | -1055 | 182 | 73.98 |
| | | 0.03 | | 0.12 | 0.42 | | -1057 | 180 | 73.74 |
| | | 0.00 | | 0.135 | 0.435 | | -1059 | 178 | 73.62 |
| 0.10 | 1.00 | 0.90 | Ca | 0.00 | 1.00 | 3.349 | -232.5 | 481.5 | 65.7 |
| | | 0.70 | | 0.10 | 1.10 | mol $kg^{-1}$ | -237.5 | 476.5 | 65.0 |
| | | 0.50 | | 0.20 | 1.20 | $CsBr/H_2O$ | -242.5 | 471.5 | 64.3 |
| | | 0.30 | | 0.30 | 1.30 | (note 2) | -247.5 | 466.5 | 63.6 |
| | | 0.10 | | 0.40 | 1.40 | | -252.5 | 461.5 | 62.5 |
| | | 0.00 | | 0.45 | 1.45 | | -256.5 | 457.5 | 62.1 |
| 0.10 | 1.00 | 0.90 | Mg | 0.00 | 1.00 | 3.830 | -756.0 | 482.0 | 65.7 |
| | | 0.70 | | 0.10 | 1.10 | mol $kg^{-1}$ | -760.0 | 478.0 | 65.0 |
| | | 0.50 | | 0.20 | 1.20 | $CsBr/H_2O$ | -764.5 | 473.5 | 64.3 |
| | | 0.30 | | 0.30 | 1.30 | (note 1) | -770.0 | 468.0 | 63.6 |
| | | 0.10 | | 0.40 | 1.40 | | -774.0 | 464.0 | 62.5 |
| | | 0.00 | | 0.45 | 1.45 | | - (note 3) | | 62.1 |

Notes:
1 Shift relative to infinite dilution 44.15 parts/$10^6$ to low field.

2 Shift relative to infinite dilution 25.48 parts/$10^6$ to low field.
Data of Halliday 1969.

3 Erratic results obtained from this sample.

4 Dielectric constants calculated from experimental molar decrements for various ions reported by Hasted, Ritson and Collie 1948.

TABLE 2.5

It is further assumed

iii) that the Cs-$H_2O$ interaction does not change significantly with ionic strength.

Thus it is postulated that only binary interactions with counterions are significant in causing shifts. According to previous theory this shift is given by equation (2.48) which may for present purposes be expressed as

$$\delta_{obs} = Ac_{Br^-}f(\varkappa) \tag{2.65}$$

Although $\varkappa$ is dependent on the ionic strength, $c_{Br^-}$ is merely the $Br^-$ volume concentration, which here is held constant.

From equation (2.48) the ratio of the observed shifts for two solutions 1 and 2 should be found to be:

$$\frac{\delta^1_{obs}}{\delta^2_{obs}} = \exp\left(\frac{e^2}{R_e kT}\left[\frac{\exp[\varkappa_1(R_e-a)]}{\epsilon_1(1+\varkappa_1 a)} - \frac{\exp[-\varkappa_2(R_e-a)]}{\epsilon_2(1+\varkappa_2 a)}\right]\right) \tag{2.66}$$

where $\varkappa_1$, $\varkappa_2$ are given by equation (2.45) for ionic strengths $I_1$ and $I_2$. In this equation it is recognised that the dielectric constant may be a function of ionic strength. The effect of salts on the dielectric constant of water is well-known (Hasted, Ritson and Collie 1948), but is small for uni-univalent electrolytes, and has hitherto been neglected. It is much more marked for multivalent ions, and the decrease of solution bulk dielectric constant has been included in the analysis of the data. The calculated changes are based upon the molar decrements of these authors and are listed in Table 2.5.

Figure 2.11 a, b show the experimental shift data (plotted in the ratio form of equation (2.64)) compared with the predictions of the HRS theory. Although there can be little doubt that the variation of shift with ionic strength is somewhat less than predicted, the extent of the agreement may be considered most satisfactory. The results show that

Figure 2.11

$^{133}Cs$ shift variation with ionic strength for $Cs^+/Na^+/M^{2+}/Br^-H_2O$ systems

a M = Mg ●

b M = Mg △

N = Ca ○

Full curves show predicted variation from equation (2.66)

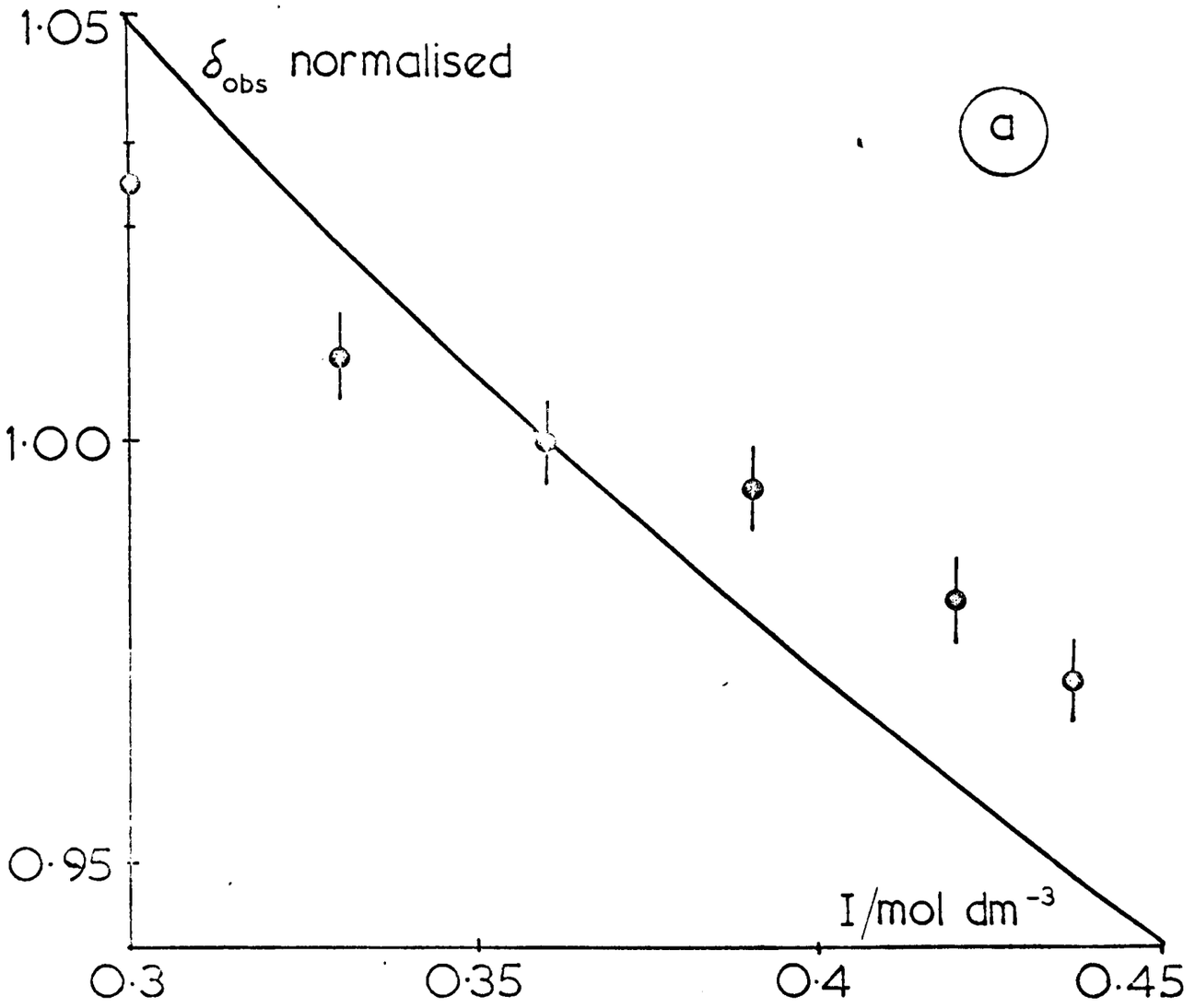
Cs shifts referenced to infinite dilution

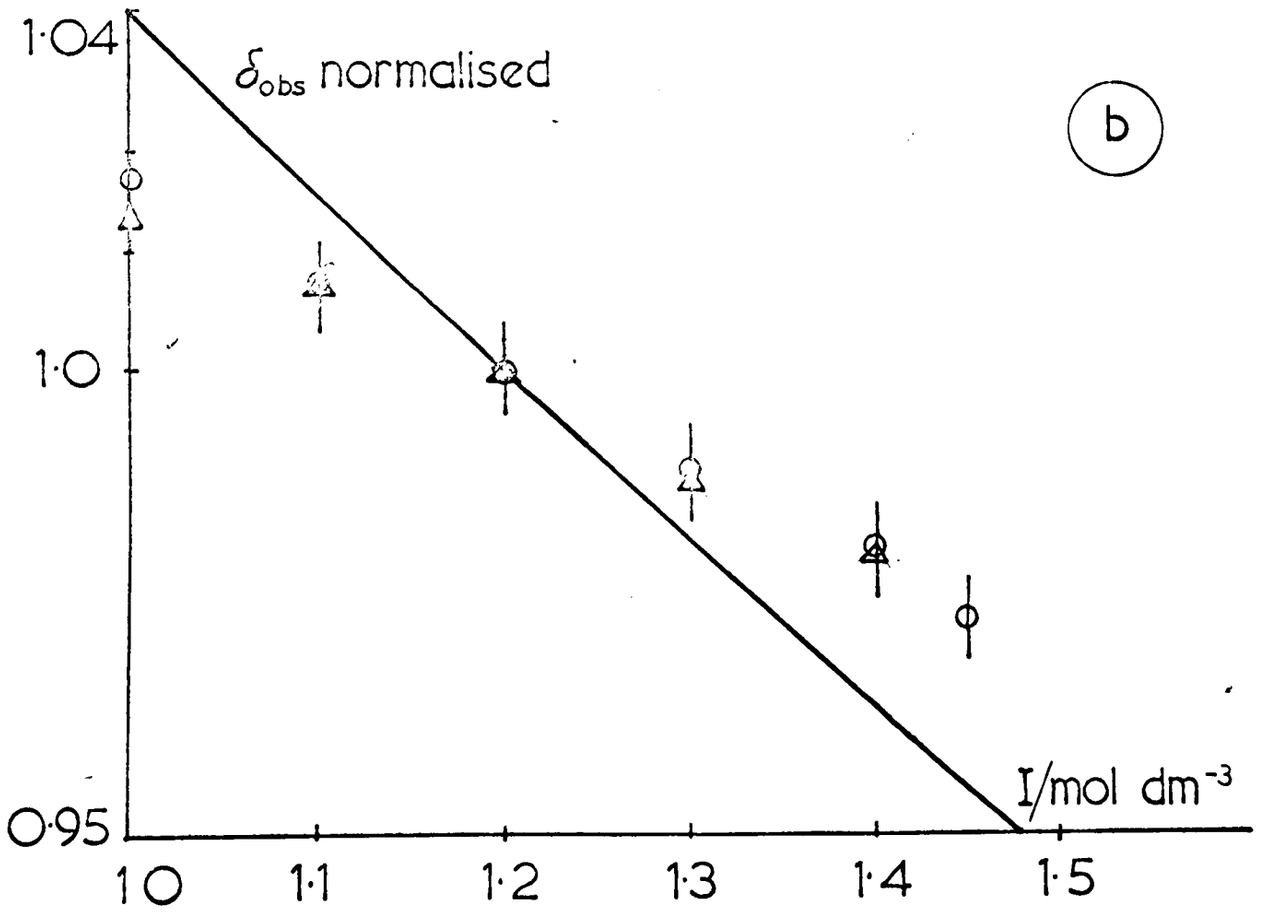
$R_e$ = 0.435 nm

a = 0.365 nm

T = 298K

Variation of dielectric constant with ionic strength shown in Table 2.5.


1·05
1·00
0·95
$\delta_{obs}$ normalised
a
I/mol dm$^{-3}$
0·3
0·35
0·4
0·45


1·04
1·0
0·95
$\delta_{obs}$ normalised
b
I/mol dm$^{-3}$
1·0
1·1
1·2
1·3
1·4
1·5

despite massive composition changes in the system the $^{133}Cs$ resonance shows only a very small high field shift with increasing ionic strength. This is entirely in accord with the predictions of the theory, which also estimates the magnitude of the effect well.

The almost exact concordance of shift data from $Mg^{2+}$ and the $Ca^{2+}$ systems of equal ionic strengths (see Table 2.5) firmly supports the assumption made earlier that the terms $\delta(Cs^{+}-M^{2+})$ are negligible. If they made appreciable contributions they would be unlikely to be equal, and some difference between the $Mg^{2+}$ and the $Ca^{2+}$ data would be expected. It is probable therefore that the discrepancy between the calculated curve and the experimental points lies in the term $\delta(Cs^{+}-H_2O)$.

## 4. Conclusion

The material presented in earlier sections of this Chapter has led to the point where the following conclusions may be drawn together.

1. The empirical log-log law of Halliday, Richards and Sharp (equation (2.41)) is only expected to hold over a limited concentration range, which for aqueous solutions happens to span almost the whole of the range which is experimentally accessible for $^{133}Cs$ n.m.r. Deviations from this law at concentrations below about 0.01 mol $dm^{-3}$ (aqueous solutions) can be detected, but here data are in agreement with the full HRS theory.

2. The log-log law is less satisfactory for non-aqueous solutions, since the concentration range over which it is expected to hold extends into the region where the theory itself appears to break down. This failure is presumably due to the generally low dielectric constants of non-aqueous solvents, and the consequential theoretical difficulties of the Debye-Hückel model.

It seems probable that the discrepancies found by HRS between theory and experiment for certain nonaqueous solvents are attributable to the incorrect assingment of infinite dilution resonance frequencies, coupled with the use of data taken from solutions containing rather high concentrations of salt. It is notable in this respect that rather good agreement was obtained in the case of pure MeOH, where all the data were restricted to low concentration solutions because of solubility limitations.

3. The determination of the infinite dilution shift calls for some care in the choice of extrapolation procedures. It is evident that any method based on the general validity of the log-log law is erroneous; on the other hand, the use of a curve fitting method based on the full HRS theory (in the $R_e$ approximation, see section 3 i(a)) seems reasonable, provided high concentration data are not used. Evidence has been presented that the bulk solvent dielectric constant is acceptable, at least until more accurate data at very low concentrations become available for study.

4. The results of experiments on MeOH and HOAc-$H_2O$ systems indicate - perhaps surprisingly - that the HRS theory accounts satisfactorily for the $^{133}Cs$ ion shifts up to tenth molar concentrations by characterising the solvent simply through a dielectric constant parameter. No account has been taken of ion-pairing as such.

There can be no question that dielectric saturation occurs in the vicinity of dissolved ions, and that the dielectric approximation breaks down at small interionic separations. On the other hand the potential at any point in the vicinity of an ion due to its ionic atmosphere is the result of long range interactions especially at low concentrations. It is this part which is concentration dependent and which may be important in determining the concentration dependence of the shift. In addition, there is evidence (Stokes and Robinson 1965) that the region of appreciable dielectric saturation about an ion may be confined to the first solvent layer.

In this connection it is important to recognise that the large singly charged $Cs^+$ ion may be untypical; it would be of great interest to have at hand data from other singly- and multiply-charged ions. Unfortunately the $^{133}Cs$ nucleus is a singularly favourable species for study by n.m.r., exhibiting as it does very large shifts and very sharp resonances.

In the theoretical introduction to this chapter, attention was drawn to the approximations upon which the Debye-Hückel pair distribution function depended. It is appropriate now to discuss these approximations in the light of the experimental results which have been presented.

Much discussion of the validity of the Debye-Hückel theory has concerned the nature of the central approximation (Poirier 1966) which has proved difficult to assess. This will not be pursued here. A simpler aspect of the Debye-Hückel theory which limits its range of application concerns the magnitude of the interionic Coulomb energy in certain situations. In order to bring the Poisson-Boltzmann equation (2.24) into consistency with the principle of linear superposition of charges, the restriction

$$eZ_\gamma \Phi_\alpha \ll kT \qquad (2.67)$$

was made. The potential energy of two small oppositely charged univalent ions in contact in water is sufficiently great for this to cause some difficulties and the problem becomes more acute in solvents of low dielectric constants and for multiply-charged ions. Interestingly, increasing electrolyte concentration reduces this problem: for the potential energy of an ion at any point R from an oppositely charged ion decreases with concentration as a result of the increased screening.

The most widely used method of overcoming the restriction of the Debye-Hückel theory to large ions and high dielectric constants is that of Bjerrum (Davies 1962; Fowler and Guggenheim 1939). In this theory, the

Debye-Hückel theory is deemed to hold except within a sphere of radius q about each ion. q, the Bjerrum critical distance, is defined by

$$q = \frac{|Z_\alpha Z_\beta| e^2}{2\epsilon kT} \tag{2.68}$$

and it is clearly the value of interionic separation for which the Coulomb energy equals twice the thermal energy. This boundary is not entirely arbitrary, as it can easily be shown that the probability of finding a counterion on the surface of the sphere R = q is less than for a sphere of any other radius about the central ion. In any case, it may be shown also that the Bjerrum q may be replaced by 2q or q/2 with very little impact on the predictions of the Bjerrum theory (Fowler and Guggenheim 1939). It has been said that outside the q spheres the Debye-Hückel theory holds; inside, Bjerrum proposed that the screening effect of the ionic atmosphere be ignored, and the Debye-Hückel potential

$$\Phi = \frac{e}{\epsilon R} \quad \frac{\exp[(-\varkappa(R-a)]}{1 + \varkappa a} \tag{2.31}$$

be replaced by the direct Coulomb potential

$$\Phi_b = \frac{e}{\epsilon R} \tag{2.69}$$

Every ion within a distance q of another ion of opposite charge is assumed to be paired with it. The ion pairs are considered to be uncharged entities of unit activity, making no contribution to the conductivity. The number of ions within this range may easily be calculated

$$N_b = 4\pi \frac{cN}{10^3} \int_a^q R^2 \exp\left(\frac{-Z_\alpha Z_\beta e^2}{\epsilon kTR}\right) dR \tag{2.70}$$

and it can be shown that the degree of association is

$$(1-\alpha) = 4\pi \frac{cN}{10^3}\left(\frac{|Z_\alpha Z_\beta|e^2}{\epsilon k T}\right)^3 Q(b) \qquad (2.71)$$

where $Q(b) = \int_2^b x^{-4}\exp(x)dx$

$$x = -\frac{Z_\alpha Z_\beta e^2}{\epsilon kTR}$$

$$b = \frac{|Z_\alpha Z_\beta|e^2}{\epsilon kTa}$$

If the ion-pair dissociation is described by an equilibrium constant K, then K may be calculated from equation (2.71) since at low concentrations

$$K^{-1} \sim \frac{(1-\alpha)}{c} \qquad (2.72)$$

But $(1-\alpha)$ at any concentration may now be calculated by combining

$$K = \frac{\alpha^2 y^2 c}{(1-\alpha)} \qquad (2.73)$$

and

$$-\log(y) = \frac{A\sqrt{(\alpha c)}}{1+Bq\sqrt{(\alpha c)}} \qquad (2.74)$$

where y is an activity coefficient.
Values of this quantity have been tabulated by Bjerrum (see Harned and Owen 1958) for various values of the independent parameters.

It must be emphasised that the Bjerrum theory is not an extension of the Debye-Hückel theory to high concentrations, but a modification to make it applicable to low concentrations of small ions in low dielectric constant solvents. The assumption of low concentrations is clear in

equation (2.70) where the screening of the ionic atmosphere is totally neglected; indeed the Bjerrum potential of equation (2.69) is the same as the limiting Debye-Hückel potential as $\varkappa \rightarrow 0$.

The Bjerrum theory calculates a value of K at very low concentrations, ans then uses this together with the law of mass action and the extended Debye-Hückel formula for activity coefficients to calculate $(1-\alpha)$ at higher concentrations. It is therefore expected to be only as reliable as this formula is.

The chemical shift of an ion on such a model is determined entirely by the ion-pair concentration. If $\sigma_{ii}$ and $\sigma_{is}$ are the shielding constants of an ion nucleus in an ion pair and in the free ion in solution respectively, then the average shielding constant of the ion is

$$\sigma = (1-\alpha)\ \sigma_{ii} + \alpha\sigma_{is} \qquad (2.75)$$

or $$\sigma - \sigma_{is} = (1-\alpha)(\sigma_{ii}-\sigma_{is})$$

Therefore the observed chemical shift relative to infinite dilution ($\delta_{obs}$) is

$$\delta_{obs} = (1-\alpha)\ \delta_{ii} \qquad (2.76)$$

At very low concentrations where $K^{-1} \sim (1-\alpha)/c$ it follows from equation (2.76) that $(\delta_{obs}/c)$ is proportional to $K^{-1}$. Thus

$$\delta_{obs}/c = (1-\alpha)\delta_{ii}/c \simeq K^{-1}\ \delta_{ii} \qquad (2.77)$$

(At higher concentrations $(1-\alpha)$ must be computed by successive approximations from equations (2.73) and (2.74)). It follows from equation (2.77) that

$$\log(\delta_{obs}/c) = pK + \log(\delta_{ii}) \qquad (2.78)$$

should hold at very low concentrations.

It is not possible to test this relationship with any precision in the absence both of very low concentration shift data and of activity data at higher concentrations. Nevertheless it is possible to make a preliminary comparison of the ion shifts data with the Bjerrum theory. It is known (Prue 1966) that the Bjerrum theory predicts an approximately linear dependence of pK on $1/\epsilon T$. Thus

$$\log(\delta_{obs}/c) = pK + \text{a constant} \qquad (2.79)$$

implies

$$\log(\delta_{obs}/c) = P.1/\epsilon + \text{a constant (P constant)} \qquad (2.80)$$

for a particular salt in a series of solvents at the same temperature. Unfortunately, very low concentration shift data are not available. Figure 2.12 shows plots of $\log(\delta_{obs}/c)$ versus $1/\epsilon$ for (a) the system CsBr/HOAc-$H_2O$ discussed in Section 3 iv and (b) various data of Halliday (1969), in which data from as low concentrations as practicable have been used. There is substantial agreement with expectations, although it must be stated that these concentrations are really too high for any conclusion to be drawn from this result. However, more strenuous tests clearly can be devised, to test in particular the concentration dependence of the shifts in a particular solvent.

It is clear from equation (249) that the HRS model also predicts a linear relationship between $\log(\delta_{obs}/c)$ and $1/\epsilon T$ at low concentrations when $\kappa$ is very small. The question of where and how the two models differ in their predictions at higher concentrations will require further attention. It should be noted that since both the Debye-Hückel and the Bjerrum theories are simply different mathematical treatments of one physical view of electrolyte solutions, a large measure agreement may be found. The Fuoss modification of the Bjerrum theory (Robinson and Stokes 1965) closely resembles the HRS of the Debye-Hückel theory, and comparison of these theories of ionic distribution in solution on one hand and chemical shift data on the other may be useful.

Figure 2.12

$\log\left(\frac{\delta obs}{c}\right)$ versus $1/c$ for Cs salts in various solvents at 298K.

a) $^{133}Cs$ shifts CsBr/HOAc/$H_2O$.

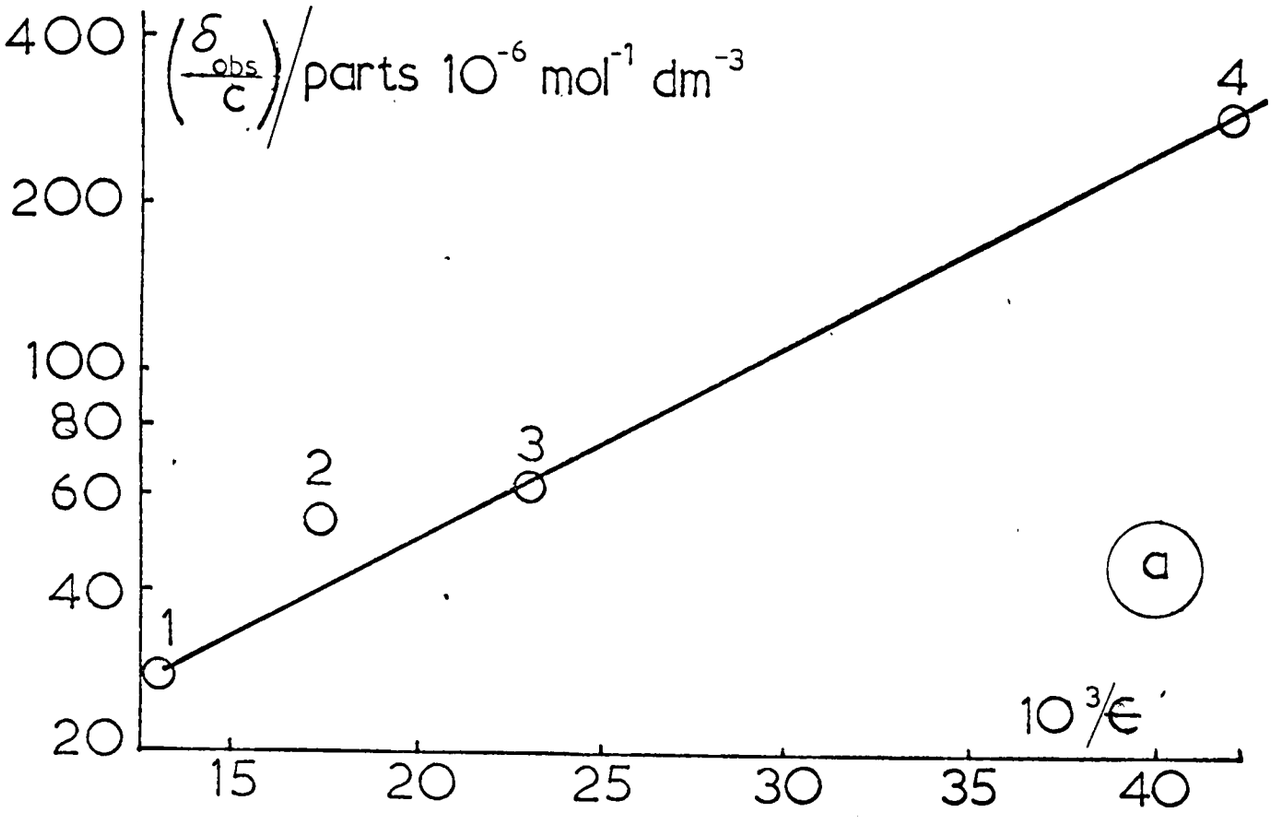
1 $H_2O$ data of Halliday 1969
2 0.80 mole fraction $H_2O$
0.20 mole fraction HOAc
3 0.60 mole fraction $H_2O$[c]
0.40 mole fraction HOAc
4 0.30 mole fraction $H_2O$
0.70 mole fraction HOAc

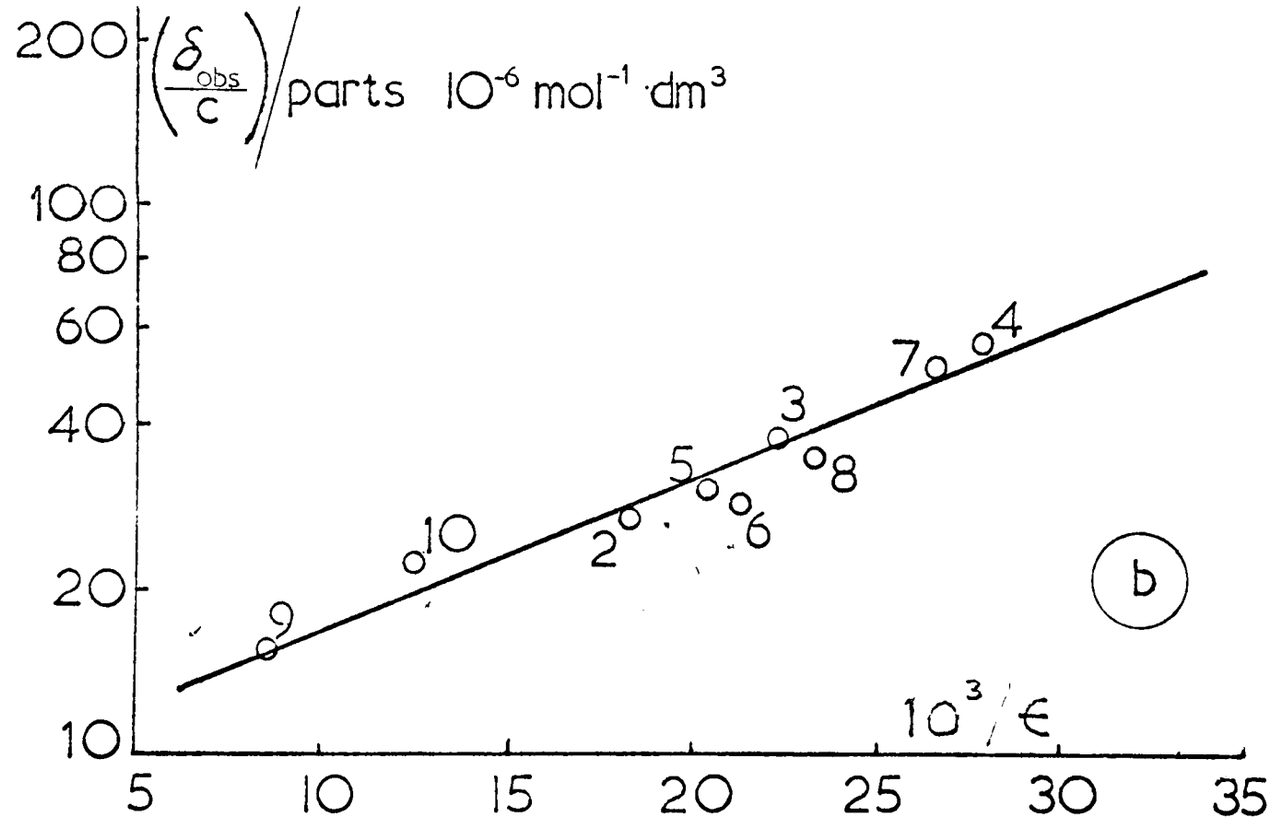
Shifts measured relative to infinite dilution:
see Table 2.4

b) $^{133}Cs$ shifts CsCl various solvents.

1 MeOH
2 0.36 mole fraction MeOH
0.64 mole fraction $H_2O$
3 0.57 mole fraction MeOH
0.43 mole fraction $H_2O$
4 0.84 mole fraction MeOH
0.16 mole fraction $H_2O$
5 0.28 mole fraction EtOH
0.72 mole fraction $H_2O$
6 1,2,3-propanetriol
7 1,2-ethanediol
8 0.18 mole fraction pyridine.
0.82 mole fraction $H_2O$
9 $H_2O$
10 0.05 mole fraction glycine
0.95 mole fraction $H_2O$

Data from Halliday, Richards and Sharp 1969.


400
200
100
80
60
40
20
$\left(\frac{\delta_{obs}}{c}\right)$/parts $10^{-6}$ mol$^{-1}$ dm$^{-3}$
1
2
3
4
a
$10^3/\epsilon$
15
20
25
30
35
40


200
100
80
60
40
20
10
$\left(\frac{\delta_{obs}}{c}\right)$/parts $10^{-6}$ mol$^{-1}$ dm$^3$
9
10
2
5
6
3
8
7
4
b
$10^3/\epsilon$
5
10
15
20
25
30
35

The full discussion of the HRS theory and the new experimental data presented in this Chapter appear to show that considerable confidence may be placed in that theory. It is becoming clear that this is true up to rather higher concentrations than is usual with a theory based on a Debye-Hückel model (albeit extended). It seems probable that the reason for this lies in the fact that to a good approximation the ion shift may be discussed in terms of the ion-counterion pair distribution function; the effect of the ions of the dynamics of the particles, especially of the solvent molecules, has no important influence on the $Cs^+$ ion chemical shift. This is in marked contrast with the complicated analysis required in the theory of phenomena such as conductivity.

It seems that the $Cs^+$ ion shifts may be understood rather simply as a direct probe of interionic collisions in solution, and in this rather direct interpretation may lie their value. There seems to be reason to hope that further measurements of ion resonances may prove useful in the study of, amongst other things, solvation phenomena and concentrated solution structure.

# CHAPTER III

## An n.m.r. study of chlorine exchange in aqueous solutions of chloride in the presence of chlorine

## 1. Introduction

The study of halogen nuclear magnetic relaxation times from suitable chemical systems in dynamic equilibrium provides a hitherto relatively unexploited means of determining kinetic information. For halogen nuclei, nuclear electric quadrupole coupling provides the dominant mechanism for the relaxation of the orientational spin states. Motion of the spins between sites which show appreciable differences in the strength of the coupling produce observable effects on the measured relaxation rate of the nucleus. These effects depend on the kinetic parameters relating to the motion of the spins.

A particularly suitable class of systems for investigation is that comprised by dynamic equilibria in which a halide ion exchanges in and out of a bound site in which there is a degree of covalency. The halogen nucleus in the free ion in solution occupies a site of almost pure spherical symmetry, and thus has a relatively long relaxation time, exhibiting a narrow n.m.r. absorption line. A binding site, such as a metal ion which forms halo-complexes, introduces a field gradient into this environment, shortening the relaxation time of the nucleus and producing a much broader line. If the free ion is the predominant species, then the exchange processes lead to a perturbation of the halide ion n.m.r. signal.

Since the relaxation time of the nucleus in the bound site is governed by the product of the nuclear electric quadrupole coupling constant and a motional correlation time, another class of systems suitable for study is afforded by equilibria involving exchange of spins between sites characterised by different correlation times. The binding of halide ions to a macromolecule is such a system.

Previous investigations of the type described have been reported by Meyers (1958) and later by Genser (1962) on the iodine-triiodide equilibrium(by $^{127}I$ n.m.r.), by Hertz (1961) on the exchange of bromide ligands

by $Zn^{2+}$, $Cd^{2+}$, and $Hg^{2+}$, and by O'Reilly (1963a) on the exchange of iodide ions by $Hg^{2+}$ complexes.

The equilibria I and II established in aqueous solution between $Cl_2$ and $Br_2$ in the presence of chloride ions are suitable for investigation by this method

$$Cl_2 + Cl^- \rightleftharpoons Cl_3^- \qquad \text{I}$$

$$Br_2 + Cl^- \rightleftharpoons Br_2Cl^- \qquad \text{II}$$

and a study of these systems by $^{35}Cl$ and $^{37}Cl$ n.m.r. is described in this chapter.

## 2. Theory of chemical exchange effects on the n.m.r. spectra of quadrupolar nuclei

The study of chemical rate processes is a well-established branch of n.m.r. spectroscopy, although as mentioned in the Introduction the majority of applications has been to the proton. Several ways of incorporating the effects of chemical exchange into the theoretical description of the resonance phenomenon have been developed. Of these the early formulations were in essence modifications of the Bloch Equations, the simple forms of which for a non-exchanging system may be written:

$$\dot{M}_+ = -\left[1/T_2 + i\,(\omega_o - \omega)\right] M_+ + i\omega_r M_z \qquad (3.1)$$

$$\dot{M}_z = \omega_r M_y - \frac{(M_z - M_o)}{T_1} \qquad (3.2)$$

where $M_+ = M_x + iM_y$

These are the equations of motion for a magnetic moment $\underline{M}(M_x, M_y, M_z)$ in the presence of a static magnetic field $\underline{H}_o$ along the +z-axis, and a smaller magnetic field $H_1$ rotating in the plane of xy at a frequency $\omega$. The coordinate system of equations (3.1) and (3.2) rotates about z

in phase with $H_1$ (such that $H_1$ lies along x in the rotating frame). If $\underline{M}$ is identified with the resultant magnetic moment of a number of nuclear spins, of the same species, having gyromagnetic ratio $\gamma$, then in addition $\omega_o = \gamma H_o$ and $\omega_r = \gamma H_1$.

When $\gamma H_1$ is small compared with $1/T_2$ then $M_z$ may be put equal to $M_o$. The solution of the Bloch equation for the transverse magnetisation is now

$$M_+(t) = \frac{i\omega_r M_o}{\alpha}\left(1-e^{-\alpha t}\right) + M_+(o)e^{-\alpha t} \qquad (3.3)$$

where $$\alpha = \frac{1}{T_2} + i(\omega_o - \omega)$$

In seeking a description of the slow passage n.m.r. experiments the time-functional terms in (3.3) are dropped. $\underline{M}+$ is separated into real and imaginary parts, which yield expressions for the shape of the u- and v-mode (in and out of phase with $H_1$) components of the n.m.r. signal.

Gutowsky, McCall and Slichter (1953) suggested that the effects of chemical exchange could be incorporated into the solutions of the Bloch equations by writing one such full solution for each site i, and then integrating this over a distribution of residence times for that site. With appropriate boundary conditions, this procedure yields an expression for $M_+$ as a function of $\alpha_i$ and kinetic parameters.

Alternatively it is possible to incorporate chemical exchange features into the Bloch equations themselves, rather than their solutions. A formulation of this type, which will be adopted throughout this chapter, was first suggested by McConnell (1958), but is supported by the results of the stochastic theory of n.m.r. lineshapes (Johnson, 1966). A very recent paper by Khazanovich (1969) presents a derivation of the McConnell equations by statistical mechanical methods.

Under steady state conditions the following equation describes the motion of the magnetisation vector at each site:

$$-M_+^i \left( \frac{1}{T_2^i} + i\,(\omega_i - \omega) + \frac{1}{\tau_i} \right) + \sum_{j \neq i} M_+^j \frac{p_{ji}}{\tau_j} = -i\omega_r M_o^i \qquad (3.4)$$

It is clear that the third term of the first bracket, $\tau_i^{-1}$, allows for the fact that the transverse magnetisation of the i site is continually reduced by transfer of nuclei from i sites to other available positions. In addition, transverse magnetisation is gained at the i site by transfers of nuclei into such sites from elsewhere in the system. In equation (3.4), the mean lifetime of nuclei in the sites are denoted by $\tau_i$ and their processional frequencies by $\omega_i$. i and j are general site labels. The $p_{ji}$ are the fractional probabilities that the transfer of a nucleus from j will be into i.

One such equation may be written for the transverse magnetisation of each site, and thus in general, using matrix notation:

$$\underline{\alpha} \underline{M}_+ = -i\omega_r \underline{M}_o \qquad (3.5)$$

where the matrix $\underline{\alpha}$ contains all the damping terms acting on $\underline{M}_+$.

The shape of the absorption mode n.m.r. signal is given by

$$\underline{M}_y (\omega) = \mathrm{Im}\,[-i\omega_r \underline{\alpha}^{-1} \underline{M}_o] \qquad (3.6)$$

This last equation draws attention to the fact that much of the difficulty in obtaining analytical solutions to these extended Bloch equations derives from the labour of rationalising their complex terms.

In situations (such as all of those discussed in this Chapter) where free halide ions (the major species, a) are moving in and out of bound sites

(provided by various minor species, i) then there is ample justification for the assumption that

$$M_o^i / M_o^a \sim 0 \quad (i \neq a) \tag{3.7}$$

In other words, the total equilibrium magnetisation is only negligibly different from that provided by the halide ions themselves. It may then be assumed that all terms $M_o^i$ are zero except $M_o^a$. This reasonable simplification serves to reduce the manipulative difficulty of the algebra considerably.

The procedure adopted will be to solve the matrix equation for $M_+^a$ and after rationalisation to select $M_y^a$ . The analytical solution at this point is a frequency-functional expression for the n.m.r. absorption spectrum. It is evident that the complete calculated spectrum would have contributions from all other $M_y^i$ also. In the present case considerations of both relative populations and relative spin-spin relaxations for the a site and the minor sites i justify the belief that these contributions are very small. Thus, the problem is treated as a perturbation of the pure a site spectrum caused by the occurrence of exchange damping. The characteristic feature of this treatment is that the spectrum calculated consists of a single line (the perturbed a site line) which continues to conform to the Lorentzian shape function even in the presence of chemical exchange. As a result calculations and experimental data can be defined in terms of a shift and an observed relaxation time, as canthe unperturbed spectrum. A more detailed discussion of these matters is given in Appendix III.

We turn now to the construction of the $\underline{\alpha}$ matrix and the solutions of the modified Bloch equations appropriate to the $Cl^-$ - halogen equilibria with which this chapter is largely concerned.

## The $Br_2/Cl^-$ system

Insofar as the only polyhalide anion present in solution is assumed

to be the species $Br_2Cl^-$ (of configuration Br-Br-Cl), this system may be considered as an example of a chlorine <u>two site problem</u>, represented by the equilibrium:

$$Br_2 + Cl^- \underset{k_b}{\overset{k_f}{\rightleftarrows}} Br_2Cl^- \quad K \qquad \text{III}$$

Daniele (1960) has reported the results of an ultraviolet spectrophotometric study of this equilibrium. However evidence will be presented later that this equilibrium does not adequately account for the Raman spectrum of bromine dissolved in aqueous chloride solutions and that other species are probably present. Further discussion of these observations is postponed until Section 6 of this chapter. Here the construction of the matrix for the nominal two-site exchange case defined by equilibrium (III) above will be carried through. We assume that Cl atoms may occupy the terminal positions only in the polyhalide anion and thus that only one site is available to the Cl nucleus in addition to the major site, the free ion. The values of the $p_{ji}$ (the fractional transfer probabilities, which are essentially stoichiometry factors) appropriate to this case, together with the site labels, and the relations between the $\tau_{ij}$ and the forward and backward rate constants $k_f$ and $k_b$ are listed in Table 3.1(a). The solution of the resulting equations for the broadening parameter $\Delta$ is

$$\Delta = \left(\frac{1}{T_2}\right)_{obs} - \left(\frac{1}{T_2}\right)_a = \frac{k_f[Br_2]^\circ}{1+K[Cl^-]} \left\{ \frac{\left(\frac{1}{T_{2b}} + k_b\right)\frac{1}{T_{2b}} + \Delta\omega_b^2}{\left(\frac{1}{T_{2b}} + k_b\right)^2 + \Delta\omega_b^2} \right\} \qquad (3.8)$$

where $k_f/k_b = K$ and $\dfrac{[Br_2]^\circ}{1+K\,[Cl^-]} = [Br_2]$

with the initial or added quantity of $Br_2$ being denoted by $[Br_2]^\circ$.

The limiting cases of (i) fast <u>exchange</u> and (ii) <u>slow exchange</u> are obtained by taking the limit of $\Delta$ as (i) $k_bT_{2b}$,/ $k_bT_{2b}/\Delta\omega_b \to \infty$ (ii) $k_bT_{2b} \to 0$, thus

(i) $\text{Lim } (\Delta) = \dfrac{[Br_2Cl^-]}{[Cl^-]T_{2b}}$ ; $\left(\dfrac{1}{T_2}\right)_{obs,\ fast\ exchange} = \dfrac{f_{Cl^-}}{T_{2a}} + \dfrac{f_{Br_2Cl^-}}{T_{2b}}$

$$\simeq \frac{1}{T_{2a}} + \frac{f_{Br_2Cl}}{T_{2b}} \qquad (3.9)$$

(ii) $\text{Lim } (\Delta) = k_f \dfrac{[Br_2]^o}{1+K[Cl^-]} \cdot \left(\dfrac{1}{T_2}\right)_{obs,\ slow\ exchange} = \dfrac{1}{T_{2a}} + \dfrac{1}{\tau_{ab}}$ (3.10)

| | | j | |
|---|---|---|---|
| | $p_{ji}$ | a | b |
| i | a | - | 1 |
| | b | 1 | - |

$Cl^-$ $(Br\text{-}Br\text{-}Cl)^-$

Site label a b

$\tau_{ab}^{-1} = k_f[Br_2]$

$\tau_{ba}^{-1} = k_b$

TABLE 3.1 (a)

| $p_{ji}$ | | j | | |
|---|---|---|---|---|
| | | a | b | c |
| i | a | - | 0 | 1/3 |
| | b | 0 | - | 2/3 |
| | c | 1 | 1 | - |

| | $Cl^-$ | Cl-Cl | $(Cl\text{-}Cl\text{-}Cl)^-$ |
|---|---|---|---|
| site label | a | b b | c c c |

TABLE 3.1 (b)

| $p_{ji}$ | | j | | | |
|---|---|---|---|---|---|
| | | a | b | c | d |
| i | a | - | 0 | $\frac{1}{2}$ | 0 |
| | b | 0 | - | $\frac{1}{2}$ | 1 |
| | c | 1 | $\frac{1}{2}$ | - | 0 |
| | d | 0 | $\frac{1}{2}$ | 0 | - |

| | $Cl^-$ | Cl-Cl | Cl-Cl-Cl |
|---|---|---|---|
| site labels | a | b b | c d c |

$\tau_{bc} = \tau_{bd} = k_f[Cl^-]$

$\tau_{ac} = k_f[Cl_2]$

$\tau_{ca} = \tau_{cb} = \tau_{db} = kb$

TABLE 3.1 (c)

where $f_A$ represents the fraction of the total chlorine nuclei in the species A.

The limiting cases correspond with intuitive expectations. Thus, in the fast exchange limit the value of $(1/T_2)$ observed is simply the mean of the $(1/T_2)_i$ weighted by the fractional populations of each site. The total chlorine concentration appears as $[Cl^-]$ in accord with the initial assumption that the chloride ion is the predominant species of the system. The meaning of the slow exchange limit requires some comment. It is clear that $k_f \rightarrow 0$ as $k_b T_{2b} \rightarrow 0$ since $k_f/k_b = K$. Thus strictly Lim $(\Lambda) = 0$, $(k_b T_{2b} \rightarrow 0)$. However it is useful to consider the case of very slow exchange as a limiting form of equation (3.8). If the exchange lifetimes are long compared with $T_{2b}$ then magnetisation in the xy plane which is lost from the A site as a result of chemical transfer will return to A only after its phase has been completely randomised by $T_2$ processes in B. Thus the rate constant for transfer of nuclei from site A to site B describes an essentially irreversible damping of the amplitude of $M_+^a$. For this limiting case, the observed line may thus be described as the Lorentzian defined by an effective $T_2$ as shown.

The $Cl_2/Cl^-$ system.

This system has a greater complexity that that discussed in the preceding paragraph since it must be treated as at least a three-site and more fully as a four-site chlorine exchange problem. On the other hand the fact that all the reacting particles are chlorine atoms introduces the useful simplification that the configuration of the ploy halide anion is no longer at issue. In this section the solutions to both the three-site and the four-site treatment of this system will be described. The author is indebted to Dr.DW. Kydon for making available the solution to three-site exchange case.

The values of the $p_{ji}$, and the site labels for the three-site treatment are tabulated in Table 3.1 (b). The expression for the line-broadening

parameter $\Delta$ is

$$\Delta = \frac{k_f[Cl_2]^o}{1 + K[Cl^-]} \cdot \left\{\frac{A + B + C + D}{E + F + G + H}\right\} \qquad (3.11)$$

where $A = \left(\frac{1}{T_{2b}^2} + \Delta\omega_b^2\right)\left(\frac{1}{k_b^2 T_{2c}^2} + \frac{5}{3k_b T_{2c}} + \frac{2}{3} + \frac{\Delta\omega_c^2}{k_b^2}\right)$

$$B = \frac{2Kk_b[Cl^-]}{T_{2b}}\left(\frac{1}{k_b^2 T_{2c}^2} + \frac{1}{k_b T_{2c}} + \frac{1}{9} + \frac{\Delta\omega_c^2}{k_b^2}\right).$$

$$C = K^2 k_b^2 [Cl^-]^2 \left(\frac{1}{k_b^2 T_{2c}^2} + \frac{1}{3k_b T_{2c}} + \frac{\Delta\omega_c^2}{k_b^2}\right)$$

$$D = \frac{4}{3}K\,[Cl^-]\,\Delta\omega_b\Delta\omega_c$$

$$E = \left(\frac{1}{T_{2b}^2} + \Delta\omega_b^2\right)\left\{\left(\frac{1}{k_b T_{2c}} + 1\right)^2 + \frac{\Delta\omega_c^2}{k_b^2}\right\}$$

$$F = \frac{2Kk_b[Cl^-]}{T_{2b}}\left(\frac{1}{k_b T_{2c}^2} + \frac{4}{3k_b T_{2c}} + \frac{1}{3} + \frac{\Delta\omega_c^2}{k_b^2}\right)$$

$$G = K^2 k_b^2 [Cl^-]^2 \left[\left(\frac{1}{k_b T_{2c}} + \frac{1}{3}\right)^2 + \frac{\Delta\omega_c^2}{k_b^2}\right]$$

$$H = \frac{4}{3}K[Cl^-]\,\Delta\omega_b\Delta\omega_c$$

The complexity of this expression derives as mentioned earlier from the algebraic rationalisation required to extract the imaginary part of $M_+^a$. As is shown in more detail in Appendix III, the situation is simplified if the contributions to the relaxation from $\Delta\omega_i$ are sufficiently small that they may be neglected. In this case (the experimental justification for which will be discussed later) it is found that the dominator of expression (3.11) becomes a perfect square such that the following reduced form for $\Delta$ is obtained:

$$\Delta = \frac{k_f[Cl_2]^o}{1 + K[Cl^-]} \cdot \frac{\left\{ \frac{1}{T_{2b}T_{2c}} + k_b\left( \frac{K[Cl^-]}{T_{2c}} + \frac{2}{3T_{2b}} \right) \right\}}{\left\{ \frac{1}{T_{2b}T_{2c}} + k_b \left( \frac{K[Cl^-]}{T_{2c}} + \frac{1}{T_{2b}} \right) + \frac{1}{3} k_b^2 K[Cl^-] \right\}} \qquad (3.12)$$

The limiting forms of this latter expression are

(i) fast exchange

$$\lim_{\substack{k_bT_{2b} \to \infty \\ k_bT_{2c} \to \infty}} (\Delta) = \frac{3[Cl_3^-]}{[Cl^-]T_{2c}} + \frac{2[Cl_2]}{[Cl^-]T_{2b}} \qquad (3.13)$$

(ii) slow exchange

$$\lim_{k_bT_{2b} \to 0} (\Delta) = k_f \frac{[Cl_2]^o}{1+K[Cl^-]} \qquad (3.14)$$

The manipulative labour involved in obtaining the full analytical solution (3.11) is very great. It is further evident that such expressions lack physical clarity, although this is not true of the limiting forms. It appears to be preferable, for systems involving exchange between more than two or three sites in which both $T_{2i}$ and $\Delta\omega_i$ must be considered, to obtain the computed spectra directly by evaluation of the matrix equation (3.6): see below, and Appendix III.

Analytical solutions to the four-site treatment of the system have been obtained for the case where $\Delta\omega_i$ (i = b,c,d) are negligible. The site labels and the $p_{ji}$ appropriate to this model are given in Table 3.1 (c). The expression for the broadening parameter $\Delta$ is

$$\Delta = \frac{k_f[Cl_2]^o}{1+K[Cl^-]} \cdot \frac{A + B + C}{D + E + F + G} \qquad (3.15)$$

where $A = \dfrac{1}{T_{2b}T_{2c}T_{2d}}$

$$B = k_b\left(\frac{1}{T_{2b}T_{2c}} + \frac{K[Cl^-]}{T_{2c}T_{2d}} + \frac{1}{2T_{2d}T_{2b}}\right)$$

$$C = k_b^2\left(\frac{1}{2T_{2b}} + \frac{K[Cl^-]}{2T_{2c}} + \frac{K[Cl^-]}{4T_{2d}}\right)$$

$$D = \frac{1}{T_{2b}T_{2c}T_{2d}}$$

$$E = k_b\left(\frac{1}{T_{2b}T_{2c}} + \frac{K[Cl^-]}{T_{2c}T_{2d}} + \frac{1}{T_{2d}T_{2b}}\right)$$

$$F = k_b^2\left(\frac{1}{T_{2b}} + \frac{K[Cl^-]}{2T_{2c}} + \frac{3K[Cl^-]}{4T_{2d}}\right)$$

$$G = \frac{1}{4}k_b^3 K[Cl^-]$$

Again, we list the limiting cases of slow and fast exchange:

(i) $\underset{k_bT_{2i}\to 0}{\text{Lim}}\ \Delta = k_f[Cl_2] = k_f\dfrac{[Cl_2]^\circ}{1+K[Cl^-]}$ (3.16)

(ii) $\underset{k_bT_{2i}\to \infty}{\text{Lim}}\ \Delta = \dfrac{[Cl_2]^\circ}{1+K[Cl^-]}\left\{\dfrac{2}{T_{2b}[Cl^-]} + \dfrac{2K}{T_{2c}} + \dfrac{K}{T_{2d}}\right\}$ (3.17)

$$= \frac{2[Cl_2]}{[Cl^-]T_{2b}} + \frac{[Cl_3^-]}{[Cl^-]}\left(\frac{2}{T_{2c}} + \frac{1}{T_{2d}}\right)$$

In addition, a complete numerical solution for the four-site case in which shift parameters are retained has been computed. The details of the method used will be found in Appendix III; it is sufficient here to say that this is a numerical solution to the matrix equation (3.6). This solution may be easily extended to the general exchange problem involving n sites. The form of the computation is such that all elements of the $\underline{M}_y$ vector may be calculated in a straightforward manner as a function of $\omega$, although for present purposes it is adequate to obtain only $M_y^a$.

It is appropriate, by way of general conclusion to this section, to comment on the choice of methods for calculating the effect of chemical exchange on the n.m.r. spectra of the $^{35}Cl$ (or other similar quadrupolar) nucleus.

The modified Bloch equation method here used is comparatively easily set up and solved. The theory is essentially classical: situations in which for example the scalar coupling of spins must be considered requires treatment by quantum mechanical methods (Johnson, 1966).

One assumption of the modified Bloch equations must be mentioned and justified: that the spin dephasing in the transition state is negligible. This requires that the lifetime of the transition state and the proportion of particles in the transition state configuration at any time be small; and also that the magnetic properties of the transition state be normal. This appears to be amply justified: for example, the lifetime of the transition state, estimated approximately from the absolute theory of reaction rates (Laidler, 1959), is about 1ps. This time is several orders of magnitude less than the precession period of the spin, and thus the condition is fulfilled.

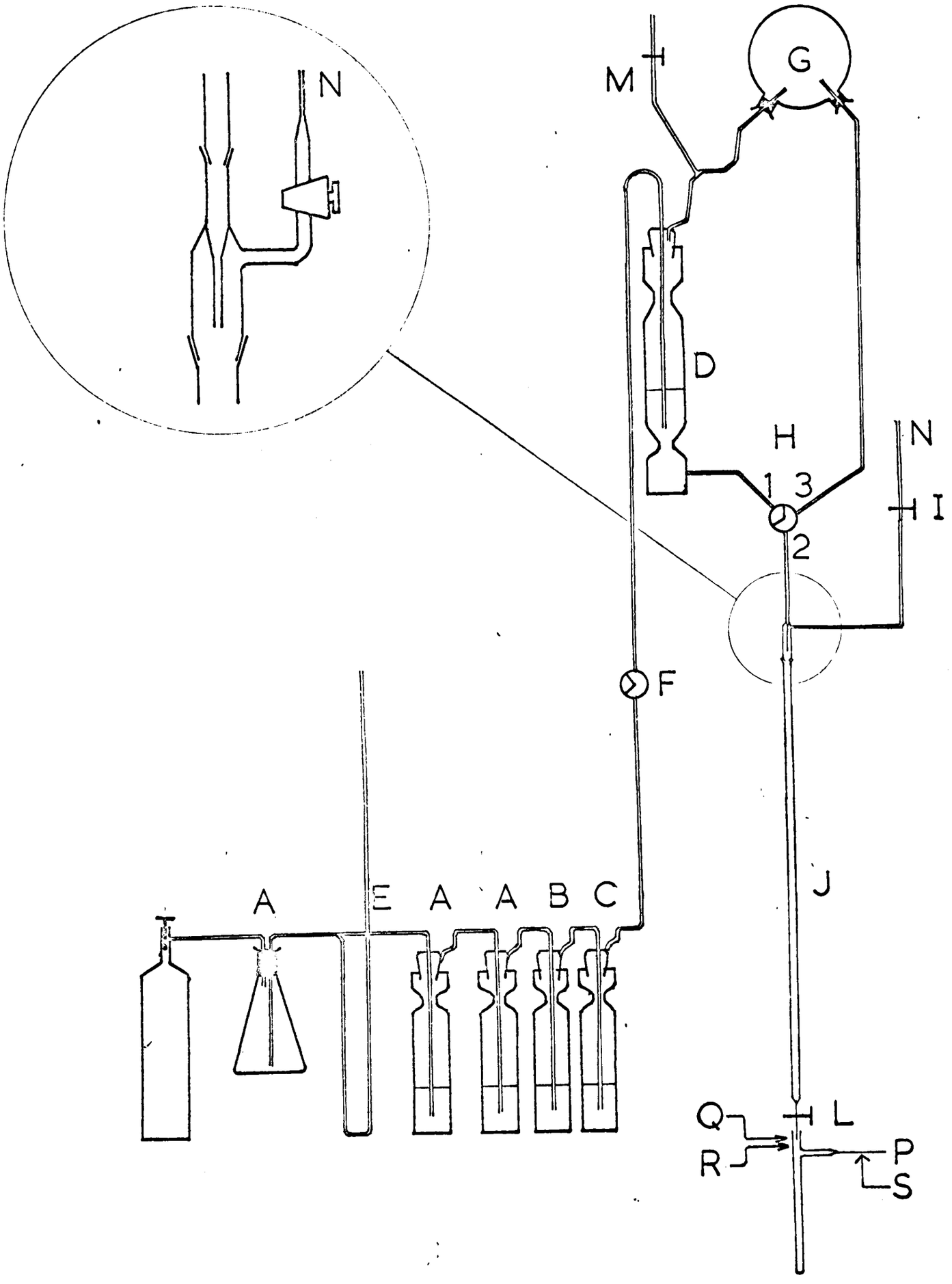
## 3. Experimental Aspects

### i. Preparation of samples and their analysis

Considerable difficulty was encountered initially in the preparation of samples containing reproducible and accurately known amounts of chlorine. Ultimately an essentially closed system was evolved: the arrangement of the line is shown in Figure 3.1. It was found that even a very brief exposure of one or two seconds of an aqueous chlorine solution to the atmosphere could result in appreciable loss of chlorine. The system used avoided exposure of this sort and maintained a pure chlorine atmosphere over all liquids in the apparatus. Only at the final stage, in which the aliquots of solution are sealed into sample tubes for n.m.r. measurements did equilibration of the chlorine gas between aqueous solution and an air space

Figure 3.1

Apparatus used in the preparation of chlorine-containing samples


N
M
G
D
H
N
1 3
I
2
F
A
E
A
A
B
C
J
Q
L
R
P
S

above the liquid phase occur. As a result of using sample tubes of standardised dimensions this feature was made reasonably reproducible.

Commercially-obtained chlorine gas (Air Products Ltd., 99.5%) was taken through potassium permanaganate solution (A) to remove HCl, washed (B) and dried by bubbling through concentrated $H_2SO_4$ (C) before passing through a storage vessel of doubly-distilled wateracidified with $HNO_3$ to pH1.7, which when thoroughly saturated with chlorine gas formed the source of chlorine water for the experiments described.

A blow-off manometer, filled with $KMnO_4$ solution, was inserted at E. The first part of the apparatus could be flushed with chlorine gas to the three-way tap F, or the whole system by appropriate manipulation of taps H(3-2), M, I and L. In particular the burette J was flushed out with chlorine gas before being filled with chlorine water from the storage vessel by closing tap M, the main exhaust point, and opening L.

The successful transfer of liquids in a closed system of this type depends to a large extent on the adequacy of the provision for displacement of the air or gas within it. In the apparatus described here, the presence of a positive internal pressure of chlorine enabled chlorine gas to be expelled at several points when necessary without fear of contamination by air. Thus chlorine water was transferred from the storage vessel D to the burette J by linking 1 - 2 through tap H and opening tap I, which allowed the chlorine gas displaced by the descending liquid to escape through a narrow spill at N. Similarly, in the design of the sample tubes it was found necessary to provide a spilled side-arm, P, to allow for displacement of air during the filling.

The ballast G smooths changes in the chlorine pressure during movement of liquid.

The standard sample tubes, made of extra-light wall pyrex glass tube (7mm. o.d.), were filled by volume, first with an appropriate quantity of NaCl stock solution and doubly-distilled water; they were then transferred to the burette J for addition of chlorine water. The total volume of solution sealed into the tubes was always 4.00ml. The sample tube fitted tightly on a graded rubber sleeve at Q, and after filling, was sealed with a hot flame at R and S. The filling operation was carried out according to a carefully timed programme in order that losses of chlorine should be made as constant as possible.

It should be noted that the original requirement for a system which could provide sets of sealed samples containing accurately equal quantities of chlorine was found to be extremely difficult to fulfill. In any case, an intrinsic obstacle in achieving this is imposed by the dependence of the solubility of chlorine on the chloride ion concentration of the solution. The requirement was eventually relaxed by the decision that the chlorine content of each tube should be assessed by destructive analysis. Nevertheless it was found an extremely useful feature of the preparative arrangement here described that series of samples graded in concentrations could be confidently prepared.

In analysis the sample tubes were broken at the weak neck just above the liquid surface into a flask containing an excess quantity of KI solution. By breaking at this point only the chlorine present in the liquid phase in the tubes was included in the analysis. After complete mixing with the KI and conversion of the chlorine to iodine the flask could be opened and a normal titration with thiosulphate carried out. The thiosulphate (N/100) was carefully standardised against both $KIO_3$ and $KBrO_3$.

The use of u-v spectrophotometry to supplement and confirm the wet analysis is discussed in Section 3 (iv) below.

The spectrum of chlorine dissolved in water was eventually obtained

from glass sample tubes containing water in contact with chlorine liquified under pressure. (The vapour pressure of liquid chlorine at room temperature is 7.6 bar). A thick-walled 14mm. pyrex test-tube was carefully joined to a length of 8mm. pyrex tube, narrowed and thickened at one point for sealing off. The tube was half-filled with .5M $H_2SO_4$, and chlorine was introduced through a teflon catheter. After bubbling for several hours, the tube was cooled in a block of solid $CO_2$, and liquid chlorine allowed to accumulate. When about $\frac{1}{2}$ml of liquid had collected, the tube was carefully sealed at the neck, and allowed to warm up and equilibrate. Similar tubes were prepared containing water, 1M $HClO_4$ and 1M $HNO_3$.

Materials:

NaCl, KI, $Na_2S_2O_3$, $KIO_3$, $KBrO_3$, HCl, $HClO_4$, $HNO_3$, $KMnO_4$, $H_2SO_4$
all AnalaR grade.
$N(n\text{-}Pr)_4Cl$ Eastman chemical.
$N(t\text{-}Bu)_4Cl$ BDH laboratory reagent.

ii. N.m.r. spectrometry.

N.m.r. linewidth measurements were made on a modified Varian Associates 4200B Spectrometer. Modulation and phase-sensitive detection were provided by a Princeton Applied Research Model 120 Lock-In Amplifier, which was operated at either 20Hz or 417Hz. Initially, signals were collected by pen-recorder; later, they were accumulated in a Data Laboratories Ltd. Biomac 1000 C.A.T., working in the signal-averaging mode. From this unit, spectra were output to a paper tape punch and to a pen-recorder. The standard spectrometer field sweep was used, and the address of the C.A.T. was advanced either internally or externally by triggering from the square-wave output of a Hewlett-Packard low frequency function generator. For the measurement of the very broad chlorine resonance from chlorine water, a Biomac NMR Interface was employed, the field being swept synchronously by a

ramp output from the C.A.T. itself.

$T_2$ values were obtained by direct measurement of linewidths and by various curve-fitting procedures discussed below, on the basis of the Lorentzian lineshape, for which:

width (Hz) of absorption line at half-height $\Delta\nu_{\frac{1}{2}} = (\pi T_2)^{-1}$

width (Hz) of derivative of absorption line between extreme

$$\Delta\nu_S = (\sqrt{3}.\pi T_2)^{-1}$$

$H_1$ and $H_m$ (modulation) amplitudes were carefully monitored, by standard procedures. Detailed saturation curves (signal amplitude as a function of $H_1$) were obtained on a number of selected samples to ensure that the spectra obtained were not broadened instrumentally. Wherever possible spectra were measured by sidebands to avoid the problem of modulation distortion effects. In the few cases where low frequency modulation was used to obtain absorption signals in the derivative form, modulation amplitudes were measured and kept within acceptable limits (Howarth and Richards 1966; Thompson 1968). In addition, an experimental study of the instrumental line-broadening caused by the use of excessive modulation amplitudes was made before any data were collected.

Temperature stability in the probe was maintained by a gentle flow of compressed air or nitrogen (obtained from liquid $N_2$ boil-off). Control was provided by an electrical heater, governed by a platinum resistance thermometer relay loop.

iii. <u>The measurement of n.m.r. linewidths</u>.

It is usual to obtain $T_2$ values from n.m.r. lines recorded by slow passage through resonance simply by measuring the width $\Delta\nu_{\frac{1}{2}}$ of the absorption between the points at which the amplitude has fallen to one half of its maximum value. The, for a Lorentzian line, $(\pi T_2)^{-1} = \Delta\nu_{\frac{1}{2}}$. Although

this method is satisfactory for strong signals, it is less so for noisy data. In fact, it appears to be highly inefficient in that most of the information contained within the resonance line is rejected. In addition the measured half-height linewidth depends sensitively on the estimated position of the baseline and on the line peak, both of which may be very poorly defined in a noisy resonance.

In an attempt to increase the accuracy of $T_2$ measured from linewidths, a method was devised in which a small set of independently measured widths ($2\Delta W_i$) across a resonance line together with the set of the corresponding amplitudes ($A_i$) measured from an arbitrary baseline are used to estimate a number of values of $T_2$ from each record of the resonance line. Referring to Figure 3.2 it can be easily shown that for a line conforming with the Lorentzian shape function

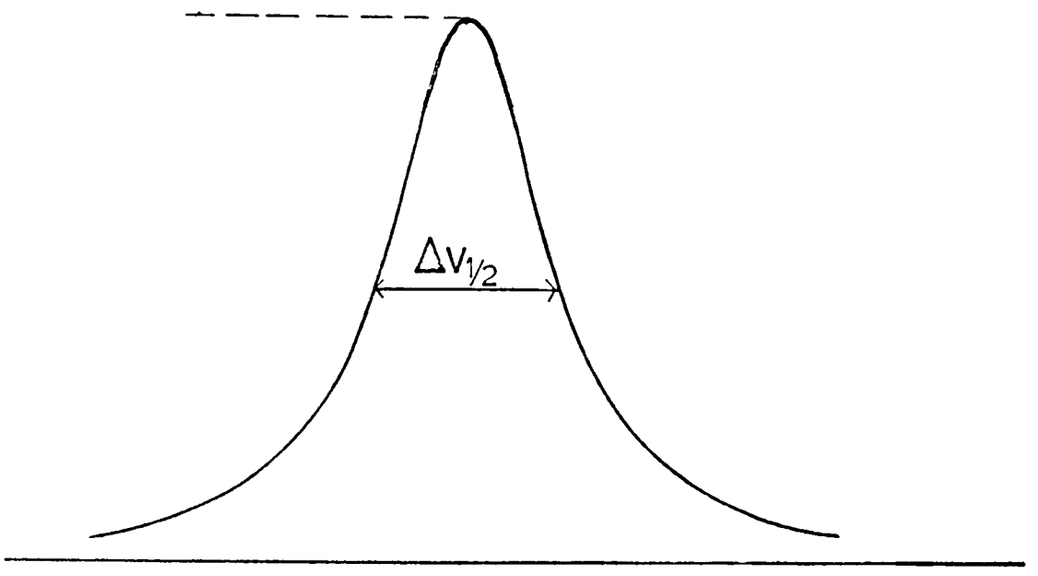
$$f(\omega) = \frac{T_2}{\pi} \quad \frac{1}{1+(\omega-\omega_o)^2 T_2^2} \tag{3.18}$$

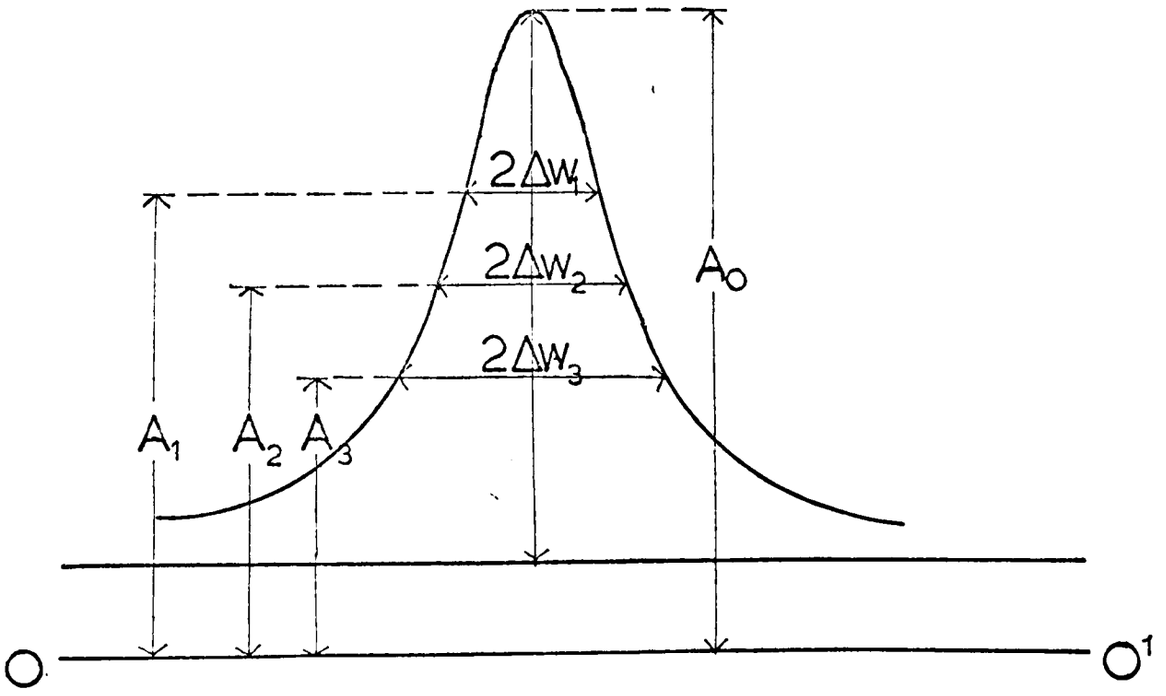
$$T_2 = \frac{\left(\frac{\Delta W_i^2 - \Delta W_k^2}{\Delta W_i^2 - \Delta W_j^2}\right) - \left(\frac{A_k - A_i}{A_j - A_i}\right)}{\Delta W_k^2 \left(\frac{A_k - A_i}{A_j - A_i}\right) - \Delta W_j^2 \left(\frac{\Delta W_i^2 - \Delta W_k^2}{\Delta W_i^2 - \Delta W_j^2}\right)} \tag{3.19}$$

$A_o$, the amplitude of the signal at the resonance frequency $\omega_o$, may of course be included in the data set $A_i$. It is clear that one value of $T_2$ may be obtained from three such measurements; however, four such measurements allow the possibility of a three-way permutation of the data and hence three values of $T_2$ may be computed. Twenty values are obtained from six measurements. It is important that the quantities $|(A_i-A_j)|$ and $|(A_i-A_k)|$ be large enough to be determined relatively accurately. The criterion applied initially was that these quantities should not be less than about one-fifth of signal amplitude. Table 3.2, columns 3 and 4 compare the results of applying this procedure to weak $Cl^{37}$ resonance lines with the results of

Figure 3.2

Diagram defines notation used in discussion of line-fitting procedures on Lorentzian resonances


$\Delta\nu_{1/2}$


$2\Delta w_1$
$2\Delta w_2$
$2\Delta w_3$
$A_0$
$A_1$
$A_2$
$A_3$
O
O'

| isotope Cl | estimated signal:noise ratio (one pass) | directly measured $\Delta\nu_{\frac{1}{2}}$ Hz | linewidth from set of widths and amplitudes | linewidth from limited Lorentz fit | 1000 point Lorentz least-sq. fit |
|---|---|---|---|---|---|
| 37 | 3:1 | $46.2\pm1$[a]<br>$49.6\pm1$[a]<br>$52.5\pm2$[d] | $48.0^{b}\pm 4$ | 51.0 | $48.6\pm .4$[c] |
| 37 | 2:1 | $92\pm 6$[e] | $91\pm 5$[f] | $93\pm 4$[g] | - |
| 37 | less than 2:1 | $140\pm 12$[h] | | | $131\pm 5$[j] |

Notes:

a mean from 6 spectra

b from set of 10 measurements from one spectrum taken in groups of 3

c 1 spectrum

d mean of three spectra

e mean of 5 spectra

f four measurements from each of 3 spectra

g seven measurements on each of 8 spectra

h four measurements on each of 7 spectra

j one spectrum

TABLE 3.2

direct half-height measurements. The comparison is disappointing. In retrospect, it is clear that the half-height width measurement is a special case of the three-point fit described here, in which the width and amplitude differences of equation (3.19) are maximised. For the baseline, the width of the line goes to infinity and the amplitude to zero; for the peak, the width goes to zero. On the other hand, when the $A_i$ differ by less than about $0.4A_o$ the calculated $T_2$ becomes very sensitive to small errors in the measured widths and amplitudes. As can be seen from Table 3.2, the standard deviation in values of $T_2$ calculated from a set of 10 such measurements is considerably greater than the standard deviation in $T_2$ calculated from 6 simple half-height linewidth measurements.

Nevertheless the uncertainty in unambiguously determining the base-line of a noisy spectrum, together with the conviction that some improvement in the definition of $T_2$ should be possible by the appropriate averaging or fitting procedure suggested that a complete least squares fit of the data to a Lorentzian line equation should be attempted.

The data smoothing procedure used to fit the n.m.r. absorption line to a Lorentzian shape function is based on the estimation of four parameters A, B, $\omega_o$ and N by the principle of least squares. The data (in the form of 1000 16-bit binary-coded values of the signal amplitudes $y_i$ at frequencies $\omega_i$) are constrained to the equation

$$f(\omega, A,B,N,\omega_o) = \frac{A}{1+N(\omega-\omega_o)^2} + B \qquad (3.20)$$

It should be noted that the dependence of f upon all parameters except B is non-linear. For any set of values of A,B,N, and $\omega_o$ and for each value $\omega_i$ of the independent variable, an $f_i$ may be calculated and compared with the corresponding observed value $y_i$. The best set of the parameters is that which minimises thesum of the squares of the residuals $|f_i-y_i|$ over all the data. In the present case all data points were given equal weight.

The programme developed (CH031, Appendix I), is based on a differential correction technique. Assuming trial values, $A^o$, $B^o$, $N^o$ and $\omega_o^o$, of the parameters, computed residuals are used to obtain improved values of A, B, N and w. The function (3.20) is expanded in a Taylor series about ($A^o$, $B^o$, $N^o$, $\omega_o^o$) retaining only first derivatives. The solutions of the set of normal equations in this case are <u>first-order</u> estimates of the quantities $A^* - A^o$ etc. where $A^*$ denotes the best value of A. Since the correction of the trial values is accurate only to first-order (due to the neglect of all derivatives beyond the first in the Taylor series expansion) the algorithm is used iteratively; in practice, convergence is rapid.

The run-time for the programme developed with only three degrees of freedom ($A^*$, $B^*$ and $N^*$ estimated) and only every fourth input data point used was 75s per iteration, on the Elliott 903 computer available. The incorporation of a fourth degree of freedom to fit the data to a best value of $w_o$ would have resulted in a prohibitively lengthy computation. Instead $w_o^*$ was first determined separately as the abscissa of the centroid of the distribution of data $(w_i, y_i)$, that is

$$\omega_o^* = \frac{\int_o^\infty f(\omega)\omega\, d\omega}{\int_o^\infty f(\omega)\, d\omega} \simeq \frac{\sum_1^{1000} (y_i - B')\omega_i}{\sum_1^{1000} (y_i - B')} \quad (\omega_i \text{ equally spaced}) \qquad (3.21)$$

where B' is an approximate value of the baseline[B] of the Lorentzian determined as the mean value of the first twenty $y_i$ of the 1000 input to the programme. In fact any $B' \geq B^*$ will give a good $\omega_o'$, providing that summation covers most of the values of i for which $y_i$ is appreciable. This restriction is designed to ensure that the data $(\omega_i, y_i)$ included in the summations are symmetrically distributed about $\omega = \omega_o^*$. In practice the best procedure is to converge on a good $\omega_o'$ from an initial value $\omega_o^o$ by repeating the calculation with summations over a range P extending from $x = \omega_o' - P$ to $x = \omega_o' + P$. This convergence is rather slow but adequate for this purpose.

iv. Spectrophotometric measurements.

Visible and near ultra-violet absorption spectra at room temperature were made on a Unicam SP800 Spectrophotometer, which was operated in the range 15000 - 42000 $cm^{-1}$.

Spectrophotometric records of the spectra from the sealed tubes prepared for n.m.r. measurements were made by supporting these long, flat-bottomed tubes in a standard 1cm path-length silica cell, which contained a mixture of 81% $CCl_4$/19% $C_6H_6$. The refractive index of this liquid matches that of the pyrex glass and reduces the scattering of light from the cylindrical surfaces of the sample tubes and helps to reduce the deviation of the light beam.

Several more accurate measurements were made using the apparatus shown in Figure 3.3 (a). In this device, a known volume of chlorine-chloride solution may be trapped below the taps A and B, and observed spectrophotometrically at the silica cell C. Then, with the bulb D containing a small quantity of strong KI solution, the tap A may be opened, and the total chlorine in the system converted to iodine by inversion. The device may now be opened and the $I_2$/KI washed out and titrated.

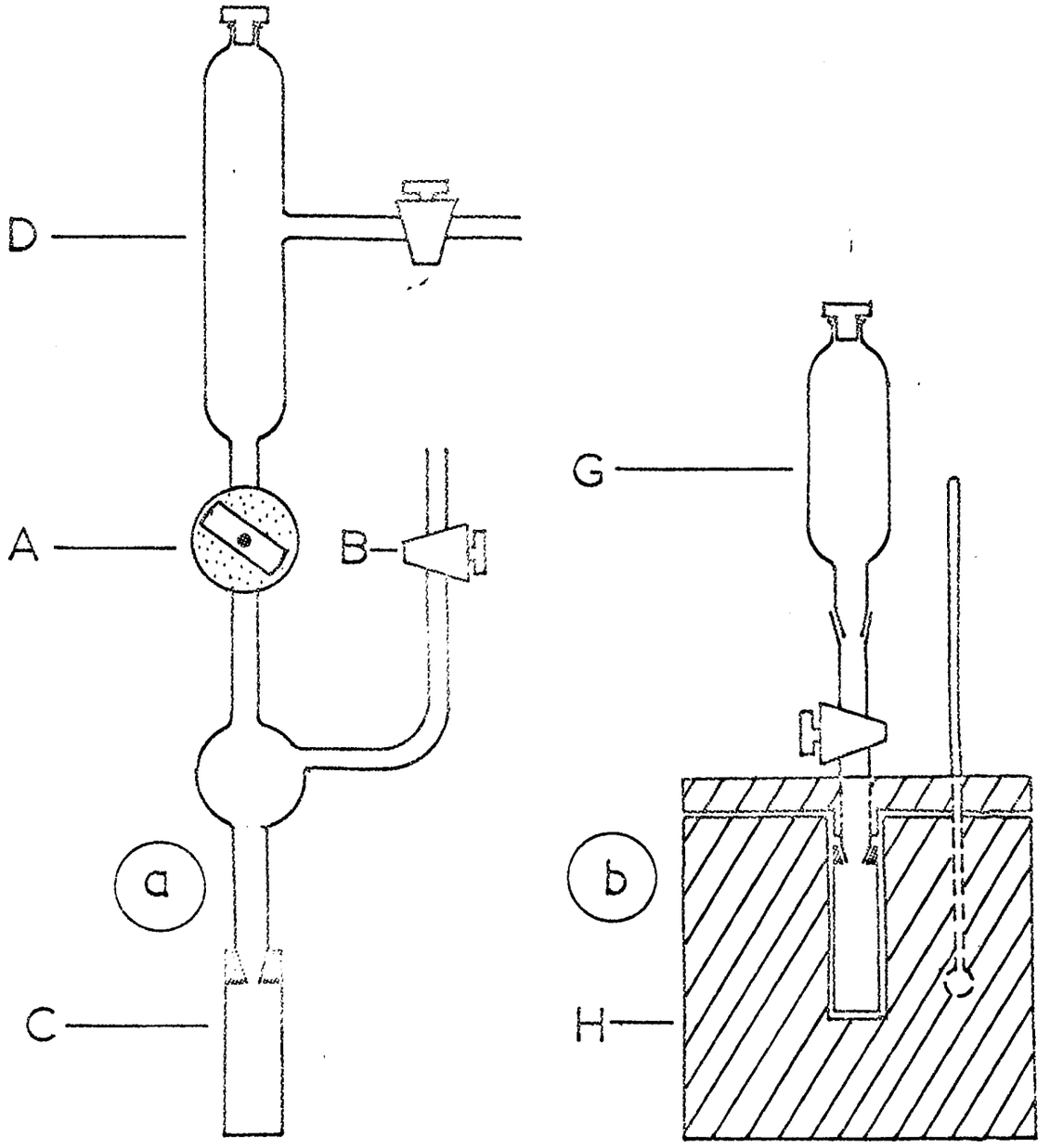
Figure 3.3 (b) shows a modification of this apparatus which was used in the variable temperature measurements of the $Cl_2$-$Cl^-$-$Cl_3^-$ equilibrium constant. The main requirement is that the volume of solution be small enough to be uniformly heated by the brass support block H; in addition, for reasons of space the mixing vessel G was not fixed in place on the cell section until after the spectrophotometry. The variable temperature measurements were carried out on a Cary 14 instrument.

Figure 3.3

Apparatus used in spectrophotometric study of chlorine/chloride ion solutions.

a Basic apparatus
b Modification used in variable temperature work

For key, see text.


D
A
B
a
C
G
b
H

## 4. Determination of subsidiary parameters

As is evident from section 2, in which expressions are derived which relate the observed broadening of the $Cl^-$ n.m.r. line caused by $Cl_2$ with the exchange rate constant, a knowledge of the chemical shifts and the relaxation times of the Cl nucleus in the covalent sites is an essential preliminary to the determination of a rate constant. In fact, if these parameters are known, then in principle a single measurement of $\Delta$ yields a value of $k_b$. Conversely, experimental data for the concentration or temperature dependence of $\Delta$ would in principle enable $T_{2b}$, $T_{2c}$ and $T_{2d}$ to be determined experimentally. However the comparatively limited accuracy of the experimental determination of $\Delta$ suggests that a preferable procedure lies in attempting independent measurements or estimates of $T_{2i}$ and $\Delta\omega_i$. This aspect of the present problem is discussed in this Section. Then section 5 contains the results of the computations made on the basis of these estimates and the equations of Section 2. The comparison of the computed and the experimental results is given in Section 6.

### i. The chemical shifts of $^{35}Cl$ and $^{37}Cl$ in $Cl_2$ and $Cl_3^-$.

The $^{35}Cl$ n.m.r signal of a sample of pure liquid chlorine has been recorded over a range of temperature. Both the shift and linewidth parameters were measured and are listed in Table , from where it may be seen that the $^{35}Cl$ chemical shift relative to aqueous saturated NaCl almost certainly lies below an upper limit of 500 p.p.m. There is no evidence in this data for important temperature dependence of the shift. After several unsuccessful attempts were made to observe the $^{35}Cl$ resonance from chlorine water under normal conditions, the signal was eventually recorded from a sample containing chlorine under pressure. (For experimental details, see Section 4.i.) Signal-averaging of 2150 passages through resonance produced a signal-to-noise ratio of 4.5:1. The shift relative to aqueous $Cl^-$ was approximately 430p.p.m. to low field. This and other details are assembled in Table 3.3.

It would be surprising if the chemical shift of $Cl_3^-$ were of a different order from that of $Cl_2$ itself. The results of measurements made on systems thought to contain the trichloride ion in relatively high concentrations support this view. It is known ( Chattaway and Hoyle 1923) that higher tetra-alkylammonium chlorides absorb equimolar quantities of chlorine very slowly to form solid trichlorides. There is also spectroscopic evidence (Evans and Lo 1966a) that the solution of these materials in benzene and methyl cyanide contains the trichloride ion. $^{35}Cl$ n.m.r. spectra were recorded from chlorinated solutions of tetra-n-propylammonium chloride in methyl cyanide and also from solutions of the chlorinated solid tetrabutylammonium chloride in the same solvent. In all cases the ratio of trichloride/chloride, as determined by thiosulphate titration, was not greater than 10%. The experiment was hampered by the broadness of the $^{35}Cl$ line observed from these salts even in the absence of $Cl_2$. This fact made shift determinations very inaccurate; the data obtained indicate that the $Cl_3^-$ shift to low field of $Cl^-$ is approximately $150\pm150$ parts/$10^6$.

ii. Relaxation times in the bound sites.

The values of the parameter $T_{2b}$, $T_{2c}$ and $T_{2d}$ for the $Cl^-/Cl_2$ exchange and of the parameter $T_{2b}$ for the $Br_2/Cl$ system have, with one exception, proved not to be independently determinable by direct n.m.r. experiment. The exception is provided by $Cl_2$, the $^{35}Cl$ linewidth of which as a function of temperature is given in Table 3.3. It has not been possible to obtain the remaining species in sufficiently high concentrations to make direct observation on their $^{35}Cl$ resonances possible.

Alternatively values of $T_2$ may be estimated from the known nuclear electric quadrupole coupling constants and estimates of correlation times, using the relation:-

$$\left(T_2^{-1}\right)_q = \frac{3}{40} \cdot \frac{2I+3}{I^2(2I-1)} \left(1 + \frac{\eta^2}{3}\right)\left(\frac{e^2Qq}{\hbar}\right)^2 \tau_c \qquad (3.22)$$

In the following sections, such estimates of the relaxation times of the

| system | T | shift[1,2] | $\Delta\nu_s$ | $T_2$ | $\eta^3$ | $T_2\eta/T$ |
|---|---|---|---|---|---|---|
| | (K) | (p.p.m.) | (kHz) | ($\mu$s) | (cp) | ($\mu$s-cp/K) |
| liq. $Cl_2$ | 206 | $-130\pm150$ | $14.4\pm.75$ | $12.8\pm.5$ | 0.655 | $.040\pm.002$ |
| liq. $Cl_2$ | 220 | $-340\pm150$ | $11.3\pm.75$ | $16.3\pm.7$ | 0.573 | $.042\pm.002$ |
| liq. $Cl_2$ | 235 | $-340\pm150$ | $9.7\pm.5$ | $18.9\pm.8$ | 0.490 | $.039\pm.002$ |
| liq. $Cl_2$ | 298 | $-370\pm75$ | $6.0\pm.5$ | $30.6\pm1.0$ | - | - |
| $Cl_2/H_2O$ | 300 | $-430\pm75$ | $13.0\pm.5$ | $14.1\pm0.5$ | 0.84 | $.040\pm.002$ |

Notes:

1. Measuring frequency (liquid $Cl_2$ system): 5.344 MHz
2. Shift expressed relative to $^{35}Cl$/saturated aqueous NaCl at 25°C.
   A <u>negative</u> shift is to <u>low</u> field of reference.
3. International Critical Tables (VII), interpolated.

TABLE 3.3

various bound sites participating in the exchange equilibria are made from considerations of:

1. experimentally available quadrupole coupling constants, mostly determined by pure quadrupole resonance spectroscopy;
2. correlations between observed quadrupole coupling constants and other molecular parameters;
3. the Townes-Daily analysis of these quadrupole coupling constants;
4. n.m.r. correlation times calculated from quadrupole coupling constants and nuclear magnetic relaxation times, where both are known.

a. The quadrupole coupling constants of the halogens and polyhalides

The halogens and their compounds have been more intensively studied by pure quadrupole resonance spectroscopy than any other class of chemical materials. The halogens, the interhalogens and the polyhalides form a sub-group of such compounds for which the quadrupole coupling constant data are reasonably complete. Nonetheless there are notable gaps in it. Some values, especially of the elementary halogens, have been determined from the microwave spectra. The question of the reliability of using in the liquid phase coupling constants determined in the solid or gas phase will be discussed below.

First a general introduction to the quadrupole coupling constant is presented with particular emphasis on a semi-empirical method of calculating this parameter which will be used throughout this section.

Direct observation is possible in n.q.r. spectroscopy of the transitions between the energy levels of the nuclear quadrupole moment in the gradient of the static electric field of the molecule. The relation between the quadrupole coupling constant ($e^2Qq/h$), expressed in frequency units and the n.q.r. frequency $\nu$ is

$$\nu = E/h = \frac{(e^2Qq/h)}{4I(I-1)} [3m^2-I(I+1)] \qquad (3.23)$$

where I is the nuclear spin quantum number. The selection rule $\Delta m = \pm 1$ governs

transitions. The isotopes $^{35}Cl$, $^{37}Cl$, $^{79}Br$ and $^{81}Br$, for which $I = 3/2$, each show a single n.q.r. line, whose frequency is given by

$$\nu = \frac{1}{2} \quad \frac{e^2Qq}{h} \tag{3.24}$$

$^{127}I$ ($I = 5/2$) shows an n.q.r. spectrum of two lines, at frequencies $\nu_1 = \frac{3}{10}(e^2Qq/h)$ and $\nu_2 = \frac{3}{20}(e^2Qq/h)$. The nuclear quadrupole moments Q are known fairly accurately from atomic beam measurements and the observed nuclear quadrupole coupling constants of an isotope $\alpha$ in a series of compounds provide a direct (relative) measure of the field gradient (tensor) at $\alpha$. The interpretative aspect of n.q.r. spectroscopy is concerned with relating these observed field gradients with what is independently known of the electronic structure of the molecules.

The field gradient at a nucleus $\alpha$ in a molecule is made up of a number of contributions which may first be divided thus:

$$q_z^\alpha = q_{z,el}^\alpha + q_{z,nucl}^\alpha \tag{3.25}$$

$q_{z,nucl}^\alpha$ is simply calculable from the classical electrostatics of point charges, provided the molecular geometry is known.

$$q_{z,el}^\alpha = \sum_p \langle \Psi_p | \mathcal{H}_q | \Psi_p \rangle \tag{3.26}$$

where the electrons are labelled by p.

$$\mathcal{H}_q = \frac{3\cos^2\theta_{p\alpha} - 1}{r_{p\alpha}^3} \tag{3.27}$$

From this point the calculation of $q_z^\alpha$ may be carried through at various levels of approximation, depending on the nature of the electronic wave functions used. Townes and Dailey have given an approximate semi-empirical method of analysing quadrupole coupling constants founded on a simple molecular orbital description. This analysis has formed the basis of nearly

all non-exact discussions of the parameter.

Townes and Dailey (1949) sought to express $q_z^\alpha$ in the form

$$q_z^\alpha = A(q_z^\alpha)^\circ \qquad (3.28)$$

where $(q_z^\alpha)^\circ$ is the field gradient of the $\alpha$ nucleus in the free atom. A is then determined by the electronic structure of the molecule, making the following assumptions:

1. only valence shell electrons need be considered; the inner electrons are unperturbed by bond-formation. (This assumption, apparently drastic in view of the sensitivity of the field gradient to effects near the nucleus, may be largely mitigated by the fact that the effect is probably almost constant from molecule to atom.)
2. that contributions $q^\alpha_{z,nucl}$ from the nuclear charges are cancelled by contributions to $q^\alpha_{z,el}$ from atomic orbitals centred on these other nuclei.

We may consider an interhalogen species such as BrCl as an example. A bonding molecular orbital $\sigma_b$ may be formed between the $p_z$ orbitals of Br and Cl:

$$\sigma_b = \frac{1}{(1+\lambda^2+2\lambda S)^{\frac{1}{2}}} \left(\phi^{Cl}_{p_z} + \lambda\phi^{Br}_{p_z}\right) \qquad (3.29)$$

On the other hand, a better description of the bonding may require that the $\sigma_b$ be formed from s,p,d hybrids of Br and Cl. Thus

$$\phi^{Cl}_{hy} \simeq (1-a_s^2 - a_d^2)^{\frac{1}{2}}\, \phi^{Cl}_{p_z} + a_s\phi^{Cl}_s + a_d\phi^{Cl}_d \qquad (3.30)$$

$$\phi^{Br}_{hy} = (1- b_s^2 - b_d^2)^{\frac{1}{2}}\, \phi^{Br}_{p_z} + b_s\phi^{Br}_s + b_d\phi^{Br}_d \qquad (3.31)$$

and then

$$\sigma_b' = \frac{1}{(1+\lambda^2+2\lambda S)^{\frac{1}{2}}} (\phi^{Cl}_{hy} + \phi^{Br}_{hy}) \qquad (3.32)$$

and from (3.26) the contribution to the electric field gradient at the Cl nucleus ($\alpha$ = Cl) from the two electrons in the bonding orbital is

$$q^{Cl}_{\sigma_b} = 2\left(\frac{1}{1+\lambda^2+2\lambda S}\right)\left(\langle\phi^{Cl}_{hy}|\mathcal{H}_q|\phi^{Cl}_{hy}\rangle + \lambda^2\langle\phi^{Br}_{hy}|\mathcal{H}_q|\phi^{Br}_{hy}\rangle + 2\lambda\langle\phi^{Br}_{hy}|\mathcal{H}_q|\phi^{Cl}_{hy}\rangle\right) \tag{3.33}$$

From assumption (i) above, the last two terms are dropped.
From (3.30) it follows that

$$\langle\phi^{Cl}_{hy}|\mathcal{H}_q|\phi^{Cl}_{hy}\rangle = (1-a_s^2 - a_d^2)\langle\phi^{Cl}_{p_z}|\mathcal{H}_q|\phi^{Cl}_{p_z}\rangle + a_d^2\langle\phi^{Cl}_{d}|\mathcal{H}_q|\phi^{Cl}_{d}\rangle + 2a_s a_d\langle\phi^{Cl}_{d}|\mathcal{H}_q|\phi^{Cl}_{s}\rangle \tag{3.34}$$

because

$$\int Y_{l_1 m_1}|\mathcal{H}_q|Y_{l_2 m_2} \neq 0$$

$$\text{only if } |\, l_1 - l_2\,| = 2,\ 0$$

In the special case $l_1 = l_2 = 0$ the integral is also zero.
The Townes-Dailey theory next (i) neglects the contributions to (3.34) from the d-orbital term and the s-d cross terms and

(ii) sets $\langle\phi^{Cl}_{p_z}|\mathcal{H}_q|\phi^{Cl}_{p_z}\rangle$

(the field gradient due to 1 p-electron) equal to the free atom value ($p^5$ configuration) with a change of sign, $-q^{Cl}_{at}$.

It is customary (Gordy 1955) to compensate for the error involved in approximation (ii) above by omitting the term $2\lambda S$ in the denominator of the coefficient of eqn. (3.33).

$$q^{Cl}_{\sigma_b} = -\frac{2}{1+\lambda^2}(1-a_s^2-a_d^2)\, q^{Cl}_{at} \tag{3.35}$$

In addition, four electrons occupy the degenerate pair of p orbitals $p_x$, $p_y$. If no pi-bonding interaction occurs, these are lone-pair orbitals having essentially free-atom values.

Since

$$Tr\ (q) = 0$$

and $$q_{xx} + q_{yy} = 2q_{xx} = - q_{zz}$$

it follows that

$$q_{p_x,p_y} = 4 \times (+ \frac{1}{2} q_{at}^{Cl}) \qquad (3.36)$$

Finally, if hybridisation has occurred, then the 3s orbital has lost its spherical symmetry and is no longer pure, and gives rise to a contribution to the field gradient, $q_s$. This may be calculated from the condition that this orbital be orthogonal to $\phi_{hy}^{Cl}$. Thus

$$q_s = - 2a_s^2 q_{at}^{Cl}$$

and summing contributions, the result

$$q_{\sigma_b}^{Cl} = \left[ \frac{2}{1+\lambda^2} (1-a_s^2 - a_d^2) + 2a_s^2 - 2 \right] q_{at}^{Cl} \qquad (3.37)$$

is obtained.

For the elemental halogens, $\lambda = 1$. It is found (Table 3.4) experimentally that $q_{X_2}/q_{at} \simeq 1$ for $Cl_2$, $Br_2$ and $I_2$. From equation (3.37) this requires $a_s^2 \cong a_d$. It has been supposed from this that $a_s = a_d = 0$ as the condition $a_s = a_d$ is unlikely to hold for all three molecules. However the Townes-Dailey analysis is undoubtedly over-simplified and probably should not be used for anything but qualitative treatments of quadrupole coupling constants. In the present context its value is in providing a physical basis firmly if crudely grounded in bonding theory against which to discuss the coupling constant data available for the halogens and polyhalide ions. Out of this estimates will be made of several coupling constants not yet measured and required in the analysis of the halogen/chloride exchange equilibria.

| Nucleus | $e^2Qq_{at}$ MHz | molecule | $e^2Qq$ MHz |
|---|---|---|---|
| $^{35}Cl$ | 109.746 | $Cl_2$ | 108.95 |
| $^{37}Cl$ | 86.510 | | |
| $^{79}Br$ | 769.756 | $Br_2$ | 765.86 |
| $^{81}Br$ | 643.032 | | |
| $^{127}I$ | 2292.712 | $I_2$ | 2156 |

Ref. Lucken 1969.

(Data determined by atomic beam methods or from atomic spectra.)

TABLE 3.4

It is the purpose of this section to determine the $^{35}Cl$ quadrupole coupling constants of the species $Cl_3^-$ and $Br_2Cl^-$. As these have not yet been measured by n.q.r. spectroscopy, they will be estimated from available data on related species.

The application of the Townes-Dailey theory to the polyhalide species ions has been recently discussed by Lucken (1969). It has been pointed out above that equation (3.37) contains more parameters than can be determined from the results of one observation. It is nevertheless a striking feature of these simple halogen species and the uncharged halogens and interhalogens that none of the quadrupole coupling constants is in serious conflict with the hypothesis of pure p-$\sigma$ bonding, involving no hybridisation with s or d orbitals. This conclusion may be conveniently expressed in terms of the $p_\sigma$ populations of each atom in the molecule. If hybridisation is assumed not to occur, then the Townes-Dailey theory suggests that the observed quadrupole coupling constant will be made up of two main contributions, a quantity ($4 \times \frac{1}{2}q_{at}$) from the $p_x$ and $p_y$ lone pairs, and a quantity ($-n \times q_{at}$) from the bonding orbital, where n is the number (fractional) of p-electrons participating in the $\sigma$ bond. Thus

$$q_z^{Cl} = (2 - n)q_{at}^{at} \qquad (3.38)$$

If the assumption of no hybridisation is correct, then the total $p_\sigma$ electron population of the molecule will be approximately integral and, for example, equal to 2 for a halogen $X_2$ species, and 4 for a trihalide $X_3^-$ species. If such results are not found, then any discrepancy casts doubt on the assumption of no hybridisation. In fact as shown in Table 3.5 the evidence strongly confirms this simple model. Again, as pointed out previously, the presence of several adjustable parameters in the theory easily allows a different interpretation in individual cases. It is only when all the available data are taken together that the conclusion of simple $p_\sigma$ bonding in these species becomes much preferable to explanations involving the cancellation of s and d hybridisation terms throughout the

| molecule | nucleus | eQq/h [1] | n from equation (3.38) | | theoretical n for simple $p\sigma$ bond |
|---|---|---|---|---|---|
| | | MHz | atom | molecule | |
| $Cl_2$ | $^{35}Cl$ | 109 | 1.01 | 2.02 | 2 |
| $Br_2$ | $^{79}Br$ | 766 | 1.00 | 2.00 | 2 |
| $I_2$ | $^{127}I$ | 2156 | 0.94 | 1.88 | 2 |
| BrCl | $^{79}Br$ | 877 | 0.86 | 1.92 | 2 |
| | $^{35}Cl$ | 104 | 1.06 | | |
| ICl | $^{127}I$ | 2944 | 0.71 | 1.96 | 2 |
| | $^{35}Cl$ | 83 | 1.25 | | |
| IBr | $^{127}I$ | 2731 | 0.81 | 1.87 | 2 |
| | $^{79}Br$ | 722 | 1.06 | | |
| $NH_4I_3$ | $^{127}I$ | - | 1.80<br>0.95<br>1.25 | 4.00 | 4 |
| $RbI_3$ | $^{127}I$ | - | 1.66<br>0.94<br>1.37 | 3.97 | 4 |
| $CsI_3$ | $^{127}I$ | - | 1.64<br>0.94<br>1.37 | 3.95 | 4 |
| $KICl_2$ | $^{127}I$, $^{35}Cl$ | - | 1.65<br>0.65<br>1.65 | 3.95 | 4 |

Note 1 data from Lucken 1969

TABLE 3.5

entire series of molecules.

Thus n.q.r. spectroscopy provides some evidence that a simple $p\sigma$ bond is present in the halogens and that a three-centre two-electron bond is present in the trihalide species. Thus for $Cl_3^-$, a bonding orbital and a non-bonding orbital

$$\sigma_b = \phi^1_{p_z} + \lambda\left(\phi^2_{p_z} + \phi^3_{p_z}\right)$$

$$\sigma_{nb} = \phi^2_{p_z} - \phi^3_{p_z}$$

which are both filled provide an explanation of the bonding. $\sigma_{nb}$ is localised largely on the terminal atoms.

Figures 3.4-3.6 show the results of a number of attempts to correlate the known coupling constants of various molecules with other molecular parameters.

i. Figure 3.4 indicates the approximate linearity of $e^2Qq/h$ for the halogens, interhalogens and trihalides with the Pauling electronegativity differences of adjacent atoms. This correlation is not at all unexpected; Gordy (1953)has suggested that the ionic character of a bond may be given by

$$i = \frac{1}{2}\left|\chi_A - \chi_X\right| \qquad (3.39)$$

where $\chi_A$ and $\chi_X$ are the electronegativities of A and X. However an ionic character parameter may also be defined in terms of $\lambda$:

$$I = \frac{1 - \lambda^2}{1 + \lambda^2} \qquad (3.40)$$

If i and I are assumed to be equivalent, then $e^2Qq/h$ and the electronegativities may be directly related:

Figure 3.4

Correlation between nuclear quadrupole coupling constants and Pauling electronegativity differences (adjacent atoms) for a number of simple halogen compounds

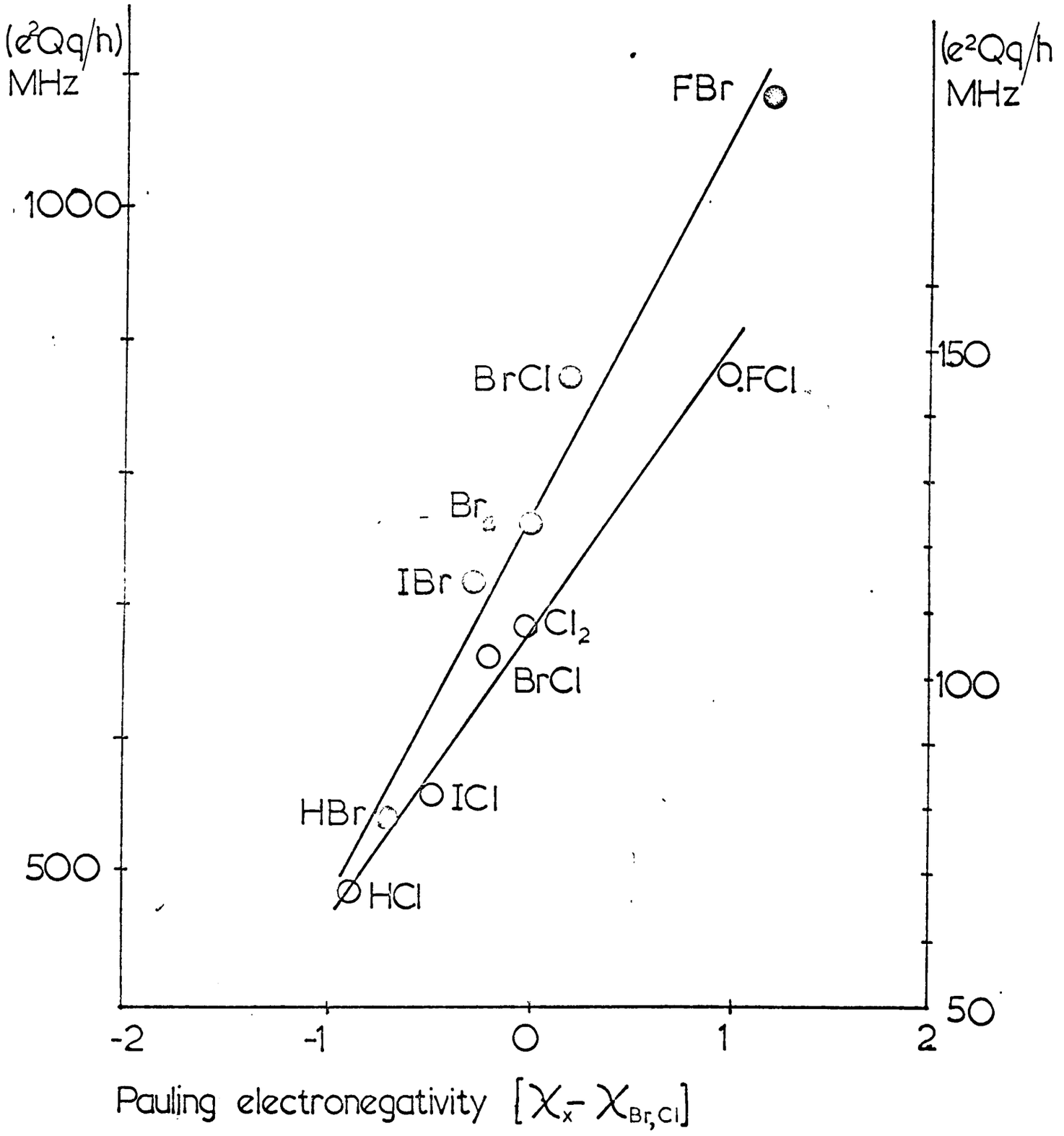

(e²Qq/h) MHz
1000
500
(e²Qq/h MHz
150
100
50
FBr
BrCl
FCl
Br₂
IBr
Cl₂
BrCl
ICl
HBr
HCl
-2
-1
0
1
2
Pauling electronegativity [χx - χBr,Cl]

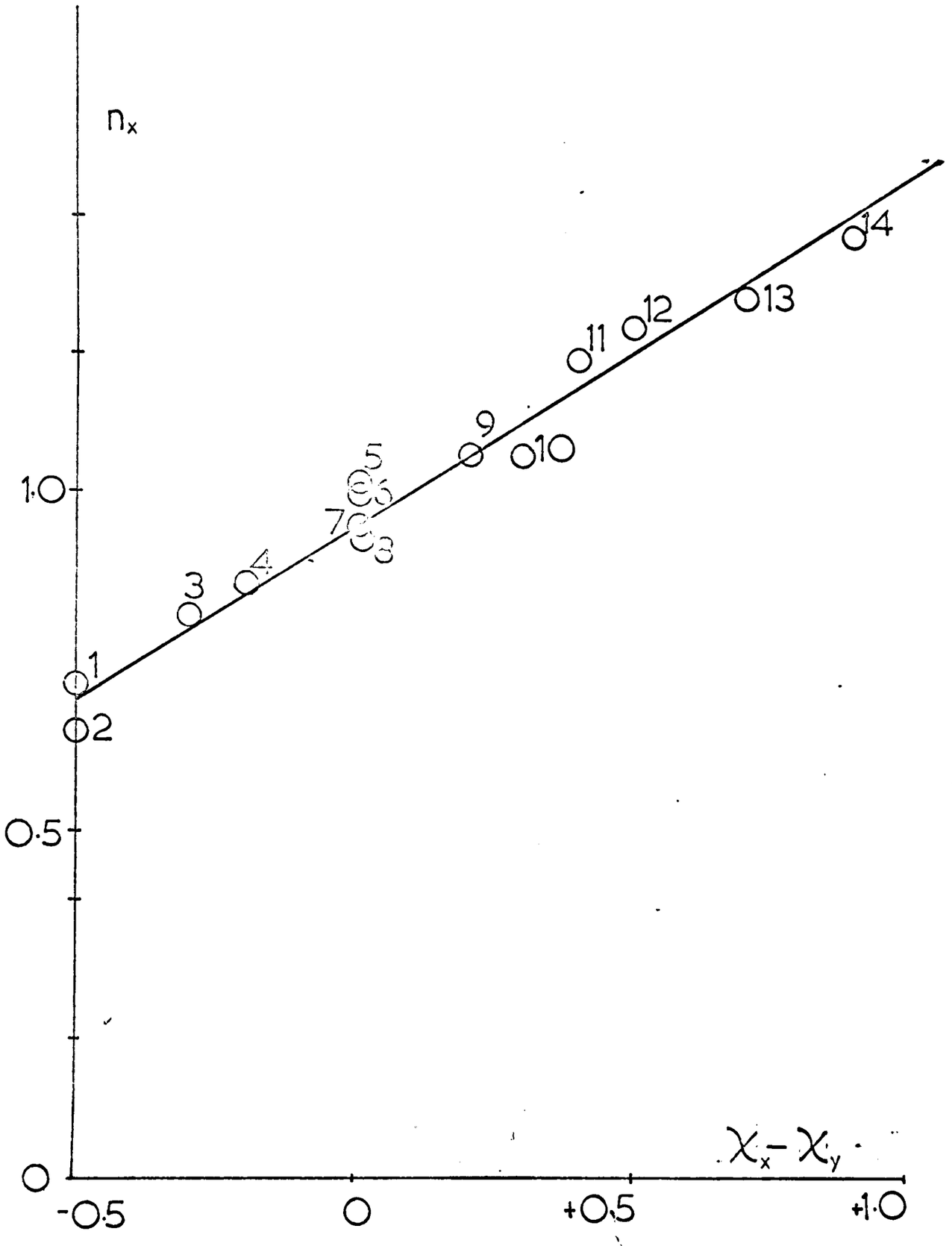
Figure 3.5

$p\sigma$ populations ($n_X$) of constituent atoms ofhalogens, interhalogens, trihalides and hydrogen halides versus Pauling electronegativity differences ($\chi_X - \chi_Y$) of adjacent atoms.

| | | | | | |
|---|---|---|---|---|---|
| 1 | ICl | (I) | 8 | $NH_4Br_3$ and $I_2$ | (-Br-) (I) |
| 2 | $KICl_2$ | (I) | 9 | BrCl | (Cl) |
| 3 | IBr | (I) | 10 | IBr | (Br) |
| 4 | BrCl | (Br) | 11 | HI | (I) |
| 5 | $Cl_2$ | (Cl) | 12 | HBr | (Br) |
| 6 | $Br_2$ | (Br) | 13 | HCl | (Cl) |
| 7 | $NH_4I_3$ | (-I-) | | | |

Values of $n_x$ calculated from nuclear quadrupole coupling constant data of Lucken (1969).

Electronegativities from Pauling (1960).


$n_x$
1·0
0·5
0
1
2
3
4
5
6
7
8
9
10
11
12
13
14
$\chi_x - \chi_y$
-0·5
0
+0·5
+1·0

$$e^2Qq^X = (1 - \frac{1}{2} \mid \chi_A - \chi_X \mid)^{at}_q \qquad (3.41)$$

Figure 3.4 shows that this simple correlation applies to a wide range of Cl-containing molecules; for a closely related series such as the trihalide anions the correlation must be considered to be a good predictor.

ii. Closely related to the $e^2Qq/h$ correlation with the electronegativity differences is the variation of the $p\sigma$ population of a particular atom with the electronegativity difference. The advantage of this for the present purpose is that it offers a means of normalising data for different atoms (I, Br and Cl) on the same scale. The central atom populations calculated from available data are listed in Table 3.5 and data of this sort are correlated with the electronegativity differences in Figure 3.5. It will be noted that the central atoms of both $Br_3^-$ and $I_3^-$ have $p\sigma$ populations of 0.95.

iii. Diesen, Wahr and Adler (1969) have suggested on theoretical grounds that a close relationship should exist between the electric field gradient generated by a chemical bond and its stretching force constant.

Their argument leads to a completely general relationship for a diatomic molecule:

$$k = e_\alpha(\frac{3}{2} q_\alpha + A) \qquad (3.42)$$

where $e_\alpha$ is the charge of nucleus $\alpha$, k is the stretching force constant, $q_\alpha = q_{zz}$ the field gradient tensor, and A is a term involving differential coefficients of the electron density function with respect to nuclear displacement. A appears to be often negligible for hydrogen; it is suggested by Diesen et al that the relation may be found to apply to other elements. $e_\alpha$ may be reinterpreted as an effective charge.

Figure 3.6

Quadrupole coupling constants of (terminal) constituent atoms of halogen species, scaled by factor $(e^2Qq_{at})^{-1}$, versus the (symmetrical) stretching force constant of bond, k. (For symmetrical triatomics, k is $k_1$ of Herzberg 1950).

| | | | |
|---|---|---|---|
| 1 | $I_3^-$ [1] | reference | GW |
| 2 | $Br_3^-$ [2] | | MF |
| 3 | $ICl_2^-$ | | HH |
| 4 | ICl | | MF |
| 5 | $I_2$ | | MF |
| 6 | IBr | | HH |
| 7 | $Br_2$ | | HH |
| 8 | BrCl | | HH |
| 9 | BrCl | | HH |
| 10 | $Cl_2$ | | EL |
| | $^{35}Cl$, | $^{79}Br$, | $^{127}I$ |

EL Evans and Lo 1966a
GW Ginn and Wood 1965
HH Hayward and Hendra 1967
MF Maki and Forneris 1967
Nuclear quadrupole coupling constant data of Lucken 1969

Notes 1. $I_3^-$: mean value of quadrupole coupling constants of both terminal atoms.

2. $Br_3^-$: mean value of the observed n.q. coupling constant of one terminal atom and the calculated value of the other; the latter calculated on the basis of $p_\sigma$ bonding.

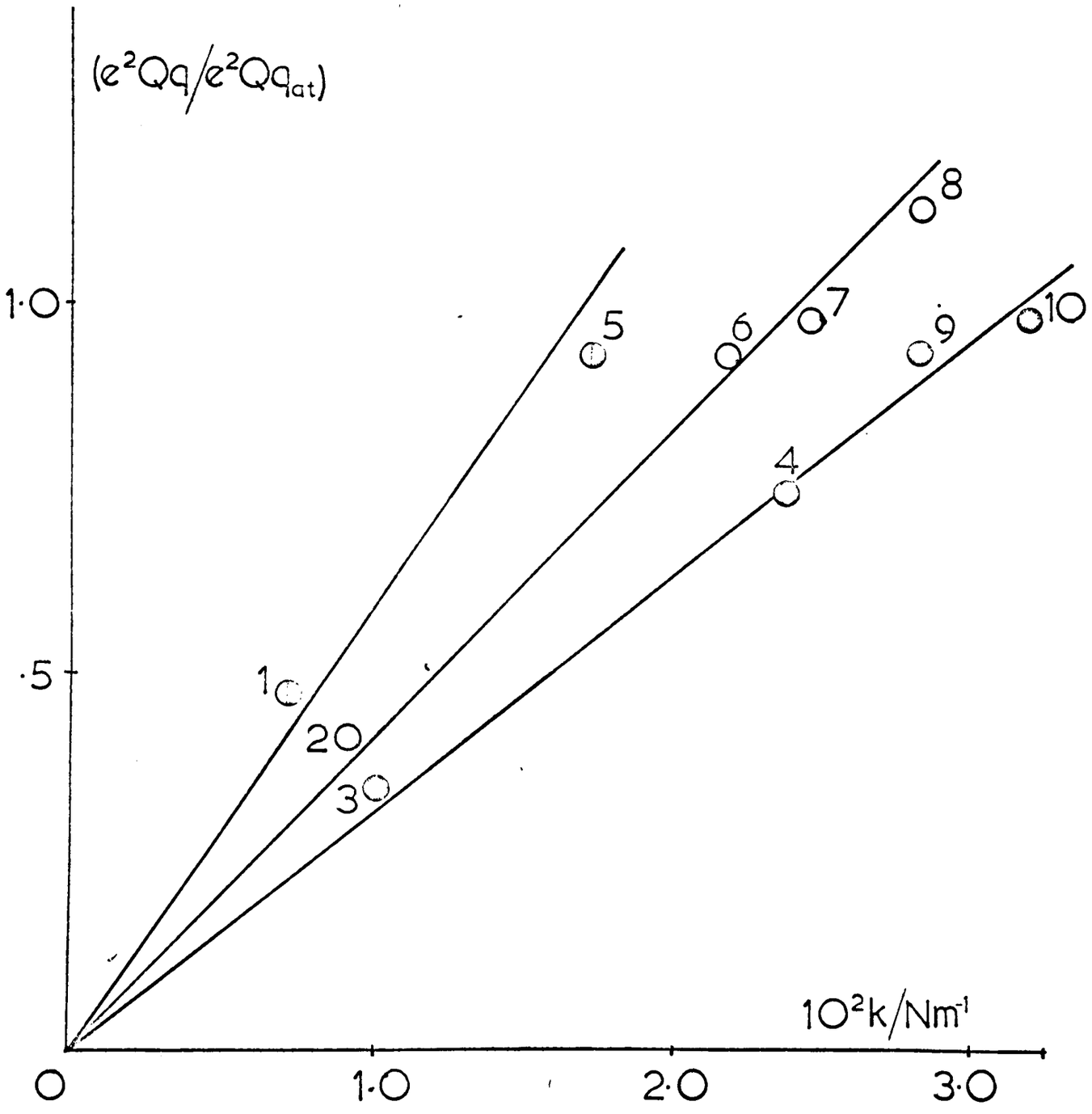

$(e^2Qq/e^2Qq_{at})$
1·0
·5
0
1·0
2·0
3·0
$10^2k/Nm^{-1}$
1
2
3
4
5
6
7
8
9
10

Figure 3.6 shows that the relation $k \propto q_\alpha$ appears to be broadly applicable to simple halogen compounds. The correlation is used here simply as further evidence in support of an estimate of the required quadrupole coupling constants.

On the basis of these data and correlations, quadrupole coupling constants can be assigned to the various species in the following way.

Table 3.5 shows that there is strong evidence of simple $p\sigma$ bonding in simple halogen molecules. It will therefore be assumed that for both $Br_2Cl^-$ and $Cl_3^-$ n = 4 ($\pm$ 0.05 assumed uncertainty). In the case of $Cl_3^-$, this assumption is equivalent to the statement that the sum of the quadrupole coupling constant of the three $^{35}Cl$ atoms equals twice the free atom coupling constant $e^2Qq_{at}$, which is given in Table 3.4. This is an important conclusion in view of the results of Section 5 which show that for the present system the predictions of the three site equations and of the four site equations are barely distinguishable. Therefore if the trichloride ion is treated as a single Cl site (as in the three site formulation of the exchange reaction) then the quadrupole coupling constant of a $^{35}Cl$ nucleus in $Cl_3^-$ simply equals two-thirds of the free atom value:

$$e^2Qq_c = \frac{2}{3} e^2Qq_{at} = 73 \text{ MHz}$$

However to make full use of the four-site treatment it is necessary to distinguish the terminal-atom and central-atom coupling constants in $Cl_3^-$. Since we have determined their sum, the task reduces to determining their ratio. This can also be done from the evidence of the $p\sigma$ populations. It is known (Lucken 1969) that n for the central atom of $Br_3^-$ is 0.95; this is the same value as found (Table 3.5) for the central atom of $I_3^-$. If we assume the value of 0.95$\pm$ 0.05 for $Cl_3^-$ also, then the ratio of the quadrupole coupling constant of the terminal atom to that of the central atom is 0.45$\pm$ 0.05. This estimate of the ratio, together with the estimate of the sum already discussed, leads directly to the most probable values

of the quadrupole coupling constants as follows:

| | | |
|---|---|---|
| $Cl_3^-$ | estimated ratio | $0.45 \pm 0.05$ |
| | estimated sum | $220 \pm 5$ MHz |
| | estimated mean | $73 \pm 2$ MHz |
| | central atom $^{35}Cl$ quadrupole coupling constant | $116 \pm 8$ MHz |
| | terminal atom $^{35}Cl$ quadrupole coupling constant | $51 \pm 5$ MHz |

In the case of $BrBrCl^-$, the dearth of n.q.r. data of any sort on unsymmetrical trihalides makes it necessary to resort to the electronegativity and stretching force constant correlations. Evans and Lo (1966b) have assigned a value of $1.0 \times 10^2 Nm^{-1}$ to the force constant $k_{BrCl}$ which suggests a $^{35}Cl$ coupling constant of about 35 MHz (see Figure 3.6). From Figure 3.5, a $p_\sigma$ population for the central atom of $\simeq 0.9$ is assigned; the remaining 3.1 units are apportioned between the terminal atoms in the same way as is found experimentally for BrCl. The resulting coupling constant is 33MHz, in very fair agreement with the previous value.

| | | |
|---|---|---|
| $BrBrCl^-$ | $^{35}Cl$ quadrupole coupling constant | $35 \pm 10$ MHz |

Correlation Times

A correlation time for the molecule $Cl_2$ in water was estimated by considering that it would be closely similar to that of MeCN in aqueous solution. The $^{14}N$ linewidth of MeCn had been reported by Herbison-Evans and Richards (1964) and its quadrupole coupling constant was known (Lucken 1969). The value derived was $1.9 \times 10^{-12}$s. The value obtained from the later experimental data on $Cl_2$ dissolved in water is $1.5 \times 10^{-12}$s (see Table 3.6).

A similar estimate of the correlation time of $Cl_3^-$ was made from the n.q.r. and n.m.r. data for the azide ion in aqueous solution. The central and terminal N atoms of this ion give rise to separate resonances and two correlation times, 4.6 and $5.6 \times 10^{-12}$s are obtained. A rounded intermediate

| system (25°) | $T_2$ ($\mu$s) | basis of $T_2$ value |
|---|---|---|
| $Cl_2/H_2O$ | 13.3 | liquid $Cl_2$ linewidth, adjusted for $\eta/T$ dependence of correln. time (1) |
| $Cl_2/H_2O$ | 11.3 | $e^2Qq/h$ of $Cl_2$, with $\tau_c$ estimated from n.m.r. and n.q.r. of MeCN, solid and aq. soln. (2) |
| $Cl_2/H_2O$ (27°) ($1NH_2SO_4$) | 14.1 | experimental determination |
| $Cl_3^-/H_2O$ | $\leq$ 4.8 (central atom) | estimated $e^2Qq/h$ and estimated correlation time (aqueous $N_3^-$) (3) |
| | $\leq$ 24.2 (terminal atoms) | |
| $Br_2Cl^-$ | $\leq$ 48 | estimated $e^2Qq/h$ and estimated correlation time |

Notes:

1. $\eta/T$, $H_2O(25°) = 3.0 \times 10^{-3}$cp/K.
2. $e^2Qq/h$, $Cl_2$= 108.95MHz; MeCN = 3.738MHz (Lucken, 1969). N.m.r. data of Herbison-Evans and Richards (1964).
3. $e^2Qq/h$, $N_3^-$ = 1.79MHz (terminal N), 1.028MHz (central N). N.m.r. data of Herbison-Evans and Richards (1964).

TABLE 3.6

value of $5 \times 10^{-12}$s is assigned to $Cl_3^-$. In view of the greater size of $Cl_3^-$ this value should probably be taken as a lower limit. In any case, this estimated correlation time is required only for guidance: in the discussion of the experimental data (Section 5) this correlation time is used as the independent adjustable parameter in the determination of the rate constant $k_b$.

For the ion $BrBrCl^-$, the same lower limit $5 \times 10^{-12}$s is considered applicable.

We may now summarise and draw together the estimates and conclusions of the previous sections concerning the shift and relaxation parameters of the bound sites. This is done in Table 3.6, which calls for only brief comment.

The parameters of $Cl_2$ were eventually determined experimentally, and the previous estimated values were therefore superseded. It is interesting that there is good agreement between the three values variously obtained.

The upper limits placed on the chemical shifts of the bound sites are such that $T_{2i}\Delta\omega_i$ are small. In the comparison of the theoretical expectations with the data the contributions of the shift terms are retained, though they are very small. In any case, the importance of such contributions in the experimental data may be assessed directly, by searching for field dependence of the line-broadening (see Section 6 (iii) e).

## 5. Discussion of effects of chemical exchange on linewidths of quadrupolar nuclei in the light of theory.

### i. Preliminaries

This section contains a short description of the behaviour of the chlorine n.m.r. line-broadenings of the $Cl^-/Cl_2/Cl_3^-$ system computed from the equations of Section 2. The emphasis is upon the general character of the results, and the dependences of the line-broadenings on various parameters are considered. In this way, this section to some extent suggests the scope of the n.m.r. line-broadening technique as a method of determining the kinetic parameters of rapidly established equilibria. In addition, this section lays the basis for the detailed consideration in the next section of the experimental data on the $Cl^-/Cl_2/Cl_3^-$ equilibrium.

The discussion is restricted to the case of one dominant species; it is difficult to formulate general conclusions about or descriptions of other, more general cases.

The four-site exchange case (equation(3.15)) is used for purposes of illustration. It is found that this is almost indistinguishable from the three-site exchange case if $T_{2c}$ for the three-site system is put equal to the weighted mean of $T_{2d}$ and $T_{2c}$ for the four-site system. The magnitudes of the $T_{2i}$ parameters used in these calculations are appropriate approximately to the $Cl^-/Cl_2/Cl_3^-$ system, (see Figure captions). In addition, the chemical shift contribution to the relaxation is ignored, since, for realistic values of the shift-between-sites parameters, this is very small.

In the following pages, it should be recalled that the equilibrium under study is

$$Cl^- + Cl_2 \rightleftarrows Cl_3^- \qquad \text{I}$$

and that the chloride ion linewidth increment is denoted $\Lambda$.

$\Delta$ will be loosely referred to throughout as the increment; it is in fact the half-linewidth increment in angular frequency units. The term "the rate constant" refers to $k_b$, the first-order rate constant for the back reaction in the equilibrium written above.

Equations (3.11) - (3.17) suggest that for the case of one dominant species the observed linewidth increment should be directly proportional to the total added chlorine concentration $[Cl_2]^o$. Consequently, it is natural to define a molar linewidth increment $\Delta_m = \Delta/[Cl_2]^o$: the (ideal) linewidth increment caused by the addition of unit amount of chlorine.

ii. <u>The dependence of the linewidth increment on the rate constant.</u>

Figure 3.7A shows the variation of $\Delta_m$ with $k_b$ ($[Cl^-]$ = 1.0 mol $dm^{-3}$). At low values of $k_b$, $\Delta_m$ is directly proportional to $k_f$. As $k_b$ increases, corresponding changes in $\Delta_m$ become more gradual. $\Delta_m$ eventually reaches a steady value, in the fast-exchange limit. Both axes of Figure 3.7 are logarithmic; when $k_b$ is less than approximately $10^4$ the broadening observed in a real system ($[Cl_2]^o \leq .02$ mol $dm^{-3}$) would probably be too minute to be observable. The region of $k_b$ within which it appears that $k_b$ can be determined satisfactorily by this method is indicated by the cross-hatching. The region of interest is therefore roughly centred upon that value of $k_b$ which is comparable with the reciprocal relaxation time of the bound sites. However this rule is only very approximate: a more precise factor is the <u>lifetime</u> ($\tau_i$) of a spin in the bound sites. In most exchanging systems at least some of the lifetimes will be proportional to concentrations, which may be varied perhaps over as much as two orders of magnitude. Thus the second line of Figure 3.7 shows the corresponding $\Delta_m$ vs. $k_b$ curve for a system containing only 0.01 mol $dm^{-3}$ concentration of chloride ion. This indicates that careful variation of concentrations may enable an unexpectedly wide range of $k_b$ to be investigated in various systems with a particular nucleus.

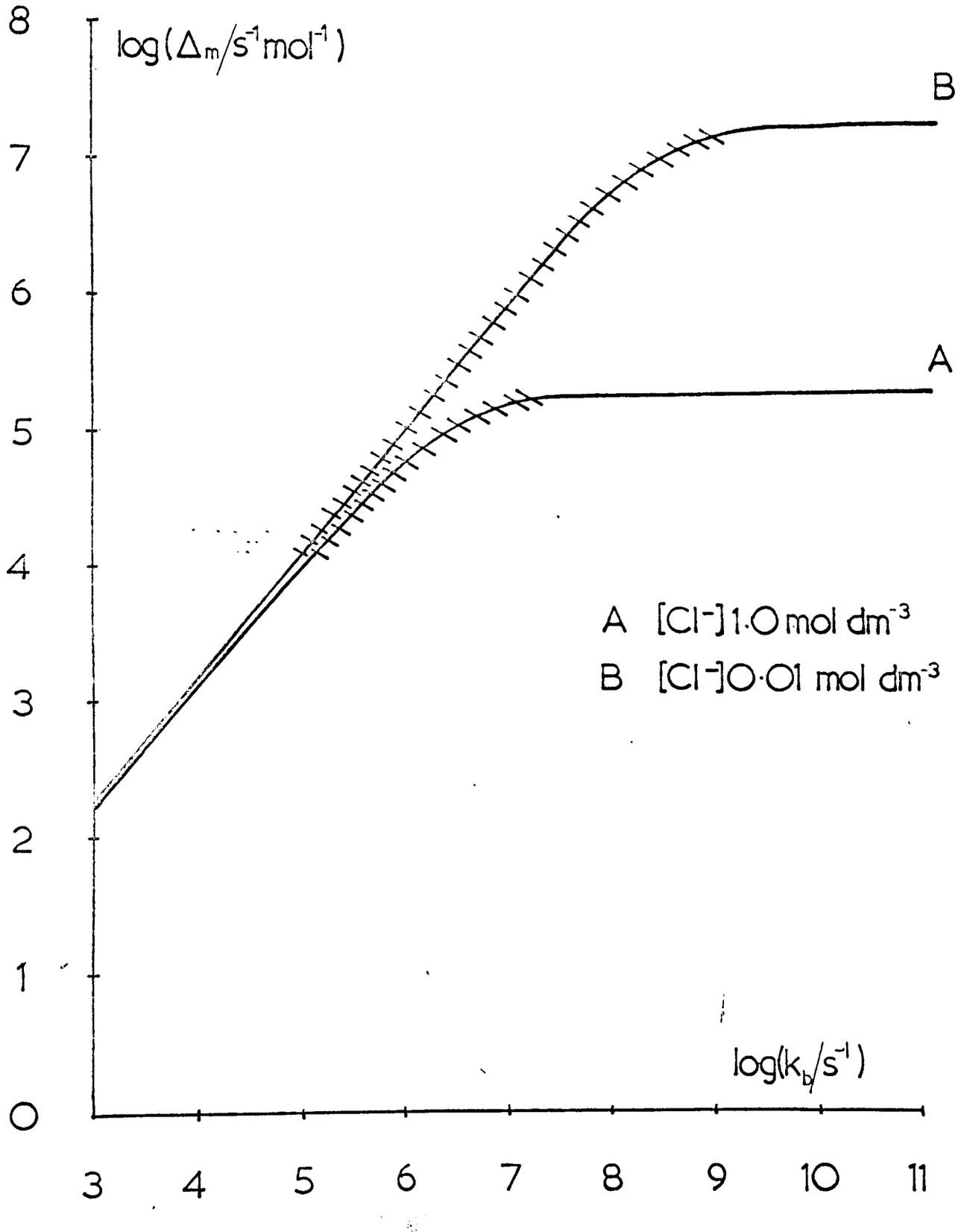
Figure 3.7

Variation of $\Delta_m$ with $k_b$, at two chloride ion concentrations

$T_{2b}$ 10.7μs

$T_{2c}$ 24.0μs

$T_{2d}$ 4.8μs


log(Δm/s⁻¹mol⁻¹)
B
A
A [Cl⁻] 1·0 mol dm⁻³
B [Cl⁻] 0·01 mol dm⁻³
log(kb/s⁻¹)
8
7
6
5
4
3
2
1
0
3
4
5
6
7
8
9
10
11

iii. Concentration dependence of the broadening as a measure of $k_b$.

The conclusions of the last paragraph suggest that the concentration dependence of $\Delta_m$ may itself be different at each value of $k_b$. This is supported by the computed results, which are shown in Figure 3.8. Here the $\Delta_m(c)$ at each value of $k_b$ have been normalised to the value $\Delta_m(1)$ computed for $[Cl^-] = 1.0$ mol $dm^{-3}$. It is clear that the concentration dependence of $\Delta_m$ shows sizeable variations with $k_b$. This of course is a direct result of the manner in which the concentrations of the sites are linked through the equilibrium constant.

In cases where a good value of the equilibrium constant is available, least-squares fitting to curves of this sort could be a sound method of determining the best value of $k_b$ from the experimental $\Delta_m$ data.

iv. $\Delta_m(k_b,c)$ for two isotopes.

We consider next an interesting feature of the exchange broadened spectra which is predicted for systems containing two isotopes, both of which are quadrupolar and observable by n.m.r. $^{37}Cl$ and $^{35}Cl$ constitute such a pair, and other notable examples are $^{79}Br$ and $^{81}Br$, $^{6}Li$ and $^{7}Li$, $^{121}Sb$ and $^{123}Sb$, $^{85}Rb$ and $^{87}Rb$, $^{69}Ga$ and $^{71}Ga$. In general the two isotopes (I and II) have different quadrupole moments (eQ) and the $T_{2i}$ values for each site i are thus different for the two isotopes:

$$T_{2i}^{I} / T_{2i}^{II} = (eQ^{II} / eQ^{I})^2 \qquad (3.44)$$

provided that I and II have the same spin. Comparison of the line-broademings produced in the resonance line of each isotope provides essentially a differential method of determining the rate constant. We can distinguish the two limiting cases in simple physical terms:
i) In the presence of very slow exchange, the linewidth increment is simply proportional to the forward rate constant, and independent of the relaxation times of the bound sites. On the timescale of the exchange process the

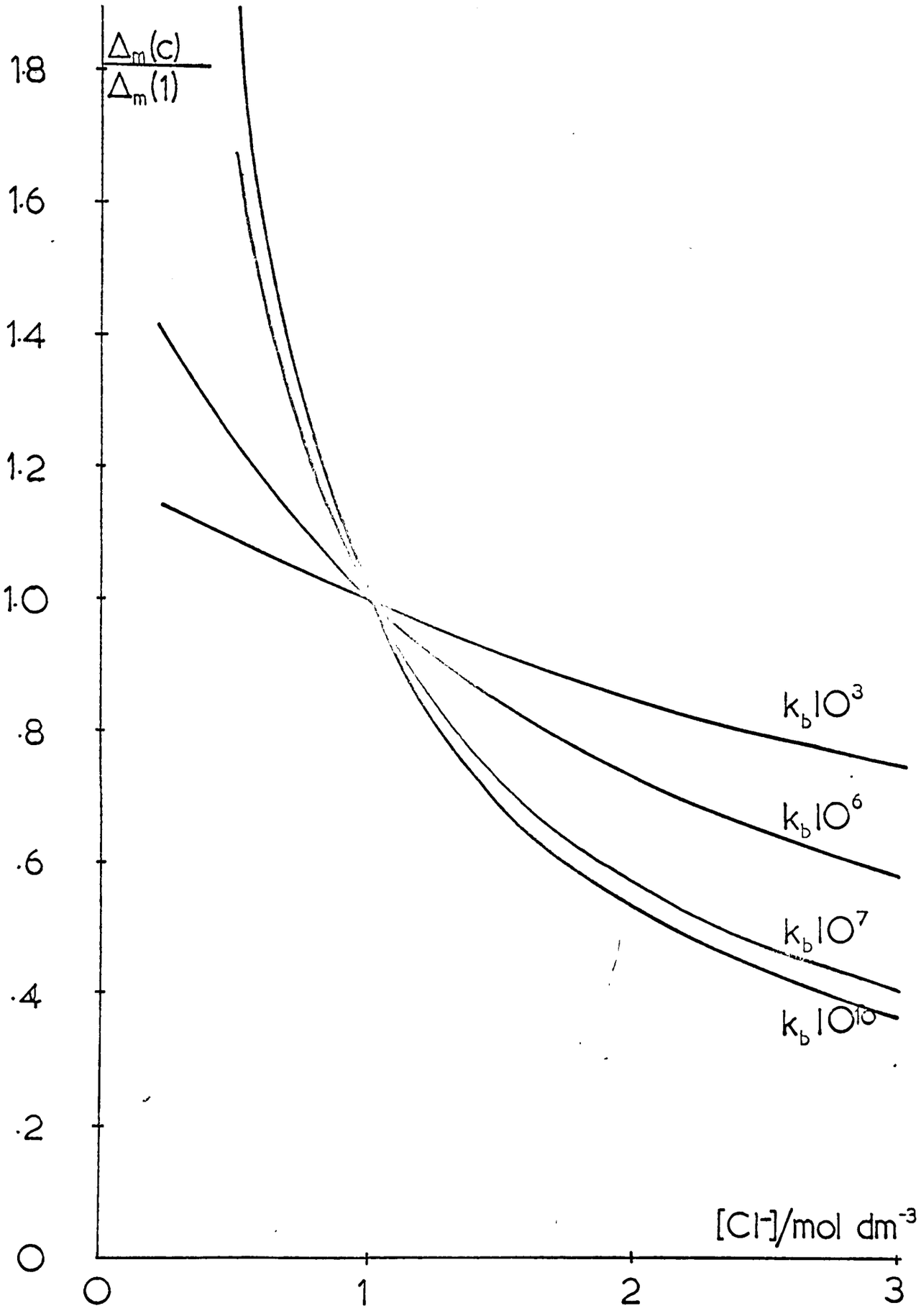
Figure 3.8

Chloride ion concentration dependence of $\Delta_m(c)$, normalised to unity at $\Delta_m(1)$, at four values of $k_b$

$T_{2b}$ 10.7μs

$T_{2c}$ 24.0μs

$T_{2d}$ 4.8μs


$\frac{\Delta_m(c)}{\Delta_m(1)}$
1·8
1·6
1·4
1·2
1·0
·8
·6
·4
·2
0
0
1
2
3
[Cl⁻]/mol dm⁻³
$k_b 10^3$
$k_b 10^6$
$k_b 10^7$
$k_b 10^{10}$

relaxation of the nuclear spin state of either isotope in a chloride ion which jumps into a minor site is relatively instantaneous. In other words, the perturbed n.m.r. line of the chloride ion is not sensitive to the differences in $T_{2i}$ between I and II, for small values of $k_f$.

ii) In the limit of fast exchange, all chlorine nuclei experience an averaged environment. In this case, the relaxation time for each isotope may be simply expressed as follows

$$(T_2^I)^{-1} = (A_I e^2 q^I Q^I)^2 \tau_c^I$$
$$(T_2^{II})^{-1} = (A_{II} e^2 q^{II} Q^{II})^2 \tau_c^{II} \qquad (3.45)$$

The quantities $q^I$ and $q^{II}$ may be equated immediately; the field gradient in a molecule should show no differences (except possibly for very light elements) upon substituting one isotope for another. The factors $A^I$ and $A^{II}$ depend on the size of the nuclear spin, I

$$A = \frac{3}{40}[(2I + 3)/I^2(2I - 1)] \qquad (3.46)$$

The two isotopes of chlorine, mass numbers 35 and 37, have the same spin, as do the pair of Br isotopes, so that for these species the A factor cancels also. In general the A factor must be retained and may lead to a useful enhancement of the utility of measurements on an isotope pair. Finally the correlation times $\tau_c^I$ and $\tau_c^{II}$ should be considered: a priori, these quantities may be expected to differ. The size of the difference will depend on the nature of the motion to which the correlation times refer. It will depend also on the mass ratio of the two isotopes, and may be expected to be larger for light elements. However, in the case of chloride ions $\tau_c^I$ and $\tau_c^{II}$ may confidently (to a very good approximation) be equated: the available evidence (O'Reilly and Schacher 1963) suggests that rotational motion in liquids, which governs the quadrupolar relaxation of these isotopes, is largely determined by molecular volume rather than by molecular masses. This approximation might not be valid for light elements

if the relaxation were governed by vibrational motion, for example (Valley 1960). The matter of the kinetic isotope effect (explicitly, the influence of isotopic mass on $k_b$, rather than on $T_{2i}$) will be raised briefly at the end of this section.

Figures 3.9 and 3.10 show the computed variation of the linewidth increments ($\Delta_m^{37}/\Delta_m^{35}$) for the two Cl isotopes as a function of $k_b$. The first figure shows the variation calculated for the three site case, at two concentrations of chloride ion. There is, as expected, a smooth sigmoidal transition from the slow exchange ratio (1.0) to the fast exchange limiting ratio (0.62). The reduction in chloride ion concentration simply produces a displacement of the transition region to higher values of $k_b$. The second figure shows the results obtained from computations on the four-site case. Here an unexpected maximum appears in the vicinity of the transition. This is apparently associated with the presence of two distinct sites in the trichloride ion with different relaxation times.

It can be seen that the concentration dependence of the increment ratio for the two isotopes ($\Delta_m^{37}/\Delta_m^{35}$) is very marked over the transition region. This is shown more clearly in Figure 3.11, where it can be seen that the theory predicts a very clear experimentally observable difference in the isotope ratio over as small a change in $k_b$ as a factor of 2 in the middle of the transition region. Thus, in principle, and in a favourable case, measurement of differential linewidth increments for such a pair of isotopes provides another experimental procedure for determining $k_b$.

Up to this point it has been assumed that the n.m.r. spectra of the $^{35}Cl$ and $^{37}Cl$ isotopes effectively constitute two observations of the same dynamical processes. In fact, it can be expected that there will be a kinetic isotope effect causing differences between the rate constants for the two isotopes. In the present case this may be assumed to be negligible. In general isotope effects are difficult to observe for elements other than

Figure 3.9

Variation of $\Delta_m^{37}/\Delta_m^{35}$ with $k_b$ for the three-site model, at two chloride ion concentrations

$T_{2b}$ 10.7μs

$T_{2c}$ 17.6μs

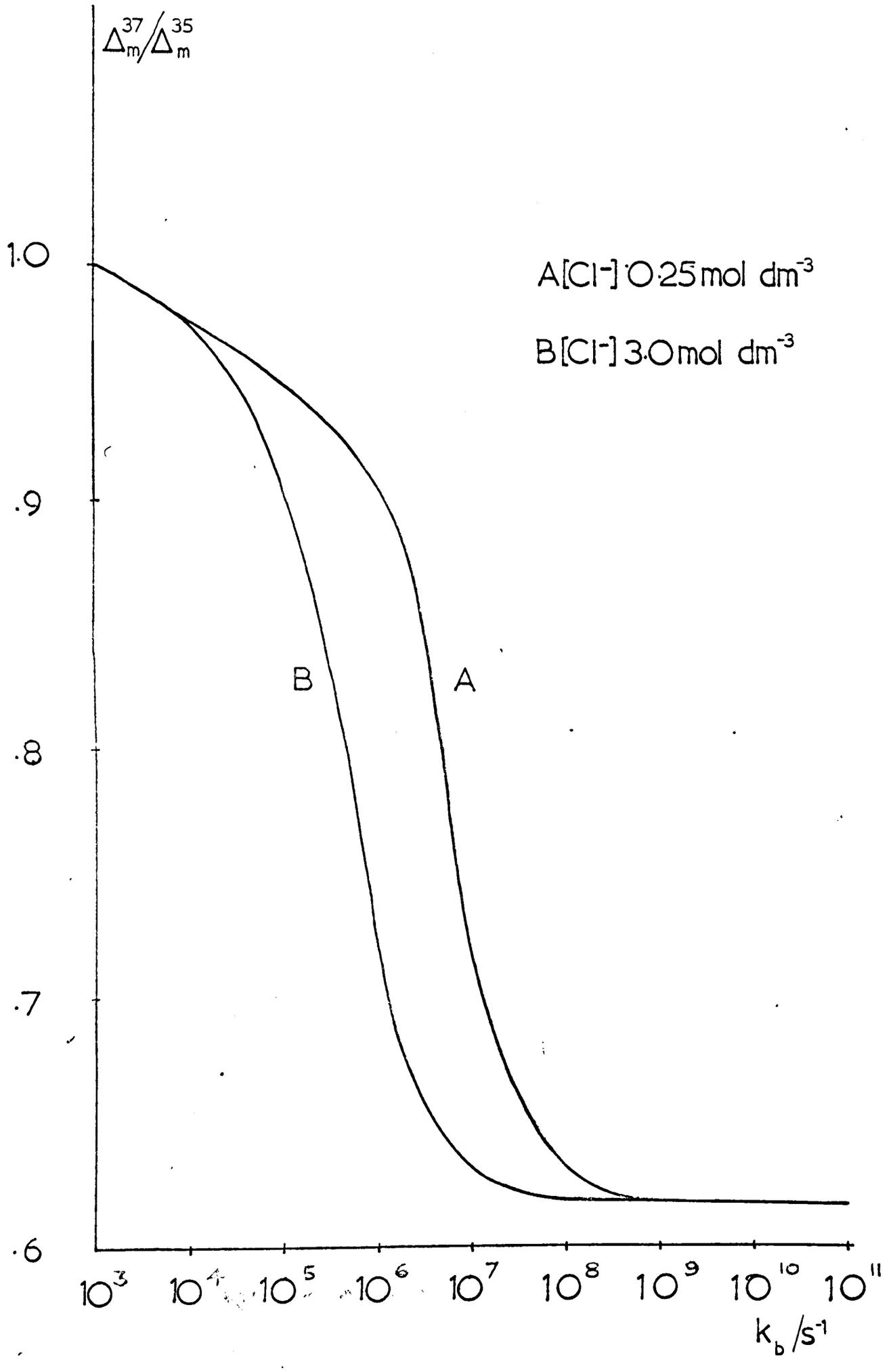

$\Delta_m^{37}/\Delta_m^{35}$
1·0
·9
·8
·7
·6
A [Cl⁻] 0·25 mol dm⁻³
B [Cl⁻] 3·0 mol dm⁻³
B
A
$10^3$ $10^4$ $10^5$ $10^6$ $10^7$ $10^8$ $10^9$ $10^{10}$ $10^{11}$
$k_b$ /s⁻¹

Figure 3.10

Variation of $\Delta_m^{37}/\Delta_m^{35}$ with $k_b$ for the four-site model, at three chloride ion concentrations

$T_{2b}$ 10.7μs

$T_{2c}$ 24.0μs

$T_{2d}$ 4.8μs

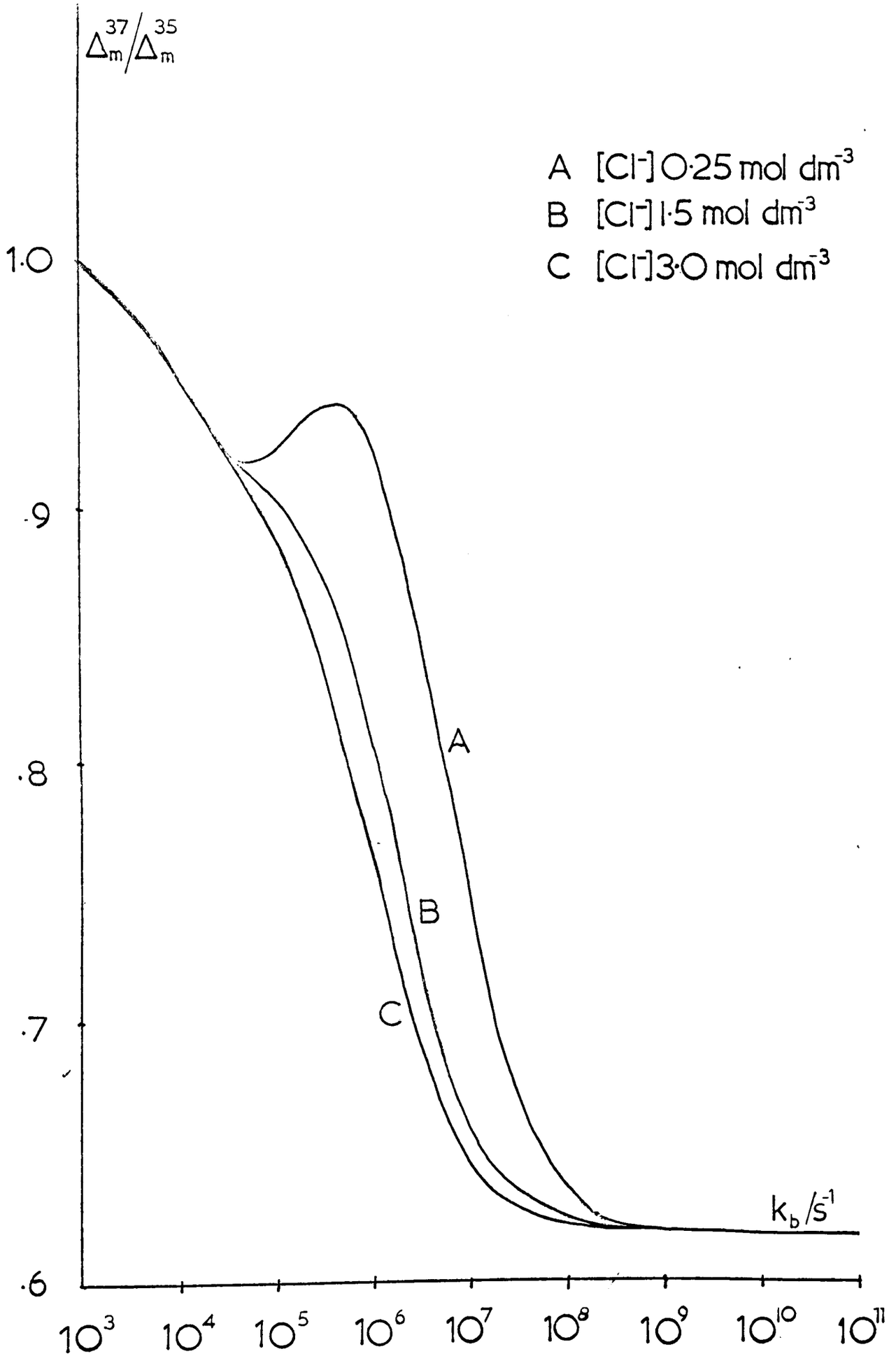
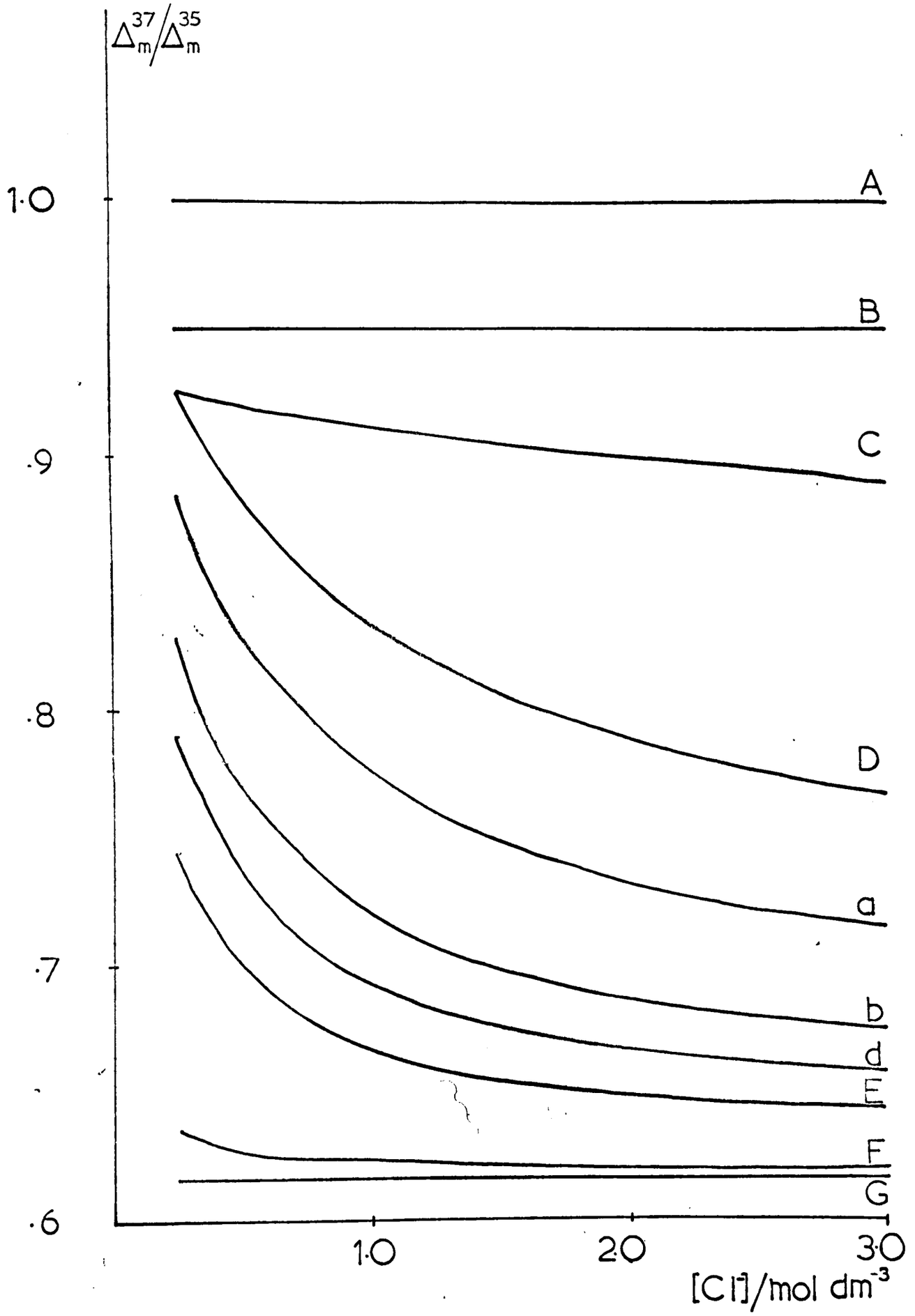

$\Delta_m^{37}/\Delta_m^{35}$
A [Cl⁻] 0·25 mol dm⁻³
B [Cl⁻] 1·5 mol dm⁻³
C [Cl⁻] 3·0 mol dm⁻³
1·0
·9
·8
·7
·6
A
B
C
$k_b/s^{-1}$
$10^3$ $10^4$ $10^5$ $10^6$ $10^7$ $10^8$ $10^9$ $10^{10}$ $10^{11}$

Figure 3.11

Chloride ion concentration dependence of $\Delta_m^{37}/\Delta_m^{35}$ at a number of different values of $k_b$.

| Key: | | $k_b/s^{-1}$ |
|---|---|---|
| | A | $1 \times 10^3$ |
| | B | $1 \times 10^4$ |
| | C | $1 \times 10^5$ |
| | D | $1 \times 10^6$ |
| | a | $2 \times 10^6$ |
| | b | $4 \times 10^6$ |
| | d | $6 \times 10^6$ |
| | E | $1 \times 10^7$ |
| | F | $1 \times 10^8$ |
| | G | $1 \times 10^{10}$ |

| | | |
|---|---|---|
| $T_{2b}$ | ($^{35}Cl$) | 10.7μs |
| $T_{2c}$ | ($^{35}Cl$) | 24.0μs |
| $T_{2d}$ | ($^{35}Cl$) | 4.8μs |
| eQ | ($^{35}Cl$) | $-7.9 \times 10^{-26} ecm^2$ |
| eQ | ($^{37}Cl$) | $-6.21 \times 10^{-26} ecm^2$ |


$\Delta_m^{37}/\Delta_m^{35}$
1·0
·9
·8
·7
·6
A
B
C
D
a
b
d
E
F
G
1·0
2·0
3·0
[Cl⁻]/mol dm⁻³

hydrogen. The theory of Bigeleisen and Wolfsberg (1958) estimates that the maximum regular Cl isotope effects (36 and 38 isotopes) are 3 and 14% respectively, against a background of Cl in natural abundance.
An example of an isotope effect in an element of similar atomic weight to chlorine is the isotopic fractionation of $^{32}S$ and $^{34}S$ which occurs in the reduction of $SO_4^=$ to gaseous $H_2S$ (Melander 1960). Experimentally this was found to be approximately two per cent. This is a favourable case in which to seek evidence of an isotope effect since each S atom reacts independently of all others. In the present case of the trichloride ion equilibrium, the systems under observation are not isotopically pure, and the isotope effect will undoubtedly be reduced by the scrambling of the isotopes in the system. Particularly for very fast opposing reactions, the determination of rate constants to the degree of accuracy necessary to reveal such isotope effects is impracticable at the present time. Only for $^6Li$ and $^7Li$ n.m.r. perhaps need such an effect ordinarily be considered. It is however possible that such an n.m.r. investigation on two isotopes could be developed in favourable situations into a useful differential method for observing isotope effects in certain elements. For example, in terms of the present treatment, deviations of the observed concentration dependence of $\Delta_m^I / \Delta_m^{II}$ from that calculated on the basis of no isotope effect might be interpreted as the result of isotopic differences between certain reaction rate constants $k^I$ and $k^{II}$.

v. Temperature dependence of the linewidth increment.

In the presence of slow exchange, the linewidthincrement is proportional to the forward rate constant. Increasing the temperature increases this rate constant, and thus enhances the line-broadening effect of the exchange. The temperature coefficient of $\Delta_m$ is also a direct measure of the activation energy of $k_f$, provided that some confirmation can be obtained that the slow exchange limit is applicable to the system. In the fast exchange limit, the temperature coefficient of $\Delta_m$ is determined by the temperature coefficient of whatever processes are responsible for relaxation

in the average environment of the system. For quadrupolar relaxation in the $Cl^-/Cl_2/Cl_3^-$ system, this may be assumed to be the reorientational motion of the molecules, and there is ample evidence that this is largely governed by the viscosity of the solution. An increase in temperature will generally reduce the viscosity of a liquid (though not invariably for aqueous electrolyte solutions), and increase the values of $T_{2i}$, causing a decrease in $\Delta_m$. Thus there is a qualitative distinction between the fast and slow exchange limits: the temperature coefficients for the two cases have different signs. In general in the transition region the temperature dependence of the linewidth increment will not accurately follow an Arrhenius law; but an observed activation energy may be calculated from an approximately linear Arrhenius plot over a short temperature range. The computed variation of such activation energies with $k_b$ is shown in Figure 3.12 for both the three-site and the four-site cases, with

$$H^{\ddagger}_{k_b} = 21.0 \text{ kJ } ( \approx 5.0 \text{ kcal})/\text{mol}$$

and

$$H^{\ddagger}_{vis} = 12.5 \text{ kJ } ( \approx 3.0 \text{ kcal})/\text{mol}$$

A sound knowledge of the temperature dependence of the equilibrium constant is a prerequisite for such a temperature study, unless the n.m.r. data itself can be used to obtain this information.

## 6. Experimental results.

### i. Visible and ultra-violet spectrophotometry.

Spectra of samples of both $Br_2/Cl^-$ and $Cl_2/Cl^-$ solutions were studied for four purposes:

(a) to investigate the possibility of using such spectra to determine sample concentrations non-destructively;

(b) to provide means of monitoring any deterioration or decomposition of the solutions sealed into the n.m.r. sample tubes;

(c) to provide independent confirmation of the method of wet analysis used to find the composition of the samples;

Figure 3.12

Apparent Arrhenius activation energy (at 298K) of $\Delta_m$ as a function of $k_b$

three-site model

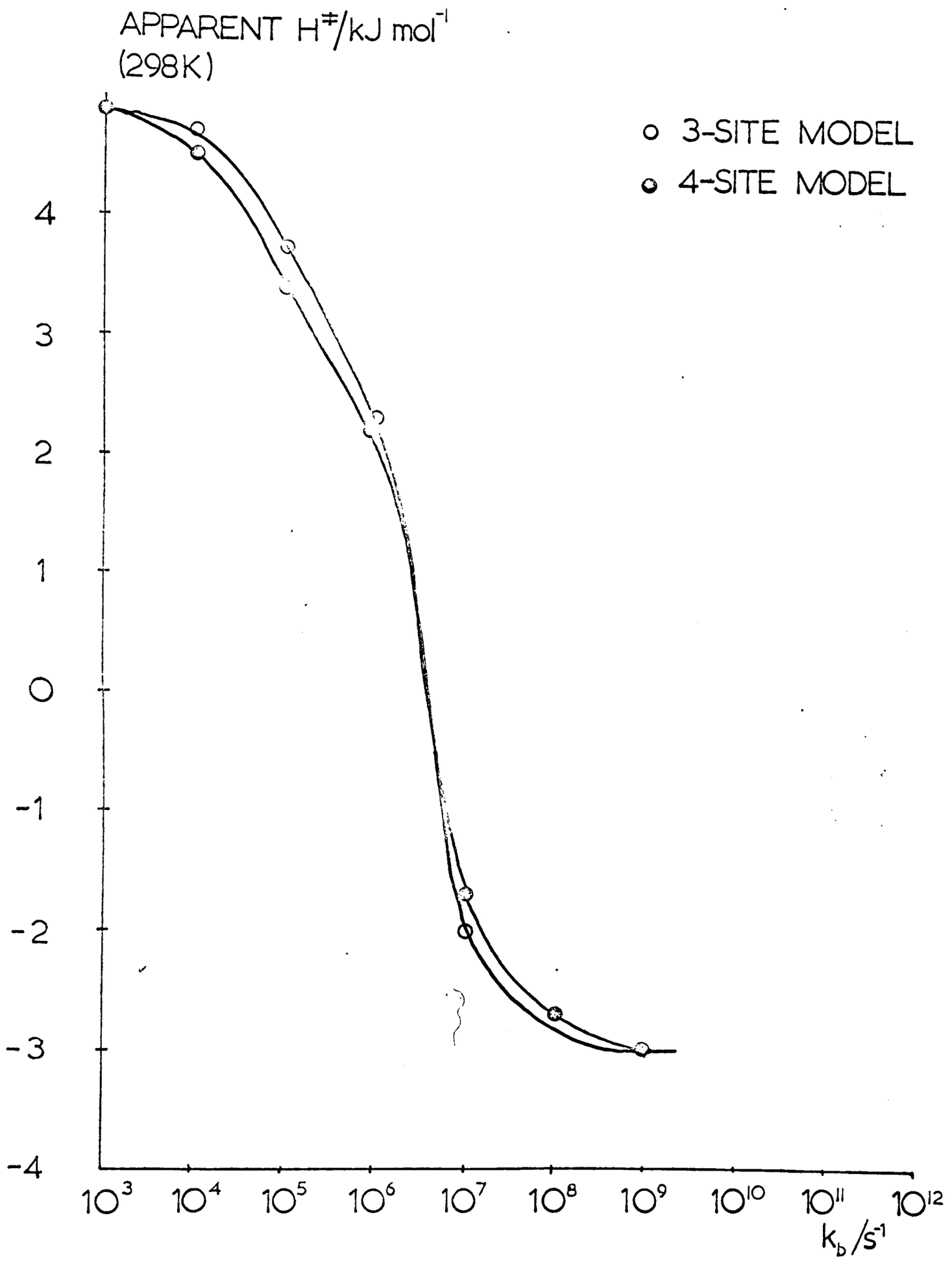
| | |
|---|---|
| $T_{2b}$ | 10.7μs |
| $T_{2c}$ | 17.6μs |

four-site model

| | |
|---|---|
| $T_{2b}$ | 10.7μs |
| $T_{2c}$ | 24.0μs |
| $T_{2d}$ | 4.8μs |

Notes:

1. Equilibrium constant assumed independent of temperature.
2. $k_b$ refers to value of $k_b$ at 298K.


APPARENT H‡/kJ mol⁻¹
(298K)
o 3-SITE MODEL
● 4-SITE MODEL
4
3
2
1
0
-1
-2
-3
-4
10³ 10⁴ 10⁵ 10⁶ 10⁷ 10⁸ 10⁹ 10¹⁰ 10¹¹ 10¹²
k_b /s⁻¹

(d) to measure the temperature variation of the equilibrium constant K.

An accurate spectrophotometric study of the $Cl_2/Cl^-$ equilibrium at 25° has been reported by Zimmerman and Strong (1957), and the absorptivity values used here are taken from this paper, as is the equilibrium constant employed. Daniele (1960) has studied the $Br_2/Cl^-$ system at 18°, 25°, 39°.

(a) The cylindrical thin-walled sample tubes devised for the n.m.r. measurements were not suitable for good quantitative spectrophotometric measurements. Nonetheless it was found possible with care to obtain from these tubes spectra reproducible to within about 2% over that region of the visible and near u-v in which the pyrex glass was sufficiently transparent. The sample tubes (which were flat-bottomed) showed variations in internal diameter of as much as ten per cent amongst a set; the effect of this on the path length was easily allowed for by direct measurement with a micrometer gauge. Even absolute $Cl_2$ concentrations obtained in this way generally showed good agreement with those obtained by destructive analysis with iodide and thiosulphate. In practice, destructive wet analysis was both more accurate and more convenient for these sealed samples.

(b) No sample deterioration was detected ($\pm$ 2%) over periods of up to two weeks in either $Br_2/Cl^-$ or $Cl_2/Cl^-$ samples.

(c) Using the apparatus shown in Figure 3.3, several more accurate spectrophotometric analyses of $Cl_2/H_2O$ solutions were made, in order to check the results of the wet analysis by iodine-thiosulphate titration. The results of these are shown in Table 3.7, which indicates that the methods are in substantial agreement. The temperature control of the Unicam SP800 instrument was poor, and the values of the stoichiometric equilibrium constant Q should not be compared directly with the value of 0.176 suggested by Zimmerman and Strong for solutions of ionic strength 1.0. An accurate determination of the temperature coefficient of the equilibrium constant is to be carried out.

| system | $A_{3250}$ | $A_{2885}$ | $A_{2537}$ | T °C | $Cl_2$ | $Cl_3^-$ | HOCl | Q | total $Cl_2$ mol/l | |
|---|---|---|---|---|---|---|---|---|---|---|
| | | | | | mol/l | | | | u-v | titrn. |
| A | 1.47 | .57 | .23 | 27 | 0.0192 | 0 | .0024 | - | .0216 | .0220 |
| B | .360 | .955 | 1.470 | 35 | 0.01163 | .00043 | 0 | .184 | .0121 | .0119 |
| C | 1.285 | .605 | (2.55)[1] | 35 | 0.01515 | .00075 | 0 | .150 | .0159 | .0156 |
| D | - | - | - | - | 0.0125 | .00003 | .0104 | - | .0230 | .0212 |

Systems:

A $Cl_2$
$HClO_4$ .98mol/l
HCl 0

B $Cl_2$
$HClO_4$ .80mol/l
HCl .20mol/l

C $Cl_2$
$HClO_4$ .667mol/l
HCl .333mol/l

D $Cl_2$, $H_2O$

Note: 1. extrapolated value.

TABLE 3.7

ii. The Raman spectrum of the system $Br_2/Cl^-/H_2O$

The Raman spectrum of a saturated solution of $Br_2$ in acidified aqueous NaCl (4 mol $kg^{-1}$) was found to show the following features:

a strong band at 278 $cm^{-1}$
a slight shoulder at 162 $cm^{-1}$
an irregularity at 230 $cm^{-1}$

A control spectrum of acidified $Br_2$ water showed one strong band at 310 $cm^{-1}$.

These results may be compared with those of Evans and Lo (1966c) who studied the $Br_2/Cl^-$ solutions in benzene and methyl cyanide. The infra-red and Raman spectra of these systems indicated that there were at least three anionic halogen species present. From a composition variation study and from previous data, these authors made the following assignment of the bands observed in the Raman spectrum:

| | |
|---|---|
| 162 $cm^{-1}$ | symmetric stretch $Br_3^-$ |
| 192 $cm^{-1}$ | $(Cl\text{-}Br\text{-}Br)^-$ |
| ~ 230 $cm^{-1}$ | |
| 273 $cm^{-1}$ | symmetric stretch $(Cl\text{-}Br\text{-}Cl)^-$ |

The present results therefore suggest that the predominant species in the aqueous $Br_2/Cl^-$ system is the symmetrical $BrCl_2^-$ ion, rather than the unsymmetrical $Br_2Cl^-$ ion, and that further clarification of the composition of this solution is desirable.

iii. N.m.r. measurements

a) Preliminaries.

One important factor which is expected to influence the size of $\Delta_m$ but which it has been convenient to ignore up to this point is the concentration dependence of the values of $T_{2i}$. This dependence comes about through the change in the bulk viscosity of the solution caused by changes in chloride ion concentration. The various figures of the previous section depict $\Delta_m$ data which are essentially normalised to the viscosity of pure water. The only satisfactory way of allowing for this important effect is to use viscosity-adjusted values of $T_{2i}$ at each concentration in the computation. This is easily achieved by employing Jones-Dole viscosity B coefficients (Stokes and Mills 1965). Electrolyte viscosities obey the Jones-Dole equation

$$\eta = \eta_o(1 + Ac^{\frac{1}{2}} + Bc) \qquad (3.47)$$

where A is very small;
thus, at a given temperature and to a good approximation

$$T_{2i}(c) \approx T_{2i}(c = 0)/(1 + Bc) \qquad (3.48)$$

since

$$T_{2i}\eta/T \approx \text{constant}$$

The value of B for NaCl is 0.087 (298K, Eisenstadt and Friedman 1967).

Next, we establish experimentally the validity of the procedure of defining a molar linewidth-increment parameter. Figure 3.13 shows that the line-broadening observed is indeed a linear function of $[Cl_2]^o$, the total added chlorine. Throughout the remainder of this Chapter therefore linewidth-increment data will be quoted as $\Delta_m$, molar increments.

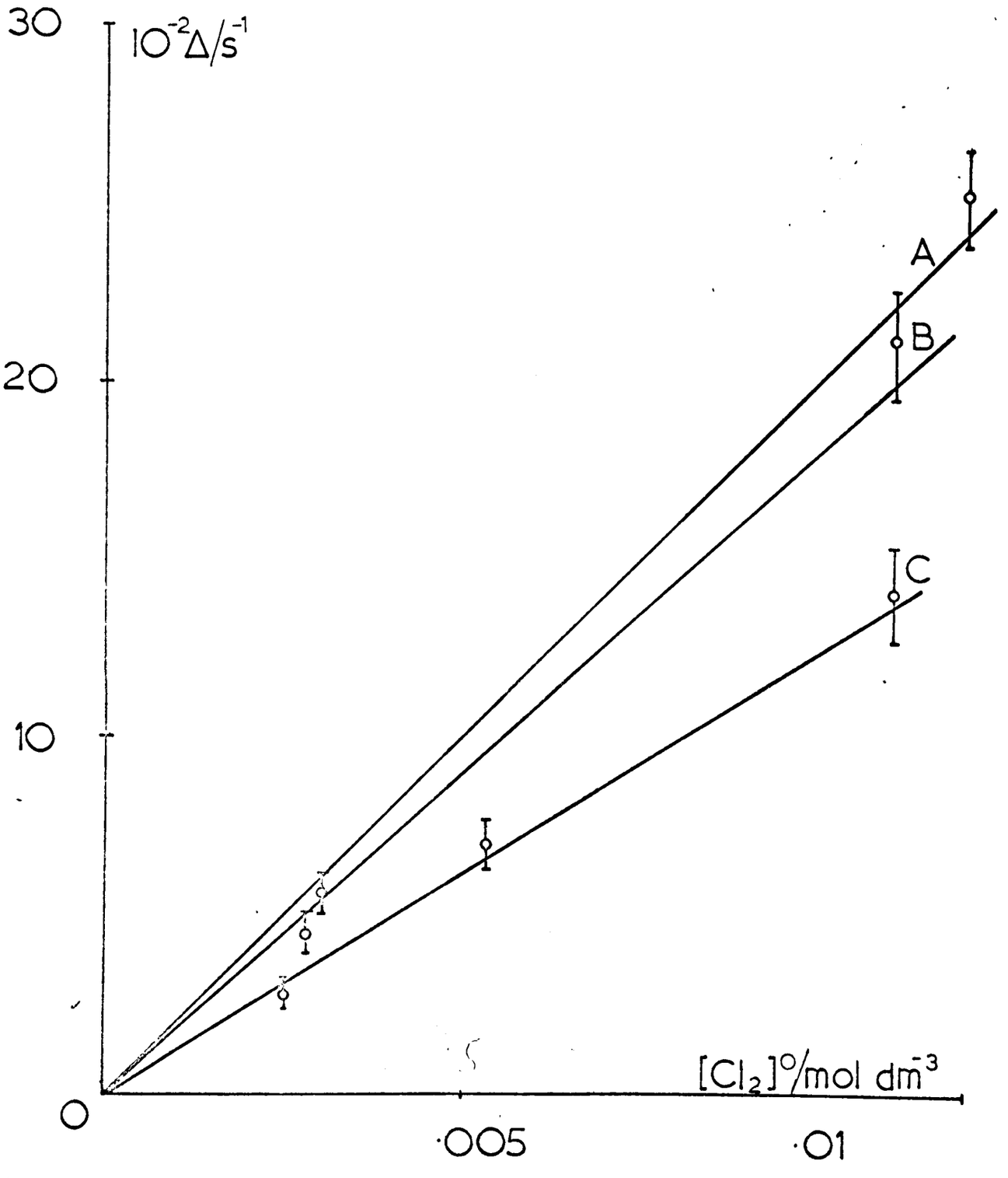
Figure 3.13

Experimental dependence of $\Delta_o$ on chlorine concentration $[Cl_2]^o$ at three chloride ion concentrations

A 1.0 mol $dm^{-3}$

B 1.5 mol $dm^{-3}$

C 2.0 mol $dm^{-3}$


30
$10^{-2}\Delta/s^{-1}$
20
10
0
A
B
C
$[Cl_2]^0$/mol $dm^{-3}$
·005
·01

b) N.m.r. data: $\Delta_m$ for $^{35}Cl$

In Section 4 of this Chapter, a set of values of the chemical shifts and relaxation times of the four sites of the $Cl^-/Cl_2/Cl_3^-$ system was estimated. Of these, the value of $T_{2b}$($^{35}Cl$ relaxation time in aqueous $Cl_2$) may now be regarded as firmly established experimentally, as may the equilibrium constant (298K) for the system. In addition, the ratio of the quadrupole coupling constants of the two sites in the $Cl_3^-$ ion will be regarded as established. Thus the object of this section is to obtain a value of $k_b$ from the best fit of the experimental data to the predictions of the four-site model, regarding only the correlation time of the trichloride ion and the rate constant ($k_b$) itself as adjustable parameters. Thus, $T_{2c}$ and $T_{2d}$ may vary proportionally ($T_{2c}/T_{2d}$ = constant). Furthermore the final best values of $T_{2c}$ and $T_{2d}$ should seem reasonable in the light of the earlier estimate.

Figure 3.14 shows the experimental $\Delta_m$ data plotted as a function of chloride ion concentration, together with a number of computed curves (see figure legend for details). This figure illustrates that for any particular set of values of $T_{2c}$, $T_{2d}$, the computed $\Delta_m$ must agree with the experimental $\Delta_m$ both in their concentration dependence and in their magnitudes. In general, for each trial value of the trichloride ion correlation time (that is, each set of $T_{2c}$, $T_{2d}$), a value of $k_b$ can be found which best matches the observed concentration dependence of $\Delta_m$ ($\Delta_m(c)/\Delta_m(1)$). This value of $k_b$ is denoted by $k_b^*$. Further, for the same value of the correlation time, a second value of $k_b$ can be found which reproduces the magnitude of $\Delta_m$ at some selected chloride ion concentration, for instance 1.0 mol $Cl^-$ $dm^{-3}$. This value of $k_b$ is denoted by $k_b^{**}$.

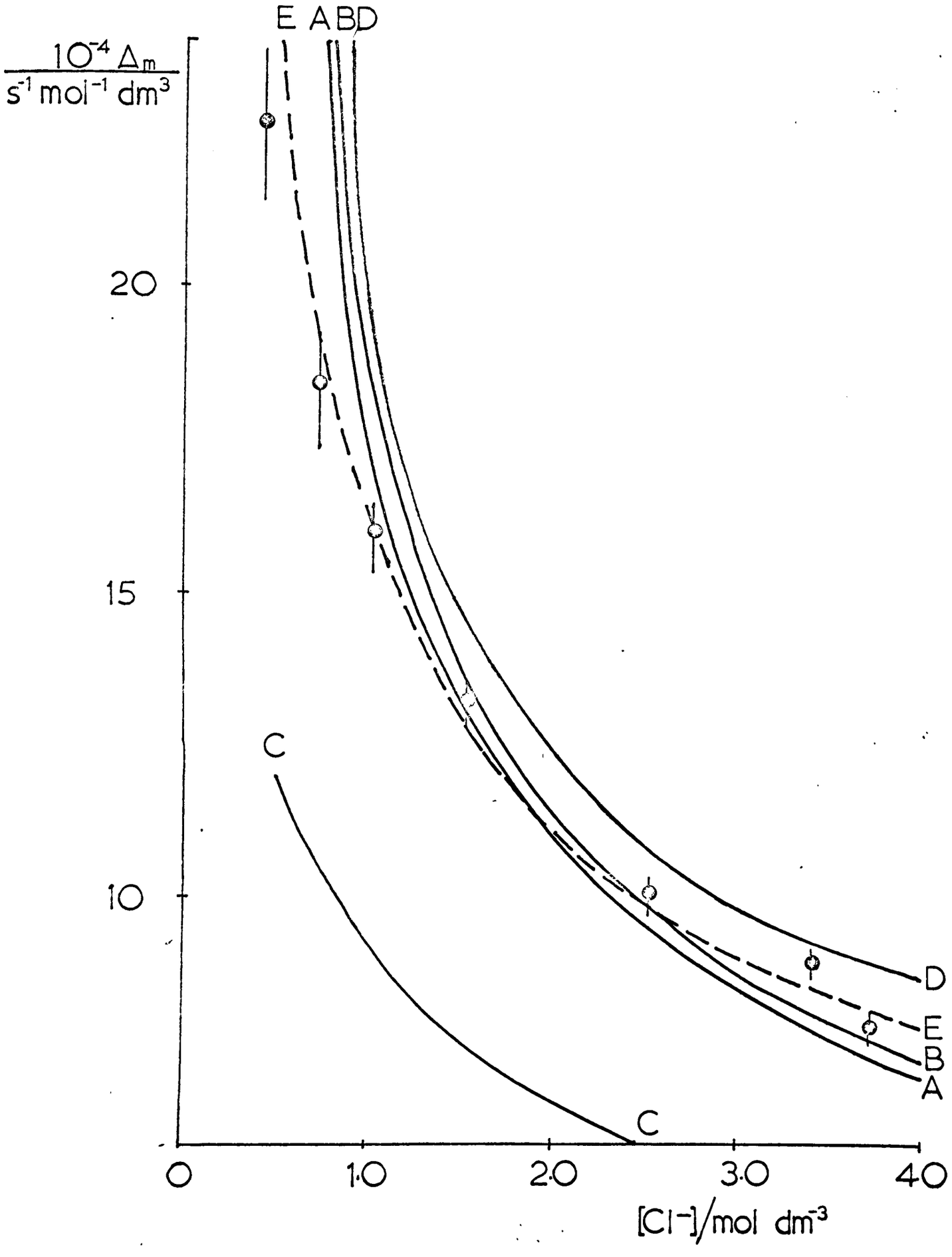
In general, $k_b^*$ and $k_b^{**}$ are not equal. Of course physically these two independent values of the rate constant must be the same, since they represent the same physical parameter. Therefore if it is possible to converge unambiguously on a value of the correlation time which causes $k_b^*$ and $k_b^{**}$

Figure 3.14

Experimental values of $\Delta_m$ (filled points), showing dependence on chloride ion concentration, compared with calculated viscosity-corrected values

| | $T_{2b}/\mu s$ | $T_{2c}/\mu s$ | $T_{2d}/\mu s$ | $k_b/s^{-1}$ |
|---|---|---|---|---|
| A | 14.0 | 22.0 | 4.4 | $4 \times 10^7$ |
| B | 14.0 | 22.0 | 4.4 | $2 \times 10^8$ |
| C | 14.0 | 20.0 | 4.0 | $2 \times 10^6$ |
| D | 14.0 | 20.0 | 4.0 | $2 \times 10^8$ |
| E | 14.0 | 15.0 | 3.0 | $8 \times 10^6$ |

E represents the "best" curve


E A B D
$10^{-4}\,\Delta_m$
$s^{-1}\,mol^{-1}\,dm^3$
20
15
10
C
D
E
B
A
C
0
1·0
2·0
3·0
4·0
$[Cl^-]/mol\ dm^{-3}$

to become equal, then this unambiguously fixes the "best" value of the true rate constant. In the present case, this procedure can be carried out extremely satisfactorily as adjustment of the correlation time causes $k_b^*$ and $k_b^{**}$ to vary in opposite directions, as is clear from Figure 3.15. Moreover the intersection of the points ($k_b^*$, $k_b^{**}$) in this figure with the diagonal line which represents the condition $k_b^* = k_b^{**}$ is sharp.

In summary: that value of the correlation time for which $k_b^*$ and $k_b^{**}$ are equal is taken to be the "best" value of the correlation time, and the corresponding $k_b^* = k_b^{**}$ is taken as the "best" value of the rate constant, $k_b$.

Figure 3.15 shows the application of this procedure to the experimental data of the previous figure. The best values of the parameters are:

$$k_b = 8 \times 10^6 \ s^{-1}$$

$$T_{2c} = 15 \ \mu s$$

$$T_{2d} = 3.0 \mu s$$

It should be noted that the trial correlation time varies by only a factor of two between the extreme points, A and E, of Figure 3.15, and that the best value of $\sim 8 \times 10^{-12}$ s agrees very adequately with the lower limit of $\sim 5 \times 10^{-12}$ s which was set upon this quantity in Section 4.

c) Discussion of experimental data for $^{35}Cl$ and $^{37}Cl$.

In Section 5 (iii) it was shown that the concentration dependence and the magnitude of the ratio of $\Delta_m$ for two isotopes are expected to be sensitive measures of the rate constant $k_b$. Having established the "best" value of $k_b$ in terms of the procedure and definition given above, we may compare the observed and computed isotope linewidth increment ratio. This is shown in Figure 3.16, where two further computed curves corresponding to other values of the rate constant are also drawn. In view of the large

Figure 3.15

Plot of $\log(k_b^*/s^{-1})$ <u>versus</u> $\log(k_b^{**}/s^{-1})$
(see text)

$T_{2b}$ 14.0μs

| | | | | |
|---|---|---|---|---|
| A | $T_{2c}$ | 24μs | $T_{2d}$ | 4.8μs |
| B | | 22μs | | 4.4μs |
| C | | 20μs | | 4.0μs |
| D | | 18μs | | 3.6μs |
| E | | 12μs | | 2.4μs |
| F | (best values) | 15μs | | 3.0μs |

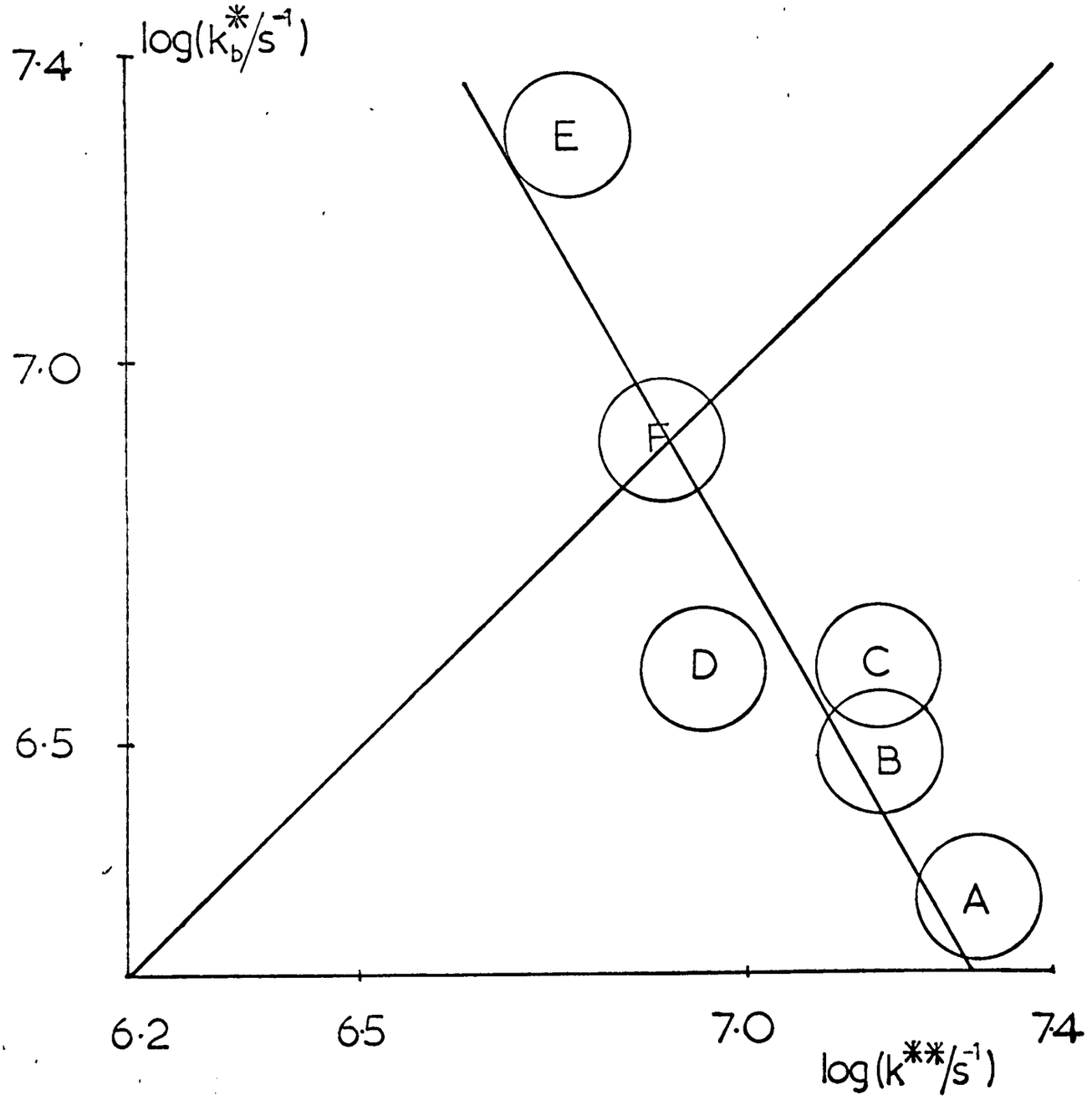
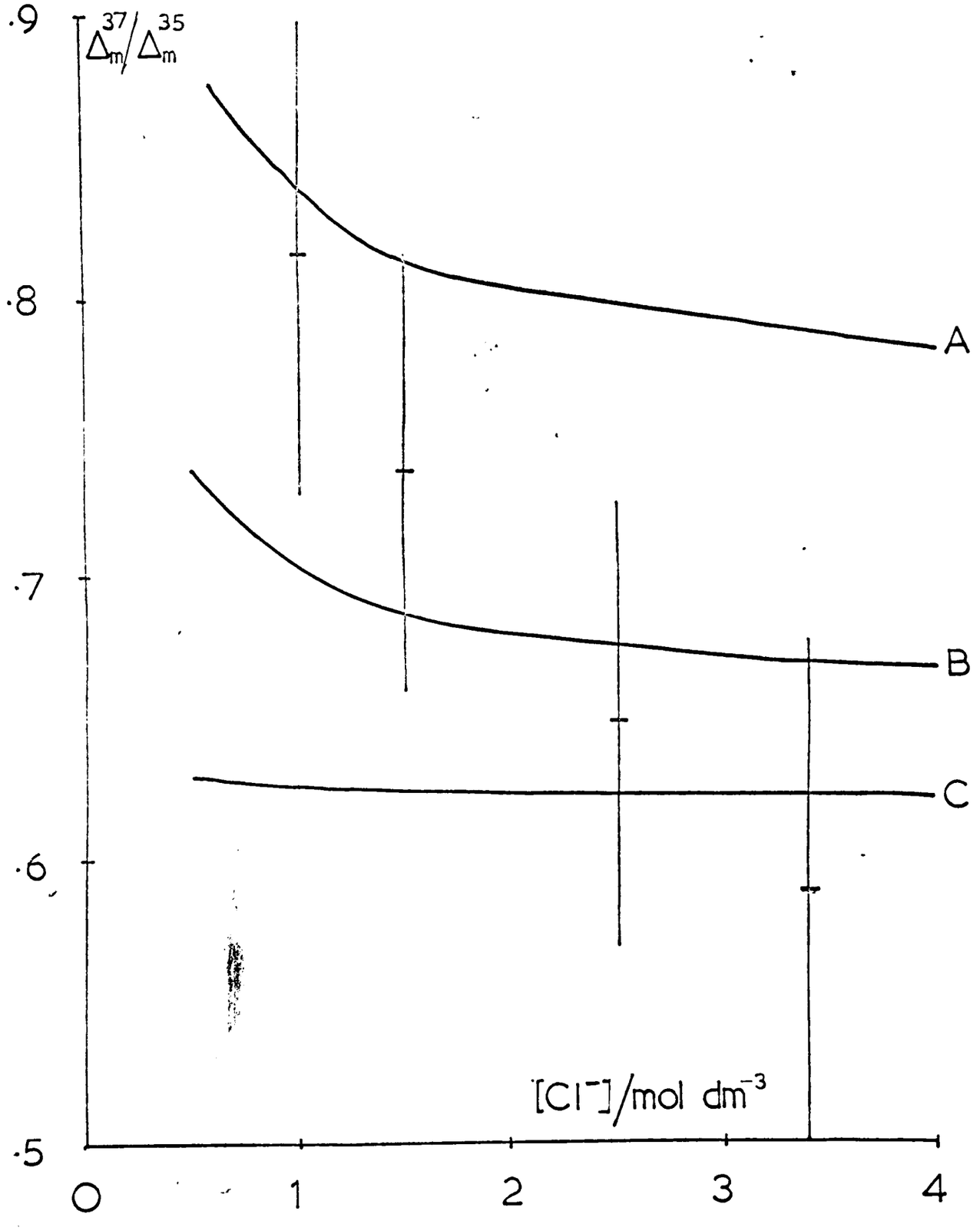

log(k_b*/s^-1)
7·4
7·0
6·5
E
F
D
C
B
A
6·2
6·5
7·0
7·4
log(k**/s^-1)

Figure 3.16

Experimental values of the ratio ($\Delta_m^{37}/\Delta_m^{35}$), as a function of chloride ion concentration, compared with calculated values (best values of parameters)


·9
·8
·7
·6
·5
$\Delta_m^{37}/\Delta_m^{35}$
A
B
C
[Cl⁻]/mol dm⁻³
0
1
2
3
4

errors in the experimental ratios, the agreement is considered satisfactory.

The error limits on the experimental data appear very large, but correspond to only ± 2Hz ($^{35}Cl$) and ± 4Hz ($^{37}Cl$) at 3.4 mol $Cl^-$ $dm^{-3}$, for instance. Unfortunately, the unbroadened $^{37}Cl$ resonance of the chloride ion is only a few cycles wide, and its observed linewidth is largely determined by the magnet inhomogeneity of the spectrometer. The subtraction of the ubroadened $^{37}Cl$ linewidth from the corresponding exchange broadened linewidth to obtain $\Delta$ must involve some error (especially for narrow lines) because the magnet profile is not accurately Lorentzian. It is straining the capacity of a conventional broad-line spectrometer to obtain accurate $T_2$ values of narrow $^{37}Cl$ resonances from linewidth measurements, and such data are better determined by spin-echo methods if possible.

d) Experimental temperature dependence of $\Delta_m$.

Experimentally, the study of the effect of temperature on the $Cl^-/Cl_2/Cl_3^-$ system is complicated by the fact that temperature changes also displace the equilibrium between dissolved and gaseous chlorine. However, it can be easily shown that if measurements are made over a range of temperature on one sealed tube then the concentration of dissolved chlorine (c) is given at any temperature T by

$$c = \frac{c_o kRT[(1/k_o RT_o) + F]}{1 + FkRT} \qquad (3.49)$$

where k is the Bunsen absorption coefficient for $Cl_2$ (or equivalent in coherent units);
RT has its usual meaning;
$F = V_1/V_g$, the ratio of the volume of the liquid phase to the volume of the gaseous phase;
and the subscript $_o$ refers to some reference temperature at which c ($c_o$)

is known. In the present experiment, F is easily obtained, and $c_o$ determined (at 298K) by titration in the usual way. Chlorine solubility data were taken by interpolation from International Critical Tables (III, 256).

In this way allowance may be made for the change in chlorine concentration with temperature, and linewidth increment data normalised.

In addition a knowledge of the temperature dependence of the equilibrium constant K must be available. In the present case, no such data have been reported. A spectrophotometric experiment is under way to obtain these data; in the meantime it will be assumed that this will constitute a second order correction only, the value of K appropriate to 298K will be used throughout.

Numerical data from an n.m.r. temperature study are gathered together in Table 2, Appendix II. The derived Arrhenius plot is given in Figure 3.17. The estimated activation energy is $10.9 \pm 2.1$ kJ ($\approx 2.6 \pm 0.5$ kcal)$mol^{-1}$.

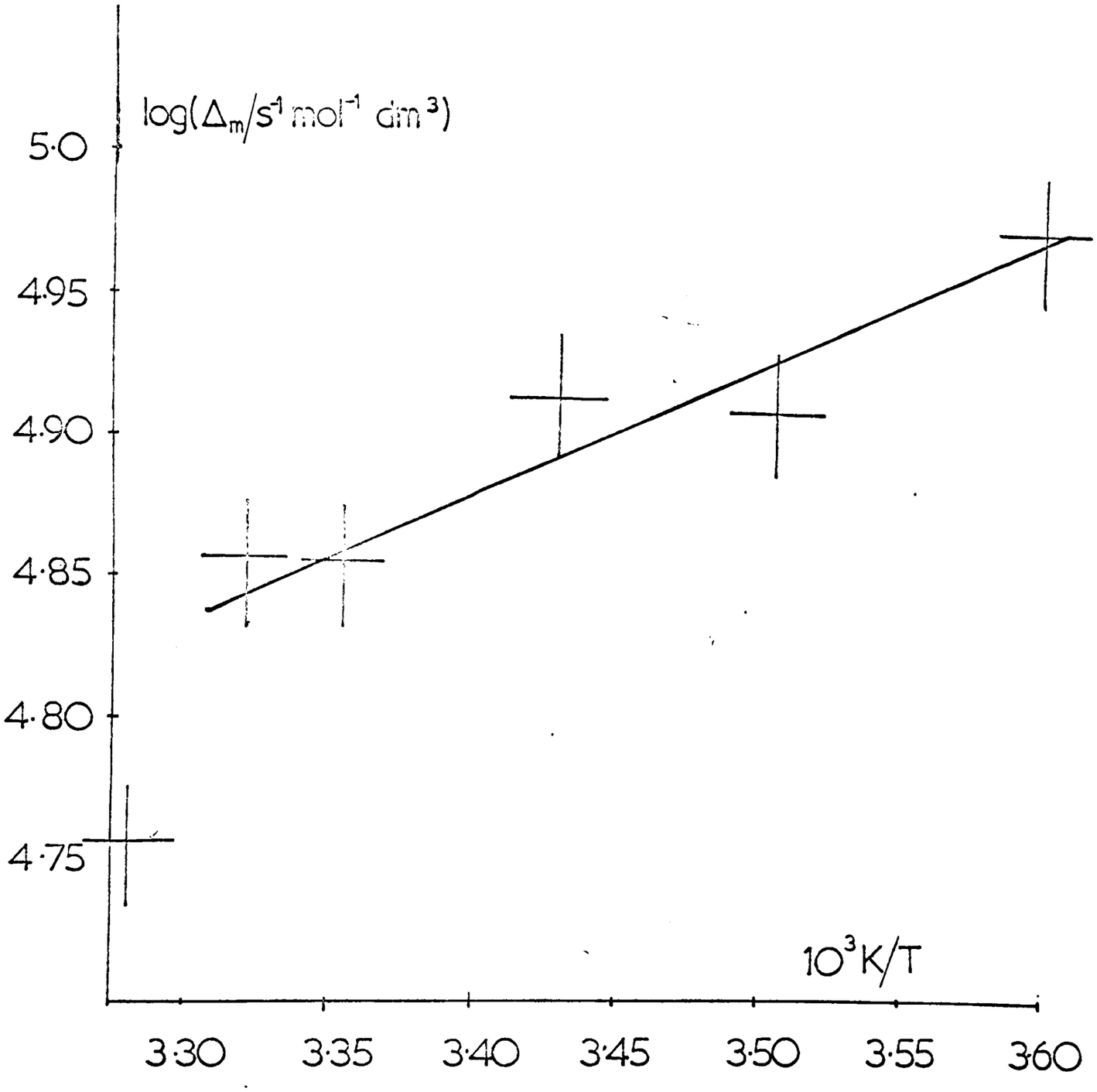
It may be seen by reference to Figure 3.12 that this is a very reasonable result, lending some support to the estimate of $k_b$ made above. However the comparison must be viewed only semi-quantitatively. The lack of any knowledge of the activation energy of the reaction makes an accurate comparison of theory and experiment impossible. The converse procedure, namely to calculate the activation energy for the reaction from $k_b$ and the measured activation energy, is in principle possible; however, the errors in the experimental quantities are such as to preclude this in the present case.

e) Field dependence of $\Delta_m$.

The inclusion of the estimated chemical shifts between sites in the calculation of $\Delta_m$ results in changes too small to show graphically; consequently, the shift parameters have been considered to be without bearing

Figure 3.17

Arrhenius plot showing experimental temperature dependence of $\Delta_m$


log(Δm/s⁻¹ mol⁻¹ dm³)
5·0
4·95
4·90
4·85
4·80
4·75
10³K/T
3·30
3·35
3·40
3·45
3·50
3·55
3·60

on the fitting of data to theory. That there is no gross field dependence of the line-broadening has been confirmed experimentally by measurements at approximately half-field on a pair of samples. No difference was detected, within the estimated experimental error between the results at the two fields.

f) Sensitivity of determined parameters to errors in subsidiary parameters

In determining a value of $k_b$ from experimental line-broadening data certain values of subsidiary parameters are assumed, as discussed in various earlier sections of this Chapter. The parameters concerned are:

a) $T_{2b}$

b) the ratio $T_{2c}/T_{2d}$ (equivalent to an assumption of the value of $e^2Qq_c/e^2Qq_d$)

c) the equilibrium constant K

The best fit between experimental data and the predictions of the four-site exchange equations is obtained by allowing $k_b$ and $T_{2c}$, $T_{2d}$ to vary (within the constraint of b) above). Figure 3.15 shows that if the assumed values of a), b) and c) are without error, then the errors in $k_b$ and $T_{2c}$, $T_{2d}$ are

$$k_b \pm 2 \times 10^6 \ s^{-1}$$
$$T_{2c} \pm 1\mu s$$
$$T_{2d} \pm 0.2\mu s$$

These uncertainties arise from the probable random errors on the data points themselves. The errors arising from other sources have been estimated by carrying through computations of $\Delta$ in which the various subsidiary parameters were allowed to vary within their error limits. The results are listed in the Table below.

| determined parameter | determined value of parameter | estimated uncertainties in determined values of parameters from various sources | | | | |
|---|---|---|---|---|---|---|
| | | from exp'tal error | from error in $K \pm 0.030$ | from error in $T_{2b} \pm 1.0\mu s$ | from error in $q_c/q_d$ $\pm 0.05$ | Total |
| $k_b/s^{-1}$ | $8 \times 10^6$ | $\pm 2 \times 10^6$ | $\pm 1 \times 10^6$ | $< \pm 1 \times 10^6$ | $< \pm 1 \times 10^6$ | $\pm 4 \times 10^6$ |
| $T_{2c}/\mu s$ | 15 | $\pm 1$ | $< \pm 1$ | very small | $\pm 2$ | $\pm 3.5$ |
| $T_{2d}/\mu s$ | 3 | $\pm 0.2$ | $< \pm 0.2$ | very small | $\pm 0.4$ | $\pm 0.7$ |
| $\tau_{Cl_3^-}/ps$ | 8 | - | - | - | - | $\pm 2$ |

Thus the final assessment of the experimentally determined value of the rate constant of the dissociation of the trichloride ion is

$$k_b = 8 \times 10^6 \pm 4 \times 10^6.$$

It should be noted that the upper limit to $k_b$ approaches the fast exchange situation where the sensitivity of the linewidth increment to the magnitude of $k_b$ is greatly reduced.

g) The n.m.r. study of the $Br_2/Cl^-$ system

The strong evidence of the Raman spectrum that aqueous solutions of bromine and chloride ions do not contain simply $Br_2$, $Cl^-$ and $(Br\text{-}Br\text{-}Cl)^-$ led to the abandonment of the n.m.r. study of the system. It is probable that the dominant species is symmetrical $BrCl_2^-$. The main impediment to the n.m.r. study lies in the absence of equilibrium constants for the various equilibria. The spectrophotometric study of Daniele appears to be inadequate in view of the new Raman data since it took account only of $Br_2Cl^-$ and $Br_2$.

## 7. General conclusions

Any substantial comment on the experimental value of the trichloride ion dissociation rate constant is made difficult by the lack of comparative data. The temperature jump relaxation method has been applied by Eigen and Kustin (1962) to the kinetics of halogen hydrolysis, but the trihalide equilibria were not studied. The early $^{127}I$ n.m.r. investigation by Meyers (1958) suggested that the triiodide-forming reaction between iodide and iodine is controlled by diffusion. However the equilibrium constant for this reaction is a thousand times greater than for trichloride formation, and Genser (1962) has criticised Meyer's formulation of the mechanism of this reaction.

Until other data become available, either on related systems or on the present system by alternative methods, then further comment is unprofitable.

It is clear from the development of this Chapter that the n.m.r. line-broadening technique can, in favourable circumstances, provide unambiguous kinetic information. Nonetheless the method is not entirely easy to apply. It may be contrasted in some respects with the widely-used relaxation methods of studying fast reactions, in which the rate at which a chemical equilibrium is re-established after a perturbation is observed directly. Here the (overall) kinetics are measured directly against a laboratory clock. The experimental quantity, a relaxation time describing the rates of change of concentrations of chemical species, depends formally only upon the kinetic parameters and the concentrations.

The n.m.r. method is not direct in this sense. It might be described as a competition method, in which the competing processes are chemical exchange and nuclear magnetic relaxation. The relaxation processes operating at each site provide a set of internal clocks which must be calibrated against the laboratory clock. This amounts to determining in some way a set of subsidiary site parameters. This extra step must introduce some error (although the importance of this in individual cases may differ greatly) and

may often be difficult to carry out. Furthermore, attention has been drawn earlier in this Chapter to the reduced sensitivity of the n.m.r. method in the cases where exchange is a very slow or a very fast process in relation to nuclear relaxation. The direct fast-reaction relaxation methods are more flexible, and now extend even to the investigation of diffusion-controlled reactions (see for example Laidler 1965) which are beyond the range of the n.m.r. method except in special cases.

In response to these criticisms, the n.m.r. method must be allowed certain virtues. Chief amongst these is the fact that it makes possible the study of processes involving particular atoms or groups of atoms; for example the role of one particular ligand species in a complex set of equilibria might be investigated. In addition n.m.r. provides a direct means of observing the role of the solvent in reactions, a matter which many kinetic methods find difficult.

# APPENDIX I

## Lorentzian line-fitting program

```
C  COMPUTES ITERATIVE LEAST SQUARES FIT OF DATA TO LORENTZIAN
C  SIGNAL AMPLITUDES INPUT IN BINARY CODE
GLOBAL,CH031,SQRT]
DIMENSION X(1050),Y(1050)
READ(1)N
PAUSE
C  SIR SEGMENT INTERFACES BINARY CODED INPUT TO FORTRAN PROGRAM
DO7I=1,N
NA=0
CODE
START   4   +0
        15  2048
        12  +1
        14  25
        5   HIGH
        4   +0
        15  2048
        1   HIGH
        5   NA
HIGH    +0
FORTRAN
7   Y(I)=NA
C  EVERY FOURTH INPUT DATUM TAKEN FOR FITTING
N=N/4
DO10J=2,N+1
K=4*J-3
10  Y(J)=Y(K)
PAUSE
READ(1)ISA,IDA,ISO,CAL,TRYA,TRYN,TRYB,C
WRITE(2,111)ISA,IDA,ISO
111  FORMAT(10H    SAMPLE,I5,10H     DATE ,I5,10H   ISOTOPE,I3)
M=0
A=.25
C  X(I) GENERATED IN RAD/SEC UNITS REFERRED TO OMEGAZERO AS ORIGIN
DO6I=1,N
X(I)=-C+A
A=A+1.
PI=3.1416
6   X(I)=2.*PI*X(I)*CAL
WRITE(2,99)
```

```
C  SEGMENT: ITERATIVE DIFFERENTIAL CORRECTION OF TRIAL VALUES
DO40K=1,5
4 S11=0.0
S22=0.0
S12=0.0
S13=0.0
S23=0.0
S33=0.0
SA=0.0
SB=0.0
SN=0.0
SR=0.0
WRITE(2,98)N,TRYA,TRYN,TRYB
99  FORMAT(30HDATA POINTS    TRIAL  VALUES  )
98  FORMAT(I10,F10.3,F12.7,F10.3)
DO20I=1,N
F=TRYA/(1.+X(I)*X(I)*TRYN)+TRYB
DIFFA=1./(1.+X(I)*X(I)*TRYN)
DIFFN=(-TRYA*X(I)*X(I))/((1.+X(I)*X(I)*TRYN)*(1.+X(I)*X(I)*TRYN))
DIFFB=1.
R=F-Y(I)
RA=-R*DIFFA
RN=-R*DIFFN
EL11=DIFFA**2
EL22=DIFFN**2
EL12=DIFFA*DIFFN
EL33=1.0
S11=EL11+S11
S12=EL12+S12
S22=EL22+S22
S13=DIFFA+S13
S23=DIFFN+S23
S33=EL33+S33
SA=RA+SA
SN=RN+SN
SR=R**2+SR
20  SB=-R+SB
COF13=S12*S23-S22*S13
COF23=S11*S23-S12*S13
COF33=S11*S22-S12*S12
COF11=S22*S33-S23*S23
COF12=S12*S33-S23*S13
COF22=S11*S33-S13*S13
DET=S13*COF13-S23*COF23+S33*COF33
DELA=(SA*COF11-SN*COF12+SB*COF13)/DET
DELN=(-SA*COF12+SN*COF22-SB*COF23)/DET
DELB=(SA*COF13-SN*COF23+SB*COF33)/DET
  TRYA=TRYA+DELA
TRYN=TRYN+DELN
TRYB=TRYB+DELB
40  M=M+1
```

```
C   SEGMENT: COMPUTES ERROR IN LINEWIDTH
5   ERROR=SQRT(SR/N)
ERROR=ERROR/(TRYA*PI*SQRT(TRYN))
WRITE(2,98)N,TRYA,TRYN,TRYB
AT2=1./(PI*SQRT(TRYN))
WRITE(2,102)AT2,ERROR
102   FORMAT(35HCOMPUTED  LINEWIDTH AND  ERROR      ,2F10.2,5H    HZ)
END
```

CH031:  INPUT KEY

| | |
|---|---|
| N | NUMBER OF DATA POINTS |
| ISA | SAMPLE CODE NUMBER |
| IDA | DATE |
| ISO | ISOTOPE MASS NUMBER |
| CAL | CALIBRATION OF DATA ADDRESS INTERVAL IN HZ UNITS |
| TRYA | TRIAL VALUE OF TRUE PEAK HEIGHT |
| TRYN | TRIAL VALUE OF TRUE (T2)**2 (SEC**2 UNITS) |
| TRYB | TRIAL VALUE OF TRUE BASELINE ORDINATE |
| Y(I) | Y DATUM (SIGNAL AMPLITUDE) 16-BIT BINARY |

```
C  PROGRAM CONVERGES ON CENTRE OF DISTRIBUTION OF BINARY INPUT DATA
GLOBAL,CH032)
DIMENSIONIY(1050)
M=992
JA=1
K=0
DO6I=1,992
N=0
CODE
START    4   +0
         15  2048
         12  +1
         14  25
         5   HIGH
         4   +0
         15  2048
         1   HIGH
         5   N
HIGH   +0
FORTRAN
6   IY(I)=N
DO12I=1,20
12   K=IY(I)+K
K=K/20
DO7J=1,5
SUMA=0.
SUMB=0.
DO13I=JA,M
SUMA=SUMA+I*(IY(I)-K)
13   SUMB=SUMB+IY(I)-K
C=SUMA/SUMB
WRITE(2,86)C,K
86   FORMAT(5H   C= ,I5,5H   K= ,I5)
JA=C-150.
7   M=C+150.
END
```

# APPENDIX II

Numerical data relating to
Chapter III

| sample number | $[Cl_2]^\circ$ mol $dm^{-3}$ | $[Cl^-]$ mol $dm^{-3}$ | isotope | $\Delta\nu_{\frac{1}{2}}$ Hz | $\Delta\nu_{\frac{1}{2}}$ Hz | $10^{-4}\,\Delta_m$ $s^{-1}\,mol^{-1}\,dm^3$ |
|---|---|---|---|---|---|---|
| 15 | .0013 | 3.7 | 35 | 50 | 33 | 7.97 ± .2 |
| 32 | .0021 | 3.4 | 35<br>37 | 77<br>48 | 60<br>34 ± 4 | 8.98 ± .2 |
| 33 | .0024 | 2.5 | 35<br>37 | 95<br>65 | 77<br>51 ± 5 | 10.1 ± .3 |
| 34 | .0025 | 1.5 | 35<br>37 | 122<br>92 | 105<br>78 ± 5 | 13.2 ± .4 |
| 35 | .0028 | 1.0 | 35<br>37 | 160<br>131 | 143<br>117 ± 5 | 16.0 ± .6 |
| 36 | .0030 | 0.7 | 35 | 193 | 176 | 18.4 ± 1.0 |
| 37 | .0028 | 0.4 | 35 | 218 | 201 | 22.6 ± 1.2 |

Note: a considerable quantity of early data is not included in this Table: these data showed greater scatter and were obtained before the line-fitting procedures were developed. As these early data referred to samples containing rather high $Cl_2$ concentrations, some of them have been included in Figure 3.13.

$^{35}Cl$ and $^{37}Cl$ linewidth data from $Cl^-/Cl_2$ systems of various concentrations

TABLE 1

| T/K | $10^3 K/T$ | $\Delta\nu_{\frac{1}{2}}$/Hz | $\Delta\nu_{\frac{1}{2}}^{ref}$/Hz | $\Delta\nu_{\frac{1}{2}}'$/Hz $=\Delta\nu_{\frac{1}{2}}-\Delta\nu_{\frac{1}{2}}^{ref}$ | $\frac{k}{\text{mol dm}^{-3}\text{ bar}^{-1}}$ [3] | $\frac{[Cl_2]^o}{\text{mol dm}^{-3}}$ [1] | $\frac{10^{-4}\Delta_m}{\text{s}^{-1}\text{ mol}^{-1}\text{ dm}^3}$ |
|---|---|---|---|---|---|---|---|
| 305 | 3.28 | 50 | 19.5 | 30.5 | .077 | .00164 | 5.7 |
| 301 | 3.32 | 61 | 20.5 | 40.5 | .084 | .00176 | 7.2 |
| 298 | 3.355 | 63 | 22 | 41 | .090 | .00180 [2] | 7.2 |
| 291.5 | 3.43 | 75 | 24 | 51 | .108 | .00195 | 8.2 |
| 284.5 | 3.51 | 82 | 27 | 55 | .133 | .00213 | 8.1 |
| 278 | 3.60 | 100 | 31 | 69 | .172 | .00231 | 9.35 |

Notes:
1 Calculated from equation (3.49)
2 Determined by titration
3 International Critical Tables (III 256)

$[Cl^-] = 3.7$ mol dm$^{-3}$

$f = V_l/V_g = 0.456$

$^{35}Cl$ linewidth data from $Cl^-/Cl_2$ systems at various temperatures

TABLE 2

# APPENDIX III

## Solutions of the Bloch equations modified to allow for the effects of chemical exchange

This Appendix presents details of the solutions of the Bloch equations in the presence of chemical exchange, the results of which were given in Chapter III. Whereas that Chapter is concerned mainly with one experimental system, the material given here is intended to be more general in treatment.

In the notation of Chapter III (except that $G = u + iv$ is used for $M_+ = M_x + iM_y$), the Bloch equations for n sites may be written:

$$\begin{aligned}
&\alpha_{11} G_1 + \alpha_{12} G_2 + \cdots \alpha_{1i} G_i + \cdots \alpha_{1n} G_n = i\omega_1 M_o^{(1)} \\
&\alpha_{21} G_1 + \alpha_{22} G_2 + \cdots \alpha_{2i} G_i + \cdots \alpha_{2n} G_n = i\omega_1 M_o^{(2)} \\
&\cdots\cdots\cdots\cdots\cdots\cdots\cdots\cdots\cdots\cdots \\
&\alpha_{n1} G_1 + \alpha_{n2} G_2 + \cdots \alpha_{ni} G_i + \cdots \alpha_{nn} G_n = i\omega_1 M_o^{(n)}
\end{aligned} \tag{A1}$$

which we write in the form

$$\underline{\alpha}\ \underline{G} = i\omega_1 \underline{M}_o \tag{A2}$$

The diagonal elements of $\underline{\alpha}$ are complex:

$$\alpha_{ii} = -\left(\frac{1}{T_{2i}} + \frac{1}{\tau_i} - i(\omega - \omega_i)\right) \tag{A3}$$

We therefore define matrices $\underline{R}$ and $\underline{I}$

$$\underline{\alpha} = \underline{R} + i\underline{I} \tag{A4}$$

noting that $\underline{I}$ is diagonal, as off-diagonal elements of $\underline{\alpha}$ are real. Therefore

$$[\underline{R} + i\underline{I}]\ \underline{G} = i\omega_1 \underline{M}_o \tag{A5}$$

$\underline{G}$ is separated into a real and an imaginary part

$$[\underline{R} + i\underline{I}]\,[\underline{u} + i\underline{v}] = i\omega_1\underline{M}_o \qquad (A6)$$

Expanding and equating real and imaginary parts

$$\underline{R}\,\underline{V} + \underline{I}\,\underline{U} = \omega_1\underline{M}_o \qquad (A7)$$

$$\underline{R}\,\underline{U} - \underline{I}\,\underline{V} = \underline{O} \qquad (A8)$$

where $\underline{O}$ is the n x 1 null matrix.

These matrix equations may be written:

$$\begin{bmatrix} \underline{R} & \underline{I} \\ -\underline{I} & \underline{R} \end{bmatrix} \begin{bmatrix} \underline{V} \\ \underline{U} \end{bmatrix} = \omega_1 \begin{bmatrix} \underline{M}_o \\ \underline{O} \end{bmatrix} \qquad (A9)$$

where the square matrix of coefficients is now of order 2n, and the column vectors of order 2n x 1.

Equation (A9) is thus a full statement of the Bloch equations in the presence of chemical exchange. It may be convenient to note that $\underline{I}$ may be written as the matrix sum

$$(\omega - \omega_o)\underline{E} + \underline{I}' \qquad (A10)$$

where $\omega$, the frequency variable, is separated out. $\omega_o$ is some (arbitrary) reference frequency, $\underline{E}$ the unit matrix of order n; $\underline{I}' = \mathrm{diag}(\Delta\omega_i)$ where $\Delta\omega_i$ is the frequency shift of the ith site, referred to $\omega_o$.

Analytical solutions for the case of one dominant species.

We may define the dominance of a species $\underline{a}$ by the inequalities

$$M_o^{(i)}/M_o^{(a)} \ll 1 \quad i \neq a \tag{A11}$$

Thus the contributions of all minor species to the equilibrium static magnetisation of the system $\underline{M}_o$ are relatively negligible. In such circumstances the solution of equation (A9) is simplified: for example, for the general three-site case, (a ≡ 1)

$$G_1(\omega) = u_1(\omega) + iv_1(\omega) = \frac{\begin{vmatrix} i\omega_1 M_o^{(1)} & \alpha_{12} & \alpha_{13} \\ 0 & \alpha_{22} & \alpha_{23} \\ 0 & \alpha_{32} & \alpha_{33} \end{vmatrix}}{\begin{vmatrix} \alpha_{11} & \alpha_{12} & \alpha_{13} \\ \alpha_{21} & \alpha_{22} & \alpha_{23} \\ \alpha_{31} & \alpha_{32} & \alpha_{33} \end{vmatrix}} \tag{A12}$$

and $G_2$ and $G_3$ similarly.

Expressions of this form provide the starting point from which were obtained the analytical solutions for Δ (the line-broadening parameter) given in Chapter III. It should be recalled that the diagonal terms of $\underline{\alpha}$ are complex and the denominator must be cleared of imaginary quantities in order to obtain $v_1$ and $u_1$. The total spectrum is given by $\underline{G} = G_1 + G_2 + G_3$; only careful inspection of the relative magnitudes of the various terms can determine whether the approximation $G \simeq G_1$ is valid for the system under study. In the present case, this is confirmed by comparison of the results obtained from calculations of $G_1$ alone and the full numerical solution for $\underline{G}$ which includes $G_1$, $G_2$ and $G_3$ (see below).

Equation (A12) may be reduced to the form

$$G_1 = \frac{i\omega_i M_o^{(1)}}{\alpha_{11} + \dfrac{\alpha_{21}(\alpha_{32}\alpha_{13} - \alpha_{12}\alpha_{33}) + \alpha_{31}(\alpha_{12}\alpha_{23} - \alpha_{22}\alpha_{13})}{\alpha_{22}\alpha_{33} - \alpha_{32}\alpha_{23}}} \tag{A13}$$

where $$\alpha_{11} = -\left(\frac{1}{T_{2a}} + \sum_{i \neq a} \frac{1}{\tau_{ai}} - i(\omega - \omega_a)\right) \quad \text{(A14)}$$

which for convenience may be represented $$\alpha_{11} = -\left(\frac{1}{T_a} - i(\omega - \omega_a)\right) \quad \text{(A15)}$$

It can be shown that equation (A12) will adopt the form

$$G_1 = \frac{i\omega_1 M_o^{(1)}}{\frac{AC + BD - \frac{C^2 + D^2}{T_a}}{M_o^{(1)} C^2 + D^2} + i \frac{AD - BC + (\omega - \omega_a)(C^2 + D^2)}{C^2 + D^2}} \quad \text{(A16)}$$

$$= \frac{i\omega_1 M_o}{r + is}$$

where A, B, C, D, are real functions of the parameters appearing in the $\alpha_{ij}$.

Now

$$v_1 = \frac{\omega_1 M_o r}{r^2 + s^2} \quad \text{(A17)}$$

where

$$r = \frac{AC + BD}{C^2 + D^2} - \frac{1}{T_a} \quad \text{(A18)}$$

and

$$s = \frac{AD - BC}{C^2 + D^2} + (\omega - \omega_a) \quad \text{(A19)}$$

To the extent that r is independent of frequency and s is a linear function of frequency, then $v_1$ is a Lorentzian function of $s(\omega)$. Equation (A18) and (A19) suggest that r should be interpreted as the exchange correction to the linewidth parameter $(1/T_a)$ and s as the shift in resonance frequency ca sed by exchange. The validity of the assumption that the absorption

signal be truly Lorentzian requires careful inspection and may not be obvious; however it is of central importance if the experimentally determined quantity is a linewidth. If the spectrum is not Lorentzian, then the linewidth may be a seriously misleading parameter. In the present work the validity of a Lorentzian lineshape is confirmed for the relevant values of the kinetic and concentration parameters by comparing the linewidth increase calculated from the reduced forms with the results of the full numerical calculation of the spectrum described in the next section.

A simpler derivation of the approximate analytical expressions for the linewidth increment caused by chemical exchange is possible if the chemical shifts between the sites may be neglected by comparison with the other parameters $\tau_{ij}^{-1}$, $T_{2i}^{-1}$. Then, expression (A13) at resonance ($\omega = \omega_i$) is purely imaginary

$$G_1 = \frac{i\omega_1 M_o^{(1)}}{A} \qquad \text{(A real)} \qquad \text{(A20)}$$

If the lineshape is Lorentzian,

$$A = \left(\frac{1}{T_2}\right)_{obs} \qquad \text{(A21)}$$

and equals the observed linewidth in angular frequency units. Thus the analytical expressions (3.11) and (3.15) of Chapter III for the three and four site cases are obtained.

Numerical solution.

It is questionable whether the analytical solutions of the Bloch equations for $\underline{G}(\omega)$ possess any major advantage over a numerical evaluation of the matrix equation (A2). Whereas such solutions become algebraically intractable in the absence of simplifying assumptions, the numerical solution is almost as easily obtained for the general case as for a simple one.

Thus from (A9), the solution for $v_1$ appropriate to any four-site case with one dominant species a is given in general by

$$v_1(\omega) = \frac{\begin{vmatrix} \omega_1 M_o^{(1)} & r_{12} & r_{12} & r_{14} & \Delta\omega_1 & 0 & 0 & 0 \\ 0 & r_{22} & r_{23} & r_{24} & 0 & \Delta\omega_2 & 0 & 0 \\ 0 & r_{32} & r_{33} & r_{34} & 0 & 0 & \Delta\omega_2 & 0 \\ 0 & r_{42} & r_{43} & r_{44} & 0 & 0 & 0 & \Delta\omega_2 \\ 0 & 0 & 0 & 0 & r_{11} & r_{12} & r_{13} & r_{14} \\ 0 & -\Delta\omega_2 & 0 & 0 & r_{21} & r_{22} & r_{23} & r_{24} \\ 0 & 0 & -\Delta\omega_1 & 0 & r_{31} & r_{32} & r_{33} & r_{34} \\ 0 & 0 & 0 & -\Delta\omega_1 & r_{41} & r_{42} & r_{43} & r_{44} \end{vmatrix}}{\begin{vmatrix} r_{11} & r_{12} & r_{13} & r_{14} & \Delta\omega_1 & 0 & 0 & 0 \\ r_{21} & r_{22} & r_{23} & r_{24} & 0 & \Delta\omega_2 & 0 & 0 \\ r_{31} & r_{32} & r_{33} & r_{34} & 0 & 0 & \Delta\omega_3 & 0 \\ r_{41} & r_{42} & r_{43} & r_{44} & 0 & 0 & 0 & \Delta\omega_4 \\ -\Delta\omega_1 & 0 & 0 & 0 & r_{11} & r_{12} & r_{13} & r_{14} \\ 0 & -\Delta\omega_2 & 0 & 0 & r_{21} & r_{22} & r_{23} & r_{24} \\ 0 & 0 & -\Delta\omega_3 & 0 & r_{31} & r_{32} & r_{33} & r_{34} \\ 0 & 0 & 0 & -\Delta\omega_4 & r_{41} & r_{42} & r_{43} & r_{44} \end{vmatrix}} \qquad \text{(A22)}$$

where $(r_{ij}) = \underline{R}$ and $\mathrm{diag}(\Delta\omega_i) = \underline{I}$, referring to equation (A9). If $v_1$ is Lorentzian, then the coefficient of $\omega_1 M_o^{(1)}$ evaluated at resonance equals $(T_2)_{\text{observed}}$.

However the restriction that only $M_o^{(1)}$ contributes significantly to $\underline{M}_o$ is easily relaxed by completing the column vector $\underline{M}_o$ with the remaining elements, $M_o^{(2)}$, $M_o^{(3)}$ and $M_o^{(4)}$. The $\underline{M}_o^{(i)}$ are directly proportional to the concentrations of the ith species. We are thus relaxing the restriction that the system be prepared with one dominant species, a.

Finally, the remaining elements of the $\underline{G}$ vector should be evaluated. If $\underline{v} = \sum_4 v_i$ is computed at each of a series of frequencies the complete spectrum is generated.

The full numerical solution

The program (CH0024) developed is listed in the following section.

The central feature of the computation of the complete spectrum is the evaluation of the eighth order determinants. The direct computation of such determinants is lengthy, and in the program below use is made of a Gauss-Jordan elimination procedure (McCalla 1967), which reduces the matrix of the determinant to a unit matrix by elementary row operations. In so doing, the determinant is calculated as the cumulative product $\prod_{kk}^{8} a_{kk}^{k}$ of the 8 diagonal elements where $a_{kk}^{k}$ is the value of $a_{kk}$ at the kth. stage of the elimination. The elimination itself is carried out according to the recursion formulae

$$a_{kj}^{k} = a_{kj}^{k-1} / a_{kk}^{k-1} \qquad j = k, 8 \ (k = 1,8) \qquad \text{(A23)}$$

$$a_{ij}^{k} = a_{ij}^{k-1} - a_{ik}^{k-1} \, a_{kj}^{k} \quad (i \neq j)$$

where the original matrix is $(a_{ij}^{o})$.

Program run-time on Elliott 903 is 45s for each frequency point.

To illustrate the use of this program, Figures 1 and 2 show the behaviour of the complete computed spectra of two model systems. Because the MATRIX CONSTRUCTION segment of the program conforms with the stoichiometry of the $Cl^-/Cl_2/Cl_3^-$ system of Chapter 3, these model systems all refer to reactions of the type

$$X + X\text{-}X \rightleftarrows X\text{-}X\text{-}X$$

Any other exchange process can be treated by trivial alterations to this program segment, just as the program may be generalised to any number of sites by extending the range of the DO loops and arrays of the program.

The model systems are:

i) exchange between four sites of equal $T_2$, but between which there are large chemical shifts;

Figure 1

Complete computed spectrum for four-site exchange of quadrupolar nucleus in model system

$$\underset{a}{X} + \underset{b}{X\text{-}X} \rightleftarrows \underset{c\ d\ c}{X\text{-}X\text{-}X}$$

$T_{2a} = T_{2b} = T_{2c} = T_{2d} = 200\mu s$

Chemical shift between adjacent sites = $5 \times 10^4$ Hz angular frequency

Site concentrations

| | |
|---|---|
| a | 2.00 mol $dm^{-3}$ |
| b | 4.00 mol $dm^{-3}$ |
| c | 1.11 mol $dm^{-3}$ |
| d | 0.55 mol $dm^{-3}$ |

Key:

| | |
|---|---|
| A | $k_b = 0$ |
| B | $10^3\ s^{-1}$ |
| C | $10^4\ s^{-1}$ |
| D | $10^5\ s^{-1}$ |
| E | $10^7\ s^{-1}$ |

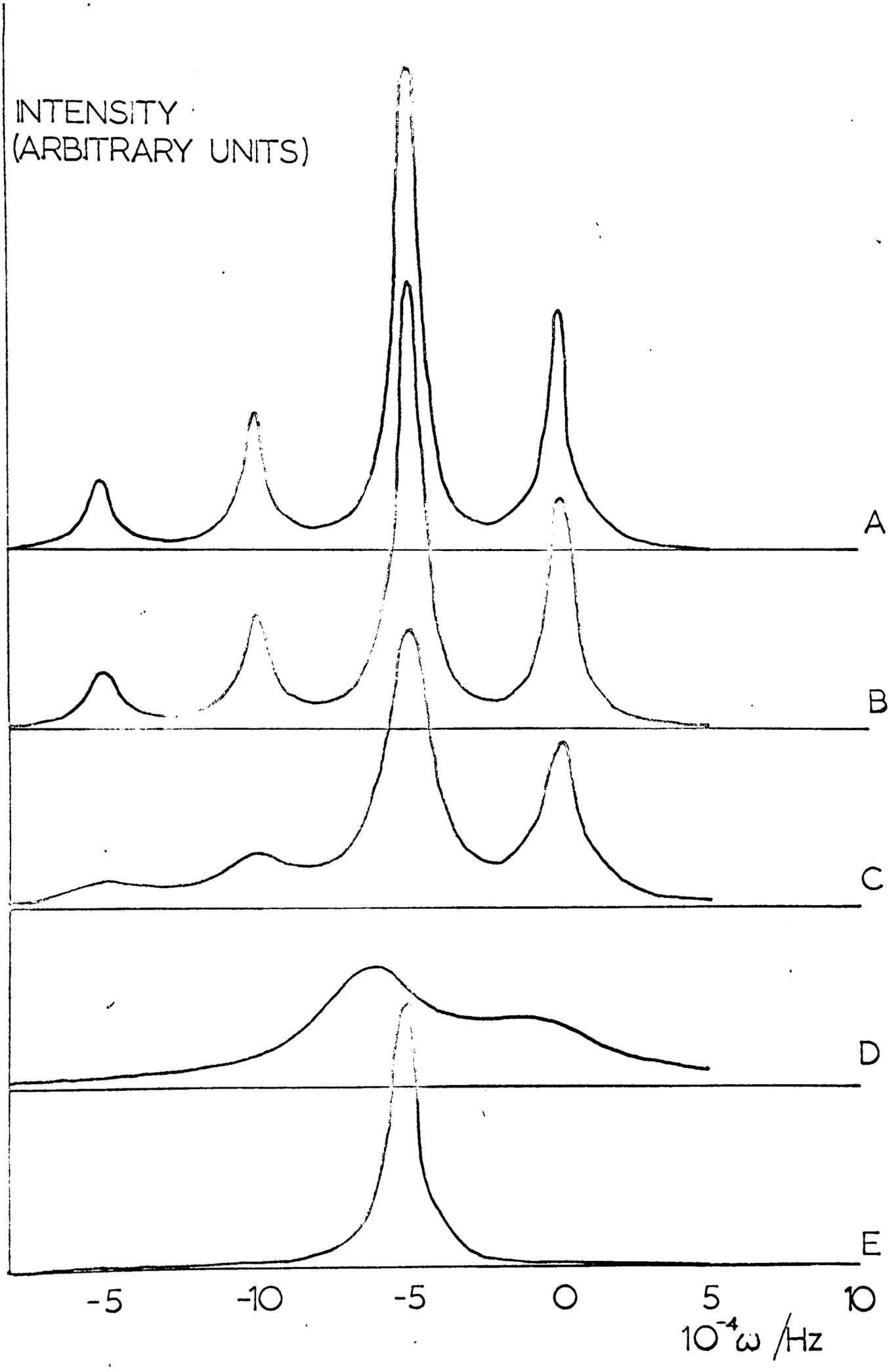

INTENSITY
(ARBITRARY UNITS)
A
B
C
D
E
-5
-10
-5
0
5
10
$10^{-4}\omega$ /Hz

Figure 2

Complete computed spectrum for four-site exchange of quadrupolar nucleus in model system

$$\underset{a}{X} + \underset{b}{X\text{-}X} \rightleftarrows \underset{c\ d\ c}{X\text{-}X\text{-}X}$$

$T_{2a} = 1000\mu s$

$T_{2b} = T_{2c} = T_{2d} = 200\mu s$

No chemical shifts between sites.

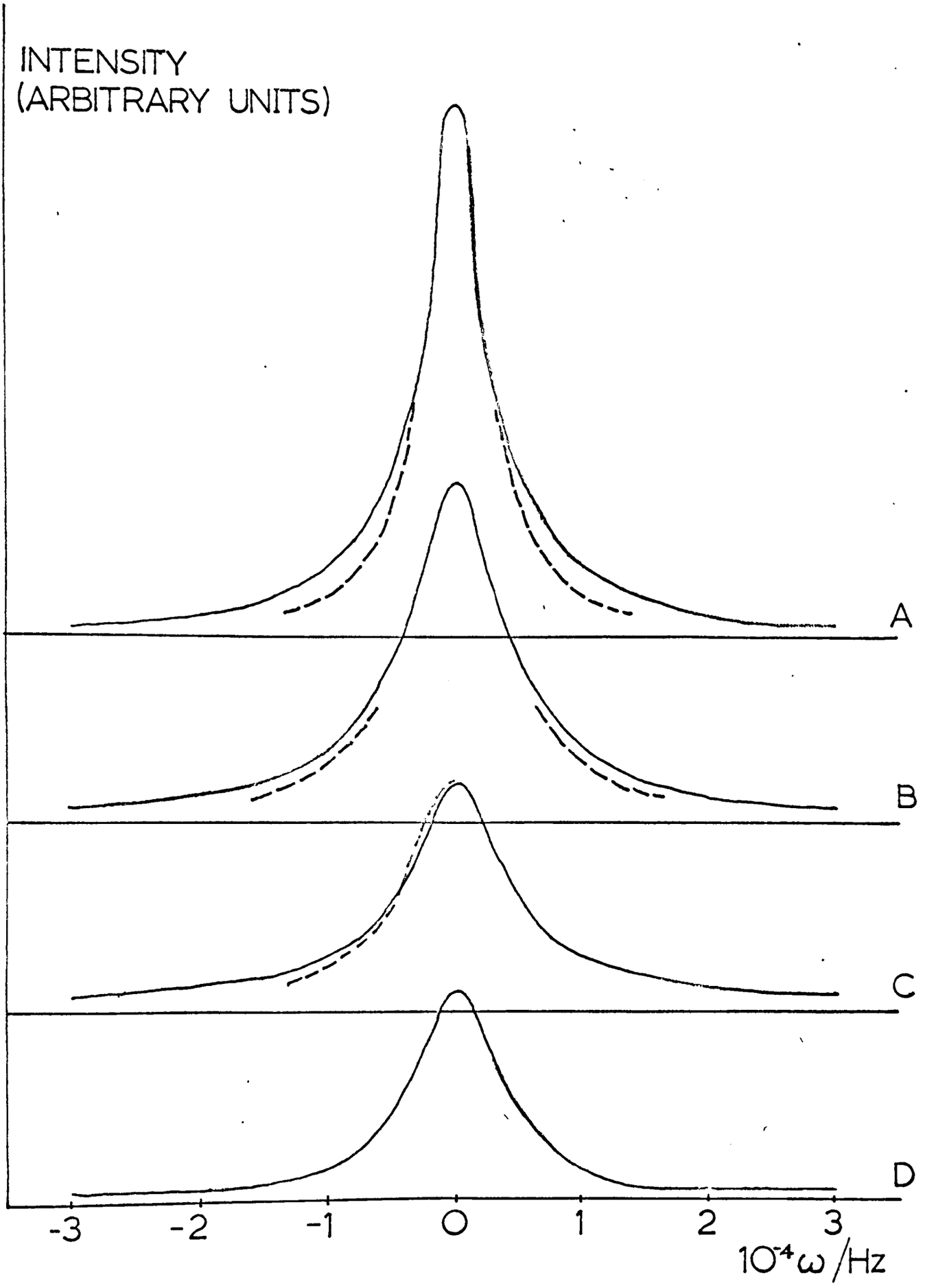
Site concentrations

| | |
|---|---|
| a | 1.00 mol $dm^{-3}$ |
| b | 2.00 mol $dm^{-3}$ |
| c | 0.55 mol $dm^{-3}$ |
| d | 0.28 mol $dm^{-3}$ |

Key:

| | |
|---|---|
| A | $k_b = 10^3\ s^{-1}$ |
| B | $10^4\ s^{-1}$ |
| C | $10^5\ s^{-1}$ |
| D | $10^6\ s^{-1}$ |

The corresponding Lorentzian functions of $(\omega-\omega_o)$, normalised to the computed lineshapes in width and in intensity, are indicated by broken lines.


INTENSITY
(ARBITRARY UNITS)
A
B
C
D
-3
-2
-1
0
1
2
3
10⁻⁴ω/Hz

ii) exchange between four sites, one (a) of which has $T_2$ five times longer than the remaining three; there is no chemical shift between sites.

The computed spectra of the first system show the familiar coalescence of a structured n.m.r. spectrum with increasing exchange rate constant.

The second set of spectra illustrates the obvious but important fact that the superimposition of a number of Lorentzian lines (unshifted) does not produce a compound Lorentzian lineshape. Thus the computed lines of Figure 2 show distinct deviations from Lorentz shape in all but the last case. This is in keeping with our expectation that the spectral line should become Lorentzian in the fast exchange limit.

```
C  NUMERICAL SOLUTION TO THE FOUR SITE PROBLEM WITH SHIFT
C  COMPUTES SPECTRUM INTENSITY AS FUNCTION OF ANGULAR FREQUENCY
C  NB:  INPUT DATA IN MICROSECOND TIME UNITS
GLOBAL,CH0024)
DIMENSION R(6,6),S(10,10),W(6),DET(5),C(4)
READ(1)CL20,CL0,AKB0,STEPCL,STEPKB
READ(1)T2A,T2B,T2C,T2D,WA0,WB0,WC0,WD0,NCL,NKB,X,NUM
A1=T2B*1.E-6
A2=T2C*1.E-6
A3=T2D*1.E-6
A0=T2A*1.E-6
WRITE(2,105)A0
WRITE(2,103)A1,A2,A3
WA00=WA0*1.E6
WB00=WB0*1.E6-WA00
WC00=WC0*1.E6-WA00
WD00=WD0*1.E6-WA00
WA00=0.
WRITE(2,110)
WRITE(2,106)WA00
WRITE(2,104)WB00,WC00,WD00
AKB=AKB0
DO2IJ=1,NKB
AKB=AKB*STEPKB
B1=AKB*1.E6
WRITE(2,101)B1
WRITE(2,102)
WRITE(2,107)
CL=CL0
DO2KJ=1,NCL
CL=CL+STEPCL
C(1)=CL
C(2)=2.*CL20
C(3)=(2.*.191*CL*CL20)/(1+.191*CL)
C(4)=.5*C(3)
WRITE(2,108)
WRITE(2,109)C(1),C(2),C(3),C(4)
DO20I=1,4
DO20J=1,4
20   R(I,J)=0.
WA=WA0
WB=WB0
WC=WC0
WD=WD0
```

```
C  MATRIX CONSTRUCTION SEGMENT
DO2IND=1,NUM
WA=WA+X
WB=WB+X
WC=WC+X
WD=WD+X
R(1,1)=-CL20*.191*AKB/(1.+.191*CL)
R(3,1)=-R(1,1)
R(1,1)=R(1,1)-1./T2A
R(2,2)=-(1./T2B)-(AKB*CL*.191)
R(3,2)=.5*AKB*CL*.191
R(4,2)=R(3,2)
R(1,3)=.5*AKB
R(2,3)=.5*AKB
R(3,3)=-(1./T2C)-AKB
R(2,4)=AKB
R(4,4)=-(1./T2D)-AKB
W(1)=-WA
W(2)=-WB
W(3)=-WC
W(4)=-WD
DO40L=1,5
DO10I=1,8
DO10J=1,8
10  S(I,J)=0.
DO11I=1,4
DO11J=1,4
11  S(I,J)=R(I,J)
C  DETERMINANT EVALUATION SEGMENT
DO120I=5,8
DO120J=5,8
M=I-4
N=J-4
120  S(I,J)=R(M,N)
DO13I=5,8
N=I-4
13  S(I,N)=-W(N)
DO14I=1,4
N=I+4
14  S(I,N)=W(I)
IF(L-5)85,86,85
85  DO87I=1,8
S(I,L)=0.
87  S(L,L)=C(L)
```

```
86  CONTINUE
DET(L)=1.
DO29M=1,8
DET(L)=DET(L)*S(M,M)
DO30J=(M+1),8
30  S(M,J)=S(M,J)/S(M,M)
S(M,M)=1.
DO12I=1,8
68  IF(I-M) 31,12,31
31  DO41J=(M+1),8
41  S(I,J)=S(I,J)-S(I,M)*S(M,J)
12  S(I,M)=0.
29  CONTINUE
40  CONTINUE
DEL=(DET(1)+DET(2)+DET(3)+DET(4))/DET(5)
DEL=-DEL
WA1=WA*1.E6
2   WRITE(2,100)WA1,DEL
100   FORMAT(2E14.5)
101   FORMAT(5H  KB=,E12.5)
102   FORMAT(14H   FREQUENCY  ,14H  INTENSITY   )
103   FORMAT(4HT2B=,E12.5,7H   T2C=,E12.5,7H   T2D=,E12.5)
104   FORMAT(4HWB =,E12.5,7H   WC =,E12.5,7H   WD =,E12.5)
105   FORMAT(4HT2A=,E12.5,3HSEC)
106   FORMAT(4HWA =,E12.5)
107   FORMAT(10H   RAD/SEC)
108   FORMAT(25HSITE CONCENTRATIONS MOL/L)
109   FORMAT(3H A ,F8.5,3H B ,F8.5,3H C ,F8.5,3H D ,F8.5)
110   FORMAT(30HSHIFTS RELATIVE TO A REF RAD/S)
END
```

CH024: INPUT KEY

| | | |
|---|---|---|
| CL20 | TOTAL CHLORINE CONCENTRATION | |
| CL0 | (INITIAL) CHLORIDE ION CONCENTRATION | |
| AKB0 | INITIAL ASSUMED RATE CONSTANT | |
| STEPCL | CHLORIDE ION CONCENTRATION INCREMENT | ** |
| STEPKB | RATE CONSTANT INCREMENT | ** |
| T2A | T2 OF A SITE (MICROSECONDS) | |
| T2B | T2 OF B SITE (.MICROSECONDS) | |
| T2C | T2 OF C SITE (MICROSECONDS) | |
| T2D | T2 OF D SITE (MICROSECONDS) | |
| WA0 | OMEGA - OMEGAA | * |
| WB0 | OMEGA - OMEGAB | * |
| WC0 | OMEGA - OMEGAC | * |
| WD0 | OMEGA - OMEGAD | * |
| NCL | NUMBER OF TIMES CHLORIDE ION CONCENTRATION IS TO BE STEPPED | ** |
| NKB | NUMBER OF TIMES RATE CONSTANT IS TO BE STEPPED | ** |
| X | FREQUENCY INTERVAL BETWEEN POINTS IN COMPUTED SPECTRUM (1/MICROSECONDS) | |
| NUM | NUMBER OF POINTS TO BE COMPUTED IN SPECTRUM | |

** PROGRAM WILL CALCULATE COMPLETE SPECTRUM FOR EACH OF A NUMBER (NCL) OF CHLORIDE ION CONCENTRATIONS AT EACH OF A NUMBER (NKB) OF RATE CONSTANTS. THE CHLORIDE ION CONCENTRATIONS AND THE RATE CONSTANTS USED ARE OBTAINED BY ADDING SUCCESSIVE INCREMENTS (STEPCL AND STEPKB) TO THE INITIAL VALUES (AKB0 AND CL0) OF THESE PARAMETERS.

* OMEGA IS THE FREQUENCY AT WHICH THE SPECTRUM INTENSITY IS TO BE CALCULATED IN A PARTICULAR LOOP, AND OMEGAX THE X-SITE LARMOR FREQUENCY. THESE AND ALL OTHER FREQUENCIES ARE EXPRESSED ON MICROSECOND TIME SCALE

# REFERENCES

Abragam A 1961 The principles of nuclear magnetism: Oxford

Arnold M and Packer KJ 1968 Molec Phys 14 241

Assink RA and Jonas J 1969 J phys Chem 73 2445

Atkins PW 1969 Molec Phys 17 321

Atkins PW Loewenstein A and Margalit Y 1969 Molec Phys 17 329

Bigeleisen JW and Wolfsberg M 1958 Adv chem Phys 1 33

Bloembergen N Purcell EM and Pound RV 1946 Phys Rev 69 37

Bloembergen N and Sorokin PP 1958 Phys Rev 110 865

Borovikov YuYa and Fialkov YuYa 1965 Sov Electrochem 1 989

Garrington A Dravnicks F and Symons MCR 1960 Molec Phys 3 174

Chattaway FD and Hoyle G 1923 J Chem Soc 123 654

Daniele G 1960 Gazz chim Ital 90 1597

Davies CW 1962 Ion association: London

Deverell C 1966 D Phil thesis: Oxford

Deverell C 1969 Prog NMR Spectroscopy 4 235

Deverell C Frost DJ and Richards RE 1965 Molec Phys 9 565

Diesen RW Wahr JC and Adler SE 1969 J chem Phys 50 3635

Dwek RA and Richards RE 1967 Disc Faraday Soc 43 196

Eigen M and Kustin K 1962 J Am chem Soc 84 1355

Eisenberg D and Kauzmann W 1969 The structure and properties of water: Oxford

Eisenstadt M and Friedman HL 1967 J chem Phys 46 2182

Endom L Hertz HG Thül B and Zeidler MD 1967 Ber Bunsenges physik Chem 71 1008

Engel G and Hertz HG 1968 Ber Bunsenges physik Chem 72 802

Evans JC and Lo GY-S 1966a J chem Phys 44 3638

Evans JC and Lo GY-S 1966b J chem Phys 44 4356

Evans JC and Lo GY-S 1966c J chem Phys 45 1069

Fowler RH and Guggenheim EA 1939 Statistical thermodynamics: Cambridge

Frank HS and Wen W-Y 1957 Disc Faraday Soc 24 133

Genser EE 1962 US at Energy Comm UCRL-9846

Gordy W 1953 Microwave spectroscopy: New York

Gordy W 1955 Disc Faraday Soc 19 14

Hafemeister DW and Flygare WH 1965 J chem Phys 43 795

Gutowsky HS McCall DM and Slichter CP 1953 J chem Phys 21 279

Hall C Haller GL and Richards RE 1969 Molec Phys 16 377

Hall C Richards RE Schulz GW and Sharp RR 1969 Molec Phys 16 529

Halliday JD 1969 D Phil thesis: Oxford

Halliday JD Hill HDW and Richards RE 1969 J sci Instrum (ser 2) 2 29

Halliday JD Richards RE and Sharp RR 1969 Proc roy Soc A313 45

Harned HS and Owen BB 1958 The physical chemistry of electrolytic solutions: New York

Hasted JB and El Sabeh SHM 1953 Trans Faraday Soc 49 1003

Hasted JB Ritson DM and Collie CH 1948 J chem Phys 16 1

Herbison-Evans D and Richards RE 1964 Molec Phys 7 515

Hertz HG 1961a Z Elektrochem 65 20

Hertz HG 1961b Z Elektrochem 65 36

Hertz HG 1967 Prog NMR Spectroscopy 3 159

Hertz HG Stalidis G and Versmold H 1969 preprint received: no publication information available

Hertz HG and Zeidler MD 1964 Ber Bunsenges physik Chem 68 821

Herzberg G 1950, 1959 Molecular spectra and molecular structure: Toronto

Hill NE 1954 Proc phys Soc 67 149

Howarth OW and Richards RE 1966 Prog NMR Spectroscopy 1 1

Ikenberry D and Das TP 1965 Phys Rev 138A 822

Itoh J and Yamagata Y 1959 J phys Soc Japan 13 1182

Johnson CS jr 1966 Adv Magnetic Resonance 1 33

Jones GT and Powles JT 1964 Molec Phys 8 607

Kay RL 1968 Adv Chem 73 1

Khazanovich TN 1969 Molec Phys 17 281

Krynicki K 1966 Physica 32 167

Laidler KJ 1965 Chemical kinetics second edn: London

Lawrence RM and Kruh RF 1967 J chem Phys 47 4758

McCall DW and Douglass DC 1965 J phys Chem 69 2001

McCalla TR 1967 Introduction to numerical methods and FORTRAN programming: New York

McConnell HM 1958 J chem Phys 28 430

Maryott AA and Smith ER 1951 Table of dielectric constants of pure liquids: National Bureau of Standards circular 514

Melander L 1960 Isotope effects on reaction rates: New York

Meyers OE 1958 J chem Phys 28 1027

Moniz WB Steele WA and Dixon JA 1963 J chem Phys 38 2418

O'Reilly DE and Schacher GE 1963 J chem Phys 39 1768

O'Reilly DE Schacher GE and Schug K 1963 J chem Phys 39 1756

Pauling L 1960 The nature of the chemical bond, third edn: Ithaca

Poirier JC 1966 Chemical physics of ionic solutions, ed Conway BE: New York

Pople J 1967 Disc Faraday Soc 43 192

Prue JE 1966 Ionic equilibria: Oxford

Résibois PMV 1968 Electrolyte theory: New York

Richards RE and Yorke BA 1963 Molec Phys 6 289

Robinson RA and Stokes RH 1965 Electrolyte solutions: London

Samoilov OYa 1965 Structure of aqueous electrolyte solutions and the hydration of ions, tr Ives DJG: New York

Simpson JH and Carr HY 1958 Phys Rev 111 1201

Speight PA and Armstrong RL 1967 Can J Phys 45 2493

Steele WA 1963a J chem Phys 38 2404

Steele WA 1963b J chem Phys 38 2411

Stokes RH and Mills R 1965 The viscosity of electrolytes: London

Swift TJ and Connick RE 1962 J chem Phys 37 307

Thompson PJ 1969 D Phil thesis: Oxford

Townes CH and Dailey BP 1949 J chem Phys 17 782

Valiev KA 1960a J exp theor Phys 10 77

Valiev KA 1960b J exp theor Phys 11 883

Valiev KA and Zripov MM 1966 J struct Chem 7 470

Wang JH 1965 J phys Chem 69 4412

Zimmermann G and Strong FC 1957 J Am chem Soc 79 2063

# SUMMARY

Summary

Chapter I begins with a brief review of the manner in which information on molecular motion in liquids may be derived from nuclear magnetic resonance relaxation time data. Emphasis is placed on solvent and solute resonance studies of electrolyte solutions.

New data is presented on the temperature, concentration and viscosity dependence of $^{81}Br^-$ and $^{23}Na^+$ ion nuclear magnetic relaxation times in several aqueous solutions. An empirical equation is proposed which describes well both the new and the previously available data. Linewidths of ion resonances studies vary linearly with $\eta/T$, but are not directly proportional to this quantity, in contradiction with the Debye-Stokes model of ionic and solvent molecular motion. Striking similarity exists between the temperature dependence of n.m.r. linewidths and that of dielectric relaxation times in alkali halide solutions, suggesting that solvent reorientation or translation in the outer hydration region is the most efficient means of quadrupolar relaxation. On this assumption approximate solvent tumbling times in the outer hydration spheres of NaBr are calculated. Contributions to relaxation from ion-ion interactions are in accord with previous theory in that they possess an activation energy of the same approximate magnitude as that for ionic self-diffusion.

Chapter II. The theory proposed by Halliday, Richards and Sharp (1969) to account for the concentration dependence of the $^{133}Cs^+$ ion shift in a number of aqueous, mixed aqueous and non-aqueous solutions of caesium salts is introduced; a detailed exposition is given, in which attemtion is drawn to its assumptions and approximations. A simple approximation in the theory, which avoids the necessity for a numerical integration, is described and justified.

The possible ways in which experimental data may be compared with this theory are discussed and illustrated. New experimental data which show the

effects on the $^{133}Cs^{+}$ ion shift of changes in temperature, dielectric constant and ionic strength are given, and fully analysed in terms of the theory by means of the precedures described. The results support the view that the theory available describes the ion shifts well even in solutions of low dielectric constant, provided that low concentraction data only are considered.

An alternative model based upon the Bjerrum ion-pair theory is considered and compared with the theory previously described. A preliminary comparison of shift data with the predictions of the Bjerrum theory is made, which indicates a qualitative concordance, although the restricted data available make detailed appraisal impossible.

Chapter III. An account is given of the use of the halogen line-broadening technique for determining the rates of chemical exchange between sites with different intrinsic relaxation times. The method is applied to the exchange of $Cl^{-}$ ion between $Cl_3^{-}$ and $Cl_2$, a "four-site chlorine exchange' problem. The appropriate algebraic solutions to the modified Bloch equations are presented, but emphasis is placed on the advantages of direct numerical computation of the spectrum. A description of the experimental procedures used includes a discussion of improvements in precision to be gained by using complete least-squares fitting procedures to abstract relaxation times from observed resonance lines. A comparison of the experimental results with theory, and in particular computed values of the broadening parameter, leads to a value of the dissociation rate constant of the trichloride ion ($8 \times 10^{6} \pm 4 \times 10^{6}$ $s^{-1}$).

Appendix I constains a listing of the program developed for finding the best Lorentzian line through experimental resonances by the criterion of least squares.

Appendix II contains a summary of experimental data relating to Chapter III in tabular form.

Appendix III contains a discussion of the solutions of the modified Bloch equations, and an account of numerical solutions in the "unrestricted" four-site case, including computed spectra. A listing is given of the program developed which provides a numerical solution to the full modified Bloch equations which enables spectra to be computed.